School of Civil and Mechanical Engineering

Department of Civil Engineering

Downscaling approach to evaluate future climate change impacts on urban hydrology

Herath Mudiyanselage Sujeewa Malwila Herath

This thesis is presented for the Degree of

Doctor of Philosophy

of

Curtin University

July 2017

DECLARATION

To the best of my knowledge and belief, this thesis contains no material previously published by any other person except where due acknowledgement has been made.

This thesis contains no material which has been accepted for the award of any other degree or diploma in any university.

Signature: 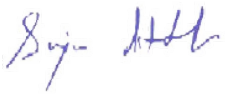

Date: 26/07/2017

ABSTRACT

Accurate design storm is one of the key elements which plays a dramatic role in urban hydrological assessments leading to urban stormwater management. IDF relations are widely used to estimate the design storm for the design of drainage and other hydraulic structures for a long time. In the recent past, unexpected urban floods occurred in major cities in the world as a result of high intensified rainfall events, motivate water professionals to re-evaluate the accuracy of available IDF relations. However, it has become a real challenge to develop an accurate and widely usable approach to develop IDF relations under changing climate. Some studies have been conducted in many parts of the world to address this issue and most of these approaches are performed well only in a particular region. Therefore, there is an essential requirement to develop a widely usable and accurate approach to determine IDF relations which present the impacts of climate change.

The main aim of this research is to develop a reliable and accurate IDF relation constructing approach under the context of climate change. Even though Global Climate Models (GCMs) are still known as a trustworthy technique to project future climate in some extend, GCMs' projections are not directly applicable in urban hydrological studies due to the low resolution. Therefore, GCMs' projections need to be subjected to a downscaling process to improve resolution in spatially and temporally.

Statistical Downscaling Model (SDSM) is used in this study to spatially downscale GCM projections (HadCM3 and CGCM3) at Perth airport region, Western Australia. For the SDSM model calibration and validation, National Centre for Environmental Prediction (NCEP) reanalysed data is used. Spatial downscaled results of Perth airport region show a general decreasing trend of annual rainfall for both scenarios. However, an increasing trend of daily rainfall can be observed for autumn seasons in 2020s and 2050s. The temporal resolution of these spatially downscaled rainfalls remain 24 hour and it should be subjected to further temporal downscaling, prior to use in IDF relations for sub-daily durations.

Generalised Extreme Value (GEV) distribution based temporal downscaling model is used for temporal downscaling of spatially downscaled rainfalls. The scaling invariant property of the extreme rainfalls are employed in the temporal downscaling model and

Non-Central Moment (NCM) method is used to estimate the GEV parameters to simulate extreme rainfall series. The accuracy of the proposed temporal downscaling approach is evaluated with the observed rainfalls in eight weather stations in Western Australia. It confirms the accuracy of proposed approach and after that it is employed on spatially downscaled daily rainfall at Perth airport region to estimate the statistical properties of sub-daily extreme rainfalls. These estimated statistical properties are used in the development of IDF relations for sub-daily rainfall events in the area. Further, the applicability of the proposed temporal downscaling approach is investigated for six weather stations in other major cities in Australia (Adelaide, Brisbane, Canberra, Darwin, Melbourne and Sydney).

Next part of the thesis focuses the empirical relationship between the extreme rainfalls and daily maximum temperature for seven major cities in Australia. Binning approach with equal numbers of pairs in a bin is used for the evaluation. It shows that the rainfall - temperature scaling relationship is limited to certain temperature range, and this relationship depends on the percentile of rainfall, the rainfall duration, analysis period and the season. Periodic analysis observes both increasing and decreasing scaling trends. According to these results, it can be expected more extreme short duration rainfalls in some regions in the future.

The final part of the thesis presents a hydrological modeling case study. This study describes a hydrological modeling approach to evaluate the combined impacts of climate change and land use change on the urban catchments. The development area of Stirling City Centre Alliance project is subjected to this study. Previously developed IDF relations to Perth airport region are used to represent the future rainfall changes under the context of climate change. The hydrological assessment results show that proposed stormwater drainage network satisfy the stormwater management requirements under existing climate. However, it does not become valid under changing climate downscaled by HadCM3-A2 scenario for future periods. Therefore, further modifications are essential for the proposed drainage network.

As a summary, overall study emphasises the importance of evaluating combined impacts of climate change and land use change in hydrological assessments. The SDSM model is feasible to describe the linkage between the daily coarse scale GCM climate predictors and the daily local rainfall (the predictand). Further proposed

temporal downscaling approach is highly accurate and widely applicable in estimating statistical properties of sub-daily rainfalls using daily rainfall series. Moreover, high intensified short duration rainfall can be expected in the future and therefore comprehensive climate change impacts assessments should be included in the urban stormwater management studies in land developments. Finally, the outcome of this research will assist water professionals in decision making and implementing more sustainable stormwater management guidelines.

ACKNOWLEDGEMENTS

I would like to take this opportunity to extend my deepest appreciation to my supervisor, Dr. Ranjan Sarukkalige for his tremendous support throughout the period which is not limited to the research. The completion of this study would not be possible without his advises and guidance. Also, I express my sincere gratitude to my co-supervisor, Professor Van Thanh Van Nguyen, for the sharing his exceptional technical knowledge with me and giving valuable guidance to fulfil this research.

I would like to acknowledge chairman of the thesis committee, Professor Hamid Nikraz, Head of the Department of Civil Engineering, Associate Professor Andrew Whyte for their valuable support throughout the study. I would like to thank Australian Commonwealth Government and Curtin University for providing me prestige Australian Postgraduate Award (APA) Scholarship. Also, I express my utmost gratitude to Department of Civil Engineering, Curtin University for providing necessary support to complete this study successfully.

I should offer my sincere gratitude to Dr. Nimal Gamage and Dr. Robin Connolly from GHD Australia, Dr. Sri Srikanth from Bureau of Meteorology, City of Stirling and DHI Australia for their support in the numerous ways to the completion of this research.

Finally, and most importantly, I should pay my tribute to my family members, especially my parents, devoted wife Thushara, my loving daughters Senadi and Senuli for their love, blessings, encouragements and generous support during my PhD studies.

PUBLICATIONS ASSOCIATED WITH THE STUDY

Herath, S.M., Sarukkalige, R. and Nguyen, V. T. V., 2017, Evaluation of empirical relationships between extreme rainfall and daily Maximum temperature in Australia, Journal of Hydrology (Accepted for publication).

Herath, S.M., Sarukkalige, R. and Nguyen, V. T. V., 2016. A spatial temporal downscaling approach to development of IDF relations for Perth airport region in the context of climate change. Hydrological Sciences Journal, 61, 2061-2070.

Herath, S.M., Sarukkalige, R. and Nguyen, V. T. V., 2015, Downscaling approach to develop future sub-daily IDF relations for Canberra Airport Region, Australia, Proceedings of the International Association of Hydrological Sciences. PIAHS, , 369, 147–155. doi: 10.5194/piahs-369-147-2015.

H.M.S.M.Herath, P.R.Sarukkalige, V.T.V.Nguyen, Evaluation of GEV parameter estimation methods to assess the scaling behavior of extreme rainfalls, 19th IAHR - APD Congress, 21-24 Sep. 2014, Hanoi, Vietnam.

H.M.S.M.Herath, B.M.A.P.Basnayaka, P.R. Sarukkalige, V.T.V.Nguyen, Behaviour of urban catchment hydrology to future climate change scenarios, 19th IAHR - APD Congress, 21-24 Sep. 2014, Hanoi, Vietnam.

Sujeewa Herath, Ranjan Sarukkalige, "Spatial and temporal downscaling approach to develop IDF curves for Melbourne airport region", 35th Hydrology and water resources symposium 2014, 24-27 Feb 2014, Perth, Western Australia.

TABLE OF CONTENTS

LIST OF FIGURES

LIST OF TABLES

LIST OF ABBREVIATIONS

AHD	Australian Height Datum
ANN	Artificial Neural Network
ARI	Average Recurrence Interval
ARR	Australian Rainfall and Runoff
ASBD	Albert Street Branch Drain
ASD	Automated Statistical Downscaling
BoM	Bureau of Meteorological
BSBD	Beryl Street Branch Drain
CBD	Central Business District
CDF	Cumulative Distribution Function
CI	Confidence Interval
CREST	Coupled Routing and Excess Storage
DAI	Data Access Integration
DEM	Digital Elevated Model
DHI	Danish Hydraulic Institute
DoW	Department of Water
DWMS	District Water Management Strategy
FSA	Flood Storage Areas
GEV	Generalised Extreme Value
GHG	Green House Gas
GPS	Global Positioning System
HD	Hydro Dynamic
IDF	Intensity Duration Frequency
IPCC	International Panel on Climate Change
LAM	Limited Area Models
LWMS	Local Water Management Strategy
MGA	Map Grid of Australia

MI	Modelling Interface
MLE	Maximum Likelihood Estimation
MLR	Multi Linear Regression
NCEP	National Centre of Environmental Prediction
NCM	Non-Central Moment
NSE	Nash- Sutcliffe efficiency
OL	Over Land
OPBD	Osborn Park Branch Drain
PWM	Probability Weight Moments
RCM	Regional Climate Models
RCP	Representative Concentration Pathways
RMSE	Root Mean Square Error
RWMS	Regional Water Management Strategy
SDSM	Statistical Down-Scaling Model
SHE	Système Hydrologique Européenne
SRES	Special Report on Emission Scenarios
SSVM	Smooth Support Vector Machine
SZ	Saturated Zone
UWMP	Urban Water Management Plan
UZ	Unsaturated Zone
WA	Western Australia
WAPC	Western Australian Planning Commission
WMO	World Meteorological Organization
WSUD	Water Sensitive Urban Design

CHAPTER 1

1. Introduction

1.1 Background

Australia is facing severe urban flooding events in the recent past like many other countries in the world. Latest urban flood incident was reported from South-East Queensland in May 2015. Queensland and New South Wales faced massive flood event due to cyclone Oswald in 2013. Also, New South Wales, Queensland and Victoria were affected by Eastern Australia Flood in 2012. The socioeconomic and environmental impacts of these floods are massive and uncountable.

Mitigation of flood damage is a very complex series of activities and it should be addressed in several ways. Especially, local agencies who are responsible for the urban stormwater management, should have a proper understanding about the occurrence of extreme storm events, climate change impacts on local catchments, land cover change and available drainage network capacities etc. Furthermore, in urban areas, stormwater management is a difficult challenge to local governments and environmental authorities rather than in rural areas. In most of the urban catchments, whole stormwater management relies on the drainage network due to the low capability of onsite infiltration systems. Therefore, drainage network should be properly designed and maintained to achieve its expected benefits.

With the requirement of accurate and reliable drainage network designing in urban catchments to facilitate the mitigation of urban flooding, nowadays, researchers are exploring new approaches to estimate the design rainfall depth accurately under the impacts of changing climate. However, most of the approaches available in the literature are valid only for specific catchments which has been subjected in the study. Hence, there is a high demand for the widely applicable approaches in flood mitigating.

1.2 Significance of the study

The current practice of stormwater management is highly based on the present Water Sensitive Urban Design (WSUD) guidelines. These WSUD guidelines provide an important framework to manage stormwater in new urban development catchments to some extent. However, current WSUD practice does not address some aspects in modern hydrology, especially it does not take climate change impact into consideration in urban hydrological assessments. Further, urban planners and designers reveal the importance of updating the design guidelines and policies to reduce the impact of natural disasters caused by climate change (Kozlowski and Yusof, 2016). Therefore, in mitigating urban flooding, both human-induced land cover change and climate change are the key factors to be taken into consideration (Alexander et al., 2007).

Assessing the land use change impacts on the catchment hydrology is a straight forward approach. Nevertheless, climate change impact assessment in the catchment scale is a complex and time-consuming process with high uncertainties. A number of studies are available in the literature which has been addressed this matter successfully (Olsson et al., 2012, Jung et al., 2015, Sachindra et al., 2014b). However, the applicability of many of these approaches is limited and highly uncertain when expanding to other areas rather than subjected study area. Therefore, a generalised study is required to encourage the urban developers and decision makers in upgrading the design guidelines to address combined impacts of land use change and climate change on urban catchments.

The general consequence of the climate change is "high intense short term rainfalls in high frequency" (Trenberth et al., 2003). These high intense rainfalls are not represented in current design storm calculations as most of the studies use Intensity Duration Frequency (IDF) relations which are already constructed based on past observed rainfalls. Therefore, development of daily and sub-daily IDF relationships, by taking future climate changes into account is an effective and accurate approach to evaluate the climate change impacts on catchment scale. Global Circulation Models (GCMs) are considered as an accurate way to evaluate climate change impacts for future periods. However, GCMs projections do not satisfy the high-resolution data requirement in local scale hydrodynamic models. Therefore, these projections need to be subjected to downscaling process to improve their resolution.

Considering these matters, this study aims to develop new IDF relations taking climate change impacts into account, by downscaling GCMs output spatially and temporally. Also, this study tries to identify some empirical relationships between extreme rainfall events and daily temperature. Therefore, the definitive target of this research is to introduce a new approach for urban stormwater management which address the impacts of climate change successfully.

1.3 Research scope and objectives

By considering the drawbacks of current urban stormwater management guidelines under changing climate, the broad objective of this study is to develop an accurate, reliable and widely usable approach to evaluate the combined impacts of land use change and climate change on urban catchments. To achieve this main objective, following sub- objectives have been aligned with this study.

- Estimate the future daily rainfall depths by spatially downscaling of GCMs predictors using regression based Statistical Downscaling Model (SDSM).
- Evaluate the capability of Generalised Extreme Value (GEV) distribution in modeling extreme rainfalls in Australia.
- Evaluate the GEV parameter estimation methods to employ in daily rainfall disaggregation.
- Develop a scaling invariant based temporal downscaling model to estimate sub-daily IDF relationships.
- Assess the capability of proposed approach to use in major cities in Australia.
- Identifying the empirical relationships between extreme rainfall events and daily maximum temperature, their changing trends and seasonal variations.
- Apply the developed IDF relations to evaluate the combined impacts of land use changed and climate change on urban catchment in Perth area via a hydrological modelling.

1.4 Overview of the thesis

There are eight chapters are included in the thesis. These eight chapters are organized into five main parts (i.e. introduction/ literature review, downscaling methodology and case studies, empirical relationships of extreme rainfalls, hydrological modeling case study and conclusion/ future studies) as shown in Figure 1.1, first chapter provides overall thesis introduction including background, significance of the study, research scopes and thesis structure.

The second chapter highlights the literature review to discuss the previous studies which are relevant to the current research. The initial part of the literature review discusses the current stormwater management practice in WA. Next part provides the details on downscaling of GCMs outputs, uncertainties of downscaling techniques and limitations etc. The third part of the chapter discusses the empirical relationships of extreme rainfall events with the atmospheric temperature in the different part of the world. Also, it provides details on physically based hydrology models, their revolution, applications and advancements.

The third chapter is allocated to discuss the methodology of spatially downscaling of daily rainfall. Perth Airport region is considered as the study area. Initially, this chapter provides a brief introduction to the study area and data set. Then it discusses the theoretical background of SDSM. It also provides the details on SDSM calibration and validation to downscale the daily rainfall for future periods using HadCM3–A2 and CGCM3-A2 scenarios. Final part describes the model results and conclusion of the chapter.

The Fourth chapter presents an evaluation of GEV distribution capability in modeling extreme daily and sub-daily rainfall events at eight weather station in WA. Also, this chapter evaluates the scaling property of observed extreme rainfall events. Further, three GEV parameter estimation techniques are evaluated and checked their suitability to use in scaling models. At the end of the chapter, developed IDF relationships using scaling models have been presented.

The fifth chapter is a further extension of third and fourth chapters. It presents an approach to developing sub-daily IDF relationships for future periods. These IDF relationships are developed by temporal downscaling of spatially downscaled daily

rainfalls for Perth airport region. For the temporal downscaling, GEV based scaling invariant model is used and future downscaled daily rainfall are obtained using SDSM. The final section of the chapter investigates the applicability of proposed approach on other major cities in Australia.

To evaluate the impacts of atmospheric temperature on rainfall patterns, empirical relationships between observed extreme daily/ sub-daily rainfalls with daily maximum atmospheric temperature are investigated in the sixth chapter. A binning technique is used in this analysis to identify the dependency of extreme rainfalls on daily maximum temperature. The first part of the chapter presents the analysing of extreme rainfall/temperature relationship of seven major cities in Australia by taking total data period as a single time slice. Further, it investigates the applicability of Clausius-Clapeyron (C-C) concept on observed extreme rainfalls and maximum temperature. Next part of the chapter describes the variation trend of extreme rainfall- temperature relationship for the 10-year time slices. Impact of seasonality on extreme rainfall-temperature relationship has been discussed at the end of the chapter

The seventh chapter is dedicated to present an application of developed theoretical findings for hydrological analysis of an urban catchment. Stirling catchment in Perth is selected as the study area. This chapter starts with briefing theoretical background of MIKE SHE physical based hydrological model and its simulating options. Then it describes the model development, model calibration and validation. Next part of the chapter presents the hydrological modelling result/discussion under proposed development and climate change.

The eighth chapter gives a general summary and conclusion on the thesis. Also, it provides outcomes of the study including recommendations for the future studies.

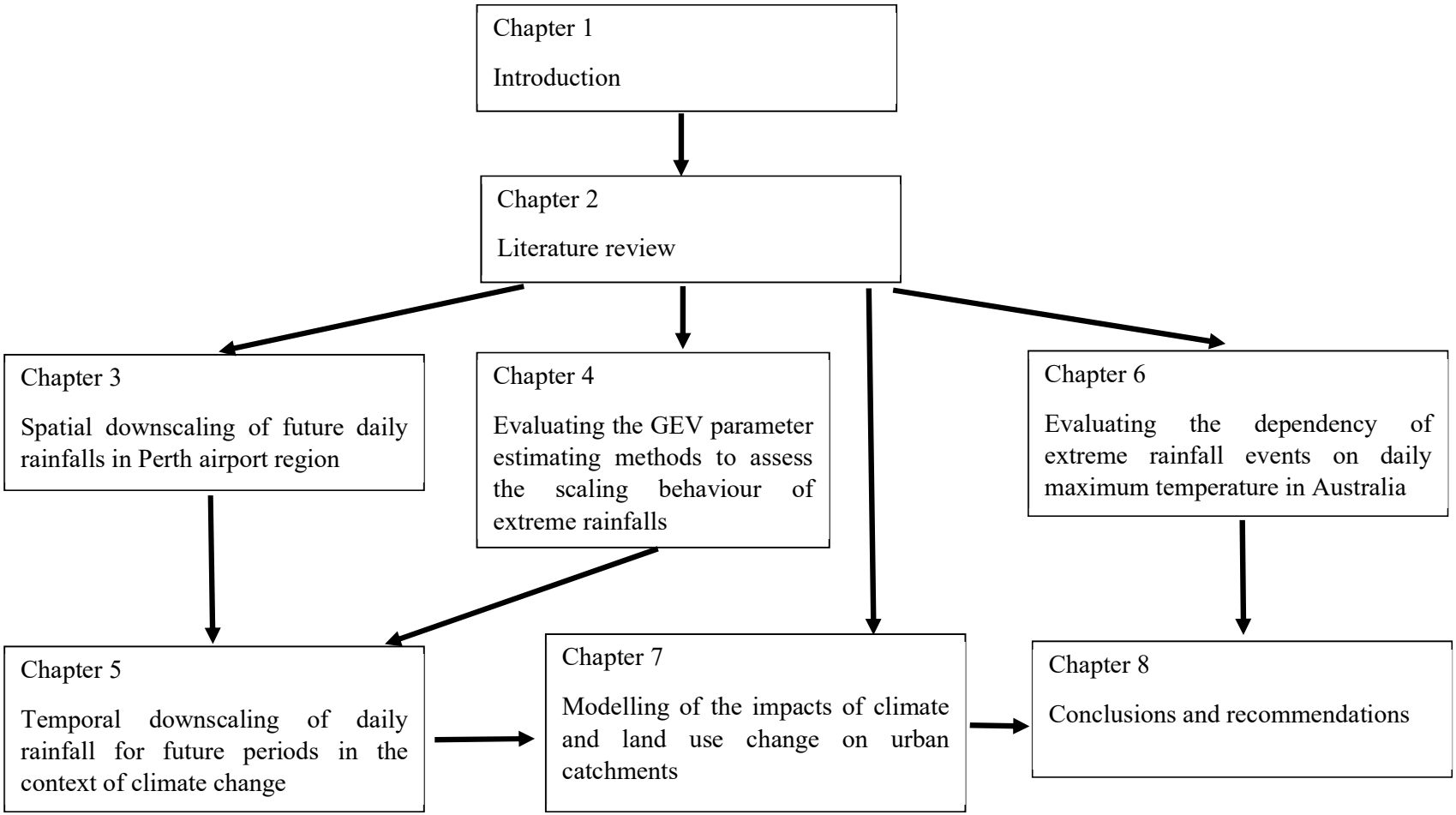

Figure 1.1: Interconnection of thesis chapters

CHAPTER 2

2 Literature review

2.1 Introduction

Stormwater management is a demanding topic, especially in urban catchments which are having more impervious areas. These impervious areas mainly consist with low infiltrative roofs, sealed roads and car parks etc. Also, these impervious areas lead high runoff volumes and shorter response time in urban catchments. Because of these reasons urban catchments are required proper stormwater management techniques to reduce the urban flooding incidents. These techniques are varied from area to area based on the available hydrological conditions. Therefore, the first two sections of the literature review is allocated to discuss the impacts of urbanization on urban hydrology and available stormwater management practices in Australia.

Furthermore, current stormwater management practices in most of the countries are not updated for a long time. Recent and future changes in determining the design storm depths in current practice does not response to the impacts of climate change on urban catchments. GCMs are considered as the best way to evaluate climate change impacts for future periods. However, GCMs projections do not satisfy the high- resolution data requirement in local scale hydrodynamic models. Therefore, these projections need to be subjected to a downscaling process to improve their resolution. The next two parts of this chapter is assigned to discuss the available downscaling approaches, their advantages and disadvantages, limitations, uncertainties and advancements etc.

Furthermore, understanding the empirical relationships of extreme rainfall event is essential in urban flood mitigating and climate change impacts assessment studies. Therefore, next section of literature review is dedicated to discuss about the empirical relationships of extreme rainfalls.

Because of the low imperviousness, urban stormwater management is highly based on the drainage network. Therefore, urban drainage networks should be properly designed. Hydrology modelling is the best way to estimate the hydrodynamic variables under different rain events. The last section of the literature review discusses the physically based hydrological modelling approaches. The beginning of the section

gives brief summary and benchmarks of the hydrology modelling revolution and the remaining sections are allocated to discuss the various models, their simulation techniques and assumptions.

2.2 Impacts of urbanization on hydrological characteristics of catchments

According to UnitedNations (2014), more than 54 % of the world population was living in cities in 2014. It was 30 % in 1950 and has been predicted as 66 % in 2050. Especially, urbanization creates more impervious areas with low infiltration. There are three main aspects of urban water systems i.e. water supply, wastewater and stormwater (Walsh et al., 2012). Urban stormwater management is correlated with urban flood protection, environmental protection, public health and sanitation. Therefore engineering, environmental science, public health and sociology disciplinarians are included in urban stormwater management (Fletcher et al., 2013)

In generally, the influence of land development and land use change is significantly high on urban hydrological cycle. It is well known that urbanization cause high runoff flows and volumes even in very small rainfall events (Fletcher et al., 2013) in urban catchments. In some regions, it has been identified as more than 100 % peak flow increment due to rapid urbanization (Rose and Peters, 2001). Because of this reason; hydraulic structures with high capacities need to be constructed to cater these high runoffs and volumes. It causes the increase of construction cost as well as reducing the usable land space. Even though most of urban drainage systems are concreted or piped, suburban and rural area is consisted with earth drains. Therefore, high runoff flows affect to earth drains severely. Bank erosion and stream widening are major problems with earth drain network with high runoff. The erosion of earth drains, reduce the reservoir capacities by sediment and it increases the probable flooding risk of surrounding area in high rainfall events. Also reducing of reservoir capacity affects the water supply throughout the year. In some countries stored water in reservoirs are used for agricultural ways and reduction of reservoir capacities cause scarcity of agricultural water demand in the dry period. Reduced lag time of catchment response is another impact of urbanization. With the reduced lag time, flash discharge can be observed and this is the main reason for urban flooding (Guo et al., 2008).

In addition to above basic facts, urbanization has an influence on rainfall timing and magnitude of the rainfall in urban areas (O'Driscoll et al., 2010). Urban heat island is one of the major problems of urbanization. In generally, the central temperature in urban areas takes higher value than surrounding sub- urban and rural area temperature. This phenomenon is known as urban heat island phenomenon (Peng et al., 2012). These urban heat islands affect to the normal convection of air masses in the area. Furthermore, surfaces of urban areas are mostly consisted with roof, asphalt, concrete etc. There is an influence on normal air circulation by these surfaces (O'Driscoll et al., 2010). These issues cause urban- induced rainfalls in urban areas. Also due to land cover change into more impervious; evapotranspiration is reduced considerably. It also affects to the natural water cycle and unpredictable rain patterns in urban catchments.

Urbanization impacts on groundwater are mainly two ways. i.e. reduce groundwater recharge and quality (Foster et al., 1996) . Most of the streams start as a water flow from saturated groundwater area. As a result of reduced groundwater recharge, the water table drops considerably, and it affects to stream base flow (Shaw, 1994). Furthermore, with the urbanization, water withdrawal is increased from surface and groundwater bodies. It also affects the reducing of base water flow and then reduced base flow affects to the ecosystems especially in the drought periods.

With these negative impacts of urbanization on natural hydrological cycle, urban stormwater management is an essential requirement in current land and urban development projects. Incapability of proper urban water management leads social, economic and environmental issues. Therefore, to achieve proper urban stormwater management benefits, different strategies and techniques have been established by responsible authorities to cover all the phases of new land development projects.

2.3 Stormwater management practices in Australia

Water Sensitive Urban Design (WSUD) is a very popular term used in Australia to describe the new Australian approach of urban planning and designing (Whelans, 1994). The broadest definitions of WSUD is

"the integrated design of the urban water cycle, incorporating water supply, wastewater, stormwater and groundwater management, urban design and environmental protection " (JSCWSC, 2009)

For the implementation of WSUD guidelines and achieve its' objectives through Best Management Practises (BMP), Western Australian Planning Commission (WAPC) has introduced stormwater management guidelines to follow throughout the land development processes as described in Figure 2.1. According to Figure 2.1, in Western Australia, assessing the impacts of land development on stormwater is basically conducted under five stages.

- Regional water management plan
- District structural plan
- Local water plan
- Subdivisional proposal
- Development

Various aspects of stormwater management are investigated in different extent at these five stages (WAPC, 2008). Figure 2.1 shows the details and flow of these stages.

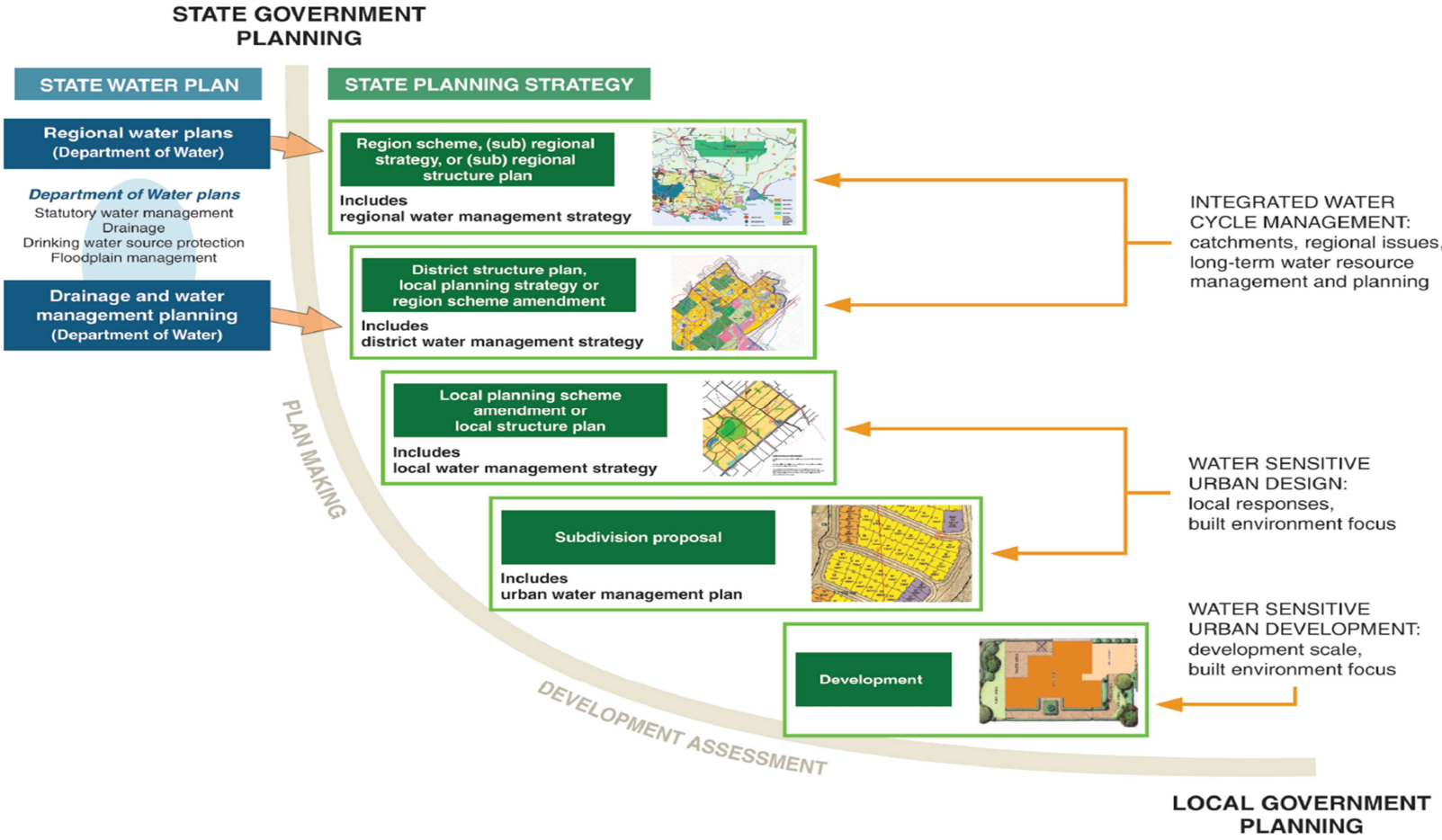

Figure 2.1: Stormwater management planning with land development process (WAPC, 2008)

2.3.1 Regional and sub-regional planning

Department of water and the Western Australian government are responsible for the preparation of regional and sub- regional plans. The main purpose of regional/sub-regional planning is the water resource management in regional scale. Regional and sub- regional water plans are supported by Regional Water Management Strategy (RWMS).

Following three main aspects are included in RWMS

- Surface and groundwater mapping, monitoring and modelling
  Identifying and mapping of surface and groundwater resources including ecosystems, boundaries, conservative areas, pre- development condition and other significances at the regional scale are included.
- Desktop historical land use assessment
  Identifying the existing and past potential of having contaminated and acid sulphate groundwater and soil.
- Water balance modelling
  Sub- catchment water balancing under pre- development condition is included here.

2.3.2 District structural planning

Next level of the water management is “the district structural plan”. Under this stage, regional scale plans and strategies are scaled down to a specific district. This plan is generally prepared by Department of Water with state government and it is supported by District Water Management Strategy (DWMS). Following main aspects are included in DWMS.

- Water balance modelling.
  Pre- development and post development water balancing in district scale, identifying required infrastructure developments etc.
- Hydrological regime of water dependent ecosystem and ecological health.
  Monitoring and determining ecological health and hydrological regimes are included here.
- Desktop historical land use assessment.

Identifying further contaminated or acid sulphate groundwater and soil in district scale.

- Groundwater modelling and monitoring.
  Assessing of groundwater quality and quantity, required controlling of groundwater levels, avoiding of groundwater dependent environmental are included.
- Surface water modelling and monitoring.
  Identifying and mapping of existing or constructed drainage network, floodplains are studied. Also, arterial drainage network identification including 100 year flow characteristics and development impact assessment on surface water are studied.

2.3.3 Local water planning

The third stage of the water management sequencing is the local water management planning. Local planning is supported by Local Water Management Strategy (LWMS). In general, following aspects are studied in LWMS.

- Water balance modelling.
  Identifying pre and post water balancing in local scale.
- Water dependent ecosystems and ecological modelling.
  Providing more detailed assessment for the DWMS findings, wetland and waterways buffer protecting, hydrological regime and ecological health assessment in local scale.
- Desktop historical land use assessment.
  Addressing the issues of the surface and shallow water which are found in DWMS stage.
- Groundwater monitoring and modelling.
  Assessing of groundwater quality and quantity, required controlling of groundwater levels, avoiding of groundwater dependent environmental in local scale.
- Surface water modelling and monitoring.
  Minimum building level, flood-bank for development, receiving of water levels are included in this stage. Further, existing surface water stream flow

monitoring, ways of catchment target flow achievement, details floodways modelling for 1 in 1 year,1 in 5 or 10 year and 1 in 100 year events are included.

- Monitoring of flows in existing streams or drainage systems.
  Identifying the quality and quantity of existing surface water to establish the pre- development status.

2.3.4 Subdivisional proposal

After the approval of LWMS; next stage is subdivision proposal. Under subdivision proposal stage structural and landscape architectural considerations need to be finalised for urban scale. Urban Water Management Plan (UWMP) is one of the key supporting document in subdivision proposal stage which addresses the urban stormwater issues. In generally UWMP includes following aspects.

- Management of water dependent ecosystems.
  Assessment of buffers for wetland and waterways to be protected, ecological health and hydrological regime monitoring, detail surveys on flora and fauna are included.
- Site investigations.
  More detailed investigations on soil properties (infiltration etc.) and contamination or acid sulphate soil.
- Groundwater monitoring and modelling.
  Assessments on groundwater recharge rates, sub- soil drainage strategies, existing and proposed groundwater level mapping.
- Surface water modelling.
  Assessments on water retention/ detention requirement for 1 in 1 year event, post development runoff control approaches, flood paths refinement for 1 in 100 year event, volumes and flood path sizing for minor and major events etc.
- Conservation and efficient use of drinking water
  Detailed modelling of water balance, water reuse strategy development for public open spaces, development and implementation of strategies for water conservations are included.

2.3.5 Development

The last stage of the process is related to the construction of buildings. Under this stage, development needs to be compliance with the UWMP proposal.

Even though this approach addresses the impacts of land use change on catchment hydrology, it does not take climate change impact into account. In other words, current approach guides developers to maintain the hydrological properties of development catchment unchanged at pre and post- development stages under changing land use. However, the expected life span of some of the urban drainage infrastructures is more than 50 years. Therefore, it is an essential requirement to evaluate combined impacts of land use change and climate change impact on the urban hydrology.

2.4 Downscaling of Global Climate Models' (GCMs') projections for urban catchments

Global Circulation Models (GCMs) are known as a primary and reliable future climate predicting tool (Maraun et al., 2010) which is based on atmospheric physics. However, GCMs are still not in a position to generate fine scale (in both space and time) climate predictions to fulfill the high-resolution data requirement to use in catchment scale studies (Arnbjerg-Nielsen et al., 2013). To fill the gap between coarse resolution output of GCMs and high- resolution data requirement of hydrological assessments, downscaling techniques are employed as a bridge. According to Mearns et al. (2003), Wilby et al. (2004) downscaling techniques are classified mainly into two categories known as dynamic and statistical. Again, statistical downscaling is sub-divided into three categories as regression-based, weather pattern based and weather generator-based approaches. Figure 2.2, illustrates the dynamic and statistical downscaling concepts graphically.

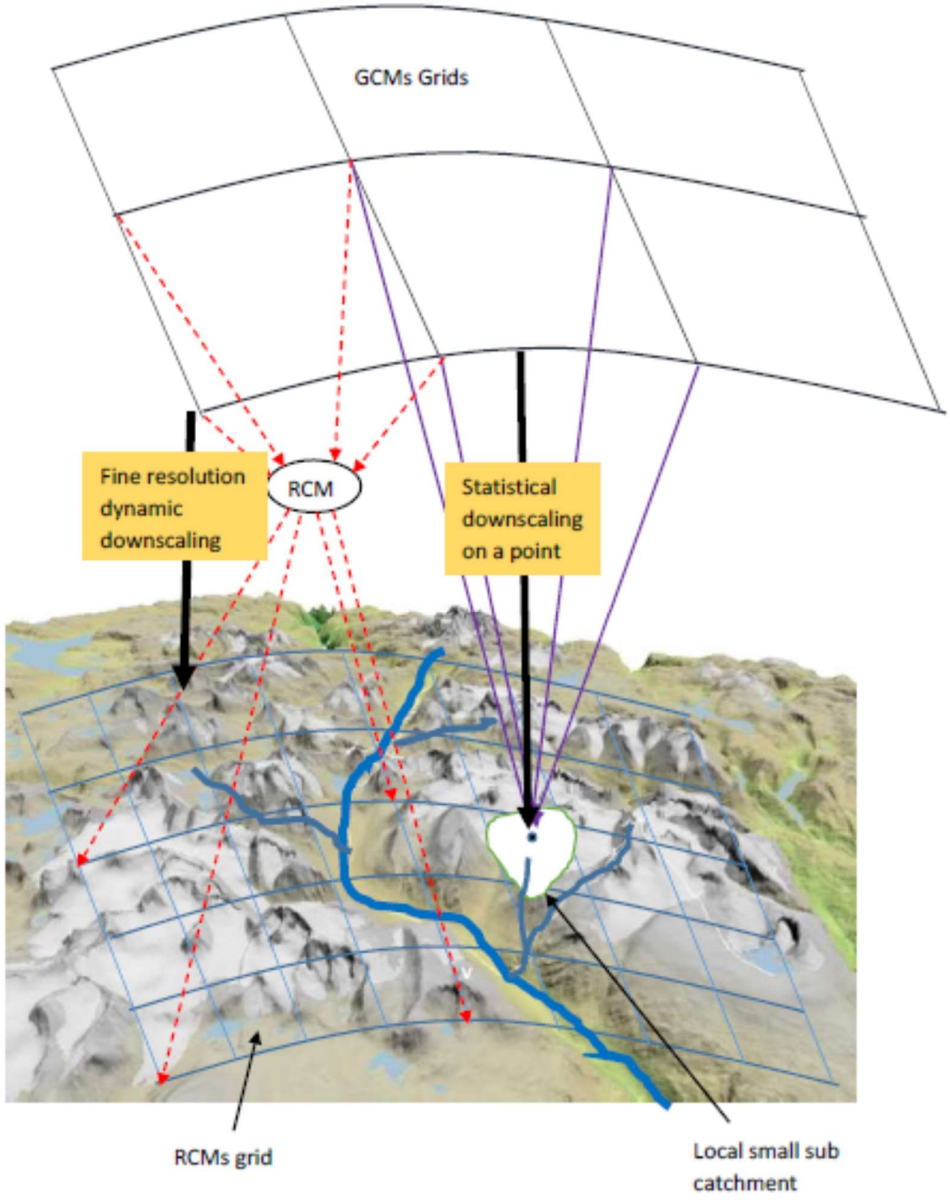

Figure 2.2: Graphical illustration of dynamic and statistical downscaling concepts

2.4.1 Dynamic downscaling

Dynamic downscaling consists with the technique of formation physical principles to capture fine spatial non-linear effects, to downscale low-resolution GCMs outputs (Xu and Yang, 2012). In this approach; GCM nested model known as Regional Climate Models (RCM) which based on atmospheric physics are used. Also, it is known as

Limited Area Models (LAMs). The concept of nested regional climate model is originally developed by Dickinson (1989) and Giorgi (1990). The RCM developed by Dickinson (1989) and Giorgi (1990) was capable of simulating climate variables for 50 km -60 km resolution grid for Western United State for three year period. Normally, in the process of downscaling, simulation boundary conditions are derived from GCM outputs. Denis et al. (2002) developed a new approach to alternate the GCM data. This new approach is known as Big- Brother Experiment and it generates high- resolution boundary. Then these high- resolution boundary data are downscaled by low- pass filtering and these filtered data are used in LAM/RCM.

With the high capability of simulating fine resolution (about 5 km grid space) climate variables, RCMs are employed in various applications in all over the world. Especially RCMs are widely used in climate prediction, paleoclimate (Hostetler et al., 2000) and anthropogenic climate change studies etc. Furthermore, RCMs are capable in seasonal and short- term weather forecasting (Rummukainen, 2010) under changing land cover conditions (Zhang et al., 2008).

Although RCMs are capable in simulating fine resolution climate data, there are some drawbacks associated with the process. With compared to the statistical downscaling approaches, dynamic downscaling/RCMs are computational costly. Also, more computational stages are included in RCMs' simulation process. Because of large number of simulation stages in the overall process, it leads to more uncertainty rather than statistical downscaling.

In addition to these basic drawbacks of RCMs/LAMs approach, some conceptual limitations are also available (Denis et al., 2002). Especially, the time taken by RCM to become climate equilibrium with GCM is known as spin- up time. In surface hydrology related simulation, spin- up time takes relatively long period due to deep soil temperature and soil moisture impacts. Sometimes spin-up time may be few months or few years. In these instances, simulation within the spin-up time need to be disregarded. Also, the accuracy of RCMs/LAMs simulations is depended on the initial boundary conditions driven by GCMs. Further, vertical and horizontal interpolation of climate projections is required in dynamic downscaling in relevant to the relations between GCMs and RCMs. It can be identified as another limitation of dynamic downscaling approaches and these interpolation errors lead to inconsistency and

imbalance of RCMs. Also, physical parameterization of RCM for the past period to continue in changing future climate is another source of uncertainty (Sachindra et al., 2014a).

2.4.2 Statistical downscaling

Statistical downscaling approaches are mainly based on the developed statistical relationships between the large scale GCM outputs and catchment scale climate variables. In generally, statistical downscaling approaches are very popular in research communities than dynamic downscaling approaches. By comparing statistical downscaling with dynamic downscaling, there are few advantages can be identified. According to Wilby and Wigley (1997), statistical downscaling approaches are simple in implementation and interpretation. Also, the required computational capacity is minimum (it means low cost) compare to the dynamic downscaling. Further, it provides a rapid assessment (does not required spin– up time etc). Also, statistical downscaling is capable to predict exotic predictors like air quality, wave height which does not predict by GCM directly. Further, the most important advantage of statistical downscaling approaches is it's capability of downscaling climate variables at a specific point. However, there are few disadvantages/ drawbacks are associated with the statistical downscaling process. Same as dynamic downscaling, GCMs boundary forcing issues affect to statistical downscaling. Therefore, uncertainties in GCMs are transferable to the subjected point through the statistical downscaling. Also, high quality observed climate data for a long period is required to the development of the relationship between large- scale GCMs climate variables and local catchment scale climate variables. Moreover, it is assumed in statistical downscaling that the developed relationships between GCMs output and past observed climate data remain unchanged for the future. Therefore, it is required to contribute past data for an adequately long period in the relationship development process. It facilitates to minimize this problem in some extent as climate change is not a sudden process (Herath et al., 2016). Also, predictor selection produces some uncertainty into the relationship. Selecting of unrelated or less potential predictors direct inaccurate predictor– predictand relationship and it end up with inaccurate downscaled results. Furthermore, statistical downscaling techniques are more capable to simulate mean value of predictand

variable rather than extreme values. However, this issue could be fixed by using a bias correction function (Nguyen et al., 2008, Herath et al., 2016). Also, the statistical downscaling process is an offline process and it does not give feedback to GCM.

2.4.2.1 Regression-based approaches

Out of four downscaling methods, regression-based statistical downscaling methods are the most popular approaches in GCMs predictor downscaling (Hessami et al., 2008) . Linear regression, Non-linear regression, Multiple regression, Artificial neural network, Canonical correction and Principal component analysis (Wilby et al., 2002) and Ridge regression (Hessami et al., 2008) are commonly used in this approach to determine the predictor- predictand relationships. Easy implementation and low computation capacity requirement are the main advantages of this method. However, high dependency on selected predictors, assuming same predictor- prediction relationship for future periods, less capability in extreme event downscaling can be identified as the main drawbacks of this approaches (Tripathi et al., 2006).

Multiple regression based Statistical Downscaling Model (SDSM), developed by Wilby et al. (2002) can be identified as the most popular tool in statistical downscaling studies. Optimization algorithms based multiple regression is used in SDSM calibration (determination of predictor-predictand relationship). SDSM is widely used in the research studies to downscale daily point precipitation, maximum and minimum temperature etc. Further, neural network approaches also are very popular in statistical downscaling. Applicability of temporal neural networks in precipitation and temperature downscaling is evaluated by Coulibaly et al. (2005) and they used the temporal neural network model to downscale daily total precipitation, daily maximum and minimum temperature at Serpent River catchment in Canada. Moreover, Automated Statistical Downscaling (ASD) tool can be identified as another popular downscaling tool which is developed by Hessami et al. (2008) based on ridge regression. Both neural network and ASD models are compared with SDSM and results indicate that overall accuracy of SDSM model is higher than others. Canonical correlation analysis is another approach of regression downscaling. Busuioc et al. (2008) successfully used canonical correlation-based statistical downscaling model to study the extreme winter precipitation in northern Italy.

Because of the wide applicability and high accuracy of regression based downscaling approaches, many recent studies used them as the downscaling tools. Sachindra et al. (2013) used Least Square Support Vector Machine (LS-SVM) and Multi Linear Regression (MLR) based approach to downscale the monthly rainfall over river catchment in Victoria, Australia. Joshi et al. (2014) used Sparse Bayesian Learning and MLR approached to downscale the hydrological indices and local climate variable in Eastern Canada to characterise the low flow regimes of three rivers. Also (Herath et al., 2016) used multiple regression based SDSM to downscale daily rainfall using HadCM3-A2 and CGCM3-A2 scenarios to develop IDF relations to represent the climate change impact on Perth, Western Australia region.

2.4.2.2 Weather pattern/type-based approaches

In weather pattern/type base approaches, large- scale atmospheric circulation patterns are classified into weather states, based on their synoptic characteristics and then link with the locally observed predictand of interest (i.e. precipitation). In the downscaling process, these developed relationships are used to simulate the predictand in local scale using large scale GCMs weather patterns for future periods. The main advantage of the weather type base downscaling approaches is its capability of capturing nonlinear predictor– prediction relationships. However, in this approach, it is assumed that the developed relationships for past observed climate data remain unchanged in the future periods too (similar as regression base approaches). In some occasions under the context of climate change, this assumption may make slightly biased simulation especially with the short period observed data. Furthermore, this approach is not suitable to simulate very rare weather types as it does not make appropriate relations between past local observed predictand and classified weather type.

Weather pattern classification is a arguable topic in the literature. In literature, there are many classifications available and in this section only discuss few of them. Vrac et al. (2007b) atmospheric patterns are classified in two ways as subjective and objective. One year later, a comprehensive weather pattern review is carried out by Huth et al. (2008) and they introduced one more classification pattern as hybrid (mix of subjective and objective patterns) to Vrac's classification. According to Huth et al. (2008) subjective classification approach (also known as manual classification) is

required expert knowledge of circulation process. However, in early years, Hess and Brezowski (1969) developed air pressure distribution based weather types over Western Europe and North Atlantic Sector and Lamb weather types over the British Isles are very popular weather type approaches in the literature (Lamb, 1972, Jones et al., 2013). High time consumption for manual classification, requirement of expert knowledge on atmospheric circulation and limitation of applicability on the other area rather than analysed window, are the main disadvantages of this approach.

With the advancement of computer technologies, objective approaches have become more convenient approach in weather typing. Objective classification (also known as automated and computer-assisted) approaches are mainly based on the complex numerical methodologies. These numerical methodologies can be categorised as Correlation type (Beck et al., 2007, Brinkmann, 2000) , Cluster analyse (Brinkmann, 1999, Esteban et al., 2005), Principle Component Analysis (PCA)(Huth, 2000, Müller et al., 2003), Multi step analysis (Schoof and Pryor, 2003), Neural network(Elizabeth et al., 2006), Other non-linear (Cannon et al., 2002), Mixed model (Vrac et al., 2007a) and Fuzzy model (Andras et al., 2002) etc. Less time consuming and unnecessity of expert knowledge are the important benefits of this approaches.

In some approaches, both subjective and objective are mixed; types classifications are subjective and cases are objective. These classifications are known as mixed or hybrid approaches. Weather classification over Louisiana, USA developed by Lewis and Keim (2015) is a very popular hybrid approach in the literature. In their study, objective Muller weather types (Muller, 1977) are used to classify daily sea level pressure and these classification used in automated correlation based subjective approach to developed hybrid weather types.

2.4.2.3 Weather generator based approaches

Simulating future weather data by adjusting weather generator parameters (which are developed based on observations) according to GCMs predictions is the concept of weather generator-based downscaling approaches. Generally, weather generators are capable of simulating ensemble daily weather data in time series with many statistical characteristics (Chen et al., 2010). Because of this capability of weather generators,

these approaches are very popular in flood risk analysis, water resource engineering and crop productivity analysis (Mavromatis and Hansen, 2001, Fowler et al., 2000, Wheater et al., 2005). Furthermore, weather generators are comparatively computationally cheap and capable of generating weather data for ungagged incomplete weather stations (Mavromatis and Hansen, 2001). However, some drawbacks are associated with most of the weather generators in rainfall downscaling. Such as poor simulating of rainfall data for inter-annual to decadal periods, inaccurate evaluations of temperature impact on rainfalls, incapability to evaluate the spatial correlation structure between multi-sites in the same area, underestimating of low-frequency events etc. (Baigorria and Jones, 2010, Chen et al., 2010).

WGEN model developed by Richardson and Wright (1984) is considered as the most popular daily weather generating model. The development of WGEN is a further extension of the model developed by Richardson (1981) to simulate daily precipitation, maximum and minimum temperature and solar radiation. LARS-WG is also widely used in weather generating approach in Europe. As a result of the Markovian approach used in WGEN generator, it is having some issues of simulating of rare events. To overcome this problem, series of serial approach (Racsko et al., 1991b) with mixed exponential distribution (Semenov and Barrow, 1997b) is used by Wilks (1999) in LARS-WG. He enhanced the capability of Richardson (Richardson, 1981) model to the concurrent simulation of precipitation, maximum and minimum temperature, and solar radiation for multi-stations further.

In the recent literature, further advancements and applications of weather generator-based downscaling approaches have been recorded. Some of them are; simulation for semi-arid climate, GCMs uncertainty propagating to impact studies, weather forecasting for sub-polar condition etc. (Forsythe et al., 2014, Hauser and Demirov, 2013, Glenis et al., 2015).

2.4.3 Temporal downscaling/ disaggregation of daily rainfalls

Most of the dynamic and statistical downscaling approaches discussed in previous sections are capable only for downscale GCMs climate data spatially. The temporal resolution of these spatially downscaled climate data still remains as one day or more

than that. Therefore, it does not satisfy the temporal resolution requirement (sub-daily) of rainfall data for the sensitive hydrological assessment in urban areas. Because of this reason, spatially downscaled rainfall data need to be subjected to a further temporal downscaling process.

Rainfall disaggregation is an interesting research topic since the early 1970s. Darío Valencia and Schakke (1972), (1973) developed rainfall desegregation model based on the seasonal variation and autoregressive simple linear regression. However, this model is not capable of disaggregating rainfall shorter than 30 days as it does not capture the intermitted and skew distribution of rainfalls (Koutsoyiannis and Xanthopoulos, 1990). A few years later, Woolhiser and Osborn (1985) developed a scheme, based on the non-dimensional Markov process to disaggregate storm depth into fractions. Also, Koutsoyiannis and Xanthopoulos (1990) developed two phases approach to desegregate monthly rainfall into hourly rate. In this approach, the first phase was consisted with external disaggregation to generate monthly rainfall depth and the second phase was consisted with internal desegregation into hourly rainfall depth. This approach was based on the Markovian and proportional bisection scheme.

Further, "Turbulence theory" (Meneveau and Sreenivasan, 1987) has been widely used in rainfall disaggregation models (Gupta and Waymire, 1993). Pui et al. (2012) studied two models known as Canonical Cascade Model and Micro Canonical Cascade Model based on Turbulence theory and scaling invariance over Australia. In this study, they found the capability of this approach in rainfall disaggregation for Perth area. Rodriguez-Iturbe et al. (1987) developed another cluster based rainfall disaggregation model known as Bartlett–Lewis model. In this model, rainfall event is considered as clusters. This concept is further extended and applied in various rainfall events byVandenberghe et al. (2011), (Smithers et al., 2002). Although these studies disaggregate rainfall into daily and hourly events, they couldn't make it in sub-hourly resolution. Other different approaches of disaggregating of rainfall are developed by Coulibaly et al. (2005) and Kumar et al. (2012) using neural networking. These approaches are also capable in disaggregating rainfall general properties up to the hourly resolution.

However, sub-daily intensities are considered as an essential design parameter in the determination of design storm events for hydrological studies in urban areas.

Furthermore, IDF relations are used in design storm estimation. Annual Maximum (AM) approach is used in many parts of the world to construct IDF relations. In the AM approach, the statistical characteristics of AM rainfall series are employed. Moreover, there are enough evidence in literature to prove the scaling behaviour of AM (annual extreme) rainfall series and it's suitability in rainfall disaggregation (Burlando and Rosso, 1996, Menabde et al., 1999, Nguyen et al., 2008, Chang, 2013). In 1990, application of extreme rainfalls' scaling concept in a statistical way is introduced by Gupta and Waymire (Gupta and Waymire, 1990). Later on this concept is improved and employed in other applications which are related to extreme rainfall events (Koutsoyiannis and Foufoula-Georgiou, 1993, Burlando and Rosso, 1996, Nguyen et al., 2002). Temporal downscaling of observed daily rainfalls into sub-daily rainfall events can be identified as the major application of scaling behaviour of extreme rainfall events. Particularly, short duration storm events data are not available in most of the rain gauge stations for a long period. To overcome this problem in constructing IDF relations, temporal downscaling is employed with a known regional scaling factor to estimate the IDF relations (Nguyen et al., 2008). There are two main temporal downscaling approaches are available in the literature which are developed by Menabde (Menabde et al., 1999) and Nguyen (Nguyen et al., 2008) using scaling phenomena of extreme rainfalls and GEV distribution. In Menabde's model, scaling of ensemble averages of AM rainfall series has been used to estimate the statistical properties of sub-daily rainfall events. In Nguyen's model, scaling of Non Central Moments (NCMs) of AM rainfall series has been used to estimate statistical properties of sub-daily rainfall events.

2.4.4 Estimation of GEV parameters using Non Central Moment (NCM)

There are many evidences in literature to prove the capability of GEV distribution in modelling annual maximum rainfall (Nguyen and Nguyen, 2008). Cumulative distribution function $F(x)$ for the GEV distribution and it is given as

$$F(x) = exp[-\{1 - \{\kappa(x - \xi)/\alpha\}\}^{\frac{1}{\kappa}}] \quad (2.1)$$

For $\kappa \neq 0$,

Further, the quantiles of GEV distribution, X_T is defined as,

$$X_T = \xi + \frac{\alpha}{\kappa}\{1 - [-ln(p)]^{\kappa}\} \quad (2.2)$$

Where, $p = 1/T$ is the exceedance probability of interest.

Where ξ, α and κ are known as the GEV parameters for location, scale and shape, respectively. These three parameters are estimated by L moment method, NCM method and maximum likelihood method.

According to Pandey (1995), k^{th} order NCM, (μ_k) of GEV distribution (for $\kappa \neq 0$) has been shown;

$$\mu_k = E\{X^k\} = \left(\xi + \frac{\alpha}{\kappa}\right)^k + (-1)^k \left(\frac{\alpha}{\kappa}\right)^k (1 + \kappa k) + k\sum_{i=1}^{k-1}(-1)^i \left(\frac{\alpha}{\kappa}\right)^i \left(\xi + \frac{\alpha}{\kappa}\right)^{k-1} \Gamma(1 + i\kappa) \quad (2.3)$$

Where Γ (.) is the gamma function. ξ, α and κ are known as the GEV parameters for location, scale and shape, respectively

Assuming the function $F(x)$ is proportional to a scaling function $F(\lambda x)$ for all positive value of scale factor(λ) , following relations has been derived (Feder, 1988)

$$F(x) = F'(\lambda)F(\lambda x) \quad (2.4)$$

Where, $F'(x) = \lambda^{-\beta}$ (β is a constant and $x^{\beta} = \frac{F(x)}{F(1)}$)

Based on above concept, relationships of k^{th} order NCM,μ_k of variable x have been derived (Gupta and Waymire, 1990) as,

$$\mu_k E\{f^k(x)\} = \alpha(k)x^{\beta k} \quad (2.5)$$

Where, $E\{f^k(1)\} = \alpha(k)$, by applying these scaling properties, the statistical properties (parameters) of the GEV distributions for two different time scales of "t "and "λt "have been defined as,

$$\kappa(\lambda t) = \kappa(t) \quad (2.6)$$

$$\alpha(\lambda t) = \lambda^{\beta}\alpha(t) \quad (2.7)$$

$$\xi(\lambda t) = \lambda^{\beta}\xi(t) \quad (2.8)$$

$$X_T(\lambda t) = \lambda^{\beta}X_T(t) \quad (2.9)$$

$$\lambda^{\beta} = \mu 1_{\lambda t}/\mu 1_t \quad (2.10)$$

Where $\mu 1_{\lambda t}$ and $\mu 1_t$ are the first NCMs of observed annual maximum rainfall for λt and t periods respectively (Nguyen et al., 1998).

Based on these relationships, statistical properties of sub-daily extreme rainfall are derived using statistical properties of daily extreme rainfalls. Further, using Equation 2.2, quantiles can be estimated for different return periods by varying the "*P*" value. Finally, estimated daily and sub daily quantiles for different return periods can be utilized to develop IDF curves for the region of study.

2.5 Uncertainty of GCMs based downscaling approaches

GCMs based downscaling approaches are considered as the most reliable approach to project impacts of future climate change on hydrological studies. However, GCMs based approaches are having some issues basically generated in GCMs, downscaling process and observations. Therefore, hydrologists who are using direct GCMs predictions or downscaled GCMs predictions should be aware of these uncertainty factors. According to Hashmi et al. (2009), uncertainty sources associated with rainfall downscaling can be categorised as;

- GCMs predictions and Green House Gas (GHG) emission scenarios based uncertainty
- Downscaling process based uncertainty
- Rainfall observation based uncertainty

2.5.1 GCMs predictions and GHG emission scenarios based uncertainty

GCMs are known as the numerical models which are developed to simulate the physical process in land, ocean, atmosphere and cryosphere based on changing the concentration of global greenhouse gas. In these models, highly complex numerical simulations are used to understand the occurrence and magnitudes of the physical processes. The approaches which use to simulate these processes are varied from one GCM to another and it leads different predictions. GCMs structure, parameterization and resolution can be identified as the main uncertainty sources in GCMs predictors (Teng et al., 2012).

Emission scenarios are known as the projections of the possible atmospheric concentration of GHG, aerosol and other pollutants in future, based on different assumptions related to population growth and technology development. International Panel on Climate Change (IPCC) released first assessment report on climate change in 1990 and after two years they released a supplementary report together with six GHG emission scenarios (numbered from a to f) known as IS92. Next, in 1995, IPCC released second assessment report and in 2000 they released a Special Report on Emission Scenarios (SRES) up to the year 2100. Under SRES release, they introduced new four scenario families to replace IS92 (IPCC, 2000). 40 emission scenarios are included into these four scenario families. Also, these scenario families are having four illustrative marker scenarios/ storylines (A1, A2 and B1, B2). The main assumptions of these marker scenarios and scenario families are summarised in Table 2.1.

Table 2.1: Marker scenarios and major assumptions

Marker scenario	Assumptions
A1 scenario family	The world is more integrated, economic growth is very high, world populations will be at peak in mid-century (2050) and decrease thereafter (low population growth), new and efficient technologies are quickly spreading, social and religion interaction. (projected CO_2 concentration is 720 ppm by 2100)
A2 scenario family	The world is more divided, Interaction between religions are very slow, world population is increasing continuously, regional economic development, high energy use, new and efficient technologies are slowly spreading, available natural resources are limited and medium to high land use. (projected CO_2 concentration is 850 ppm by 2100)
B1 scenario family	The world is more integrated, ecological friendly, economic growth and population growth is similar to A1 (low), low material intensity, low energy use, high change in land use and low available natural resources, medium spreading of efficient technology. (projected CO_2 concentration is 550 ppm by 2100)
B2 Scenario family	The population grown is moderate and economic growth is intermediate. Spreading of new technologies is less than A1 and B1. Fossil fuel energy usage is low. (projected CO_2 concentration is 620 ppm by 2100)

In 2001 and 2007 IPCC third and fourth assessment reports are released respectively. Then in 2014 IPCC released the fifth assessment report and greenhouse gas concentration scenarios. These concentration scenarios are known as Representative

Concentration Pathways (RCPs) and are based on the past research studies about GHG emission. Therefore, RCP scenarios are not fully integrated scenarios or climate projections. RCPs consists 4 scenarios (i.e. RCP2.6, RCP4.5, RCP6 and RCP8.5) which named based on the radiative forcing values by the year 2100 (radiative forcing values are +2.6, +4.5, +6, +8.5 W/m^2 respectively). These RCP scenarios and their major assumptions are presented in Table 2.2

Table 2.2: RCP scenarios and major assumptions

RCP scenario	Major assumptions
RCP 2.6	RCP 2.6 scenario is based on the study conducted by Lucas et al. (2007). Main features of RCP 2.6 scenario can be summarised as; very low GHG emission, radiative forcing value at its peak 3.1 W/m^2 in 2050 and reduce up to 2.6 W/m^2 in 2100, mean global temperature will be increased by 2ºC at the end of 2100.
RCP 4.5	This scenario is based on the studies conducted by Clarke et al. (2007) and Wise et al. (2009). It assumes employing of various technologies and policies to reduce GHG emission, radiative forcing will be stabilized before 2100 at 4.5 W/m^2.
RCP 6	The main assumption is stabilization of radiative forcing at 6 W/m^2 after 2100 as a result of implementing less effective climate policies. It is based on the study conducted by Hijioka et al. (2008).
RCP 8.5	No climate policies or strategies are associated with this projection. It assumes high GHG emission with medium technology development, high world population and high energy requirement. This scenario is based on the study done by Riahi et al. (2007)

According to the above summary of GHG emission scenarios, it is well cleared that future projections are associated with considerable uncertainty.

2.5.2 Downscaling process based uncertainty

As discussed in section 2.4, downscaling approaches are associated with their own strengthens and weaknesses. Many evidence is available in the literature which related to the uncertainty of the downscaling process. In recent literature, Gutmann et al. (2012) compared statistical downscaling and dynamic downscaling of precipitation over Colorado area in the USA. By this study, they found that both approaches are capable of improving the resolution of precipitation and spatial pattern of the precipitation. However, they concluded that both approaches are associated with significance uncertainty. Specially, predictor selection and weather generating steps are highly uncertain in statistical downscaling. Chen et al. (2012a) used SDSM and Smooth Support Vector Machine (SSVM) to downscale precipitation using HadCM2-A2 and CGCM3-A2 scenarios over Hanjiang basin, China. They concluded their study as SDSM perform better than SSVM. Sachindra et al. (2013) studied about the monthly streamflow downscaling using MLR and Least Square Support Vector Machine Regression (LS-SMV-R) in North Western Victoria, Australia. LS-SMV-R performed slightly better than MLR model in their study. However, both models were not capable of capturing high stream flows. Frost et al. (2011) studied capability of six downscaling models (i.e. the dynamical downscaling conformal–cubic atmospheric model, simple scaling model, analogue method, and three stochastic models such as generalised linear model for daily climate time series, non-homogeneous hidden markov model and modified markov model-kernel probability density estimation) to downscale multisite daily rainfalls over 30 weather stations in South–Eastern Australia. This study concludes that the simple scaling approach provides the robust results using GCM predictors and, stochastic models are capable in extreme events modelling better than other approaches. These comparisons clearly show that accuracy of downscaling data is highly depended on the followed downscaling approach.

2.5.3 Rainfall observation based uncertainty

Issues in rainfall records are also having significance impacts on downscaling. It is required rainfall records for a long duration in statistical downscaling model calibration and validation. Because of various reasons, most of the countries are facing the scarcity of accurate, reliable long duration rainfall records. Unavailability of historical records, coarse resolution of records (unavailability of sub-daily and sub-hourly records), missing records, instrumental errors, human errors (negligence) (Saidi et al., 2014) can be identified as the main sources of the scarcity of accurate and reliable long-term records. To overcome this issues, rainfall data collecting and recording organizations use various techniques such as spatial interpolation techniques (Teegavarapu, 2009), regression based approaches (Lo Presti et al., 2008), Neural network algorithms(Nkuna and Odiyo, 2011) etc. All these methods generate some uncertainty into the rainfall records and it also transfers to the downscaling models.

2.5.4 Probable solutions to decrease the uncertainty in rainfall downscaling

However, some effective approaches are available in the literature to minimise the uncertainty associated in the downscaled rainfalls. Employing of ensemble-based approaches is a very popular technique to minimise the associated uncertainty in the predictors. Ensembles from the same model and multi models (Kharin and Zwiers, 2002) can be identified as the two main techniques in predictor ensemblling. Simulating of series of ensembles using a stochastic weather generator is another ensemble approach to minimize the uncertainty associated with the simulation. Here, each ensemble member is considered as equally plausible local climate projections (Wilby and Dawson, 2007).

Another method of minimizing the uncertainty is the bias correction. In generally, the difference between the GCM predictors/downscaled predictands and corresponding observed variables are simply known as the bias. There are two main different ways to correct the associated bias; i.e. correcting of bias of raw GCM outputs, correcting of the predictand bias after the downscaling (Sachindra et al., 2014b). There are many bias correction techniques are available to use on raw GCM outputs or downscaled predictand. Nested model (Johnson and Sharma, 2012), nonlinear regression (Nguyen

et al., 2008), quantile mapping (Wood et al.), monthly mean correction (Fowler and Kilsby, 2007), equidistance quantile mapping (Li et al., 2010) approaches are widely used for the bias correction in rainfall downscaling studies.

2.6 Impacts of temperature on extreme rainfalls

Evaluating the impacts of anthropogenic climate change is essential to understand the behaviour of unexpected short duration extreme rainfall process. Anthropogenic GHG emissions have been increased conciderabaly since the end of 20th century (IPCC, 2000) and by comparing the climate model it can be identified the probable relations exist between climate change and GHG emissions (Crowley, 2000). There is high impotence of maintaining the atmospheric GHG/carbon dioxide concentration to keep atmospheric temperature steadily. Because of the high capability of GHG/carbon dioxide to absorb the reflecting radiation from the earth received from the sun. As a result of high emission of GHG to the atmosphere with the industrial revolution, natural greenhouse emission has been intensified (Tripati et al., 2009). According to Intergovernmental Panel of Climate Change (IPCC 2000), imbalance greenhouse emission promotes the changes in rainfall patterns in the world. Increase the occurrence of extreme events, flooding events due to the high-intensified precipitation and more droughts have been projected for the future periods using GCMs (Easterling et al., 2000) for some parts of the world. Therefore, to mitigate the damage from these projected future disasters, it is important to identify the empirical relationships of extreme events with other climate variables.

In the context of changing climate, research studies which evaluate the relationship between atmospheric temperature and extreme rainfalls have become a very demanding topic in last decade. Although the general acceptance of increased temperature dominates the high-intensity precipitation events in many parts of the world, there is a high uncertainty remains in this conclusion (Alexander et al., 2006, Allan and Soden, 2008). This conclusion is mainly based on the future climate projections which is governed by Clausias–Clapeyron (C-C) relationship and average relative humidity variations in the world (Soden and Held, 2006).

According to C-C relationship, water holding capacity of the atmosphere is increased by exponential rate with temperature increasing. In recent history, there are a number of studies have been conducted to find out the scaling relationship between extreme precipitation and temperature in different parts of the world. Lenderink and Van Meijgaard (2008) introduced the binning technique to evaluate the C-C scale and it can be known as a pioneer study in this research field. They used a binning technique to determine C-C scale properties of hourly rainfalls at DeBilt, The Nederlands by categorising rainfalls into 2˚C temperature bins. According to their findings, higher percentiles (99.9^{th} and 99^{th}) of rainfalls show rainfall-temperature scale up to 15% /˚C with daily mean temperature. It is an increase of more than twice as expecting by C-C scale relationship at the daily mean temperature exceed 12ºC. Seasonality of the rainfall-temperature scale is studied by Berg et al. (2009) for weather stations located in European countries. Berg et al. (2009) observed rainfall-temperature scale for both observed daily rainfall and simulated rainfall by few RCMs. They identified stronger rainfall-temperature scale for the winter season than the summer as a result of available moisture in summer season play a dominant role rather than atmospheric moisture holding capacity.

Hardwick Jones et al. (2010) investigated the C-C scaling over 137 weather stations in Australia. They studied the rainfall-temperature scale for 99^{th} and 50^{th} percentile rainfall. This study showed both positive and negative scale for 99^{th} percentile rainfall. Especially, these negative scaling weather stations were located in Northern Territory, which is having totally different climate to the other states. Also, the negative scale is observed for 99^{th} percentile rainfall event for the higher temperature (between 20ºC-26ºC) events in all stations as a result of declined maximum relative humidity at the higher temperature above 26ºC.

By moving further, Utsumi et al. (2011) assessed the relationship between extreme daily rainfall and surface air temperature in a global scale. They studied the rainfall intensity/surface air temperature relationship with the latitudes. For higher latitudes, high temperature increases the rainfall intensity and it reduces the rainfall intensities at the tropics. Also at middle latitudes, extreme daily precipitation increase at low temperature and decrease at high temperature. Also, Shaw et al. (2011) studied the relationship between the extreme hourly precipitations and surface temperature in the different hydroclimate zones in the USA. Furthermore, there are many recent studies

available in the literature,(Chen et al., 2013, Panthou et al., 2014, Sun et al., 2015, Yu and Li, 2012) which studied the relationship between extreme precipitation and surface temperature in all over the world under various climate conditions.

Although these studies generally agree with the statement of "high-temperature courses extreme precipitation events" there are many inconsistent associated with it. Mainly following behaviour of extreme rainfall/temperature can be identified.

- The relationship between extreme precipitation and atmospheric temperature depends on the study area (latitude). In some areas, it follows C-C scale and most of the areas it varies from C-C scale.
- Impact on atmospheric temperature is higher on short duration precipitation rather than long duration precipitation.
- Extreme precipitation/atmospheric temperature relation is inconsistent under different temperature.
- Seasonal variation (in some areas even monthly variations) can be observed in extreme precipitation/atmospheric temperature.

2.7 Hydrological modelling approaches to evaluate climate change impacts

2.7.1 Benchmarks of evolution of hydrological modelling

Rainfall- runoff modelling can be identified as the best way to evaluate the impact of land use change and climate change on the catchment scale. Rainfall–runoff modelling has a more than 100 year history. In the mid of 19th century basic rainfall–runoff models were used in urban sewer design, land reclamation drainage designs and spillways designs (Todini, 1988). In the early stage, rational method and the empirical formula derived from previous studies are used in numerical modelling by assuming the similar conditions. With the modelling requirement became more complex, various modifications are added to the rational methods and other methods to determine the accurate and more realistic conditions. With the introduction of hydrograph theories based on the superposition concept by Sherman (1932), new assumptions were automatically included into the rainfall- runoff modelling without any knowledge at

that time. As an example, the superposition concept assumes that the catchment behaves like causative and rainfall-surface transformation based linear time invariant system etc. Also, few disadvantages were associated with assumed unit hydrograph approach (i.e. surface runoff and base flow are separated, determinations of effective rainfall, unit hydrograph derivations etc.)

Basic stage of conceptual modelling is started in the 1950s with the finding of the differential equation capability to represent the shape of the unit hydrograph. Then the unit hydrograph was represented by the derived parameter from the catchment or a statistical way (Nash, 1958). With this advancement, conceptual modelling was used in a different hydrological application like modelling of the linear channels, linear channels and reservoirs, nonlinear reservoirs etc. However, there were some issues with the catchment based parameter estimation as those parameters are highly subjective. To overcome the drawbacks in unit hydrograph based rainfall–runoff models, different other approaches were developed in the 1960s (Crawford and Linsley, 1966, Rocwood and Nelson, 1966).

Also, Danish Hydraulic Institute (DHI) from Denmark, SOGREAH from France and the Institute of Hydrology from UK worked together to developed new physical based integrated hydrological modelling system. In the mid of 1980s they were able to develop a new hydrological model "SHE" (Système Hydrologique Européenne) and it can be identified as the beginning of the present era of hydrological modelling. SHE model was initially based on the blueprint proposed by Freeze and Harlan (1969). In that period, other physical based hydrological models' functions were limited to estimate rainfall-runoff of small catchments (Wooding, 1965). However, SHE model was capable of applying a variety of hydrological applications and was a real advance model at that time. It used integration of partial derivation equation by considering the continuity of mass and momentum. Also, it could link the sub-processes model by matching the boundary conditions.

2.7.2 Advancements and application of physically based hydrology modelling

With the development of the computers performances, many physical based hydrological models have been developed to address various hydrological aspects with

high accuracy and more realistic manner. Mainly physically based hydrology modelling approaches are used empirical relationships or non-linear partial differential equations representing the mass, momentum and energy balance (Abbott et al., 1986b). Also, these models take the primary aspects (surface runoff, channel routing, groundwater and sub-surface water movements, evapotranspiration, snowmelts etc.) of the land phase of the hydrologic cycle into the consideration. Physics based parameter estimations (these estimations are based on the scientific laws), the spatial variation of input data, the requirement of minimum calibration can be identified as the main advantages of these model. On the other hand, physically based hydrology models are time demanding and costly. Also, data requirement is relatively high (i.e. catchment data, meteorological data etc.) (Gosain et al., 2009, Chau et al., 2005).

Further, new technologies (i.e. GIS, remote sensing, LiDAR data etc.) play a vital role in the fulfilment of the data requirement of the hydrological models. Most of the commercial model (i.e MIKE SHE) are compatible with these external data sources. It facilitates user to developed, high accurate, realistic and more advanced hydrological models to simulate real runoff routing process. Also, it reduces the model development time in a considerable manner.

There are a number of physically based hydrology models are available in the literature. These models differ each other, especially from the simulation process. Also, data requirement, simulation time, computational demand and accuracy of the results are highly variable. Table 2.3 summarises the key information on some popular models among the hydrologists.

Table 2.3: Summary of popular physically-based hydrological models

Model Name	Principal reference	Major remarks on modelling approach
SHE By Danish Hydraulic Institute (DHI) from Denmark, SOGREAH from France and the Institute of Hydrology, UK.	(Abbott et al., 1986a, Abbott et al., 1986b)	Based on conservation of mass, momentum and energy or empirical relationship are given by experimental studies
MIKE SHE By Danish Hydraulic Institute (DHI).	(Refsgaard and Storm, 1995)	Developed version of SHE model. More details are included in Chapter 7
IHDM By Institute of Hydrology, Wallingford, UK.	(Beven et al., 1987)	The catchment is assumed as series of channels and hillslopes. These components are modelled individually and combined at the end.
SWAT By USDA Agricultural Research Service (USDA-ARS) and Texas A&M AgriLife Research, part of The Texas A&M University System.	(Arnold et al., 1998)	Based on the water balance at snow, soil profile, shallow and deep aquifer storages. In the modelling process, total catchments are divided into sub-catchments. These sub-catchments are subjected to further division into unique land use and soil components. These smallest components are known as the hydrologic response unit.

THALES By Department of Civil and Agricultural Engineering, The University of Melbourne, Australia.	(Grayson et al., 1992)	In the modelling, catchment is divided into an irregular grid based on streamlines and equipotential lines.
HRCDHM By Hydraulic Research Centre, San Diego(Carpenter and Georgakakos, 2004), USA.	(Carpenter and Georgakakos, 2004)	Terrain features and drainage network based sub-catchment approach are used in surface water modelling.
WATBAL By Danish Hydraulic Institute.	(Knudsen et al., 1986)	Main attention on the root zone through fully physically distributed approach. For the groundwater modelling, lumped conceptual approach is used.
PAWS By Department of Civil & Environmental Engineering, Michigan State University.	(Shen and Phanikumar, 2010)	The catchment is divided into orthogonal grids and river network is considered separately. Intersecting land cells are used to exchange water between land and river.
CREST (Coupled Routing and Excess Storage) By University of Oklahoma and NASA SERVIR.	(Wang et al., 2011)	Spatiotemporal distribution of cell to cell rainfall– runoff routing, three feedback mechanism of assisting runoff generation and routing component coupling.

TOPMODEL (semi-distributed)	(Beven and Kirkby, 1976, Beven and Kirkby, 1979)	Based on the topographic concept index. Assumed; saturated zone hydraulic gradient is approximately equal to the topographic slope of local surface, exponential relationship between downward transmissivity and depth to the water table, saturated zone dynamics and steady state are approximately equal

2.8 Summary of literature review

Urban stormwater management has become more complex with the climate change impacts on urban hydrology. The beginning of this literature review discusses the current stormwater management practice in Australia. Even though current practice evaluates the land use change impacts on hydrological characteristics in land development projects, it does not take climate change impact into account. Downscaling of GCMs projections is a very popular approach of climate change impact assessments. The middle part of this chapter describes the downscaling approaches, their drawbacks, uncertainties and probable solutions etc. Further, it is necessary to understand the occurrence of extreme rain events. Therefore, it discusses the empirical relationships of extreme rainfall events with the atmospheric temperature in the different part of the world and its characteristics. Also, physically based hydrology models are highly capable to investigate the impacts of land use change and climate change in urban areas.

CHAPTER 3

3 Spatial downscaling of future daily rainfalls in Perth airport region

The approach described in this chapter is published at

Sujeewa Herath, Ranjan Sarukkalige, "Spatial and temporal downscaling approach to develop IDF curves for Melbourne airport region", 35th Hydrology and water resources symposium 2014, 24-27 Feb 2014, Perth, Western Australia.

3.1 Introduction

Assessing the impacts of climate change on small urban catchments is one of the challenging tasks for hydrologists. Out of them, estimating the design storm depths for sub-daily rainfall duration under climate change is very important in mitigating the future flood disasters. As mentioned, two analyses, spatial downscaling and temporal downscaling is vitally important in such assessments. This chapter presents the first part (spatial downscaling) of the approach which is utilized to develop IDF relations for future periods by taking the impacts of climate change into account. The second part (temporal downscaling) of the approach has been presented in Chapter 5.

GCMs have been recognized to represent the main features of the global circulation of basic climate parameters. However, these models so far could not reproduce detailed regional climate conditions at fine temporal and spatial scales of relevance to regional hydrological studies (Xu, 1999, Nguyen et al., 2006). According to the recent literature, spatial and temporal resolutions vary in a wide range in the present GCMs and RCMs (Willems and Vrac, 2011). These resolutions are still not able to fulfill the high-resolution data requirements in urban hydrological assessments. To fill the gap between coarse resolution output of GCMs/RCMs and high-resolution data requirement of hydrological assessments, downscaling techniques are employed as a bridge.

As discussed in Chapter 2, downscaling methods are divided into four general categories (Wilby and Wigley, 1997, Mearns et al., 2003, Wilby et al., 2004). Such as

regression methods (Hewitson and Crane, 1996, Wilby et al., 1999), weather pattern approaches (Yarnal et al., 2001), stochastic weather generators (Richardson, 1981, Racsko et al., 1991a, Semenov and Barrow, 1997a, Bates et al., 1998), and limited-area regional climate models (Mearns et al., 2003). The first three types could be categorized under statistical downscaling which is based on the assumption that regional climate is affected by the local physiographic characteristics as well as the large-scale atmospheric state (Hessami et al., 2008). Limited area RCM with fine computational grids over a limited area could be categorized under dynamic downscaling. Due to their low computational cost, statistical downscaling techniques are very popular in the climate change impact assessment studies. (Khan et al., 2006). There are many statistical procedures available in the literature which are currently employed to formulate predictor– predictand relationships, such as linear and nonlinear regression, canonical correlation, artificial neural network and principal components analyses (Wilby et al., 2002). Among them, the Statistical DownScaling Model (SDSM) proposed by Wilby et al. (2002) is the most popular tool that is based on the regression concept (Khalili et al., 2013). According to the comparisons of SDSM rainfall downscaling performance with Long Ashton Research Station Weather Generator (LARS-WG) model and Artificial Neural Network (ANN) model (Khan et al., 2006), LARS –WG model (Hashmi et al., 2011), Smooth Support Vector Machine (SSVM) (Chen et al., 2012b), SDSM shows high performance in future rainfall downscaling. By considering the accuracy and wide applicability, SDSM is employed in this study to evaluate the impacts of climate change on daily rainfalls for future periods.

Taking these facts into account, the main objective of this chapter can be identified as evaluating the impacts of climate change on daily rainfall in Perth airport area for future periods. Under this broad objective following sub-objectives are aligned.

- Development of daily rainfall downscaling model
- Spatially downscaling of future daily rainfalls using HadCM3-A2 and CGCM3-A2 scenarios
- Evaluating the daily rainfall changing trends
- Evaluating the seasonal rainfall changes

3.2 Study area and datasets

Considering the availability of more accurate data with longest record periods and least missing data, Perth airport region is subjected to this study. As a main data input of the downscaling model, observed daily rainfall data (1961-1990) at Bureau of Meteorological (BoM) rain gauge station located at Perth airport are used to developed spatially downscaling model.

In addition to observed daily rainfall data, NCEP reanalysed data sets corresponding to HadCM3 and CGCM3 computational grids are used to SDSM calibration and validation. Also, HadCM3-A2 and CGCM3-A2 climate scenarios are used to the future rainfall simulation. These NCEP reanalysed data and GCM variables are downloaded from the Data Access Integration website (DAI, http://quebec.ccsn.ca/DAI/).

These data include,

- NCEP/HadCM3 and NCEP/CGCM3 normalised daily observed predictor variables for the period 1961-2001.
- HadCM3-A2 normalised daily climate predictor variables for the period 1961-2099.
- CGCM3-A2 normalised daily climate predictor variables for the period 1961-2100.

26 climate variables are included in HadCM3-A2, NCEP/HadCM3 data archive and 25 climate variables are included in CGCM3-A2 and NCEP/CGCM3 data archive. These variables are presented in Table 3.1

Table 3.1: NCEP predictor variables

No	Predictor Discription	Predictor
1	Surface airflow strength	p_f
2	Surface zonal velocity	p_u
3	Surface meridional velocity	p_v
4	Surface vorticity	p_z
5	Surface wind direction	p_th
6	Surface divergence	p_zh
7	500hPa airflow strength	p5-f
8	500hPa zonal velocity	p5_u
9	500hPa meridional velocity	p5_v
10	500hPa vorticity	p5_z
11	500hPa wind direction	p5th
12	500hPa divergence	p5zh
13	850hPa airflow strength	p8-f
14	850hPa zonal velocity	p8_u
15	850hPa meridional velocity	p8_v
16	850hPa vorticity	p8_z
17	850hPa wind direction	p8th
18	850hPa divergence	p8zh
19	*500hPa relative humidity	r500
20	*850hPa relative humidity	r850
21	500hPa geopotential height	p500
22	850hPa geopotential height	p850
23	**Near surface relative humidity	rhum
24	Surface specific humidity	shum
25	Mean temperature at 2m height	temp
26	Mean sea level pressure	mslp

(*specific humidity is used for CGCM3 **Only for HadCM3)

The study area, HadCM3 and CGCM3 grid distribution are presented in Figure 3.1

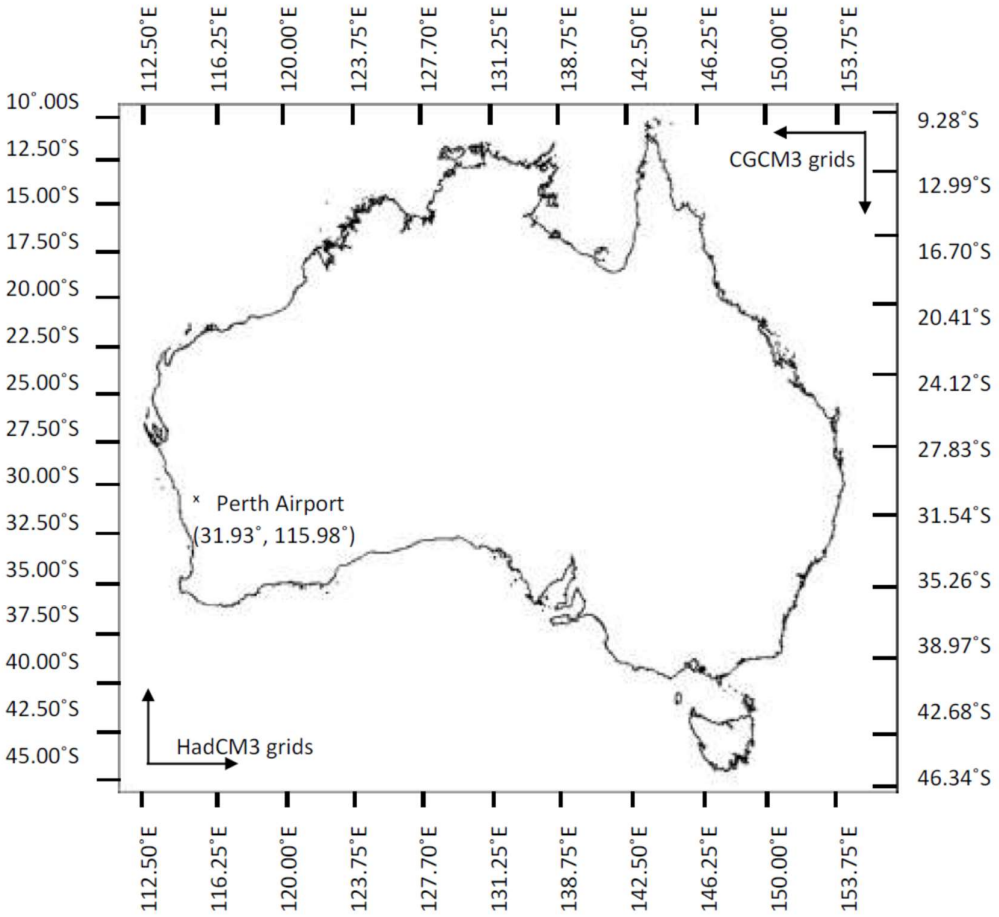

Figure 3.1: Map of study area including HadCM3 and CGCM3 grid coordinates.

3.3 Methodology: Statistical Down-Scaling Model (SDSM)

Statistical Down-Scaling Model (SDSM) is a combination of multiple regression based and stochastic weather generator methods. The main function of the regression component can be identified as the formulation of the empirical relationship between local scale predictands (daily precipitation, daily maximum temperature etc.) and large scale GCM's daily variables for the respective grid (Wilby and Wigley, 1997). The main function of the stochastic component is known as adjusting the variance of downscaled variable for the high agreement with observed data. Also, it facilitates to generate the multiple simulations with same statistical properties in slightly different time scale (Diaz-Nieto and Wilby, 2005).

Furthermore, large-scale climate variables are used in two ways in SDSM in precipitation downscaling. Initially, SDSM analyses the occurrence of wet days using climate variables. Following equation is used in SDSM to simulate the occurrence of the wet days. (Wilby et al., 2014, Wilby and Dawson, 2013).

Under the constraint of $0 \leq W_i \leq 1$, precipitation occurs when uniform random number $[0,1]$ $r \leq W_i$

$$W_i = \alpha_0 + \sum_{j=1}^{n} \alpha_j X_{ij} \quad (3.1)$$

Where,
W is the occurrence of wet day, α is the regression parameter, n is the number of predictor variables and X is the predictor variable.

At the second stage, equation 3.2 is used to estimate the precipitation depth at the return of wet day.

$$P_i^k = \beta_0 + \sum_{j=1}^{n} \beta_j X_{ij} + e_i \quad (3.2)$$

P is the depth of precipitation, $k = 0.25$ for forth route transformation (Wilby et al., 2002), β is the regression parameter, n is number of predictor variable, X is the predictor variable and e is model error.

The key steps of the SDSM downscaling process are;

i. Quality control and data transformation

Collecting and handling of accurate climate data archive for a long period is a challenge for meteorological organizations. Therefore, it is a compulsory requirement to evaluate the accuracy and missing data in climate modelling studies. Also, data transformation is required when using different data formats and different time

standards. SDSM facilitates quality controlling and data transforming to overcome these issues which are raised with climate modelling.

ii. Screening of downscaling predictor variables

Identifying the most potential GCM's variables (low resolution gridded climate variable) for the predictand at a local site is the most difficult and time consuming stage in any type of statistical downscaling approach. To assist the SDSM users in this critical step, SDSM provides three supporting techniques, such as scatter plot, seasonal correlation analysis and partial correlation analysis. These techniques assist the user in selecting most appropriate GCM predictors. Also, these selected predictors are used in the model calibration process.

iii. Model calibration

Formation of multiple regression relationships between local predictand and gridded climate variables are carried out at this stage. There are three options; annual, monthly and seasonal; are available in SDSM to generate these relationships. Further, model calibration process can be unconditional or conditional, depend on the relationship between predictor and predictand. In the unconditional modelling, a direct relationship is built between predictand and predictors while the conditional modelling intermediate process is available between predictand and predictors relationship.

iv. Weather generator

Synthesis of daily weather data using the independently observed predictor variables is the main function of weather generator. Mainly it facilitates to evaluate the accuracy of calibrated SDSM model. Further, it enables the reproducing of daily weather data for artificial time series to represent the present climate.

v. Data and graphical analysis

Statistical analysis/comparison of observed climate data with the synthesis data is carried out at this stage.

vi. Scenario generations

Generating of ensembles (number of ensembles can be changed from 20 to100) of daily weather data using GCM climate variables and generated regression

relationships in model calibration step is carried out at this stage. To use in scenario generation, all GCM predictors should be normalised and the names of predictors should be exactly same to the predictors' name used for model calibration. Figure 3.2 represents these main processes of SDSM as a simple flow chart.

Data requirement	SDSM Process	Method/ Output /Remarks
Station Data (Precipitation, Maximum or minimum temperature)	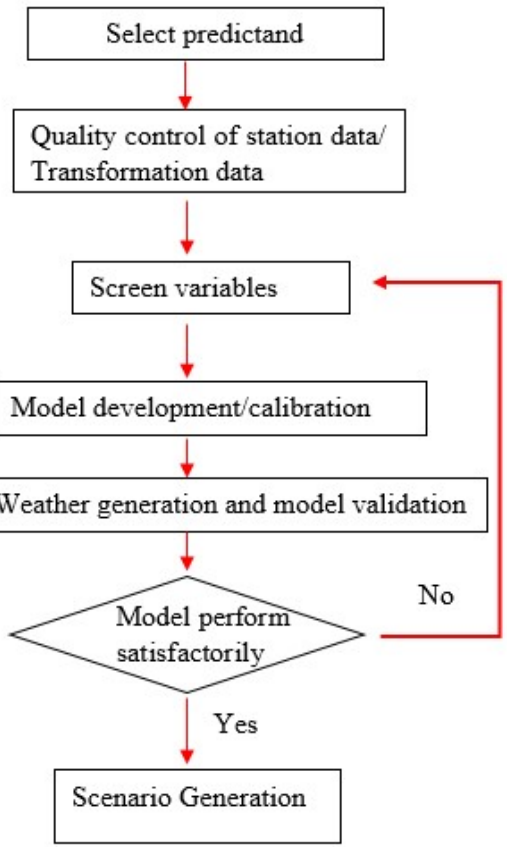	In this study observed daily rainfall at Perth airport is selected as the predictand
Station Data (Precipitation, Maximum or minimum temperature and NCEP data)		Identify • Missing data • Outliers • Gross data errors And perform required data transformation
Station data (predictand) NCEP data (Predictors)		Analyse the correlation between predicated and predictors using partial correlation matrix/coefficient, scatter plots etc.
Station data (predictand) Selected NCEP data (Predictors) (For a part of historical data period)		May required decisions on • Conditional/unconditional • Model type (monthly, seasonal or annual)
Daily rainfall data and NCEP predictors (For the remains period of historical data available)		Ensemble simulation by means of NCEP data (20 to 100)
		Performances of the downscaling model is evaluated by comparing the observed precipitation (for this study) and simulated precipitation.
Calibrated SDSM model GCM predictors		Ensemble simulation by means of GCM data (20 to 100)

Figure 3.2: Statistical downscaling process of SDSM

3.4 SDSM calibration and validation

Perth airport rain gauge station (BoM Station ID – 009021) observed daily rainfall data and NCEP reanalysed data are used to develop predictor– predictand relationships. In this study 1961-1990 period is taken as the most recent standard reference period according to World Meteorological Organization (WMO). The SDSM model is calibrated for 1961-1975 period and is carried out on a monthly basis. Data for the 1976-1990 period is used for the validation of the model. The threshold of the wet day is selected as 0.3 mm/day (Buishand, 1978, Harrold et al., 2003, Mehrotra et al., 2004). By considering the skewness of rainfall distribution, the fourth root transformation is used for the model calibration. Furthermore, SDSM model is considered as conditional for rainfall downscaling (Wilby and Dawson, 2007)

There are few methods available in SDSM to select most appropriate predictors to simulate the predictand variable. In the predictor selection process, initially, all NCEP reanalysed atmospheric variables (Table 3.1) in the region are subjected to the predictor selection analysis. Explained variance and correlation analysis facilities are employed, and the confidence level is taken as 0.05 for the analysis. Using predictor selection analysis, mean sea level pressure, geo-potential height at 500 hPa, geo–potential height at 850 hPa, relative humidity at 500 hPa and near surface relative humidity are selected as potential predictors for NCEP/HadCM3. Surface zonal velocity, airflow strength at 850 hPa are selected for NCEP/CGCM3. Explained variance for NCEP/HadCM3 and NCEP/CGCM3 are presented in Table 3.2 at monthly basis. According to Table 3.2, explained variance which describes the correlation between predictor–predictand is varied between 7.5%-49.2% for NCEP/HadCM3 and 6.3%-46% for NCEP/CGCM3 respectively for 12 months. Also, according to Table 3.2, explained variance shows high explained variance percentages for April – September period which are the rainy months in Perth region.

Table 3.2: Monthly explained variance between observed daily rainfalls and NCEP/HadCM3 and NCEP/CGCM3 variables

Month	E% for NCEP/HadCM3	E% for NCEP/CGCM3
January	7.5	12.4
February	10.4	6.3
March	13.3	15.7
April	37.1	39.3
May	41.5	46.0
June	49.2	44.0
July	43.7	45.2
August	44.2	43.7
September	35.5	44.9
October	37.7	39.2
November	20.1	19.6
December	17.1	16.8

Correlation matrix, Partial r and Probability value (known as P value) represent the relationship strength between two associated variables. High Partial r value represents strong correlation strength between variables while low P value presents a high chance of association. Correlation matrix and Partial correlation coefficients for NCEP/HadCM3 are presented in Table 3.3 and Table 3.4 respectively. Also Table 3.5 and Table 3.6 present the correlation matrix coefficient and partial correlation matrix for NCEP/CGCM3 respectively. In generally correlation parameters corresponding to the rainfall downscaling are less strong than the parameters in temperature downscaling.

Table 3.3: Correlation matrix of NCEP/HadCM3

	Rainfall	mslp	p500	p850	r500	rhum
Rainfall	1	-0.394	-0.271	-0.355	0.277	0.303
mslp	-0.394	1	0.310	0.657	-0.192	-0.137
p500	-0.271	0.310	1	0.353	0.011	-0.485
p850	-0.355	0.657	0.353	1	-0.176	-0.344
r500	0.277	-0.192	0.011	-0.176	1	0.133
rhum	0.303	-0.137	-0.485	-0.344	0.133	1

Table 3.4: Partial correlation coefficient between Perth airport daily rainfall and NCEP/HadCM3

Predictor	Partial r	P Value
mslp	-0.232	0.0000
p500	-0.069	0.0128
p850	-0.042	0.0137
r500	0.151	0.0000
rhum	0.180	0.0000

Table 3.5: Correlation matrix of NCEP/CGCM3

	Rainfall	ugl	8_fgl
Rainfall	1	0.339	0.393
ugl	0.339	1	0.821
8_fgl	0.393	0.821	1

Table 3.6: Partial correlation coefficient between Perth airport daily rainfall and NCEP/CGCM3

Predictor	Partial r	P Value
ugl	0.032	0.0256
8_fgl	0.213	0.0000

3.5 Results and Discussion

3.5.1 Evaluating the SDSM model performances for calibration and validation period.

To evaluate the accuracy of the developed downscaling model, daily rainfall series is simulated for the calibration period (1961-1975) using NCEP/HadCM3 and NCEP/CGCM3. Figure 3.3 presents a comparison of average daily rainfall between observed and simulated data for calibration period. According to Figure 3.3, average daily observed rainfall for the calibration period is 2.25mm/day and rainfall is highly seasonal. Maximum daily average rainfall (higher than 6mm/day) can be observed in the month of June for the calibration period. Also, May–September period shows comparatively high average daily rainfall over 2mm/day, while November–March period shows the lowest average daily rainfall less than 1mm/day. Furthermore, Figure 3.3 shows that simulated daily rainfalls by downscaling models using NCEP/HadCM3 and NCEP/CGCM3 highly accurate for the calibration period. Annual daily average rainfall takes 2.01mm/day and 2.11mm/day for NCEP/HadCM3 and NCEP/CGCM3 respectively. Furthermore, both models show accurate seasonal rainfall pattern throughout the year.

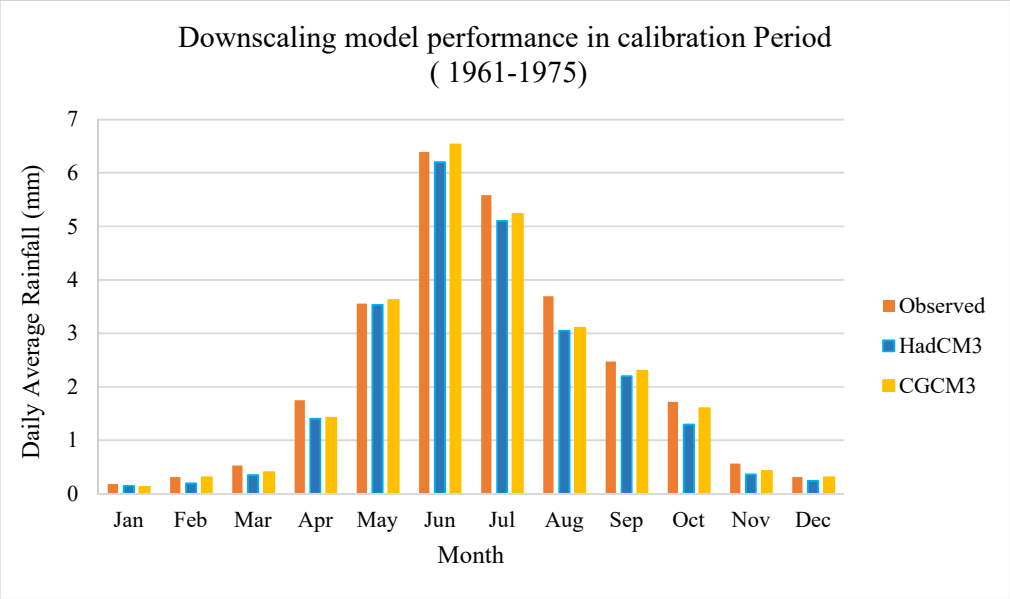

Figure 3.3: Comparison of observed and simulated daily average rainfalls for calibration period (1961-1975)

To verify the accuracy of the developed downscaling model, observed rainfall is compared with the simulated daily rainfall for a validation period (1976–1990). Figure 3.4 shows this comparison of daily average rainfall in monthly basis for the validation period. It can be clearly observed that the observed annual daily average rainfall has been decreased in the validation period (1.99mm/day). Simulated annual daily average rainfall is 1.92mm/day and 1.94mm/day for NCEP/HadCM3 and NCEP/CGCM3 respectively. However, yearly wet period (May–September) and dry period (November-March) are same as the calibration period. Furthermore, simulated results are highly consistent with observed daily rainfalls for both GCMs. Therefore Figure 3.4 depicts that the developed downscaling models are highly capable in daily rainfall downscaling using HadCM3 and CGCM3.

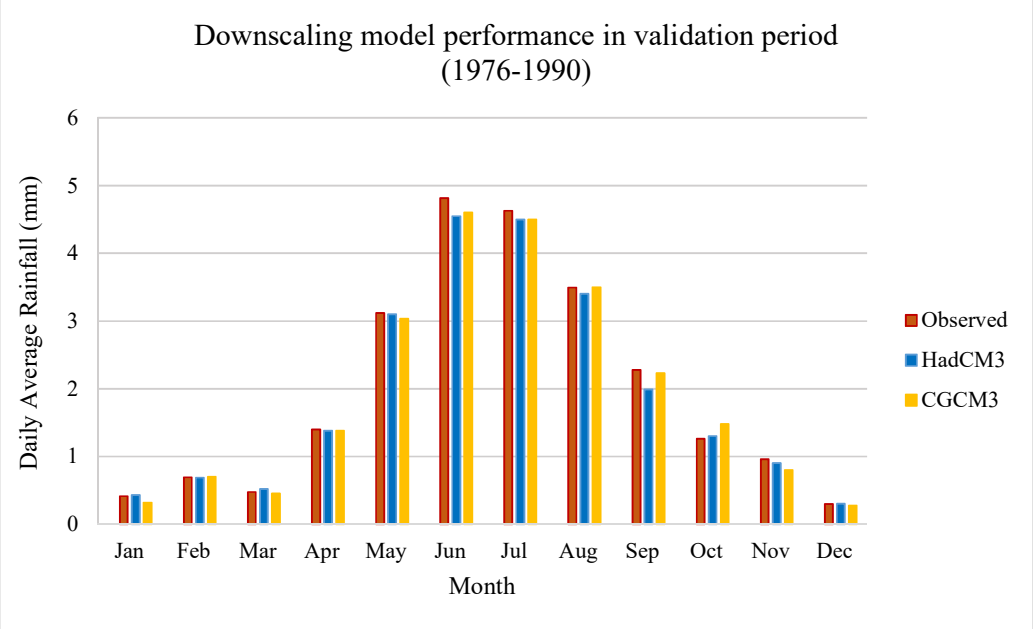

Figure 3.4: Comparison of observed and simulated daily average rainfall for validation period (1976-1990)

3.5.2 Evaluation of the spatially downscaled daily rainfall for the future periods

In the next stage, calibrated and validated SDSM is used to downscale the daily rainfall for the future periods. Here, NCEP climate predictors are replaced by the climate variables of HadCM3-A2 and CGCM3-A2 scenarios. Figure 3.5 and Figure 3.6 present the time series plot of simulated annual rainfall using HadCM3-A2 and CGCM3-A2 scenarios respectively. According to Figure 3.5 and Figure 3.6, simulated

annual rainfall series shows short-term fluctuating behaviour for both GCMs. Also, annual rainfall time series does not show simple rainfall changing trend for the future period. Therefore, 5 year moving average of annual rainfall is estimated to identify the long- term trend of simulated rainfalls. These calculated 5 year moving average results show a clear decrease in annual rainfall trend for future periods for both GCMs and these results align with the identified rainfall projections for the same region by other studies (Jakob et al., 2012). Further, average annual rainfall decreasing rate for CGCM3-A2 (1.96mm/year) takes higher value than decreasing rate for HadCM3-A2 (1.05 mm/year)

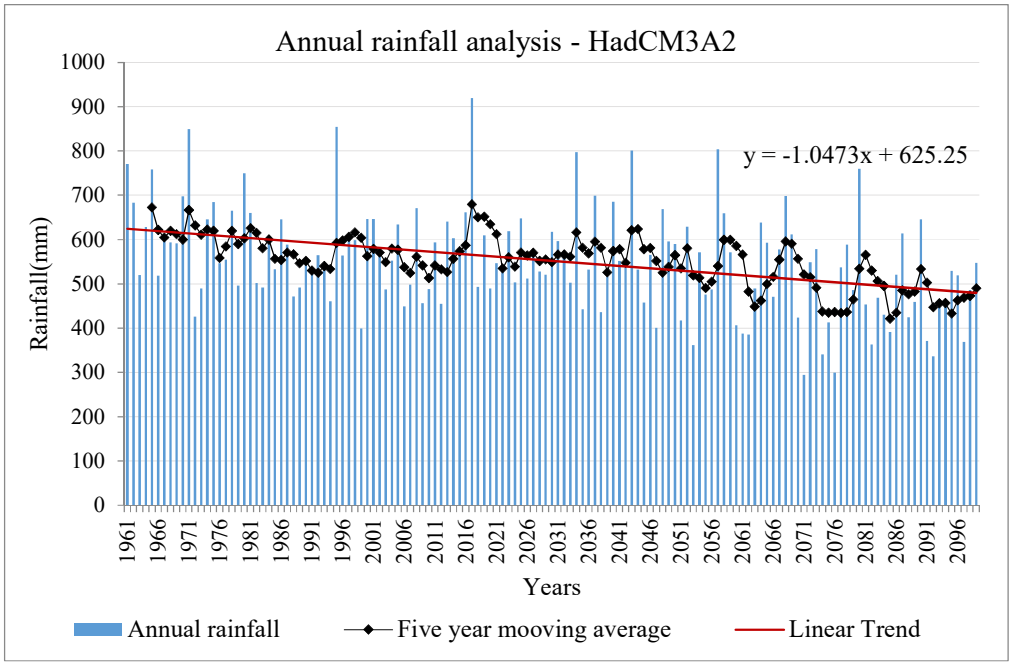

Figure 3.5: Rainfall trend analysis for annual rainfall downscaled by HadCM3-A2

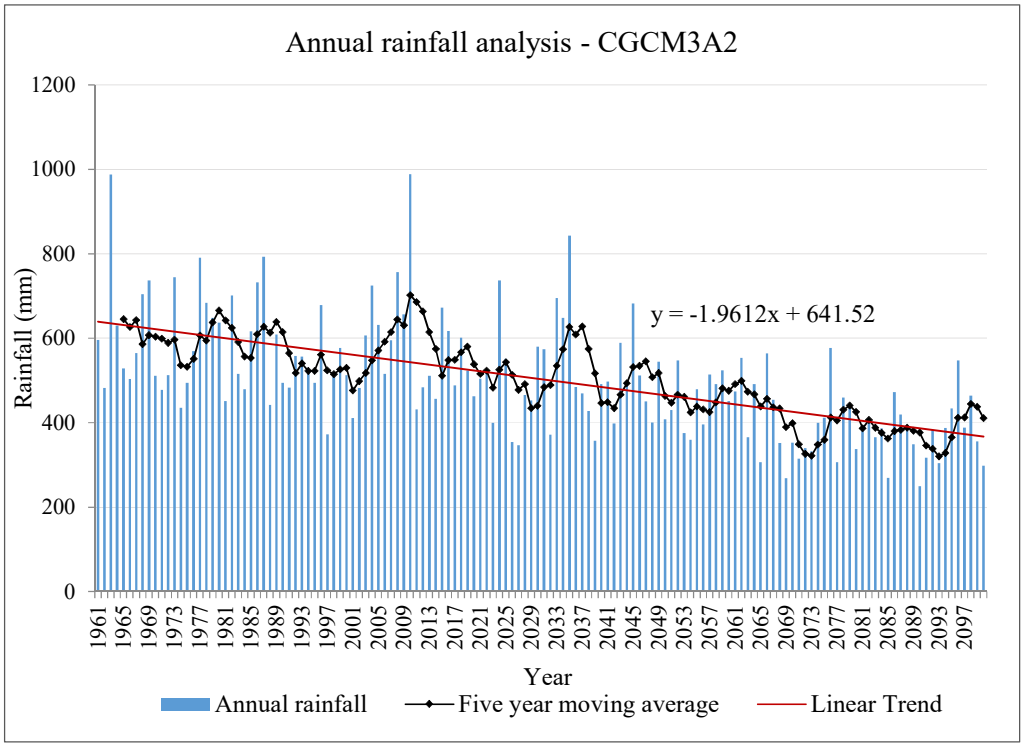

Figure 3.6: Rainfall trend analysis for annual rainfall downscaled by CGCM3-A2

Furthermore, Figure 3.7 presents the daily average rainfall changing values and percentage calculated from the total annual rainfall presented in Figure 3.5 and Figure 3.6. In this comparison, 1961-1990 period is considered as the standard reference period. Therefore, Figure 3.7 presents the daily average rainfall changing values and percentages for 2020s (2011-2040), 2050s (2041-2070) and 2080s (2071-2099/2100) periods with respect to the 1961-1990 period. According to Figure 3.7, average daily rainfall deduction can be observed for all the future periods of daily rainfall simulated using both HadCM3-A2 and CGCM3-A2 simulations. However, deduction of the percentage of simulated rainfall using HadCM3-A2 shows minimum deduction percentage than CGCM3-A2 simulations. Also, Figure 3.7 depicts, deduction percentage at 2080s takes its maximum for HadCM3-A2 and CGCM3-A2 of (approximately) 22% and 36% while at 2020s takes the minimum of 4% and 14% respectively. Therefore, according to both downscaled results, we can expect low mean annual daily rainfall in the future periods in Perth Airport region.

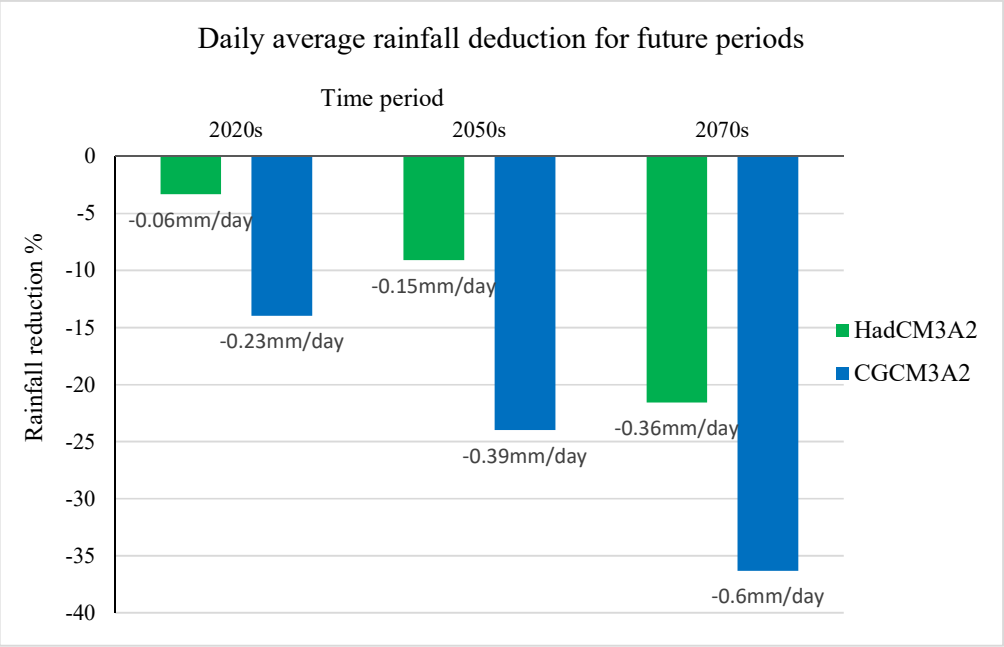

Figure 3.7: Daily average rainfall changing value and percentage for the simulated future rainfalls

3.5.3 Impacts of climate change on seasonal daily rainfall

Furthermore, spatially downscaled future daily rainfalls are analysed in seasonal basis. Figure 3.8 and Figure 3.9 present the seasonal analysis of downscaled future rainfalls using HadCM3-A2 and CGCM3-A2 respectively. The seasonal analysis is conducted under four seasons named summer (Dec-Feb), autumn (Feb–May), winter (Jun–Aug) and spring (Sep–Nov). These figures present the seasonal variation of daily rainfall for 2020s, 2050s and 2080s reference to 1960-1990 standard period. Figure 3.8 clearly shows a decreasing daily rainfall trend for all seasons except autumn in 2020s and 2050s for HadCM3-A2. 2020s autumn daily rainfall shows 13.8% increment while 2050s shows 7.3% increment. Further, climate change impacts on the summer rainfall are minimal and daily rainfall deduction percentages take very low value for the summer period (2020s – 3.2%, 2050s – 4.9 and 2080s – 8.2%). On the other hand, climate change highly affects to winter rainfall. Considerable reduction of daily rainfalls can be observed for all the winter period (2020s – 23.9%, 2050s – 41.7 and 2080s – 94.1%).

Figure 3.9 also shows decreasing daily rainfall according to CGCM3-A2 for all seasons except 2020s spring. However, spring rainfall increment is very small and it

is only 2.8%. Maximum average daily rainfall reduction can be observed for the winter seasons and it takes 58.7%, 89.4%, 116.7% for 2020s, 2050s and 2080s respectively. The impacts of climate change on summer rainfall is minimal for CGCM3-A2 simulation too.

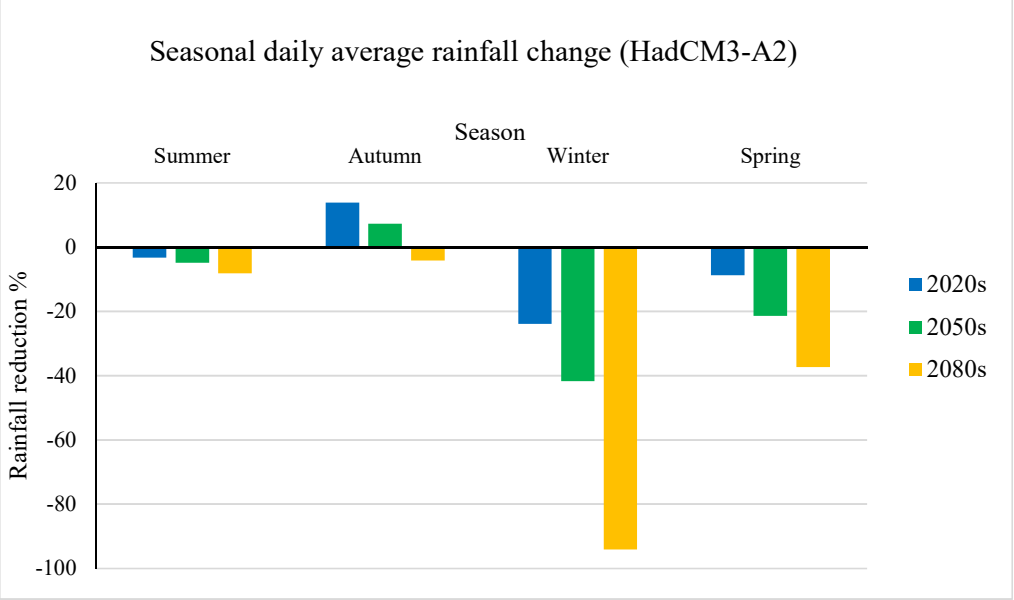

Figure 3.8: HadCM3-A2 simulated daily average rainfall changing percentage in seasonal basis for future periods

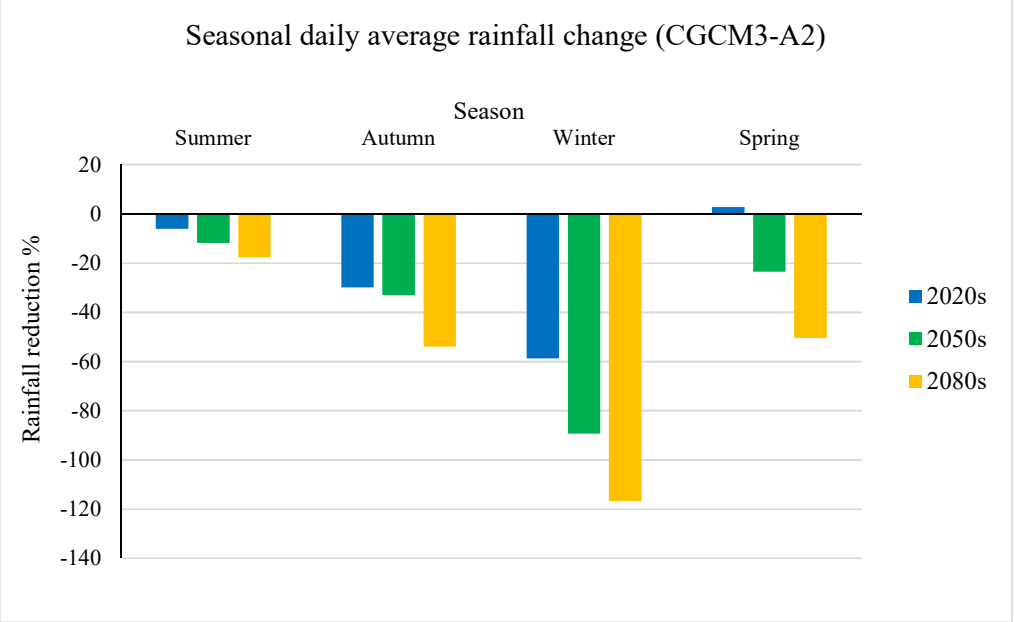

Figure 3.9: CGCM3-A2 simulated daily average rainfall changing percentage in seasonal basis for future periods

3.6 Summary

Spatial downscaling of GCM predicted rainfall data is essential to evaluate the impact of climate change on specific region/point. In this chapter, SDSM is used to downscale the future daily rainfall series for Perth airport region. SDSM background theories, downscaling model development steps, model calibration and validation process are discussed in the initial sections of this chapter.

Downscaling model is successfully calibrated for the 1961 –1975 period and validated for the 1976-1990 period confirming that the SDSM model is feasible in describing some fundamental statistical properties of the daily rainfall process. For the SDSM model calibration and validation, the normalized NCEP reanalysed data on HadCM3 and CGCM3 grids are used. In the next section, A2 scenarios of HadCM3 and CGCM3 are used to downscale the future daily rainfall series.

The overall results of both GCMs show decreasing annual rainfall for the future periods. As expected, the rate of annual rainfall decreasing is not same for HadCM3 and CGCM3. Further, downscaled result by CGCM3-A2 scenario shows a higher deduction rate of daily rainfall than HadCM3-A2 for 2020s, 2050s and 2080s with respect to 1961-1990 period.

In the seasonal analysis, an increase of daily rainfall can be observed for autumn season in 2020s and 2050s for HadCM3-A2 downscaled data. Further, increased spring rainfall for 2020s can be observed for CGCM3-A2 downscaled daily time series. However, downscaled rainfalls by both GCMs show high rainfall reduction in winter seasons for the future period.

CHAPTER 4

4 Evaluation of GEV parameter estimation methods to assess the scaling behaviour of extreme rainfalls

Extended from

> H.M.S.M.Herath, P.R.Sarukkalige, V.T.V.Nguyen, Evaluation of GEV parameter estimation methods to assess the scaling behavior of extreme rainfalls, 19th IAHR - APD Congress, 21-24 Sep. 2014, Hanoi, Vietnam.

4.1 Introduction

Rainfall disaggregation is very useful where sub-daily rainfall records are not available. In these occasions, rainfall disaggregation is used to obtained statistical properties of sub-daily extreme rainfall events at required weather stations either using available daily recorded or regional data. These generated statistical properties are used in developing IDF relations and other hydrological modelling studies.

GEV distribution is a combination of Gumbel, Frechet and Weibull distributions within the extreme value theory and it includes three parameters for location, scale and shape. Based on the value of shape parameter, (Shape parameter =0, >0 and <0) GEV distribution is known as Extreme Value Type I, Extreme Value Type II and Extreme Value Type III respectively. Further, GEV distribution is considered as high capable continuous probability distribution to model extreme climate events (Park et al., 2011, Aryal et al., 2009).

One of the major application of GEV distribution is disaggregation of extreme rainfalls. This disaggregation is mainly based on the scaling invariant property of extreme rainfall events (Burlando and Rosso, 1996, Menabde et al., 1999, Nguyen and Nguyen, 2008, Chang, 2013). However, the accuracy of the disaggregation is highly based on the GEV parameter estimation approaches. Especially some parameter

estimation methods do not comply with the mandatory requirements of GEV parameter scaling, while some methods are accurate only for some specific study areas. The purpose of this chapter is to evaluate the appropriateness of GEV parameter estimation methods in the context of rainfall disaggregation in Western Australia. Three GEV parameter estimation methods (Method of L Moment, Maximum likelihood method and Non Central Moment method) are tested in this chapter.

Therefore, main objectives of this chapter are;

- Evaluate the GEV parameter estimation methods to use in rainfall disaggregation.
- Develop IDF relations using proposed rainfall disaggregation approach.

4.2 Study area and datasets

Eight rain gauge stations in Western Australia are selected for this study. All these stations are located in South-West region in Western Australia. The rainfall pattern in this region is highly seasonal and most of the rainfall occur in the winter period (June-August). According to the Bureau of Meteorology (BoM) statistics, more than 50% of annual rainfall in the South- West region is received in the winter period (BoM, 2015). Figure 4.1 shows the locations, of selected rain gauge stations for this study.

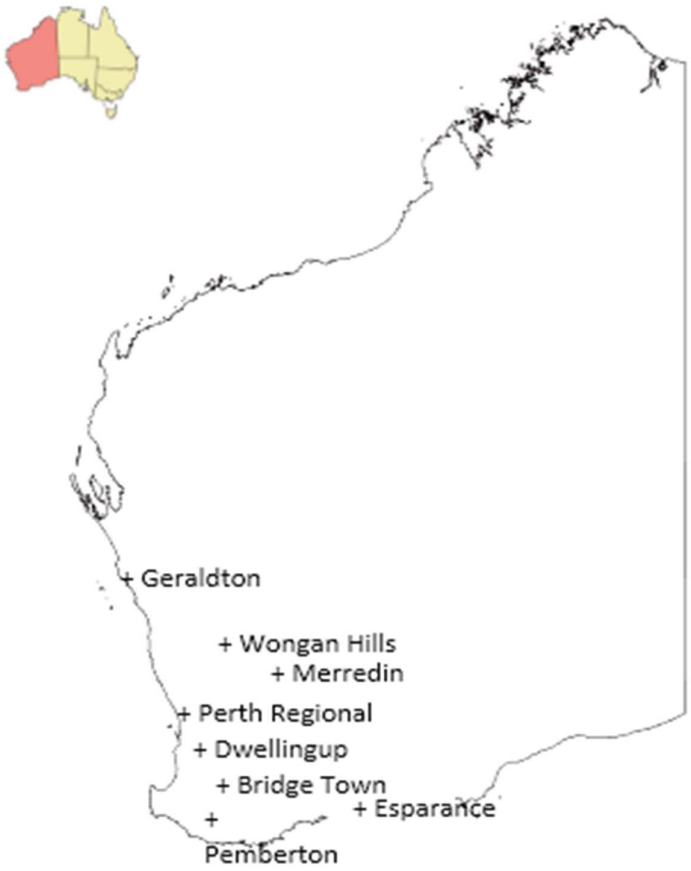

Figure 4.1: Locations of the selected rain gauge stations for the study

Observed six minutes rainfall data are collected from The Bureau of Meteorology and these data are used to analyse annual maximum rainfall for 6min., 12min., 30min., 1h, 2h, 6h, 12h and 24h periods. The length of the observed data availability is varied within 15 to 30 years in eight stations. Table 4.1 presents the coordinates of each location and period of data used in the study.

Table 4.1: Details of Weather Stations

Rain Gauge Station	BoM Station ID	Coordinates	Data Period
Bridgetown	009510	33.96^0 S, 116.14^0E	1968- 1995
Geraldton	008051	28.78^0S, 114.61^0E	1961-1976
Dwellingup	009538	32.71^0S, 116.06^0E	1965-1983
Esperance	009789	33.87^0S, 121.89^0E	1971-2001
Merredin	010092	31.48^0S, 118.29^0E	1982-1997
Pemberton	009592	34.45^0S, 116.04^0E	1996-2010
Wongan Hills	008138	30.89^0S, 116.72^0E	1974- 1999
Perth Regional	009034	31.95^0S, 115.86^0E	1956-1991

4.3 Methodology

4.3.1 GEV parameter estimation

GEV distribution is a high capable three parameter probability distribution function to model annual maximum rainfall and Cumulative Distribution Function (CDF for GEV is given at equation 2.1 in section 2.4.4. By considering the accuracy of GEV parameter estimation methods; L moment method, Non Central Moment (NCM) method and Maximum Likelihood Estimation method (MLE) are evaluated in this chapter. Initially, suitability of GEV distribution in annual maximum rainfall series modelling is evaluated for selected eight rain gauge stations.

Method of L- Moment

The method of L- Moment (Hosking, 1990) is based on the linear combinations of weighted probability moments . First three L moments of a data sets are given as $\lambda_{1,}\lambda_2 \; and \; \lambda_3$,

$$\lambda_1 = E[X] \quad (4.1)$$

$$\lambda_2 = \frac{1}{2} \mathrm{E}\,[X_{2:1} - X_{1:2}\,] \quad (4.2)$$

$$\lambda_3 = \frac{1}{3} \mathrm{E}\,[X_{3:3} - 2X_{2:3} + X_{1:3}] \quad (4.3)$$

Here, $X_{i:n}$ is the i[th] largest observation in a sample of size n.

Furthermore, Probability Weight Moments (PWM) are commonly used for L moment estimates.

r[th] PWM βr is defined as

$$\beta_r = E[X\{F(X)\}^r] \quad (4.4)$$

$F(X)$ is the cumulative distribution function of X

When b_r is the unbiased PWM estimator of β_r, b_r is defined as

$$b_r = \frac{1}{n} \sum_{j=r+1}^{n} \binom{j-1}{r} x_{j:n} / \binom{n-1}{r} \quad (4.5)$$

For $r = 1,2, \ldots (n-1)$

Then the first three L moment are given as

$$\lambda_1 = \beta_0 \quad (4.6)$$

$$\lambda_2 = 2\beta_1 - \beta_0 \quad (4.7)$$

$$\lambda_{13} = 6\beta_2 - 6\beta_1 + \beta_0 \quad (4.8)$$

Parameters of GEV distribution can be estimated by following equations

$$\kappa = 7.8590c + 2.9554c^2 \quad (4.9)$$

$$\alpha = \kappa\lambda_2 / [\Gamma(1 + \kappa)(1 - 2^{-\kappa})] \quad (4.10)$$

$$\xi = \lambda_1 + \left(\frac{\alpha}{\kappa}\right) [\Gamma(1 + \kappa) - 1] \quad (4.11)$$

When c is defined as

$$c = \frac{2\lambda_2}{\lambda_3+3\lambda_2} - \frac{ln(2)}{ln(3)} \quad (4.12)$$

Method of NCM

According to Pandey (1995) k^{th} order NCM, (μ_k) of GEV distribution (for $\kappa \neq 0$) has been shown as equation 2.3 in literature review.

By determining the first three NCMs of a data set, it is possible to derive three non-linear equations to estimate three parameters of GEV distribution.

Method of MLE

The method of Maximum Likelihood can be identified as a very popular method for GEV parameters estimation. According to Embrechts et al. (1997), likelihood function is given by

$$L(\theta; X) = \sum_{i=1}^{n} h_\theta\,(X_i) I_{\{1+\kappa(x_i-\xi)/\alpha>0\}} \quad (4.13)$$

The corresponding log likelihood function;

$$l(\theta; X) = Ln\, L(\theta; X) \quad (4.14)$$

Then the maximum likelihood estimator for θ is given by;

$$\widehat{\theta n} = arg\, max_{\theta \epsilon \Theta} l(\theta; X) \quad (4.15)$$

Where, ξ, α and κ are known as location, scale and shape parameters respectively.

Further, Matlab function "parmhat = gevfit(X)" gives the three parameters of GEV distribution fitted to extreme values series of X using MLE.

4.3.2 Evaluation of model performance

It is an essential requirement to conduct performance criteria in hydrological modelling studies to evaluate the model performances. Performance criteria evaluation

is based on the difference between observed and simulated values. In this study, two types of performance criteria; graphical analysis and goodness-of-fit analysis are conducted to evaluate the performance of proposed approach in rainfall disaggregation.

Graphical analysis

Graphical data analysis is the simplest and easily understandable performance analysis criteria to use in hydrological modelling. As this study is related to rainfall depths and their return periods, probability plots are used. Cunnane (Cunnane, 1978) plotting position formula (equation 4.16) is used in the analysis.

$$p_{i=} \frac{(r-0.4)}{(n+0.2)} \quad (4.16)$$

Where P_i = ith plotting position, $r =$ rank of the i^{th} observation when sorted by descending order, n = number of observations

Goodness-of-fit tests

Three goodness-of-fit tests are used to evaluate the performance of GEV distribution in modelling of annual maximum rainfall events and capability of scaling approach to estimate the sub-daily annual maximum rainfall depth using daily rainfall depths.

Root Mean Square Error (RMSE)

RMSE is commonly used to measure the difference between predicted and observed values. Individual differences are called residuals, and the RMSE serves to aggregate them into a single measure of predictive power. Also, low RMSE value implies the high accuracy of the prediction.

$$RMSE = \sqrt{\frac{\sum_{i=1}^{n}\left(X_{obs,i}-X_{model,i}\right)^2}{n}} \quad (4.17)$$

Where;

$X_{obs,i}$ is observed values and $X_{model,i}$ is modelled values at time/place i.

Nash–Sutcliffe Model Efficiency Coefficient (NSE)

Nash–Sutcliffe Model Efficiency Coefficient (NSE) is one of the most effective measure of model performance widely using in hydrological modelling (Wang et al., 2011). NSE takes value between -∞ to 1. $NSE = 1$ gives perfect match of model with the observed data. $NSE = 0$ corresponds to the accurate model results with the mean of the observed data. If NSE < 0, it implies the low accurate of model predictions. NSE is defined as

$$NSE = 1 - \frac{\sum_{i=1}^{n}(O_i - Si)^2}{\sum_{i=1}^{n}(Oi - O')^2} \quad (4.18)$$

Where

$$O' = \frac{1}{n}\sum_{i=1}^{n} Oi \quad (4.19)$$

n- Number of time steps, Oi – Observation at ith time step, Si –Simulation at ith time step

Percent Bias test (PBIAS)

The average tendency of simulated values is measured by percent bias test.

$$PBIAS = \frac{\sum_{i=1}^{n}(Si - Oi)}{\sum_{i=1}^{n} Oi} * 100 \quad (4.20)$$

Where,

Oi – Observation at ith time step, Si –Simulation at ith time step

The optimum value of PBIAS is 0 and the positive values indicate overestimation and the negative values indicate underestimation of the model.

4.3.3 Evaluation of scaling behaviour of rainfalls

According to the literature (Burlando and Rosso, 1996, Menabde et al., 1999) annual maximum rainfall events of the different time scales show scaling behaviour. This phenomenon is mainly used in temporal downscaling/disaggregation of daily rainfalls to estimate the statistical properties of sub-daily annual maximum rainfall depths. Furthermore, when the simple scaling relationship exists between two time periods; t and λt, then GEV parameters which are fitted to relevant annual maximum series are related as,

$$\kappa(\lambda t) = \kappa(t) \tag{4.21}$$

$$\alpha(\lambda t) = \lambda^{\beta}\alpha(t) \tag{4.22}$$

$$\xi(\lambda t) = \lambda^{\beta}\xi(t) \tag{4.23}$$

Where, ξ, α and κ are known as location, scale and shape parameters respectively and λ^{β} is the proportion between average annual maximum rainfalls of λ and λt period. Validity of this relationships are evaluated for the different parameter estimation methods in this study. Then the most appropriate parameter estimating method is utilized to develop sub daily IDF relations using daily observed data.

4.4 Results and discussion

4.4.1 Evaluation of the capability of GEV distribution in modelling of annual maximum rainfalls.

As mentioned in section 4.3.1 (Methodology), suitability of GEV distribution to describe the annual maximum rainfall series is evaluated using visual plotting and goodness-of-fit tests. For the illustration purpose Figure 4.2 describes the capability of GEV distribution in modelling annual maximum rainfall events.

Figure 4.2 presents a comparison of the capability of L moments, NCMs and MLE methods in estimating GEV parameters for 6min, 1h and 24h rainfall events of selected eight rain gauge stations. Evaluation results indicate that the L moment and NCMs

methods are more accurate than MLE method in reproducing annual maximum rainfall series for selected eight stations.

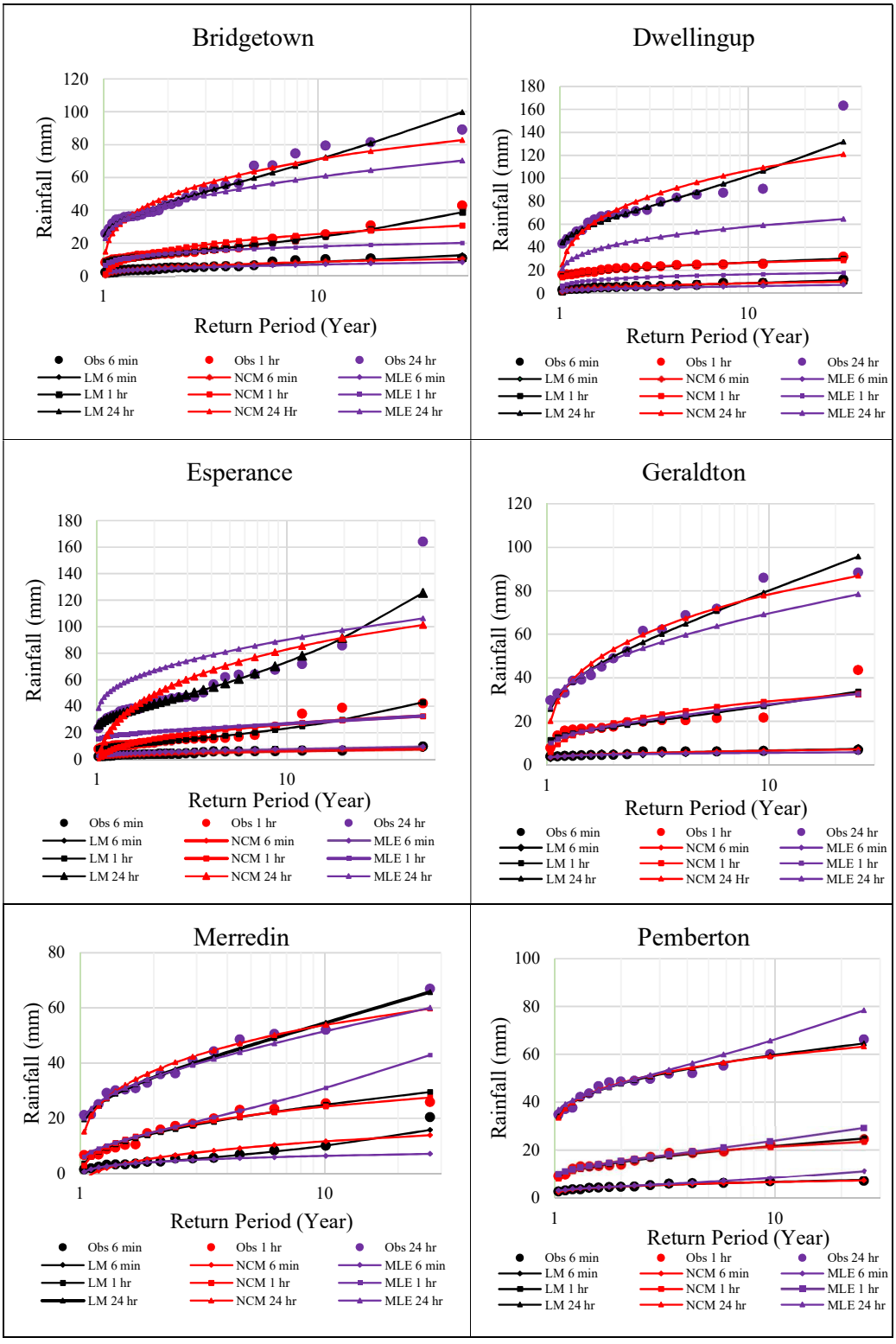

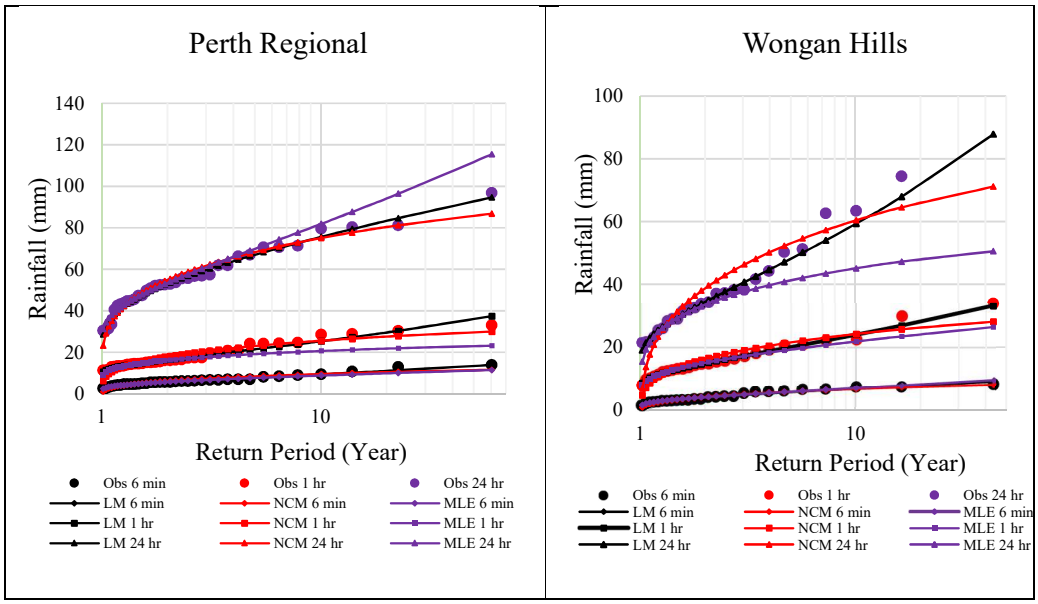

Figure 4.2: GEV fitting to observed 6 minute, 1 hour and 24 hour annual maximum rainfalls

In addition to the visual plotting, RMSE, NSE and PBIAS goodness-of-fit tests are conducted to evaluate the most accurate parameter estimation methods. Results of the goodness-of-fit tests are included in Table 4.2. According to the results of the goodness-of-fit tests and visual plotting of observed and modelled data, MLE has the lowest accuracy in GEV parameter estimation for selected stations and NCM, L moment methods are more capable in GEV parameter estimation. Therefore, NCM and L moment methods only subjected to the scaling study to develop IDF curve.

Table 4.2: Goodness-of-fit test results

		6 min			12 min			30 min			1 h			2 h			6 h			12 h			24		
		NMC	**LM**	**MLE**	**NMC**	**LM**	**MLE**	**NMC**	**LM**	**MLE**	**NMC**	**LM**	**MLE**	**NMC**	**LM**	**MLE**	**NMC**	**LM**	**MLE**	**NMC**	**LM**	**MLE**	**NMC**	**LM**	**MLE**
Geraldton	RMSE	0.343	0.350	0.663	0.392	0.405	1.986	0.839	0.841	2.874	4.309	3.273	3.588	4.066	1.871	3.971	5.376	3.582	10.328	6.968	5.615	16.530	4.363	3.554	6.631
	NSE	0.890	0.886	0.590	0.954	0.950	-0.194	0.931	0.931	0.190	0.659	0.803	0.763	0.864	0.971	0.870	0.910	0.960	0.669	0.877	0.920	0.309	0.944	0.963	0.870
	PBIAS	-0.001	-0.001	-0.083	-0.000	-0.000	0.121	-0.000	-0.000	0.103	-0.000	-0.000	-0.010	0.001	0.001	-0.051	0.001	0.001	-0.149	0.001	0.001	-0.215	-0.000	-0.000	-0.069
Bridgetown	RMSE	0.827	0.641	1.165	1.268	0.660	1.776	3.704	1.342	5.312	3.660	1.074	5.300	3.137	0.935	4.485	3.201	1.900	6.975	4.684	2.728	6.395	5.113	3.440	7.611
	NSE	0.885	0.931	0.771	0.868	0.964	0.741	0.707	0.962	0.398	0.746	0.978	0.468	0.826	0.985	0.644	0.906	0.967	0.556	0.891	0.963	0.796	0.907	0.958	0.793
	PBIAS	-0.000	-0.000	-0.107	0.000	0.000	-0.104	0.001	0.001	-0.181	0.001	0.001	-0.147	0.000	0.000	-0.099	0.000	0.000	-0.104	0.000	0.000	-0.078	0.000	0.000	-0.083
Dwellingup	RMSE	0.635	0.286	1.827	1.146	0.936	4.072	1.436	0.527	6.978	1.038	0.817	8.989	0.726	0.730	11.036	2.483	2.171	19.105	8.582	7.116	27.213	13.276	8.548	34.362
	NSE	0.916	0.983	0.305	0.884	0.923	-0.460	0.894	0.986	-1.506	0.930	0.957	-4.253	0.978	0.977	-4.175	0.955	0.965	-1.685	0.795	0.859	-1.057	0.724	0.885	-0.852
	PBIAS	0.000	0.000	-0.274	0.000	0.000	-0.367	0.000	0.000	-0.413	0.000	0.000	-0.415	0.000	0.000	-0.399	0.000	0.000	-0.426	0.000	0.000	-0.424	0.000	0.000	-0.414
Esperance	RMSE	0.455	0.332	1.092	0.971	0.366	1.886	2.016	0.951	4.188	4.762	2.476	7.710	6.743	2.775	10.455	7.674	1.986	15.343	10.303	3.126	17.734	15.645	7.314	23.902
	NSE	0.928	0.984	0.585	0.884	0.960	0.564	0.821	0.910	0.228	0.669	0.944	0.132	0.667	0.983	0.200	0.753	0.976	0.015	0.739	0.916	0.225	0.616	0.585	0.104
	PBIAS	-0.001	-0.001	0.230	0.003	0.003	0.214	0.000	0.000	0.298	0.000	0.000	0.385	0.001	0.001	0.485	0.001	0.001	0.489	0.001	0.001	0.408	0.001	0.001	0.387
Merredin	RMSE	2.451	1.200	3.542	2.151	1.125	3.176	1.671	1.418	3.236	1.653	1.675	4.693	1.428	1.439	72.877	1.739	1.568	2.936	2.020	1.811	2.457	3.004	1.627	2.570
	NSE	0.694	0.927	0.361	0.823	0.952	0.615	0.930	0.950	0.739	0.939	0.938	0.510	0.943	0.942	-1.467	0.948	0.958	0.852	0.961	0.969	0.943	0.939	0.982	0.955
	PBIAS	0.001	0.001	-0.273	0.001	0.001	-0.176	0.001	0.001	-0.156	0.001	0.001	0.148	0.000	0.000	1.710	0.000	0.000	0.055	0.000	0.000	0.021	0.000	0.000	-0.026
Pemberton	RMSE	0.208	0.213	1.219	0.272	0.254	1.361	0.691	0.543	1.209	0.830	0.679	1.477	1.551	1.363	2.391	1.661	1.699	12.387	1.021	1.030	7.578	1.490	1.315	4.094
	NSE	1.000	1.000	0.984	1.000	1.000	0.991	0.999	0.999	0.997	0.999	1.000	0.998	0.999	0.999	0.997	0.999	0.999	0.967	1.000	1.000	0.992	1.000	1.000	0.998
	PBIAS	0.000	0.000	0.135	0.000	0.000	0.102	0.000	0.000	0.056	0.000	0.000	0.048	0.000	0.000	0.056	0.000	0.000	0.194	0.000	0.000	0.097	0.000	0.000	0.046
Perth Regional	RMSE	0.820	0.348	0.720	1.281	0.723	1.117	1.710	0.550	1.588	1.934	1.231	3.320	1.090	0.727	1.191	1.003	0.750	4.132	2.794	1.289	1.441	2.974	1.843	4.798
	NSE	0.892	0.981	0.917	0.854	0.954	0.889	0.864	0.986	0.883	0.882	0.952	0.651	0.965	0.985	0.958	0.981	0.990	0.684	0.942	0.988	0.985	0.961	0.985	0.898
	PBIAS	0.000	0.000	-0.040	0.000	0.000	-0.036	0.000	0.000	-0.040	0.000	0.000	-0.100	0.000	0.000	0.016	0.000	0.000	0.057	0.000	0.000	0.011	0.000	0.000	0.042
Wongan Hills	RMSE	0.402	0.382	0.419	0.546	0.468	0.761	0.927	0.591	0.877	1.999	0.758	2.026	2.201	1.262	2.134	3.331	1.528	3.822	4.484	3.246	6.069	5.873	2.689	10.275
	NSE	0.952	0.956	0.948	0.964	0.974	0.930	0.957	0.983	0.962	0.884	0.983	0.881	0.902	0.968	0.908	0.909	0.981	0.881	0.893	0.944	0.803	0.865	0.972	0.588
	PBIAS	0.000	0.000	0.010	0.000	0.000	0.037	0.000	0.000	0.028	0.000	0.000	-0.050	0.000	0.000	-0.043	0.000	0.000	-0.065	0.000	0.000	-0.087	0.001	0.001	-0.141

4.4.2 Properties of estimated GEV parameters.

Estimated GEV parameters by L moment and NCM method are analysed. According to the literature shape parameter (κ) of GEV distribution should be a constant (Nguyen et al., 2008) for all the durations for rain gauge stations in a region. Also, this phenomenon is the fundamental requirement of extreme rainfall scaling by GEV distribution. GEV parameters estimated by NCM only shows this property for all selected rain gauge stations. For the illustration purpose estimated shape parameters of GEV distribution by NCM method and L moment are included in Table 4.3. According to the Table 4.3, it shows the estimated shape parameters by NCM method take very close values for all annual maximum series. The range of the shape parameter by NCM method shows highest value (0.1) at Geraldton station and second highest range (0.06) shows at Esperance station. The shape parameter range for all other stations by NCM method shows less than 0.05. However, shape parameter range takes high value for the L moment estimation. Merredin station shows the highest range (0.68) and Wongan Hills station shows the lowest range (0.17).

4.4.3 Evaluation of scaling behaviour of annual maximum rainfalls.

As NCM method is the most suitable GEV parameter estimating approach to study the scaling behavior of annual maximum rainfalls, NCM of observed annual maximum rainfalls is analyzed. To identify the scaling regimes, first three NCMs of observed rainfalls are calculated and plotted against its duration in

Figure 4.3. All the rain gauge stations except Geraldton, show two scaling regimes. Geraldton rain gauge station shows three scaling regimes (i.e. six minutes to 30 minutes, 30 minutes to six hours and six hours to 24 hours)

Table 4.3: Estimated shape parameter of GEV distribution by NCM method and L moment method.

Duration (h)	Bridgetown		Dwellingup		Esperance		Geraldton		Merredin		Pemberton		Perth Regional		Wongan Hills	
	NCM	LM	NCM	LM	NCM	LM	NCM	LM	NCM	LM	NCM	LM	NCM	LM	NCM	LM
0.1	0.25	-0.14	0.24	-0.10	0.22	-0.03	0.18	0.06	0.27	-0.39	0.26	0.19	0.25	-0.11	0.25	0.01
0.2	0.27	-0.17	0.27	-0.16	0.27	-0.16	0.27	0.18	0.27	-0.18	0.27	0.19	0.26	-0.05	0.27	0.04
0.5	0.28	-0.40	0.27	-0.18	0.27	-0.26	0.28	0.29	0.28	0.00	0.27	0.13	0.27	-0.15	0.28	0.03
1	0.28	-0.33	0.27	0.09	0.28	-0.40	0.28	-0.16	0.28	0.14	0.28	0.07	0.28	-0.18	0.28	-0.14
2	0.28	-0.21	0.28	0.28	0.28	-0.44	0.28	-0.19	0.28	0.29	0.28	0.00	0.28	0.05	0.28	-0.10
6	0.28	-0.01	0.28	0.12	0.28	-0.35	0.28	-0.12	0.28	0.15	0.28	0.23	0.28	0.16	0.28	-0.12
12	0.28	-0.15	0.28	0.03	0.28	-0.34	0.28	-0.18	0.28	0.07	0.28	0.22	0.28	-0.01	0.28	-0.15
24	0.28	-0.14	0.28	-0.17	0.28	-0.34	0.28	-0.01	0.28	-0.03	0.28	0.19	0.28	0.08	0.28	-0.21

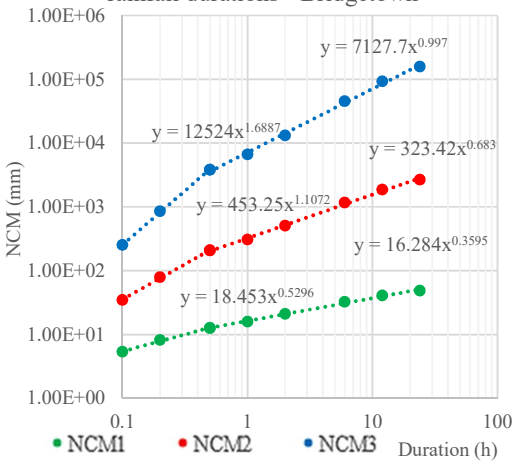
Scaling behaviour of NCM of different rainfall durations - Bridgetown
1.00E+06
1.00E+05
1.00E+04
1.00E+03
1.00E+02
1.00E+01
1.00E+00
NCM (mm)
y = 7127.7x^0.997
y = 12524x^1.6887
y = 323.42x^0.683
y = 453.25x^1.1072
y = 16.284x^0.3595
y = 18.453x^0.5296
0.1
1
10
100
Duration (h)
NCM1
NCM2
NCM3

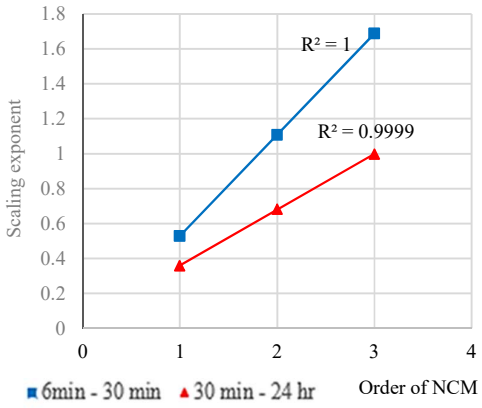
Behaviour of Scaling Exponent of NCM Bridge town
Scaling exponent
1.8
1.6
1.4
1.2
1
0.8
0.6
0.4
0.2
0
R² = 1
R² = 0.9999
0
1
2
3
4
6min - 30 min
30 min - 24 hr
Order of NCM

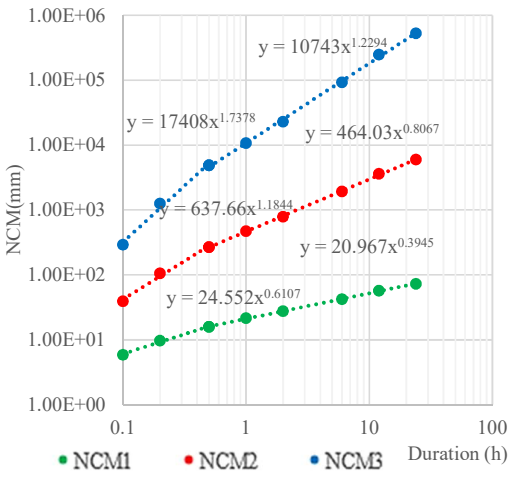
Scaling behaviour of NCM of different rainfall durations - Dwellingup
1.00E+06
1.00E+05
1.00E+04
1.00E+03
1.00E+02
1.00E+01
1.00E+00
NCM(mm)
y = 10743x^1.2294
y = 17408x^1.7378
y = 464.03x^0.8067
y = 637.66x^1.1844
y = 20.967x^0.3945
y = 24.552x^0.6107
0.1
1
10
100
Duration (h)
NCM1
NCM2
NCM3

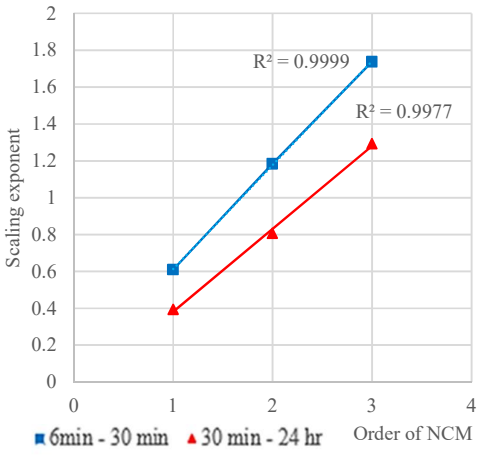
Behaviour of Scaling Exponent of NCM Dwellingup
Scaling exponent
2
1.8
1.6
1.4
1.2
1
0.8
0.6
0.4
0.2
0
R² = 0.9999
R² = 0.9977
0
1
2
3
4
6min - 30 min
30 min - 24 hr
Order of NCM

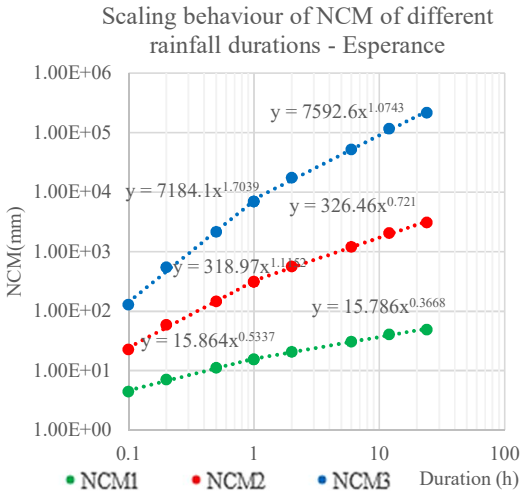
Scaling behaviour of NCM of different rainfall durations - Esperance
1.00E+06
1.00E+05
1.00E+04
1.00E+03
1.00E+02
1.00E+01
1.00E+00
NCM(mm)
y = 7592.6x^1.0743
y = 7184.1x^1.7039
y = 326.46x^0.721
y = 318.97x^1.1453
y = 15.786x^0.3668
y = 15.864x^0.5337
0.1
1
10
100
Duration (h)
NCM1
NCM2
NCM3

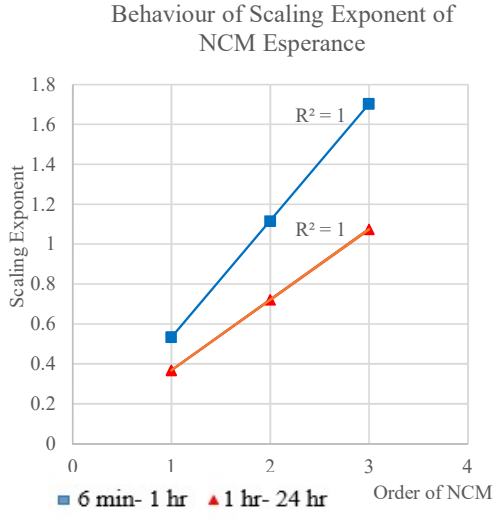
Behaviour of Scaling Exponent of NCM Esperance
Scaling Exponent
1.8
1.6
1.4
1.2
1
0.8
0.6
0.4
0.2
0
R² = 1
R² = 1
0
1
2
3
4
6 min- 1 hr
1 hr- 24 hr
Order of NCM

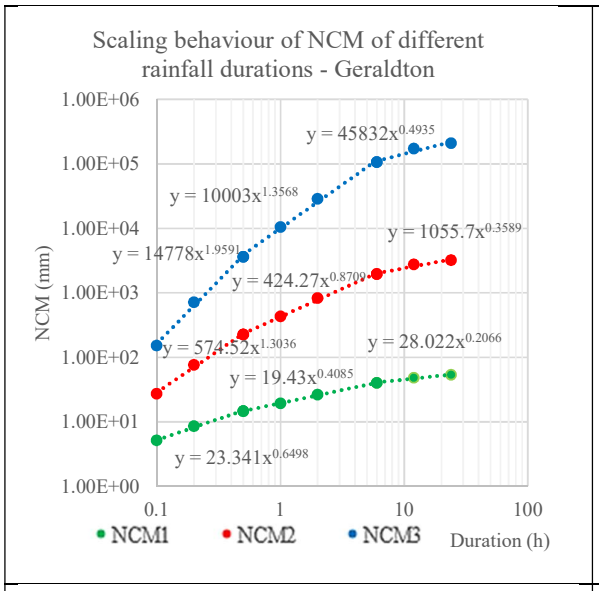
Scaling behaviour of NCM of different rainfall durations - Geraldton
NCM (mm)
1.00E+06
1.00E+05
1.00E+04
1.00E+03
1.00E+02
1.00E+01
1.00E+00
y = 45832x^0.4935
y = 10003x^1.3568
y = 1055.7x^0.3589
y = 14778x^1.9591
y = 424.27x^0.8709
y = 574.52x^1.3036
y = 28.022x^0.2066
y = 19.43x^0.4085
y = 23.341x^0.6498
0.1
1
10
100
NCM1
NCM2
NCM3
Duration (h)

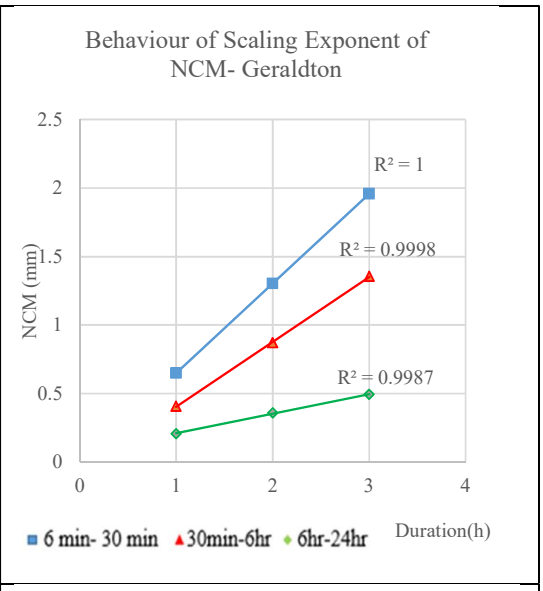
Behaviour of Scaling Exponent of NCM- Geraldton
NCM (mm)
2.5
2
1.5
1
0.5
0
R² = 1
R² = 0.9998
R² = 0.9987
0
1
2
3
4
6 min- 30 min
30min-6hr
6hr-24hr
Duration(h)

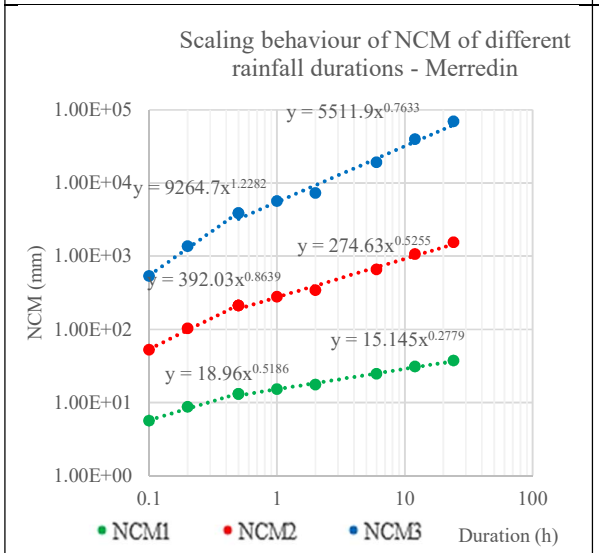
Scaling behaviour of NCM of different rainfall durations - Merredin
NCM (mm)
1.00E+05
1.00E+04
1.00E+03
1.00E+02
1.00E+01
1.00E+00
y = 5511.9x^0.7633
y = 9264.7x^1.2282
y = 274.63x^0.5255
y = 392.03x^0.8639
y = 15.145x^0.2779
y = 18.96x^0.5186
0.1
1
10
100
NCM1
NCM2
NCM3
Duration (h)

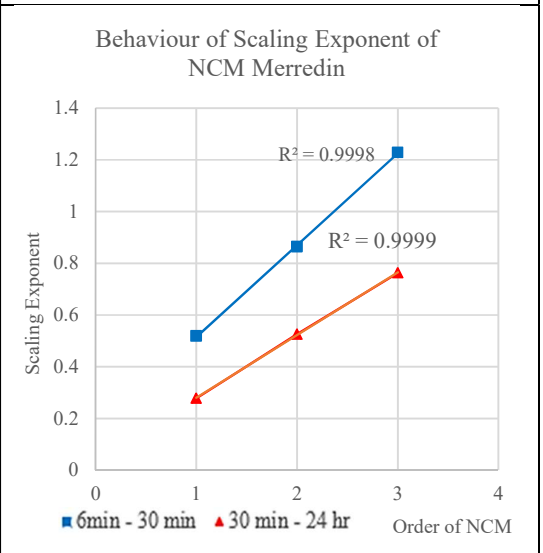
Behaviour of Scaling Exponent of NCM Merredin
Scaling Exponent
1.4
1.2
1
0.8
0.6
0.4
0.2
0
R² = 0.9998
R² = 0.9999
0
1
2
3
4
6min - 30 min
30 min - 24 hr
Order of NCM

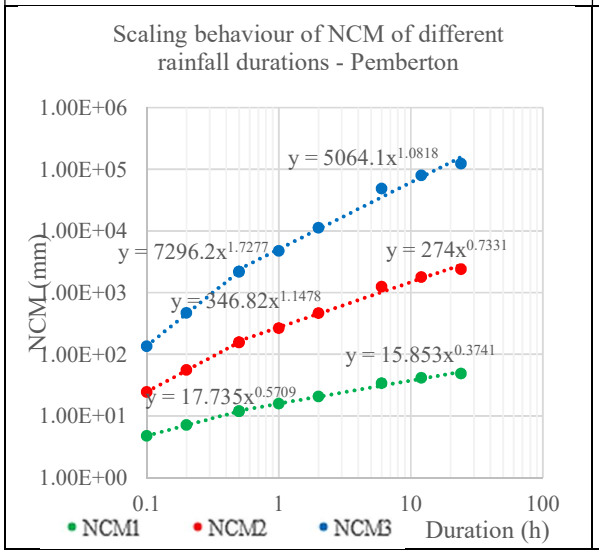
Scaling behaviour of NCM of different rainfall durations - Pemberton
NCM (mm)
1.00E+06
1.00E+05
1.00E+04
1.00E+03
1.00E+02
1.00E+01
1.00E+00
y = 5064.1x^1.0818
y = 7296.2x^1.7277
y = 274x^0.7331
y = 346.82x^1.1478
y = 15.853x^0.3741
y = 17.735x^0.5709
0.1
1
10
100
NCM1
NCM2
NCM3
Duration (h)

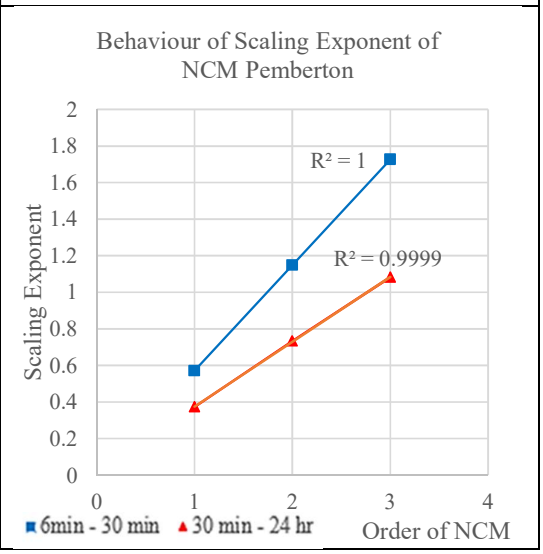
Behaviour of Scaling Exponent of NCM Pemberton
Scaling Exponent
2
1.8
1.6
1.4
1.2
1
0.8
0.6
0.4
0.2
0
R² = 1
R² = 0.9999
0
1
2
3
4
6min - 30 min
30 min - 24 hr
Order of NCM

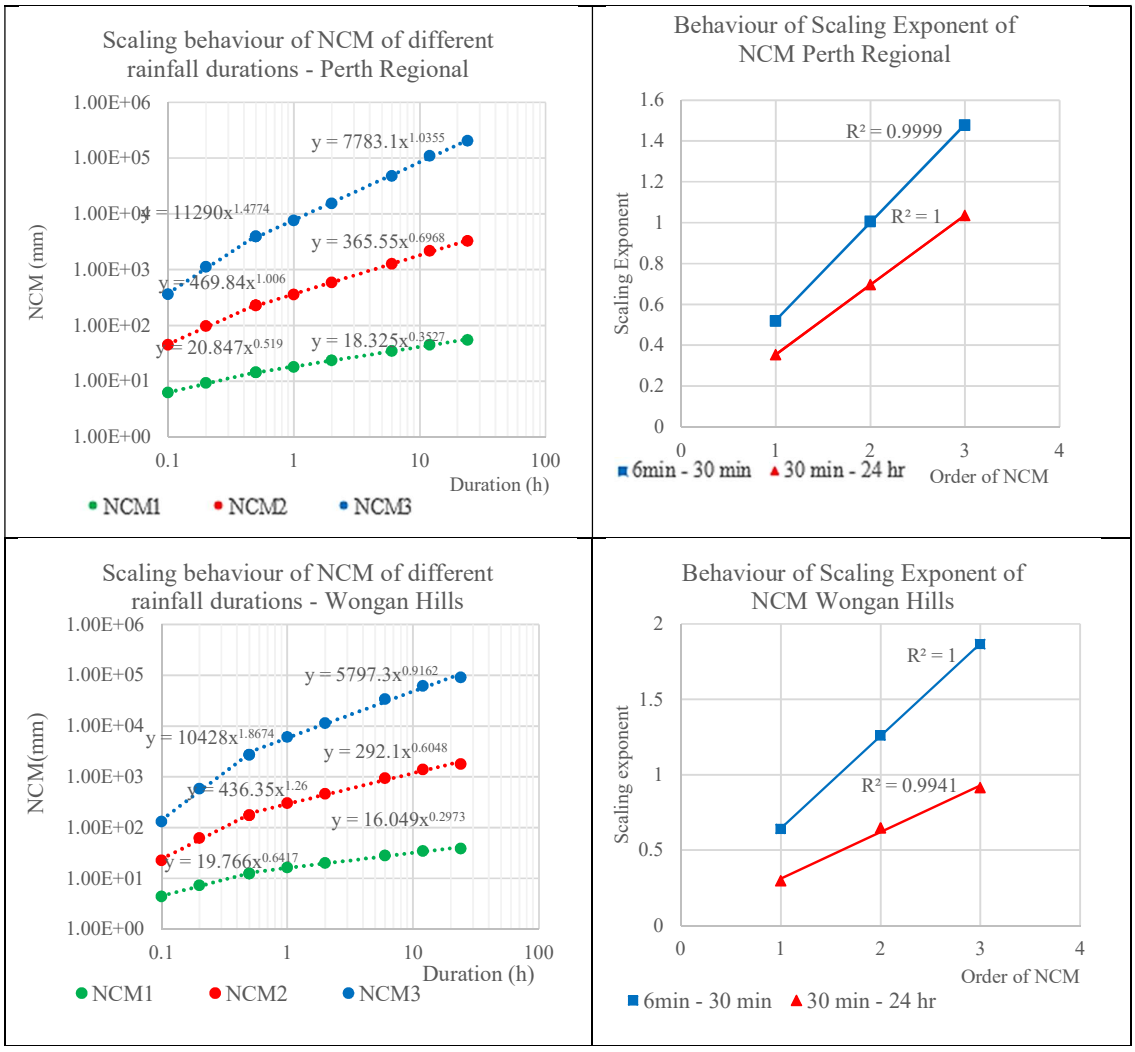

Figure 4.3: Evaluation of the scaling behaviour of annual extreme rainfall series (a) the scaling of first three NCMs (b) linearity of scaling exponents.

Table 4.4: Existing simple scaling time regimes of annual maximum rainfalls

Station	Scaling Time Regimes
Bridgetown	6min- 30min and 30min – 24h
Geraldton	6min- 30min, 30min– 6h and 6 h-24h
Dwellingup	6min- 30min and 30min – 24h
Esperance	6min- 1h and 1h – 24h
Merredin	6min- 30min and 30min – 24h
Pemberton	6min - 30min and 30min – 24h
Perth Regional	6min- 30min and 30min – 24h
Wongan Hills	6min- 30min and 30min – 24h

4.4.4 Estimation of statistical properties of sub-daily annual maximum series

In this step, the equations 4.21, 4.22 and 4.23 are used to estimate the statistical properties of sub-daily annual maximum rainfalls using statistical properties of daily annual maximum series. Then the estimated sub-daily GEV parameters are used to generate sub-daily quantiles for 6min, 12min, 30min, 1h, 2h, 6h, 12h and 24h. The estimated quantiles (from derived sub-daily data) were compared against the quantiles estimated from the observed data using RMSE, NSE and PBIAS to evaluate the accuracy of proposed approach. Table 4.5 presents the average values of these goodness-of-fit tests between the estimated quantiles by NCM scaling method and observed data. These goodness-of-fit tests show, NCM based scaling approach is highly capable to estimate the sub-daily statistical properties of annual maximum rainfalls using the statistical properties of daily rainfalls.

Table 4.5: Goodness-of-fit test results (average of 6 min to 24 h rainfall events) for scaled quantiles and observed rainfalls.

Station	RMSE	NSE	PBIAS
Bridgetown	3.27	0.82	0.00041
Geraldton	3.83	0.72	0.00042
Dwellingup	4.73	0.65	0.00038
Esperance	6.20	0.72	0.00059
Merredin	2.39	0.83	0.00048
Pemberton	1.84	0.99	0.00025
Wongan Hills	2.61	0.90	0.00051
Perth Regional	1.96	0.88	0.00029

To further confirmation of the accuracy of proposed approach, downscaled annual maximum rainfalls using NCM based temporal downscaling model is compared with the observed rainfall values. For the illustration purpose, probability plots of annual maximum rainfalls are presented in Figure 4.4 and Figure 4.5 for Wongan Hills and Dwellingup stations respectively. Figure 4.4 presents 2h and 12min rainfalls at Wongan Hills and Figure 4.5 presents 6h and 12min rainfalls at Dwellingup stations. These figures depict the accuracy of NCM scaling approach in temporal

disaggregating of daily rainfalls. Further, probability plots for all other stations are presented in Appendix.

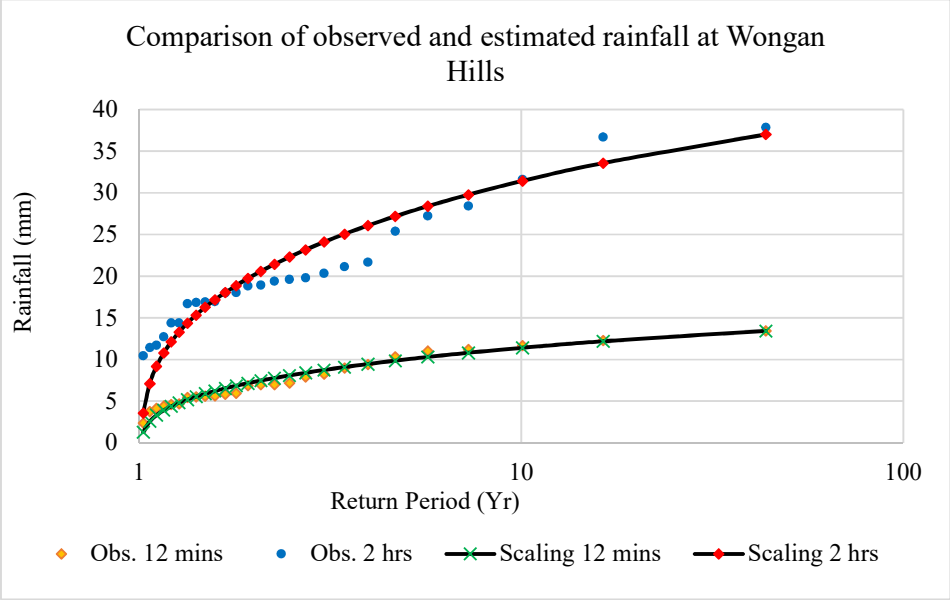

Figure 4.4: Probability plot of observed and estimated rainfalls at Wongan Hills

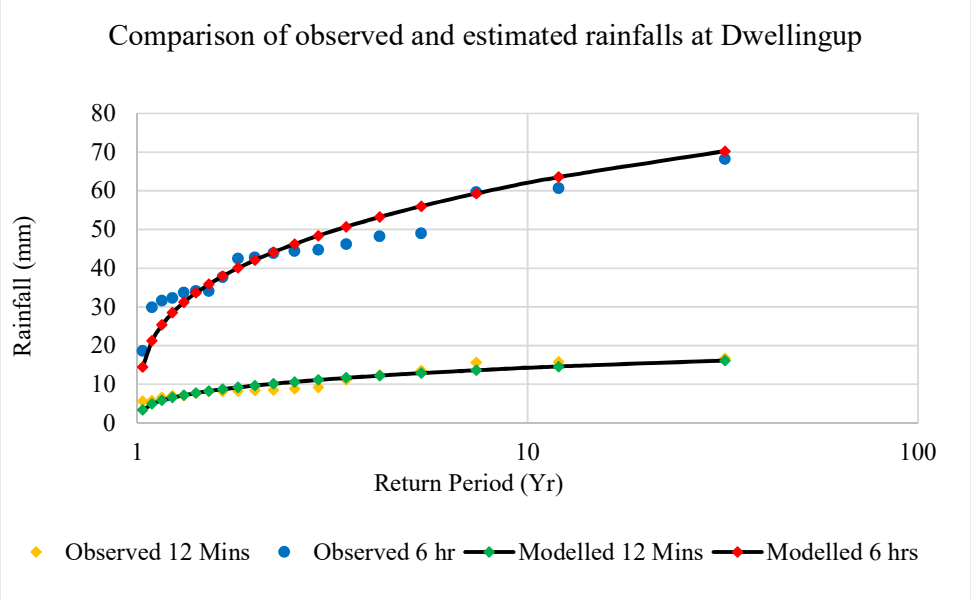

Figure 4.5: Probability plot of observed and estimated rainfalls at Dwellingup.

Also, modelled sub-daily rainfalls are compared with observed rainfalls by Quantile-Quantile (Q-Q) plot. For the illustration purpose Q-Q plot of Merredin and Geraldton

rain gauge stations are presented in Figure 4.6 and Figure 4.7 respectively. These Q-Q plots also show high accuracy of proposed NCM method to estimate the GEV parameters in scaling studies.

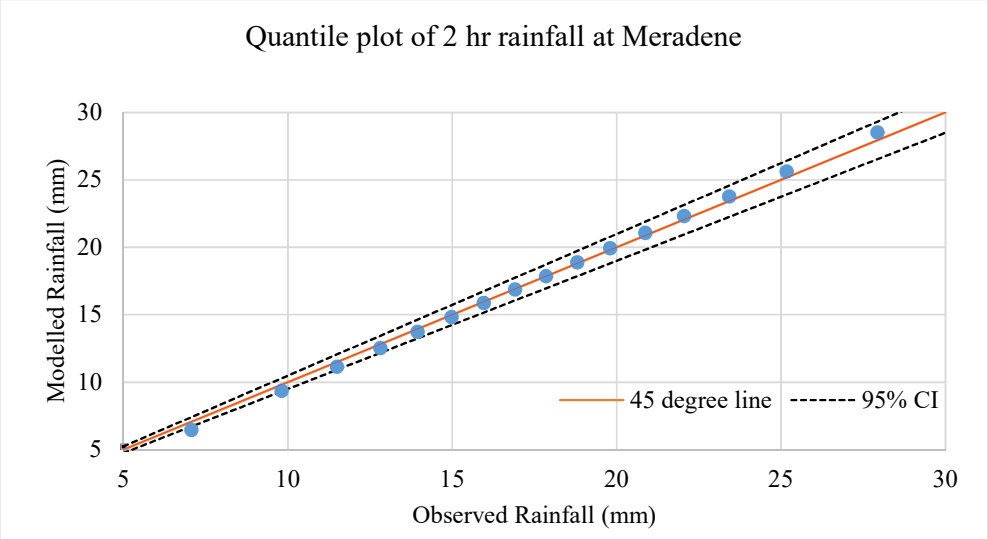

Figure 4.6: Comparison of 2h modelled and observed rainfall at Merredin

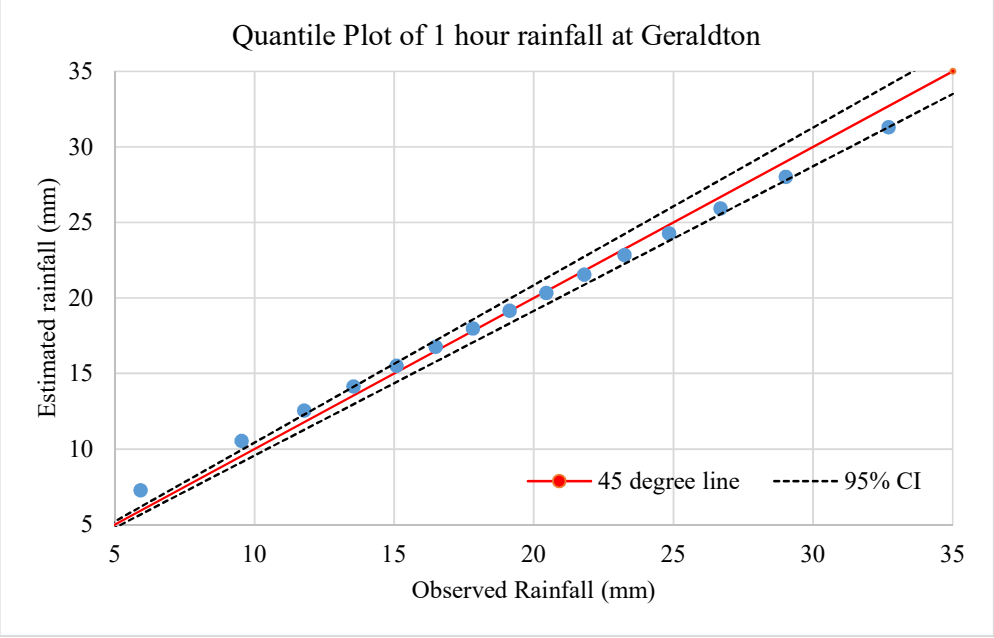

Figure 4.7: Comparison of 1 hour modelled and observed rainfall at Geraldton

Finally, estimated statistical properties of sub-daily rainfalls by proposed NCM method are used to develop IDF relations for sub-daily events. IDF relations are developed to 2, 5, 10, 20, 50 and 100 year return periods from 24 hours to 6 minutes rain durations. For the illustration purpose, developed IDF curves for Bridgetown and Geraldton are presented in Figure 4.8. Developed IDF curves for other stations are presented in Appendix. According to developed IDF curves Pemberton and Wongan Hills IDF relations show comparatively low rainfall depths respect to other six stations. Furthermore, these developed IDF curves show slightly less rainfall depth than the rainfall depth in BoM IDF curves. Table 4.6 presents a comparison between BoM and estimated 1 hour rainfall depth at 10 years return period. It shows that Pemberton estimation differs 22.8% from the BoM value. All the other stations show less than 15% difference. Differences in analysing techniques, analysing periods can be identified as the main reasons for this difference. However, Dwellingup and Perth Regional stations show high agreement between BoM and estimated depth by this study.

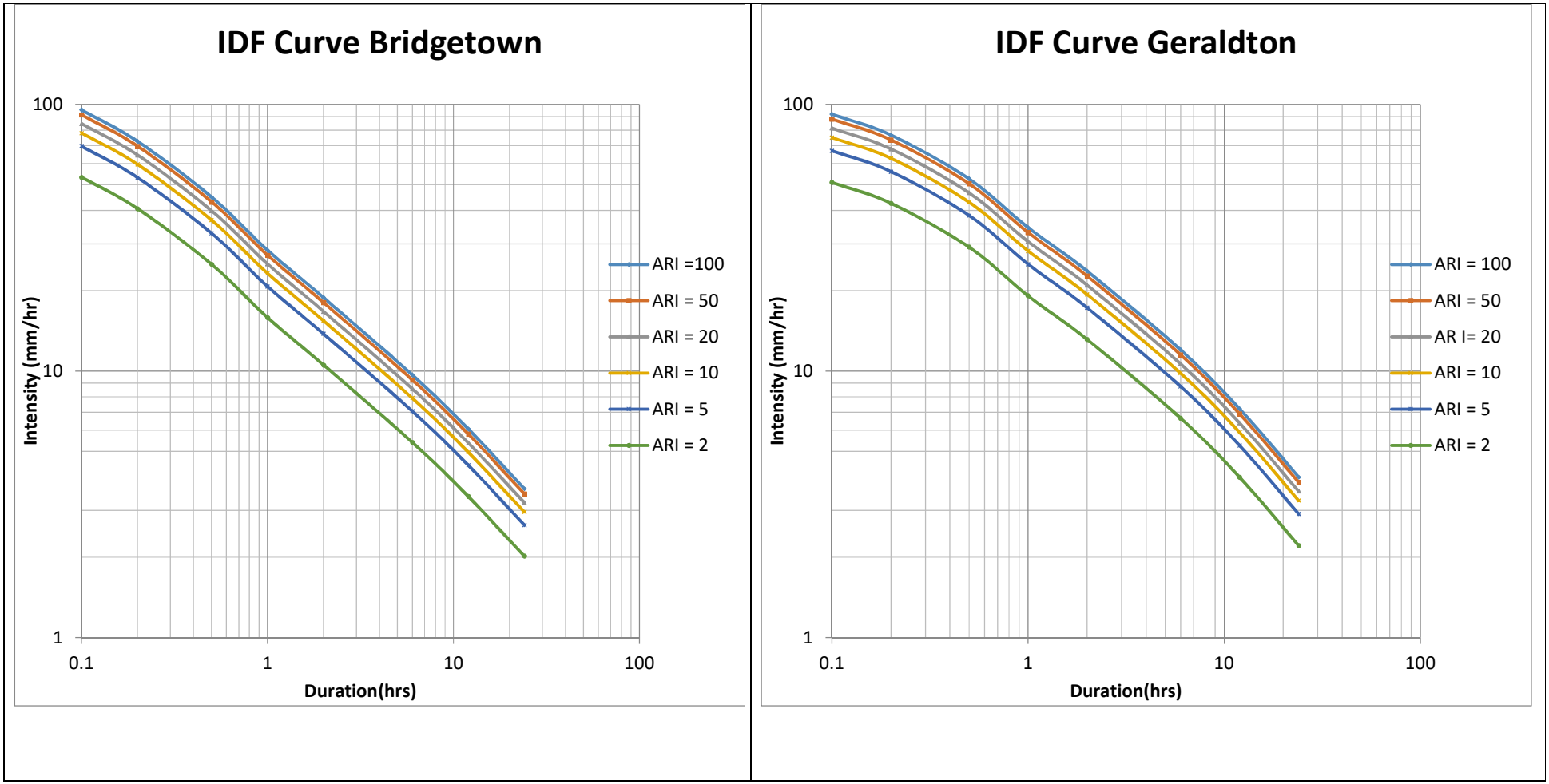

Figure 4.8: Developed IDF curves by temporal downscaling of daily rainfalls

Table 4.6:Comparison of BoM and estimated rainfall depth for 1 hour in 10 year return period

Station	BoM	Estimated	Difference (%)
Bridgetown	25.7	23.2	9.7
Dwellingup	33	31.4	4.8
Esperance	23.2	26.1	-12.5
Geraldton	31.1	28.2	9.3
Merredin	25.3	21.8	13.8
Pemberton	25	19.3	22.8
Perth Regional	25.4	24.6	3.1
Wongan Hills	28.3	25.3	10.6

4.5 Summary

IDF relations play remarkable role in estimating of design storms in hydraulic structures designing. Frequency analysis of annual maximum rainfall is a popular method of constructing IDF relations. However, observed sub-daily rainfall data are not available in most of the rain gauge stations for a long period and it causes inaccurate IDF relations. To overcome the problem of lack of sub-daily data, various techniques are used. Temporally downscaling/ disaggregation of daily rainfall into sub-daily rainfall is a one of very popular techniques. This study explains NCM based scaling approach to use in temporal downscaling of daily rainfalls at eight rain gauge stations in Western Australia.

Main outcomes of this chapter are;

- GEV distribution is a capable probability distribution function to describe the annual maximum rainfall events of the selected stations.
- L moment method and NCM method are more accurate than MLE method in GEV parameter estimating for the selected rain gauge stations.
- Only NCM method estimates constant shape parameter for annual maximum rainfalls for all the time durations of a station. Therefore, only NCM method provide a platform to temporal downscaling of daily rainfall using GEV distribution.

- Estimated GEV quantiles for sub-daily rainfall events by NCM methods are useful in constructing IDF curves for ungauged and stations with low-resolution rainfall data.

.

CHAPTER 5

5 Temporal downscaling of daily rainfall for future periods in the context of climate change

Extended from

Herath, S.M., Sarukkalige, R. and Nguyen, V. T. V., 2016. A spatial temporal downscaling approach to development of IDF relations for Perth airport region in the context of climate change. Hydrological Sciences Journal, 61, 2061-2070.

Herath, S.M., Sarukkalige, R. and Nguyen, V. T. V., 2015, Downscaling approach to develop future sub-daily IDF relations for Canberra Airport Region, Australia, Proceedings of the International Association of Hydrological Sciences. PIAHS, , 369, 147–155. doi: 10.5194/piahs-369-147-2015.

5.1 Introduction

Temporal downscaling of daily rainfalls is equally important in hydrological assessments, especially for small urban watersheds. In particular, the development of the IDF relations for sub-daily rainfalls is required for planning and design of urban drainage systems. Therefore, the main objective of this chapter is to describe an approach of temporal downscaling which estimates sub-daily IDF relations for future periods using the spatially downscaled daily rainfalls (described in chapter 3). Further, this study aims to evaluate the applicability of proposed approach for seven major cities in Australia. The results of this study will be helpful in climate change impacts assessments which are required design rainfall data with fine spatial and temporal resolution.

Seven rain gauge stations located in seven states in Australia are subjected to this study. (Adelaide, Canberra, Melbourne, Perth, Darwin airport rain gauge stations, Sydney observatory hill and Brisbane regional rain gauge station are selected for this study). Study area map is presented in Figure 5.1

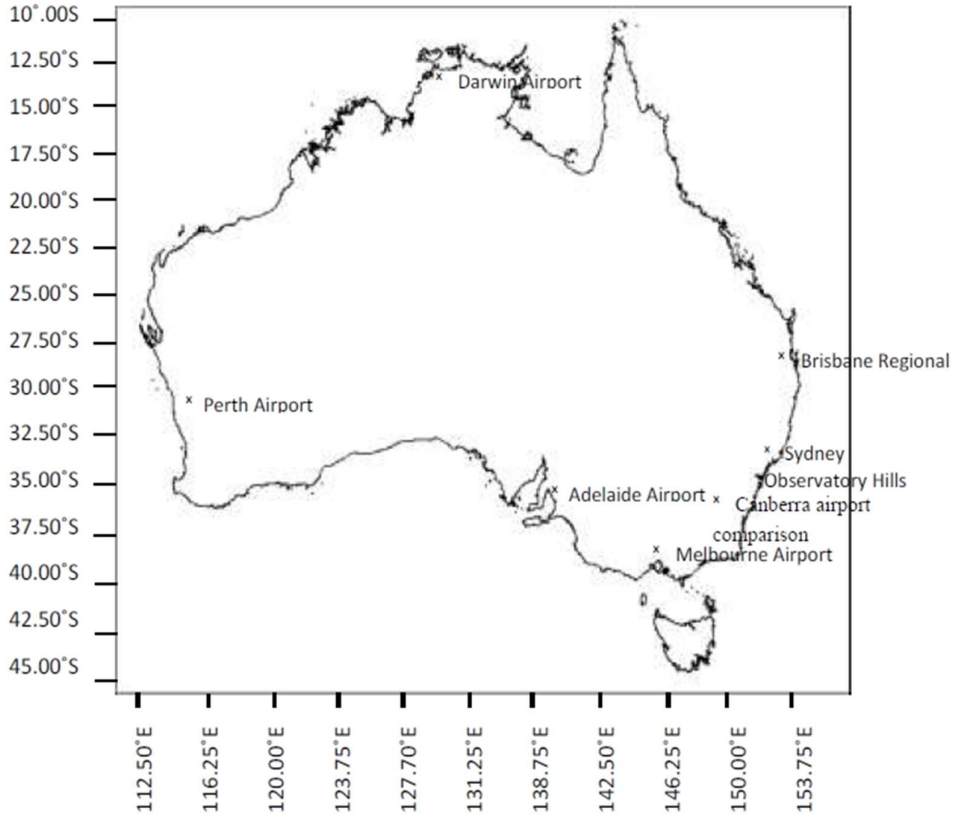

Figure 5.1: Location map of the study area

Australian BoM is one of the main organizations of providing weather and climate data in Australia. For this study, pluviometer six minute rainfall data are collected from BoM. When selecting weather stations for the study, length and completion percentages of the weather records are considered. Full detail of seven stations subjected to this study are included in Table 5.1

Table 5.1: Details of weather stations

State	Weather Station Name	BoM Station ID	Data period
New south wales	Sydney observatory hill	66062	1913-2010
Victoria	Melbourne airport	86282	1971-2010
Western Australia	Perth airport	09021	1961-2010
Northern Territory	Darwin airport	14015	1954-2010
South Australia	Adelaide airport	23034	1971-2010
Queensland	Brisbane regional	40214	1908-1994
Australian Capital territory	Canberra airport comparison	70014	1938-2010

5.2 Methodology of developing IDF relations

To illustrate the methodology of developing IDF relations for future periods, Perth airport rain gauge station is taken as a case study. Spatial downscaling of future daily rainfall for Perth airport region using HadCM3–A2 and CGCM3-A2 scenarios has been described in Chapter 3. These spatially downscaled daily rainfalls are subjected to further temporal downscaling to investigate the sub-daily IDF relations for future periods.

5.2.1 Bias correction of annual maximum daily rainfalls downscaled by SDSM

Most of the rainfall modellings in the context of climate change, bias corrections are required to obtain high accurate results. In this study regression based bias correction technique is used to improve the accuracy of spatially downscaled annual maximum daily rainfall. Literature shows that similar bias correction approach have been successfully applied in extreme rainfall downscaling studies (Nguyen and Nguyen, 2008)

Equation 5.1 and 5.2 describe the bias correction approach which is applied in this study.

$$P_\tau = P_{o\tau} + e_\tau \quad (5.1)$$

in which P_τ denotes the adjusted annual maximum daily rainfall at a probability level τ, $P_{o\tau}$ denotes the corresponding GCM–SDSM estimated annual maximum daily rainfall and e_τ denotes the residual (bias) associated with $P_{o\tau}$.

Then, e_τ is estimated using the third order regression function as follows.

$$e_\tau = a.P_{0\tau}^3 + b.P_{0\tau}^2 + c.P_{0\tau} + d + e \quad (5.2)$$

In which a, b, c and d are the parameters of the regression function, and e is the resulting error term.

5.2.2 Temporal downscaling (Temporal disaggregation)

GEV distribution is known as a highly capable cumulative distribution function to describe extreme rainfall depths. As presented at equation 2.1 in section 2.4.4 in literature review, GEV distribution is a three-parameter function and these three parameters are known as location, scale and shape parameters.

In literature, few different methods are available for estimating the GEV parameters; Method of Probability Weighted Moment (Hosking et al., 1985), Maximum Likelihood Estimation (Phien and Fang, 1989), Method of L-Moment (Hosking, 1990) and Non Central Moment (NCM) (Nguyen et al., 1998). As presented in Chapter 4, for the temporal downscaling of spatially downscaled daily data, the NCM is used in this study as it is the most appropriate method to use with the scale invariance concept (Nguyen et al., 2008, Nguyen et al., 2002, Nguyen et al., 1998) to describe the proposed downscaling approach.

The k^{th} order NCM, (μ_k) of the GEV distribution (for $\kappa \neq 0$) is presented at equation 2.3 in literature review. Using equation 2.3, three independent equations are derived to

solve the location, scale and shape parameters of GEV distribution which is fitted to 24 hours observed annual maximum rainfall series. In the next step, by considering the scaling behaviour of extreme rainfall, statistical relations are derived between observed daily and sub-daily rainfall. These relations are shown in equations 2.6, 2.7, 2.8 and 2.9 in literature review. Based on these relations, statistical properties of sub-daily extreme rainfall are estimated for sub-daily rainfalls. Finally, estimated daily and sub-daily quantiles for different return periods are utilized to develop IDF curves for the region of study.

5.3 Results: Temporal downscaling of Perth Airport

From now on, proposed methodology is illustrated by a worked example of Perth Airport rain gauge station. Spatial downscaling of future rainfall of Perth airport has been discussed in Chapter 3 using A2 scenarios of HadCM3 and CGCM3. These spatial downscaled daily rainfall series is subjected to temporal downscaling in this case study. In the later part of this chapter (section 5.4) it proves the applicability of proposed methodology for all other main cities in Australia.

5.3.1 Bias correction of spatial downscaled annual maximum daily rainfalls.

Even though the SDSM model is capable of simulating spatially downscaled daily rainfall average values, it is unable to downscale high accurate annual extreme rainfall series for a long period. Especially, when the different climate factors (which are not considered in SDSM predictor selection) leads extremely high rainfall event in a specific year, considerable difference can be identified between downscaled and observed rainfall depths. Therefore, spatially downscaled daily maximum rainfalls should be subjected to a bias correction to obtain high accurate annual maximum rainfall series.

To minimize the bias associated with spatially downscaled daily data, a regression relationship is developed between simulated annual maximum daily rainfalls and their bias for the calibration period (1961-1975). As the first step in bias correction process, associated bias [the difference between annual maximum downscaled rainfalls (mean of annual maximum rainfalls of 100 ensembles) and observed rainfalls] at probability

level τ is calculated. Then a regression function is developed to describe the bias associated with downscaled rainfall. Finally, downscaled rainfall is adjusted by estimated bias at all probability levels. Figure 5.2 and Figure 5.3 describe fitted third order regression function to bias which is associated with HadCM3-A2 and CGCM3-A2 simulated values. According to Figure 5.2, when the SDSM simulated value is at 50-60 mm range, it shows the lowest bias for both GCMs. Furthermore, the bias values show relatively high value for the both tail ends which are simulated by SDSM. Similar behaviour of SDSM model is reported in the literature by other researchers (Nguyen and Nguyen, 2008).

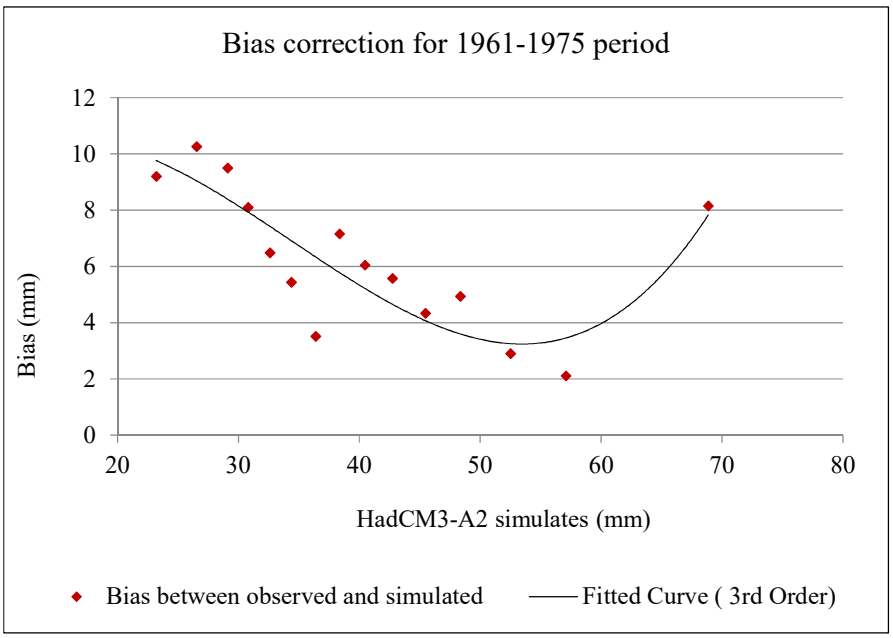

Figure 5.2: Development of bias correction function for annual maximum daily rainfall downscaled by HadCM3-A2

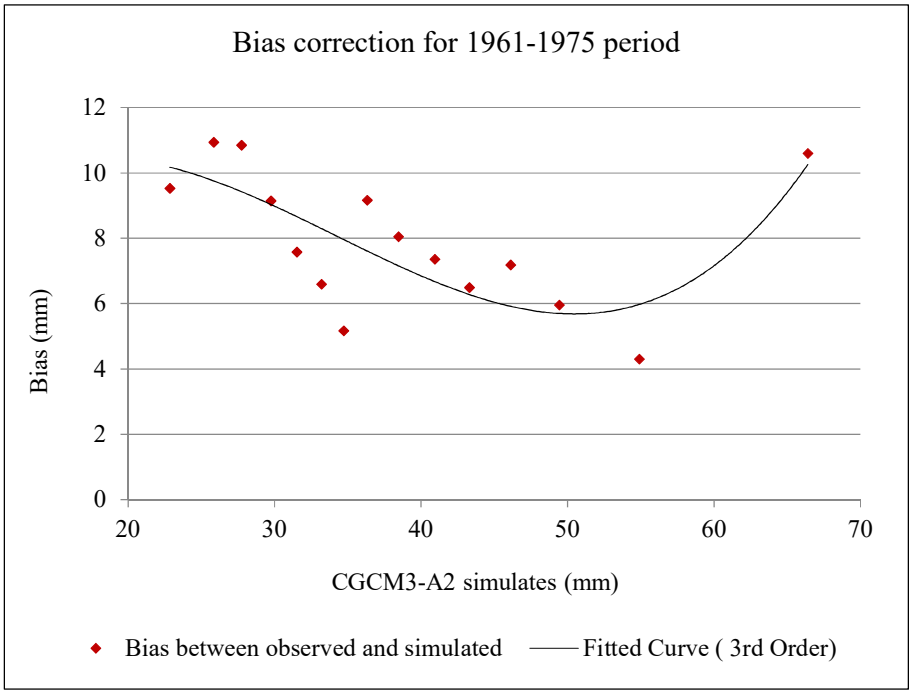

Figure 5.3: Development of bias correction function for annual maximum daily rainfall downscaled by CGCM3-A2

Bias-corrected annual maximum daily rainfall data has been used to produce probability plot to confirm the accuracy of the developed bias correction. Figure 5.4 and Figure 5.5 show the probability plots of observed annual maximum daily rainfalls and simulated rainfall from HadCM3-A2 and CGCM3-A2 for the calibration period respectively. According to Figure 5.4 and Figure 5.5, without bias correction, the simulated annual maximum daily rainfall by HadCM3-A2 and CGCM3-A2 do not show a strong agreement with the observed data. By applying a third order bias correction function, it could obtain a strong agreement with the observed annual maximum rainfalls verifying the accuracy of proposed bias correction functions.

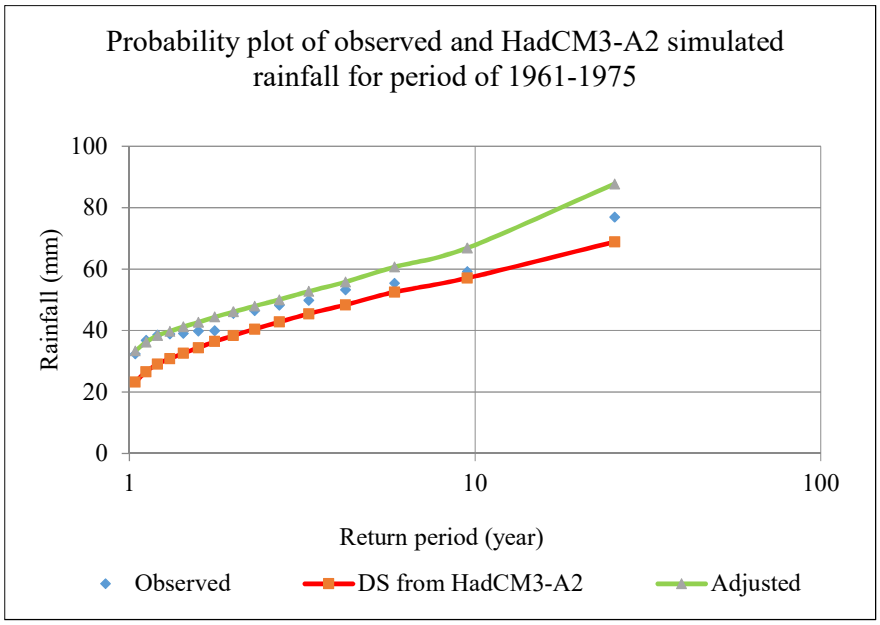

Figure 5.4: Probability plots of annual maximum daily rainfalls downscaled from HadCM3-A2 for the calibration period (1961-1975).

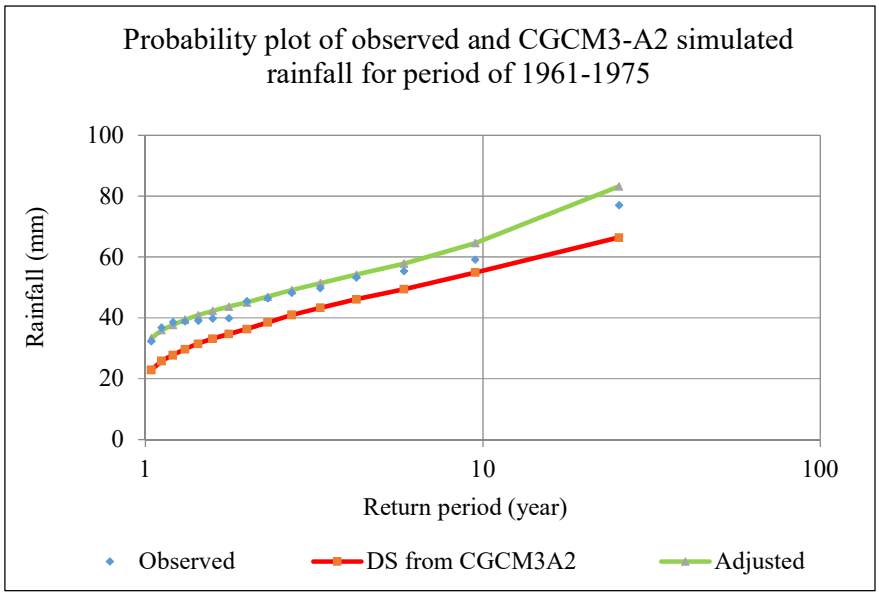

Figure 5.5: Probability plots of annual maximum daily rainfalls downscaled from CGCM3-A2 for the calibration period (1961-1975).

Furthermore, to confirm the accuracy of developed bias correction functions, same bias correction function (which is developed for the calibration period) is applied to the validation period. Figure 5.6 and Figure 5.7 present the probability plot of annual

maximum daily observed rainfalls and simulated rainfalls from HadCM3-A2 and CGCM3-A2 for the validation period (1976-1990). Moreover, Figure 5.6 and Figure 5.7 confirm the suitability of proposed third order bias correction functions in rectifying the associated bias with SDSM's estimations for the validation period. In addition to visual confirmation of bias rectification, goodness-of-fit tests are carried out on originally downscaled and bias corrected rainfalls comparing with observed data. Calculated RMSE, Nash–Sutcliffe Model Efficiency Coefficient (NSE) and Percentage bias (PBIAS) values are shown in Table 5.2. These goodness-of-fit tests confirm that high improvement can be obtained by applying third order bias correction to the downscaled annual maximum daily rainfalls over the calibrating and validating period of selected study area. By considering the accuracy of developed bias correction functions, they are utilized to improve the accuracy of simulated annual maximum daily rainfall for the future periods.

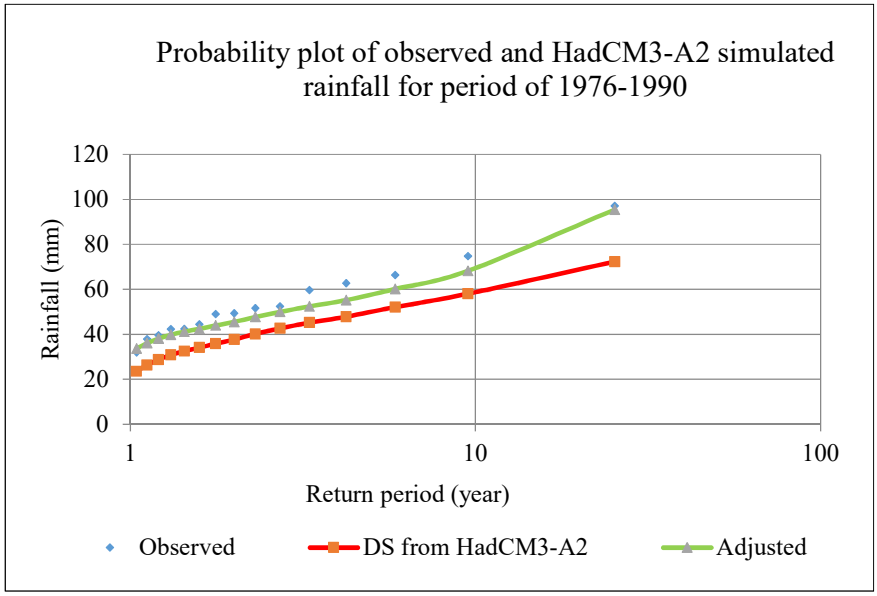

Figure 5.6: Probability plots of annual maximum daily rainfalls of downscaled from HadCM3-A2 for the validation period (1976-1990)

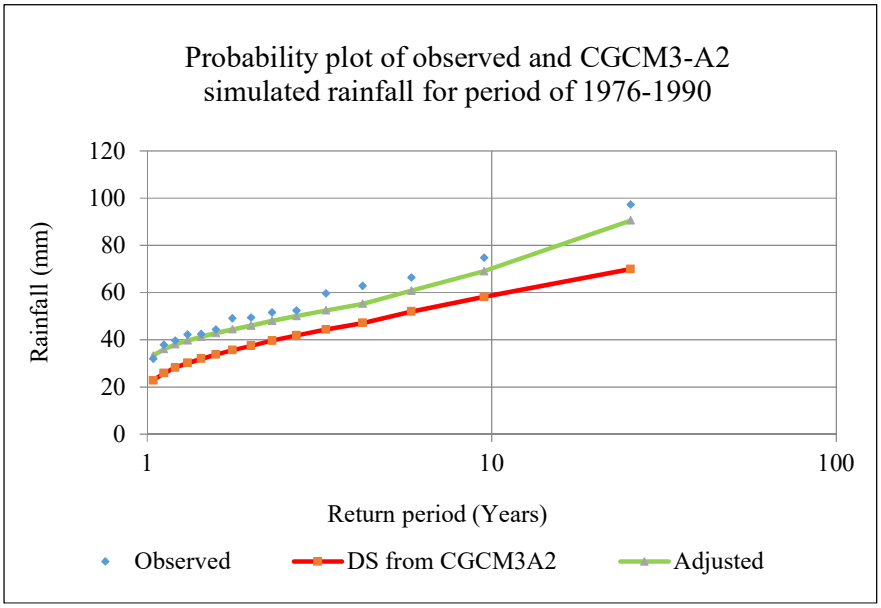

Figure 5.7: Probability plots of annual maximum daily rainfalls of downscaled from CGCM3-A2 for the validation period (1976-1990)

Table 5.2: Accuracy of proposed bias correction in terms of goodness-of-fit tests.

Goodness-of-fit test	Scenario	Period of 1961-1975		Period of 1976-1990	
		Before bias correction	After bias correction	Before bias correction	After bias correction
RMSE	HadCM3-A2	6.69	4.15	13.50	4.28
NSE		0.62	0.86	0.30	0.93
PBIAS		0.13	-0.06	0.24	0.06
RMSE	CGCM3-A2	8.17	2.64	14.15	7.33
NSE		0.44	0.94	0.24	0.93
PBIAS		0.17	-0.04	0.25	0.07

5.3.2 Temporal downscaling

Spatially downscaled rainfalls are subjected to a temporal downscaling process to develop IDF relations for sub-daily extreme rainfalls. Identifying the scaling behaviour of the observed annual maximum rainfall series is the main requirement of the temporal downscaling approach. To identify the scaling time regime of observed

rainfalls in 1961-1990 period, a log – log plot of first three non-central moments of the observed annual maximum rainfalls against rainfall durations is developed (Figure 5.8). According to Figure 5.8, power law dependency of rainfall statistical moments with duration is observed and it is identified in one time regime (30 mins to 24 h.). In addition, behaviour of scaling exponent (λ^{β}) of the first three non-central moments of the observed annual maximum rainfall is assessed and it is included in Figure 5.9. This Figure depicts the linearity of scaling exponent with the moment order. These linear relationships verify the applicability of the simple scaling model to describe extreme sub-daily rainfall events using available daily extreme rainfall.

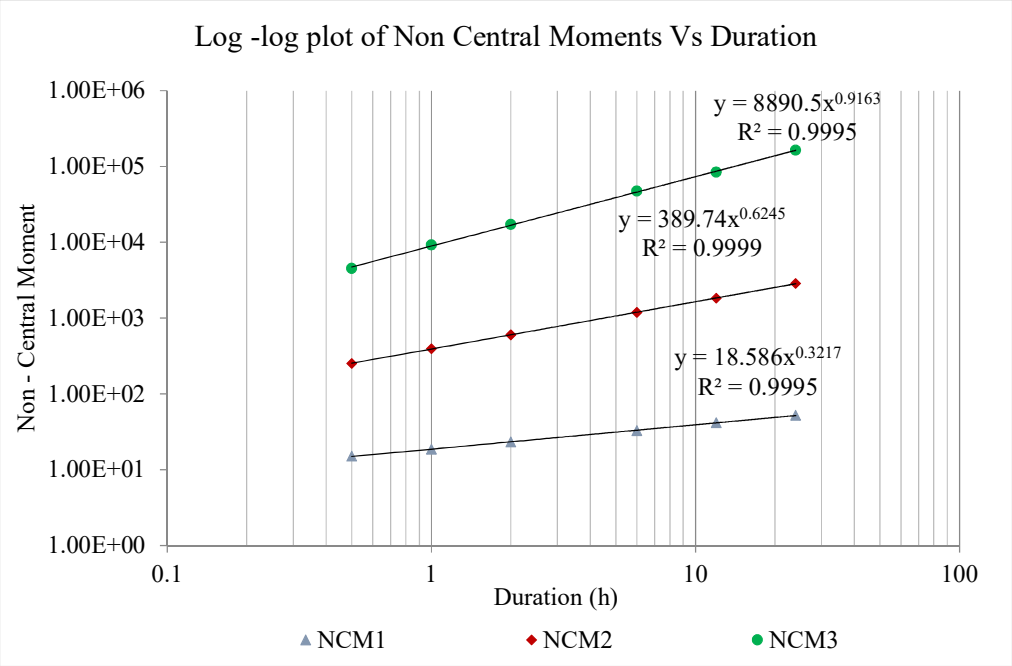

Figure 5.8: Log-Log plot of first three NCM of observed annual maximum rainfall versus durations for period of 1961-1990.

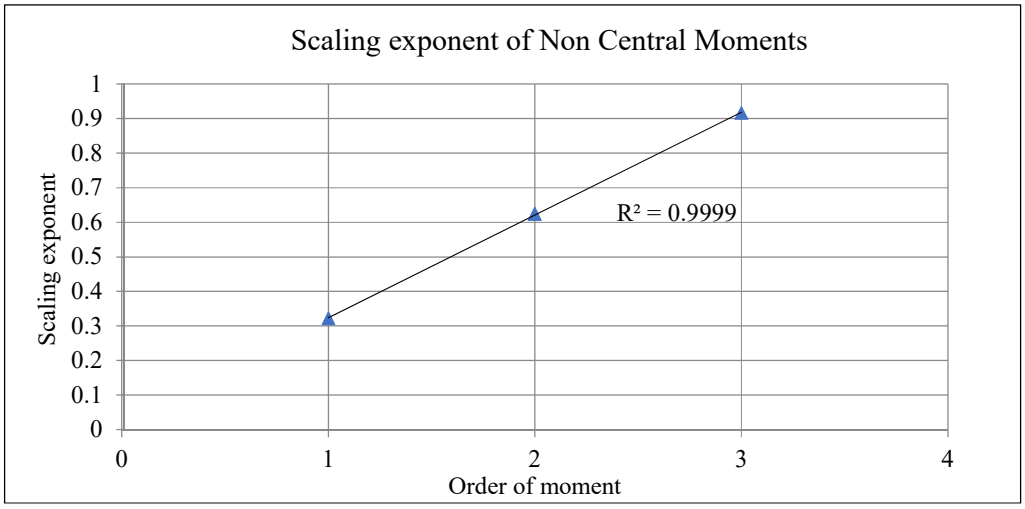

Figure 5.9: Scaling exponent of the first three NCM.

Before applying the scaling concept to daily extreme rainfall data, the suitability of GEV distribution to describe the annual maximum daily rainfall is analysed using the visual plot of fitted GEV (cumulative distribution) function against observed annual maximum rainfall data. Figure 5.10 shows that the GEV fits well to the observed annual maximum daily data, which confirms the applicability of GEV to describe the statistical properties of annual maximum daily rainfall series of the Perth airport rain gauge station.

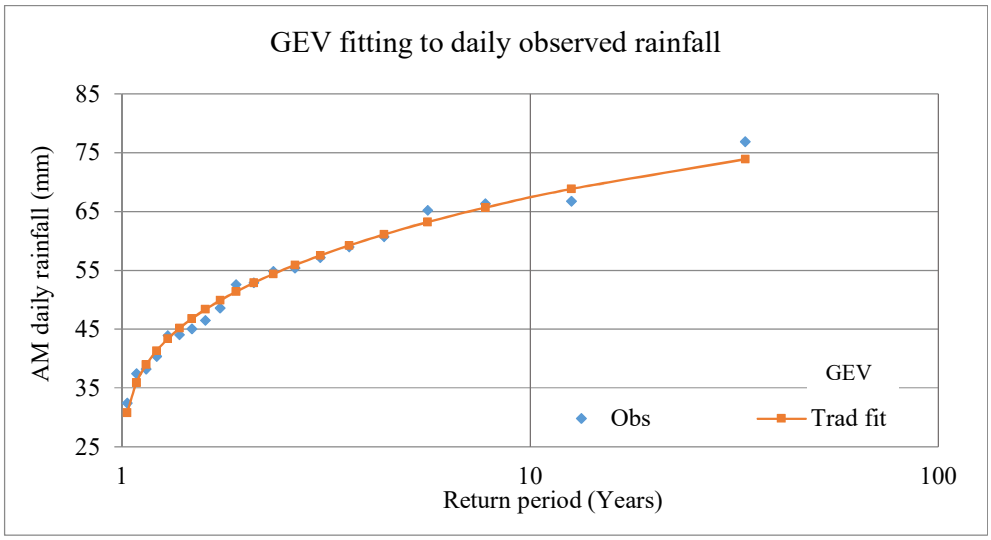

Figure 5.10: Comparison of GEV distribution fit to the observed annual maximum daily rainfalls at Perth Airport.

Then, above verified scaling concept is applied to obtain the statistical properties of GEV distributions which describe the sub-daily annual maximum rainfalls. Figure 5.11 and Figure 5.12 illustrate the capability of the scaling model to reproduce sub-daily extreme rainfall series.

Figure 5.11 portrays the comparison between the observed 30-minute rainfall extremes and the values estimated by the GEV fitted and the values estimated by the scaling GEV distribution. According to the closeness of estimated values to the perfect fit (45^0) line, suitability of proposed scaling method in sub-daily extremes modelling is verified. Further, Figure 5.12 illustrates the accuracy of estimating sub-daily rainfall by scaling bias corrected daily HadCM3-A2 simulated data. In Figure 5.12, Q-Q plot of HadCM3-A2 estimation (bias corrected) and GEV fit series show the high accuracy of scaling method in sub-daily rainfall estimation. Figure 5.13 presents similar results for CGCM3-A2. Further to evaluate the performance of constructed models, RMSE, NSE coefficient and PBIAS values are estimated for 1961-1990 period between observed sub-daily rainfalls and downscaled rainfalls. Calculated coefficients (RMSE, NSE, PBIAS) are included in Table 5.3 Estimated RMSE value for sub-daily rainfall using HadCM3 and CGCM3 varies between 1.28–4.53 and 1.31-4.7 respectively. Calculated NSE coefficients are very close to 1 (0.85- 0.93 for HadCM3-A2 and 0.83-0.92 for CGCM3-A2) and PBIAS coefficients are very close to 0 (-0.01-0.06 and 0.01-0.08 for HadCM3 and CGCM3 respectively). These agreements confirm the accuracy of proposed spatial and temporal downscaling approach in estimating the sub-daily annual maximum extreme rainfall for Perth airport region.

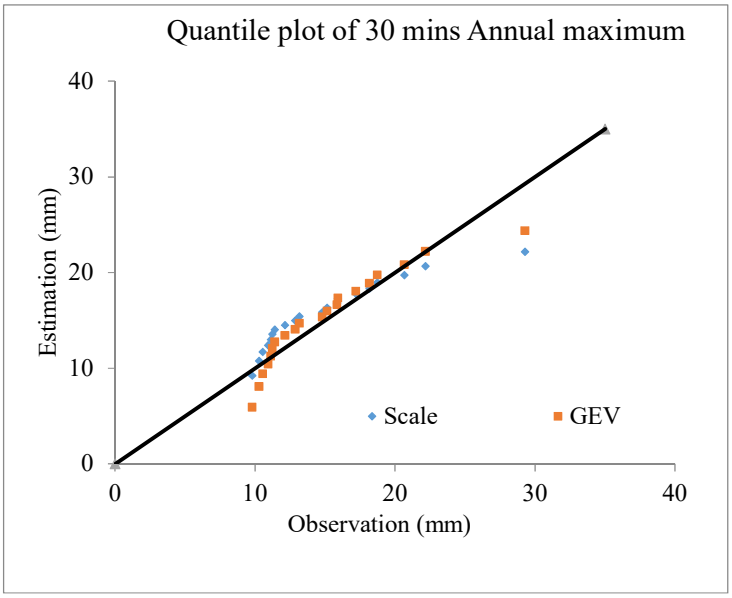

Figure 5.11: Comparison of annual maximum 30 minutes rainfalls obtained by GEV fitting, scaling and observation at Perth Airport

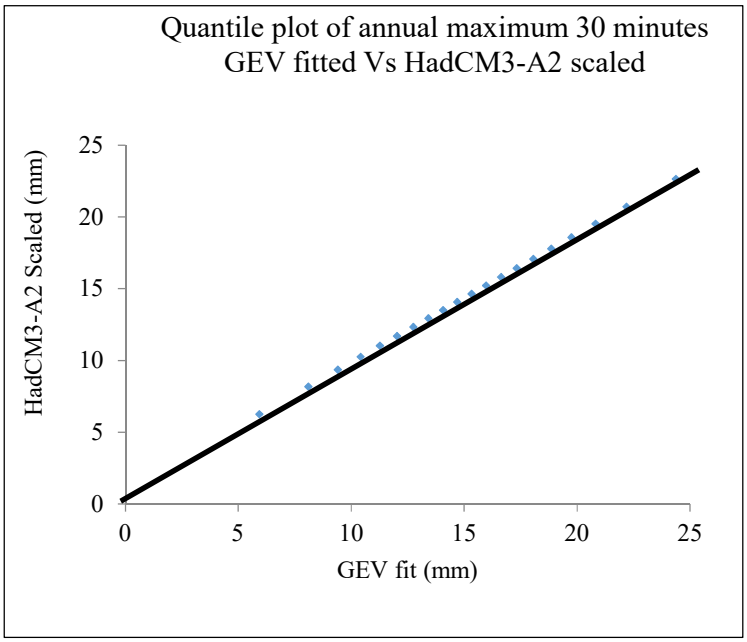

Figure 5.12: Comparison of GEV fitted annual maximum 30 minutes rainfall with scaled annual maximum daily rainfall at Perth Airport for HadCM3-A2

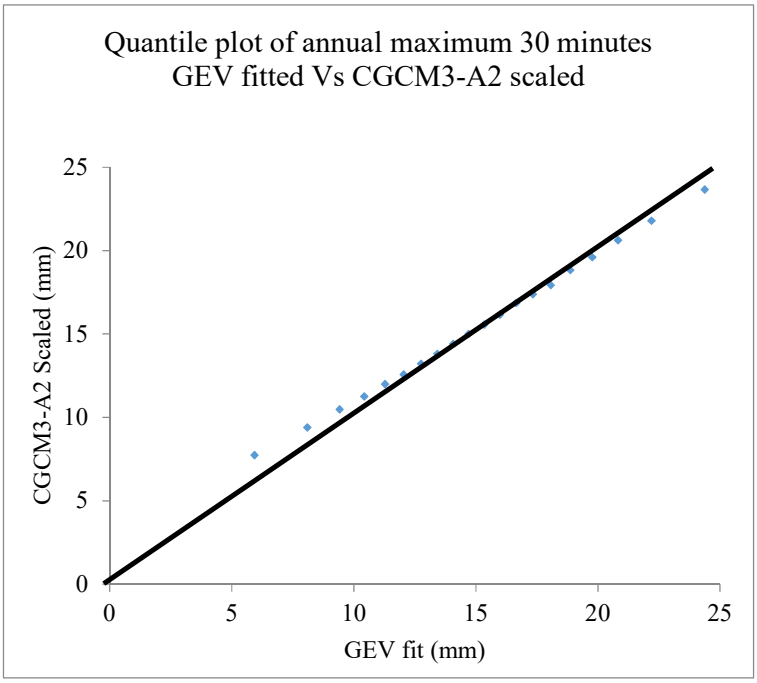

Figure 5.13: Comparison of GEV fitted annual maximum 30 minutes rainfall with scaled annual maximum daily rainfall at Perth Airport for CGCM3-A2

Table 5.3: Calculated coefficient for observed and downscaled annual maximum sub-daily rainfall for 1961-1990 period.

GCM	Efficiency Coefficient	30 min	1 hour	2 hour	6 hour	12 hour
HadCM3	RMSE	1.28	2.05	2.99	4.23	4.53
	NSE	0.93	0.90	0.85	0.86	0.85
	PBIAS	-0.01	0.01	0.02	0.06	0.06
CGCM3	RMSE	1.31	2.24	3.12	4.57	4.70
	NSE	0.92	0.88	0.84	0.83	0.84
	PBIAS	0.01	0.02	0.04	0.07	0.08

5.3.3 Future extreme rainfall patterns

To evaluate the trend of daily and sub-daily annual maximum rainfall for the future periods, the same approach is applied to the bias corrected annual maximum daily rainfall series which are simulated by HadCM3-A2 and CGCM3-A2. In temporal downscaling, it is assumed that the scaling factor which calculated for the 1961 -1990 period, remain constant for the future periods. (As the climate change is a long-term

process, impact of climate change is countered in present scaling factor). Figure 5.14 and Figure 5.15 show the probability plots of 1hour annual maximum rainfalls estimated from the downscaled annual maximum daily rainfalls using the HadCM3-A2 and CGCM3-A2 simulation results respectively. According to Figure 5.14 and Figure 5.15, downscaled results using HadCM3-A2 scenario show a low variation of extreme rainfall magnitudes than downscaled extreme rainfalls magnitude using CGCM3-A2 scenario. A similar pattern is identified for HadCM3 and CGCM3 in the literature (Nguyen et al., 2008). Furthermore, downscaled extreme rainfalls from HadCM3-A2 show different extreme rainfall patterns for different return periods. (i.e. extreme rainfalls of 2080s show the lowest value for low return period and extreme rainfall of 1961-1990 period shows lowest value for high return periods). Extreme rainfalls obtained by downscaling CGCM3-A2 show a very clear decreasing trend of extreme rainfall magnitude over future periods. Moreover, it can be seen that both HadCM3-A2 and CGCM3-A2 predict the same decreasing trend of extreme rainfalls for future periods (2020s, 2050s, and 2080s). Both GCMs give highest extreme rainfall for the 2020s (2011- 2040), next for the 2050s (2041-2070) and lowest for the 2080s (2071-2100) for Perth airport rain gauge station. A similar trend of future extreme rainfall events has been identified by other studies in the same area (Jakob et al., 2012).

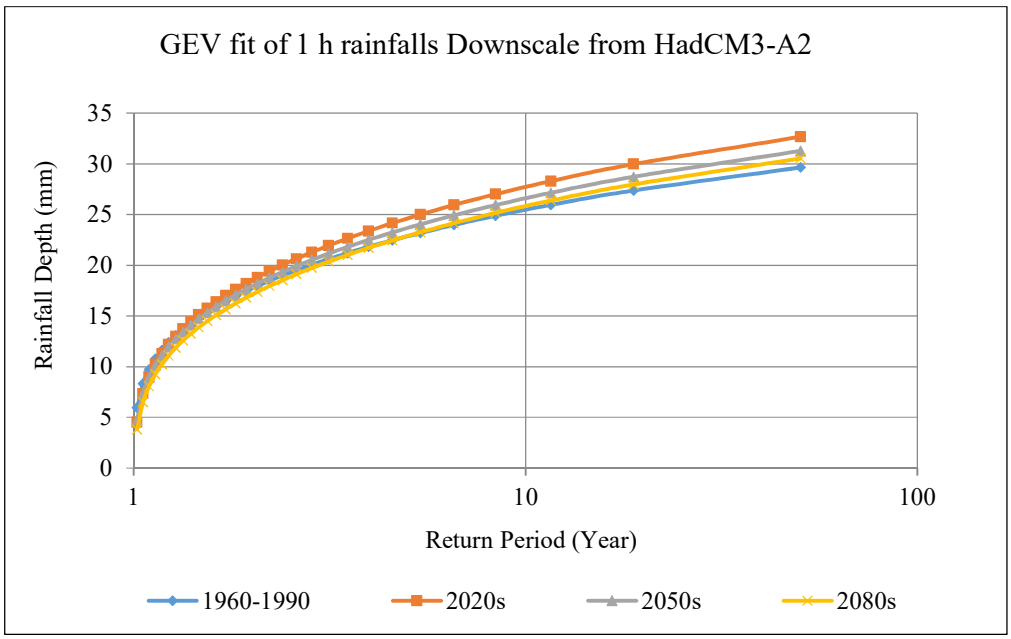

Figure 5.14: Probability plots of 1 hour annual maximum rainfalls at Perth airport for HadCM3-A2

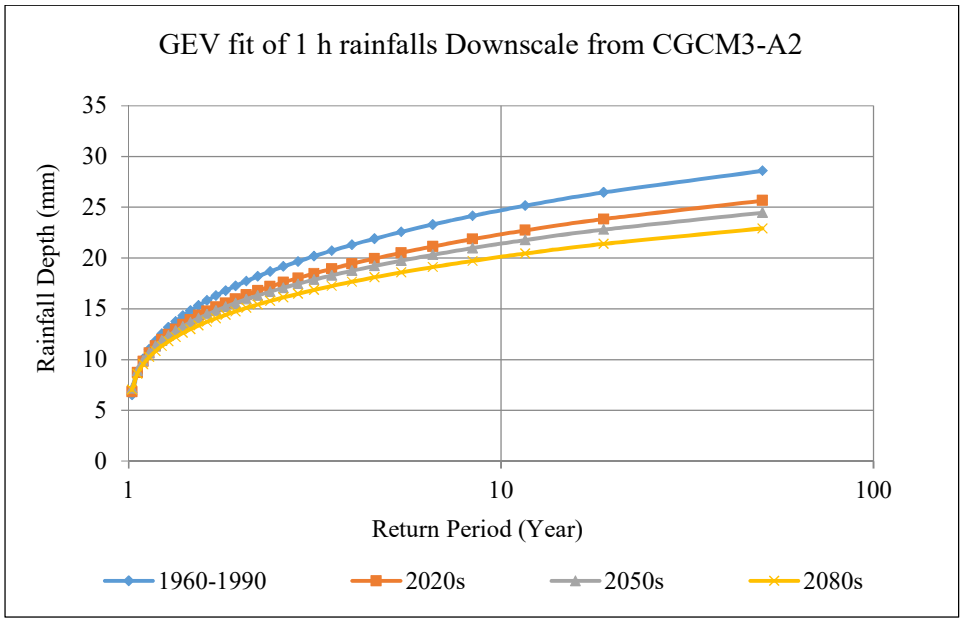

Figure 5.15: Probability plots of 1-hour annual maximum rainfalls at Perth airport for CGCM3-A2.

5.3.4 IDF relations using estimated sub-daily extreme rainfalls

Sub-daily extreme rainfalls produced by the proposed spatial-temporal downscaling approach are used to develop IDF relations for Perth airport station for current and future periods. For the illustrating purposes, Figure 5.16 to

Figure 5.21 represent the developed IDF curves for the future periods of 2020s, 2050s and 2080s using downscaled HadCM3-A2 and CGCM3-A2 rainfall. Moreover, the intensity of 1 hour rainfall events is studied for 2020s, 2050s and 2080s periods. 2020s intensities take the highest values and, then 2050s and 2080s take lowest values. Future 1 hour intensity deduction percentages for different return periods (5, 10, 20, 50 and 100 years) are presented in Table 5.4. In Table 5.4, downscaled 1 hour intensities by HadCM3-A2 and CGCM3-A2 for 2050s and 2080s are compared with 2020s intensities and both GCMs show a decreasing trend of future rainfalls. Percentage reductions of the HadCM3-A2 downscaled intensities for 2050s and 2080s vary between 3.9%-4.4% and 7%-6.5% respectively. Percentage reductions of the intensities downscaled by CGCM3-A2 take higher values than HadCM3-A2. It varies between 3.7%-4.7% for 2050s and 9.4%-10.8% for 2080s. These results differ from

the general acceptance of Green House Gas (GHG) emissions which tend to increase the extreme rainfall event. The main reasons for this difference are the impact of downscaling the rainfall over point location. It can be varied from the general behaviour of gridded forecast of GCMs. Further, the proportional relationship between daily extreme rainfalls and temperature (mean or maximum) follows C-C relation (Lenderink and Van Meijgaard, 2008) scaling relation and it valid only for a limited range of temperature (Jones et al., 2010). When the temperature takes high values, it tends to decline the extreme rainfall. Moreover, the literature shows a similar trend of extreme rainfall events in this region for future periods (Jakob et al., 2012).

Furthermore, these developed IDF relations which take climate change impacts into account will allow hydrologists to bring the impacts of climate change into their designs. Also, updated IDF curves are important in reducing the risk of decision-making process of water resources engineers in hydrological assessment by considering climate change impacts on future hydrological designs. Therefore, the IDF curves developed in this study will attract high attention among professionals and public and will be useful in designing future water resources infrastructure.

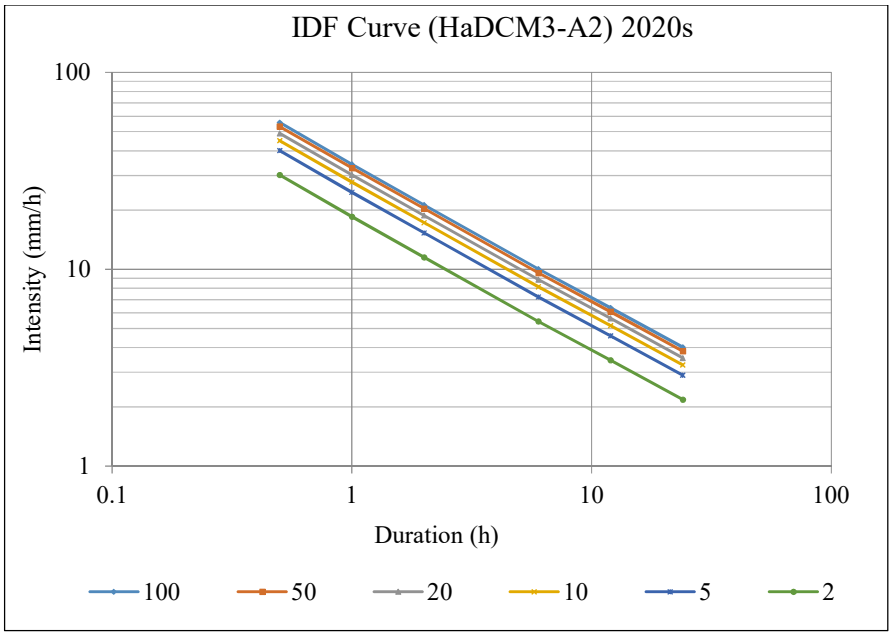

Figure 5.16: Developed IDF curves for the period of 2020s using HadCM3-A2.

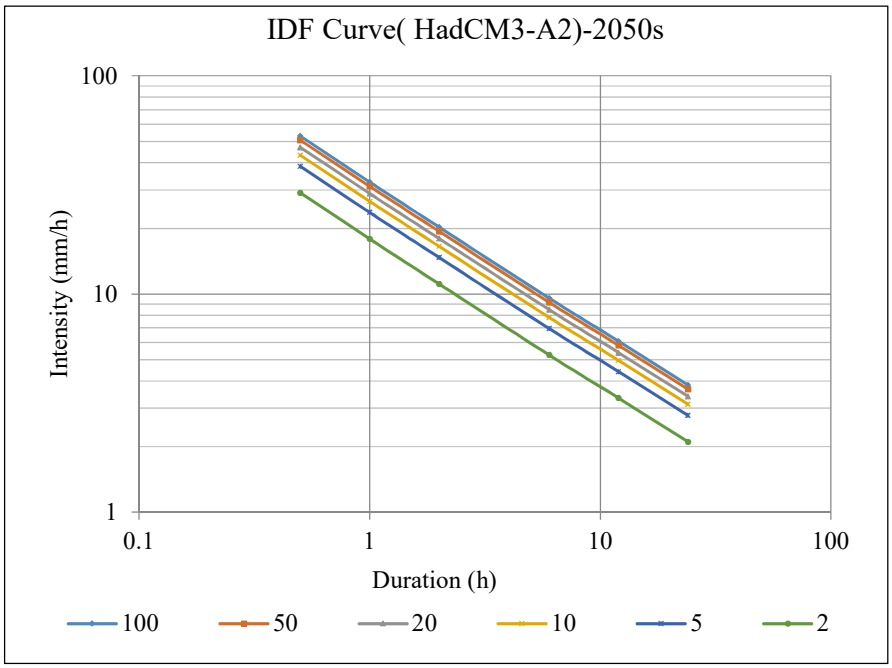

Figure 5.17: Developed IDF curves for the period of 2050s using HadCM3-A2.

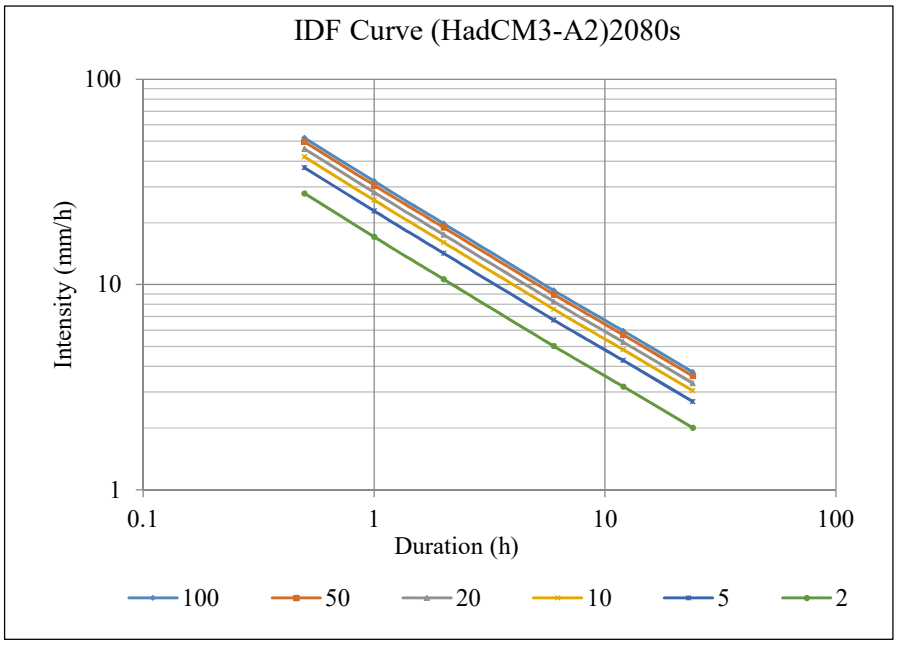

Figure 5.18: Developed IDF curves for the period of 2080s using HadCM3-A2.

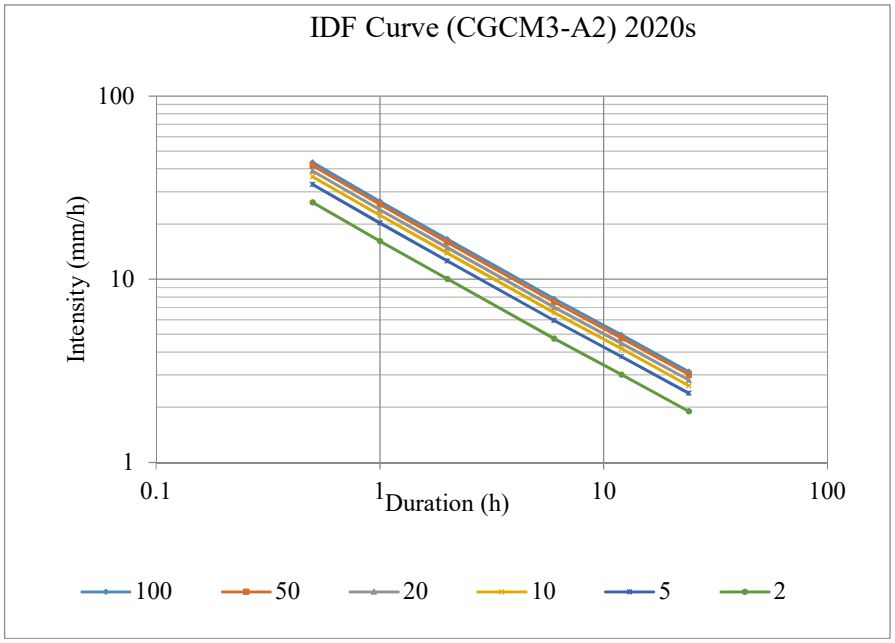

Figure 5.19: Developed IDF curves for the period of 2020s using CGCM3-A2.

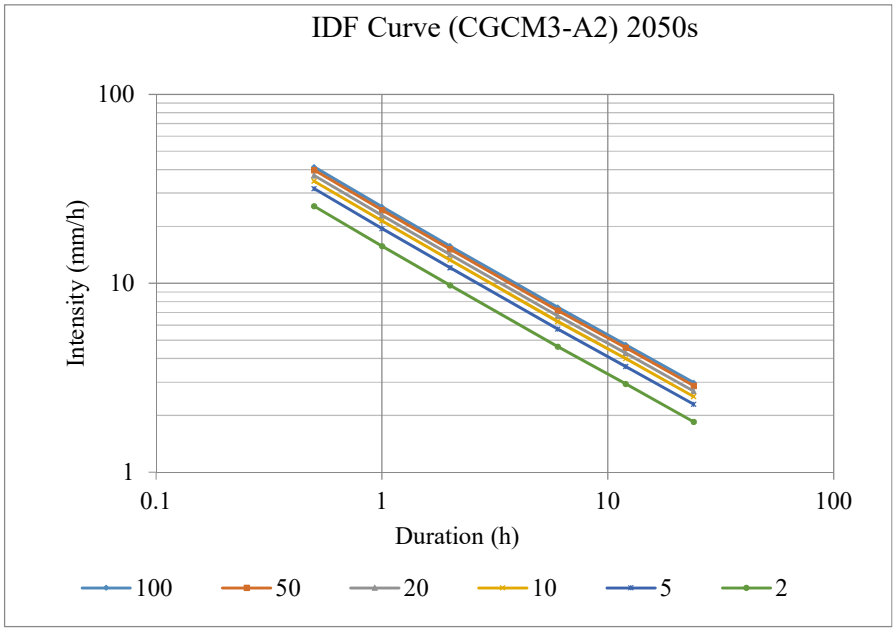

Figure 5.20: Developed IDF curves for the period of 2050s using CGCM3-A2.

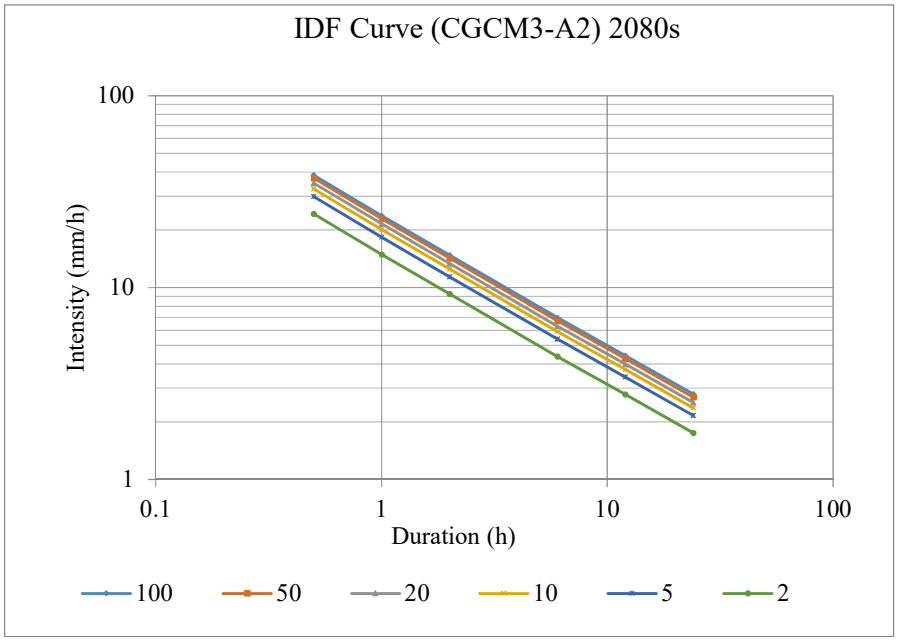

Figure 5.21: Developed IDF curves for the period of 2080s using CGCM3-A2.

Table 5.4: Variation of 1 hour rainfall intensities compare to 2020s intensities at Perth airport

ARI (years)	Variation (percentage reduction) compare to 2020s			
	HadCM3-A2		CGCM3-A2	
	2050s	2080s	2050s	2080s
5	-3.9	-7.0	-3.7	-9.4
10	-4.1	-6.8	-4.1	-9.9
20	-4.2	-6.7	-4.4	-10.3
50	-4.3	-6.5	-4.6	-10.6
100	-4.4	-6.5	-4.7	-10.8

5.4 Applicability of proposed downscaling approach for other main cities in Australia.

The demonstrated example of Perth airport rain gauge station clearly confirms the accuracy of proposed downscaling approach in developing sub-daily IDF relations for

future periods. This section shows the applicability of proposed approach for all other locations included in this study. to

Figure 5.22 illustrate the scaling behaviour first three NCMs of observed rainfalls at Adelaide airport, Brisbane regional, Canberra airport, Darwin airport, Melbourne airport and Sydney observatory hill rain gauge stations. According to Figure 5.22, it clearly depicts that all rain gauge stations show scaling behaviour in their observed annual maximum rainfall series. Except Sydney observatory hill rain gauge station, other all stations show simple scaling regime of 24 h to 0.5 h. It confirms the applicability of proposed temporal downscaling method in estimating sub-daily IDF relations same as Perth airport example. Sydney observatory hill rain gauge station shows two time regimes which exist power law dependency. It shows first time regime from 24 h to 2 h and second regime for 2 h to 0.5 h. Therefore, temporal downscaling of daily downscaled rainfall should be carried out by two steps. (i.e. 1. Estimating statistical properties up to 2 h rainfalls from statistical properties of 24 h rainfalls 2. Estimating statistical properties up to 0.5 h rainfalls from statistical properties of 2 h rainfalls).

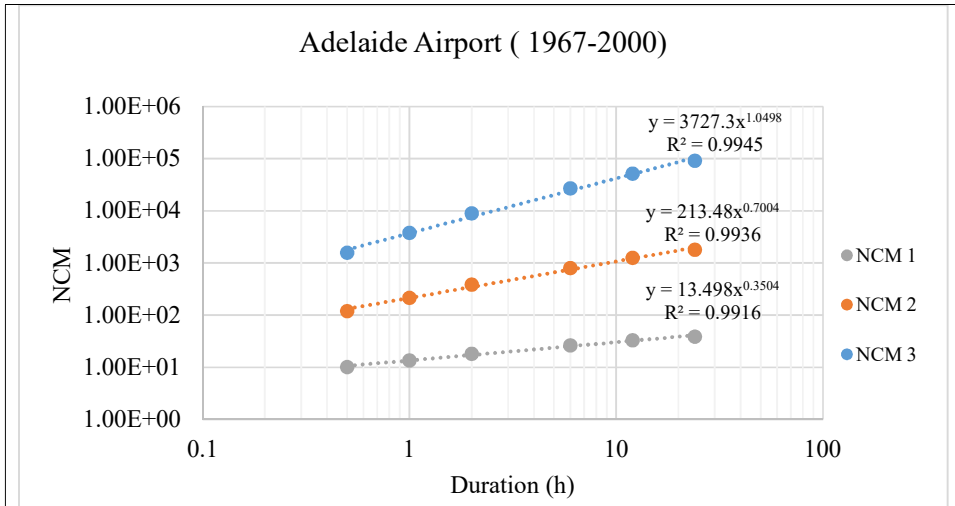
Adelaide Airport (1967-2000)
1.00E+06
1.00E+05
1.00E+04
1.00E+03
1.00E+02
1.00E+01
1.00E+00
NCM
0.1
1
10
100
Duration (h)
y = 3727.3x^1.0498
R² = 0.9945
y = 213.48x^0.7004
R² = 0.9936
y = 13.498x^0.3504
R² = 0.9916
NCM 1
NCM 2
NCM 3

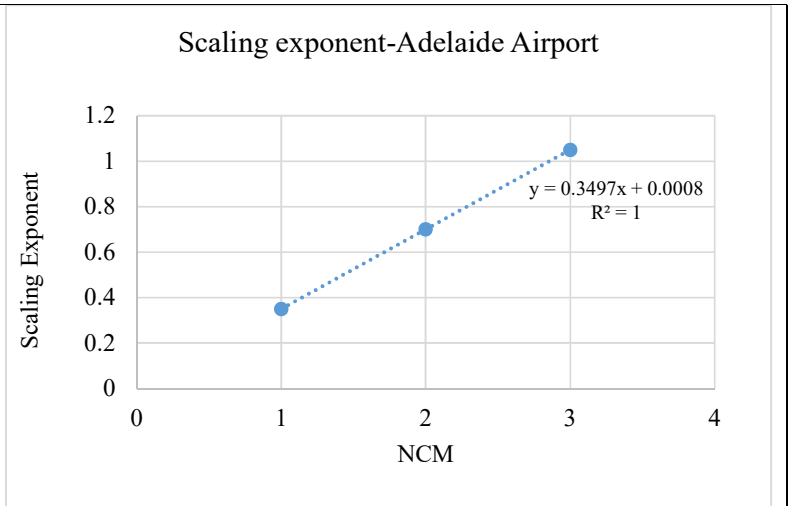
Scaling exponent-Adelaide Airport
Scaling Exponent
1.2
1
0.8
0.6
0.4
0.2
0
0
1
2
3
4
NCM
y = 0.3497x + 0.0008
R² = 1

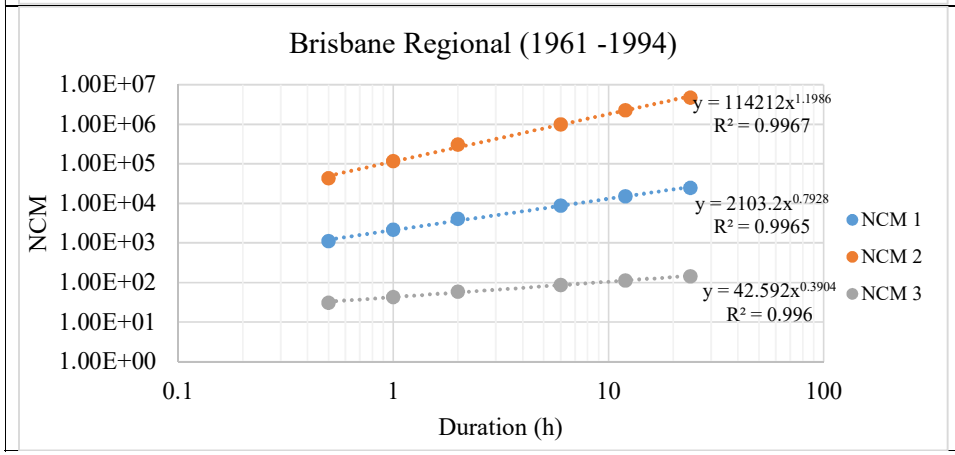
Brisbane Regional (1961 -1994)
1.00E+07
1.00E+06
1.00E+05
1.00E+04
1.00E+03
1.00E+02
1.00E+01
1.00E+00
NCM
0.1
1
10
100
Duration (h)
y = 114212x^1.1986
R² = 0.9967
y = 2103.2x^0.7928
R² = 0.9965
y = 42.592x^0.3904
R² = 0.996
NCM 1
NCM 2
NCM 3

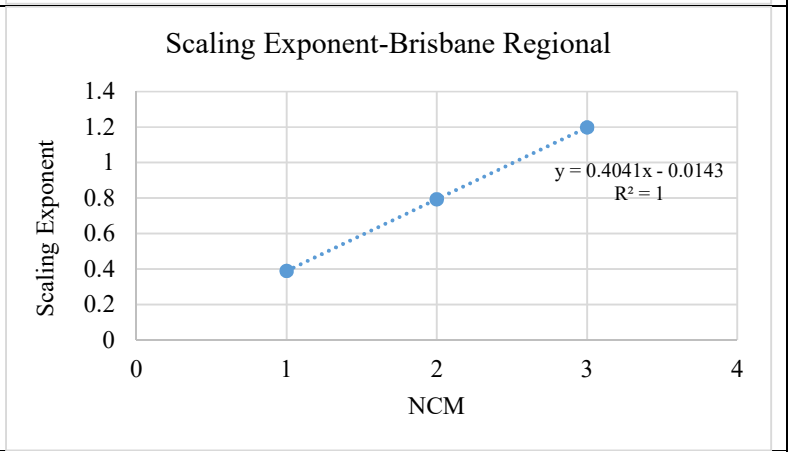
Scaling Exponent-Brisbane Regional
Scaling Exponent
1.4
1.2
1
0.8
0.6
0.4
0.2
0
0
1
2
3
4
NCM
y = 0.4041x - 0.0143
R² = 1

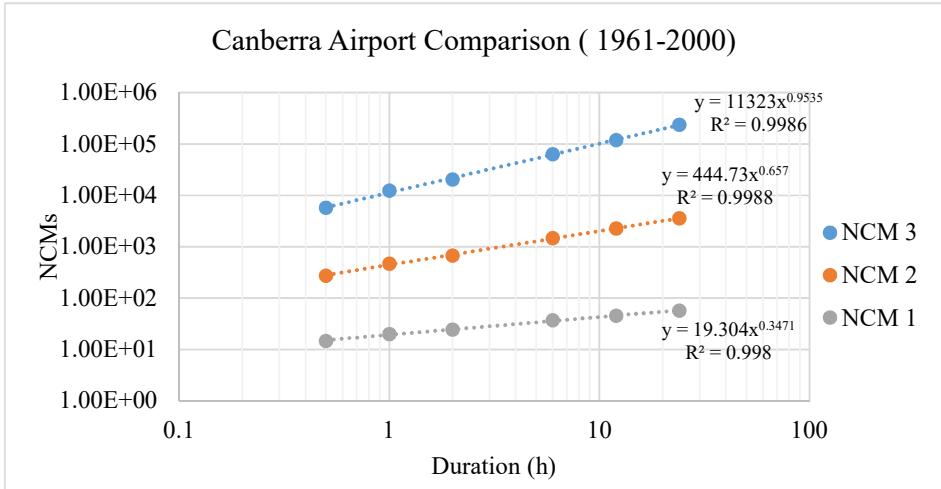
Canberra Airport Comparison (1961-2000)
1.00E+06
1.00E+05
1.00E+04
1.00E+03
1.00E+02
1.00E+01
1.00E+00
NCMs
0.1
1
10
100
Duration (h)
y = 11323x^0.9535
R² = 0.9986
y = 444.73x^0.657
R² = 0.9988
y = 19.304x^0.3471
R² = 0.998
NCM 3
NCM 2
NCM 1

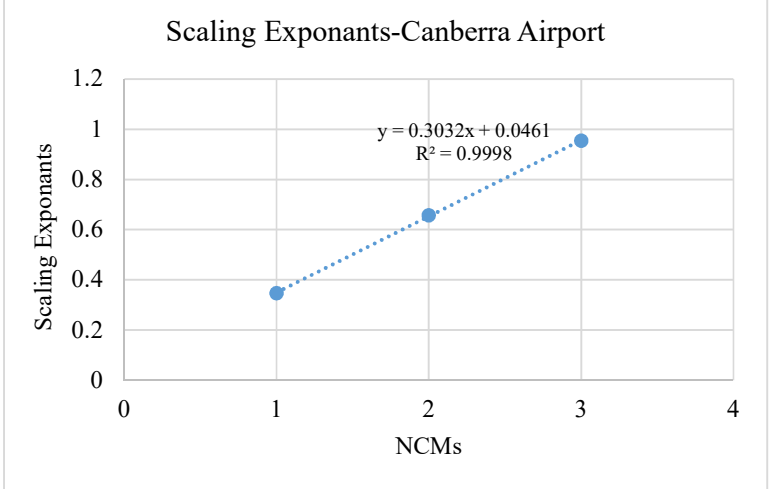
Scaling Exponants-Canberra Airport
Scaling Exponants
1.2
1
0.8
0.6
0.4
0.2
0
0
1
2
3
4
NCMs
y = 0.3032x + 0.0461
R² = 0.9998

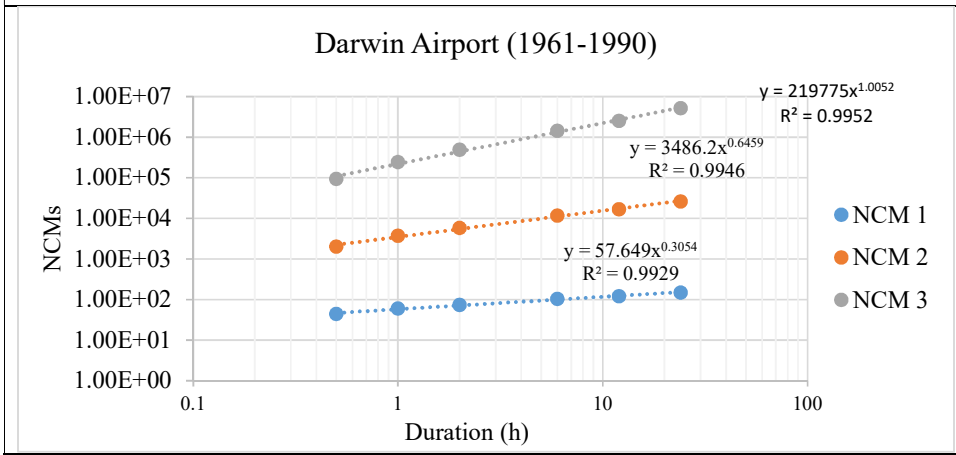
Darwin Airport (1961-1990)
1.00E+07
1.00E+06
1.00E+05
1.00E+04
1.00E+03
1.00E+02
1.00E+01
1.00E+00
NCMs
0.1
1
10
100
Duration (h)
y = 219775x^1.0052
R² = 0.9952
y = 3486.2x^0.6459
R² = 0.9946
y = 57.649x^0.3054
R² = 0.9929
NCM 1
NCM 2
NCM 3

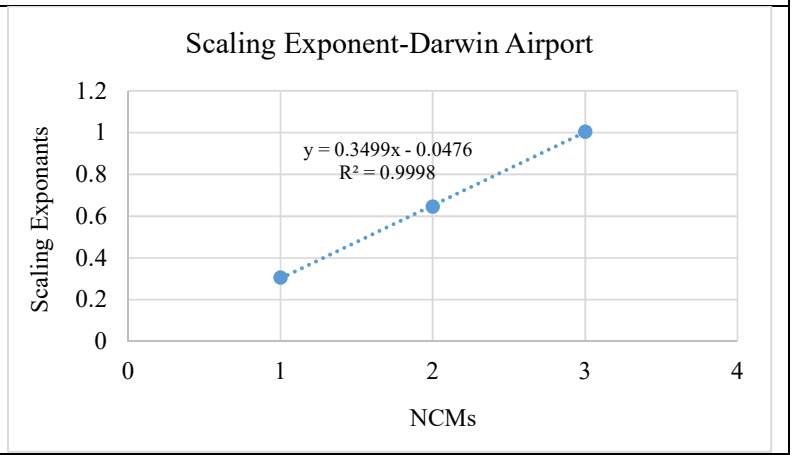
Scaling Exponent-Darwin Airport
Scaling Exponants
1.2
1
0.8
0.6
0.4
0.2
0
0
1
2
3
4
NCMs
y = 0.3499x - 0.0476
R² = 0.9998

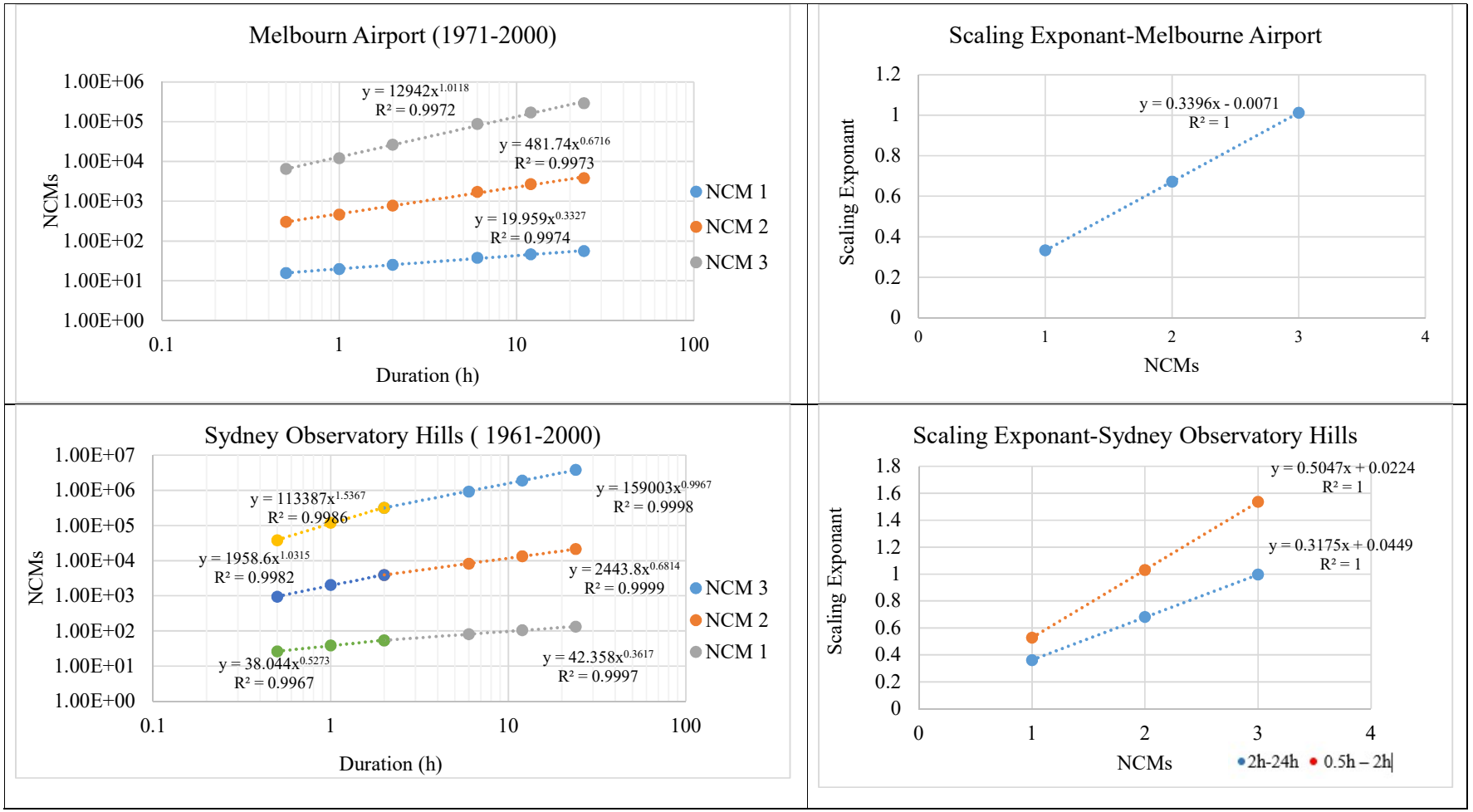

Figure 5.22: Assessing the scaling behaviour of first three NCM of observed annual maximum rainfall versus durations

5.5 Summary

Spatial and temporal downscaling of climate change triggered extreme rainfall data are essential for the estimation of design storms in the context of climate change. This study develops an approach to downscale short-time extreme rainfall to update the IDF curves in assessing the impacts of climate change on the design storms. The NCEP reanalysed data, HadCM3-A2 and CGCM3-A2 climate predictor data and the daily and sub-daily observed rainfall data at Perth airport rain gauge station are used to assess the feasibility and accuracy of the proposed spatial-temporal downscaling approach.

This study is carried out in two major steps; spatial downscaling of the daily rainfall process using the SDSM (As described in Chapter 3); and temporal downscaling of spatially downscaled daily rainfalls using an approach based on scaling concept (As described in this chapter). SDSM model is successfully calibrated for the 1961 –1975 period and validated for the 1976-1990 period confirming that the SDSM model is feasible in describing some fundamental statistical properties of the daily rainfalls. However, the downscaled annual daily maximum rainfalls are not close to the observed data. Hence, a bias-correction procedure has been proposed to improve the accuracy of the downscaled rainfall. The accuracy of proposed bias correction procedure is evaluated by the goodness-of-fit tests and visual plotting. Results show that a strong agreement between observed and downscaled daily maximum rainfalls could be achieved, based on the proposed third-order bias-correction function.

Furthermore, the annual maximum rainfall data of Perth airport rain gauge station is found to display a simple scaling regime within the time interval from 30 minutes to 24 hours. A temporal downscaling method based on the scaling of GEV distribution is then proposed to downscale the observed annual maximum daily rainfalls to sub-daily values. Results of the annual maximum rainfall data have indicated the accuracy of the suggested temporal downscaling procedure. The accuracy of the estimated sub-daily extreme rainfalls for different return intervals was checked using RMSE, NSE and PBIAS values. These results demonstrate the feasibility of establishing the linkages between the daily downscaled rainfalls and the sub-daily extreme rainfall at a given local site. Finally, IDF curves were developed for future periods by means of linkage between daily predictors of GCMs and extreme sub-daily rainfalls at Perth Airport rainfall station. Developed IDF curves show similar extreme rainfall decreasing trend for 2020s, 2050s and 2080s for both GCMs.

In the later part of this study, the applicability of proposed approach is evaluated for Adelaide, Brisbane, Canberra, Darwin, Melbourne and Sydney rain gauge stations. It shows the suitability of proposed temporal downscaling approach to develop sub-daily IDF relations for all other selected cities.

CHAPTER 6

6 Evaluating the dependency of extreme rainfall events on daily temperature in Australia

Extended from

> Herath, S.M., Sarukkalige, P.R. and Nguyen, V. T. V., 2017, Evaluation of empirical relationships between extreme rainfall and daily maximum temperature in Australia, Journal of Hydrology (Accepted for publication).

6.1 Introduction

Atmospheric temperature is one of the dominant climate variables which has a strong relationship with extreme rainfall events. The general acceptance is that increases in temperature drives high-intensity precipitation events in many parts of the world (Alexander et al., 2006, Allan and Soden, 2008, Westra et al., 2013). However, this hypothesis remains uncertain and does not mean equal influence on all regions of the world (Fischer and Knutti, 2015). Also, this hypothesis is mainly based on future climate projections as governed by the Clausius–Clapeyron (C-C) relationship and average relative humidity variations throughout the world (Soden and Held, 2006). By considering the importance of evaluating the relationship of extreme rainfalls with physical factors, this chapter is dedicated to discuss the variation of the scaling relationship between extreme daily/sub-daily rainfall events and daily maximum temperature in seven major cities in Australia.

Australian Rainfall records clearly show high variations in rainfall and their pattern over seven states. Also, impacts of climate change vary among interstates. Therefore, same rain gauge stations i.e. Adelaide Airport, Canberra Airport, Darwin Airport, Melbourne Airport, Perth Airport, Sydney (Observatory Hill) and Brisbane Regional described in Chapter 5, located across five Australian states and two territories with longest record periods and least missing data are considered for this study. Also, BoM rainfall data and daily

maximum temperature data are collected for the chosen sites. Detailed information on the seven selected stations is included in Figure 5.1 and Table 5.1 in Chapter 5.

The aim of the study described in this chapter is to evaluate the variation of the rainfall - temperature scaling relationship between daily maximum temperature and extreme rainfall events over the analysis period. Studies described in the literature do not discuss the variation in rainfall-temperature scaling relationships over long time periods as determined by analysing the data using different windows in time. Most of the studies calculate the scale by considering the whole period as one slice of time, consequently these studies do not show variations in scaling relationships for both past and present conditions. Studying variations in rainfall - temperature scale trend enables researchers to project the behaviour of extreme rainfall events in the future. Therefore, this study has three main goals:

I. identify the relationship between daily and sub-daily extreme rainfall and daily maximum temperature,
II. evaluate the variation in rainfall-temperature scale for different time slices,
III. analyse the impact of seasonality on rainfall – temperature scale.

6.2 Empirical relationships between precipitation and temperature

There are several methods available in the literature to evaluate the empirical relationships between rainfalls and temperature, though some of them are associated with high uncertainty. The 'binning' technique, developed by Lenderink and Van Meijgaard (2008) is used in this study to evaluate the empirical relationships between precipitation and temperature. For each station, the maximum rainfall depth on wet days (defined as rainfall >0.3mm/day) for a given duration is grouped with daily maximum temperature. Consistent results for daily mean temperature and daily maximum temperatures have been obtained by previous studies conducted by other researchers in Australia (Hardwick Jones et al., 2010). Initial observations clearly indicated that the variation in temperature is primarily driven by seasonality in most locations. Therefore, this study is carried out using yearly and seasonal lumped data.

Few limitations have been identified by Wasko and Sharma (2014) in applying binning technique compare to the quantile regression approach, especially these limitations and bias are associated with the approach of equal width temperature bins. Assignment of temperature bins of equal width leads to fewer pairs in the upper and lower temperature bins. Furthermore, fixing bin temperature ranges may result in empty bins being ignored and the distortion of the relationship between temperature and rainfalls. By considering the drawbacks associated with the use of equal width bins, temperature bins are assigned an equal number of pairs per bin (Hardwick Jones et al., 2010) and the median temperature value of each bin is used to identify the bin. The temperature range of each bin is then estimated to be approximately 2˚C, with the temperature range of the upper and lower tails slightly greater than 2˚C. Another minor source of sampling uncertainty is related to the number of pairs in periodic samples. (As an example, different number of pairs in a bin for 1991-2000 period and 2001-2010 period etc.). In generally, sampling uncertainty takes a high value at the presence of few number of pairs in a bin. When consider the periodic analysis of all stations, the median of the pairs in a temperature bin is 104 for this study. For the winter–spring season, the number of pairs is 51 and summer – autumn season, it is 50. Therefore, sampling uncertainty is minimum in this study.

To identify the C-C scaling relationship between extreme rainfalls and temperature, an exponential regression function is applied. According to the literature (Hardwick Jones et al., 2010, Utsumi et al., 2011), the relationship between precipitation (P) and temperature is described by Equation 6.1.

$$\mathbf{P_2 = P_1(1 + \alpha)^{\Delta T}} \qquad (\mathbf{6.1})$$

Where,

P_1 and P_2 are the precipitation percentiles at temperature T_1 and T_2 respectively. ΔT is the temperature difference between T_1 and T_2. α is the precipitation temperature scaling co-efficient, where $\alpha = 6.8\%$ ˚C^{-1} at 25 ˚C equivalent to Clausius-Clapeyron . For the rainfall - temperature scaling analysis the 99th and 50th percentiles of daily maximum 6 minute, 12 minute, 30 minute, 1 hour, 2 hour, 6 hour, 12 hour and 24 hour rainfall durations are considered.

6.3 Evaluating the Rainfall-Temperature scaling relationship for extreme rainfall and daily maximum temperature

Initially, by taking the total data period as one-time slice, the rainfall temperature scaling relationship is estimated for extreme rainfall events and daily maximum temperature. Figure 6.1 and Figure 6.2 present the distribution of the 99th and 50th percentiles of daily and sub-daily extreme rainfall with daily maximum temperature respectively. According to Figure 6.1, the 99th percentiles of maximum rainfall events show exponential relationships with daily maximum temperature. The relationships are especially strong (more positive) for the sub-daily (6 minute, 12 minute, 30 minute, 1 hour and 2 hour) rainfall durations. However, in most instances, the resultant exponential scaling rate does not agree with the generally accepted C-C scale value of 6.8%˚C^{-1}.

Figure 6.2 also shows that in general the rainfall-temperature scaling rate for the 50th percentile has a lower value than the 99th percentile scaling rate and at most stations, it is very close to zero. For some stations (Adelaide, Darwin, Perth and Sydney) the scaling rate for the 50th percentile is negative for all rain durations. The result apparent in Figure 6.1 and Figure 6.2 is that the exponential scaling relationship exists only within a certain temperature range. Especifically the graphs show a reduction of the extreme rainfall intensities with increasing temperature between 30˚C and 35˚C (except Darwin station).

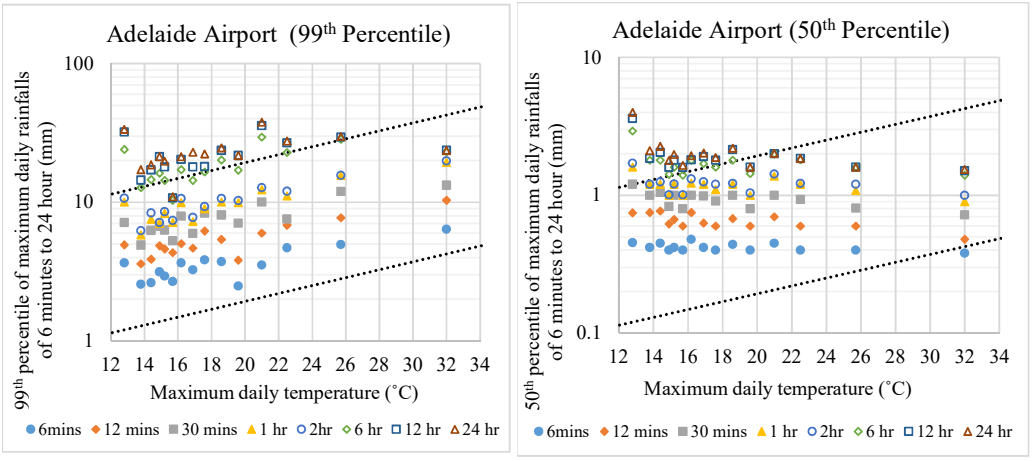

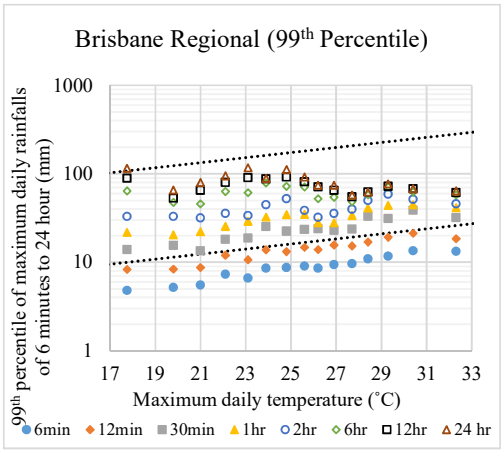
Brisbane Regional (99th Percentile)
99th percentile of maximum daily rainfalls of 6 minutes to 24 hour (mm)
1000
100
10
1
17 19 21 23 25 27 29 31 33
Maximum daily temperature (˚C)
6min 12min 30min 1hr 2hr 6hr 12hr 24 hr

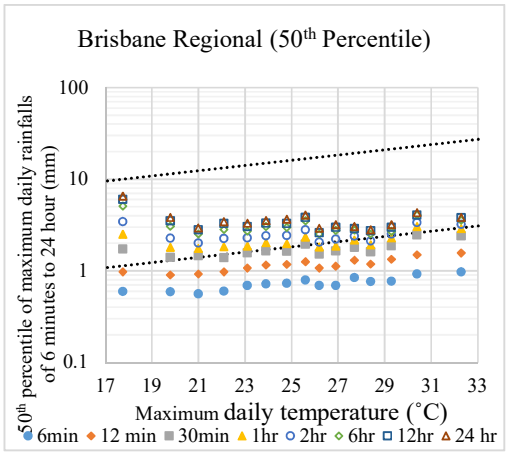
Brisbane Regional (50th Percentile)
50th percentile of maximum daily rainfalls of 6 minutes to 24 hour (mm)
100
10
1
0.1
17 19 21 23 25 27 29 31 33
Maximum daily temperature (˚C)
6min 12 min 30min 1hr 2hr 6hr 12hr 24 hr

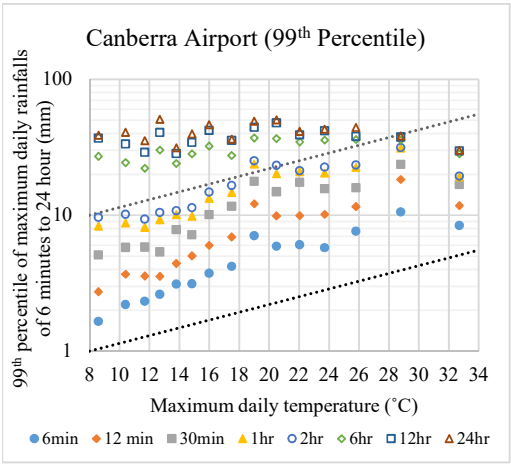
Canberra Airport (99th Percentile)
99th percentile of maximum daily rainfalls of 6 minutes to 24 hour (mm)
100
10
1
8 10 12 14 16 18 20 22 24 26 28 30 32 34
Maximum daily temperature (˚C)
6min 12 min 30min 1hr 2hr 6hr 12hr 24hr

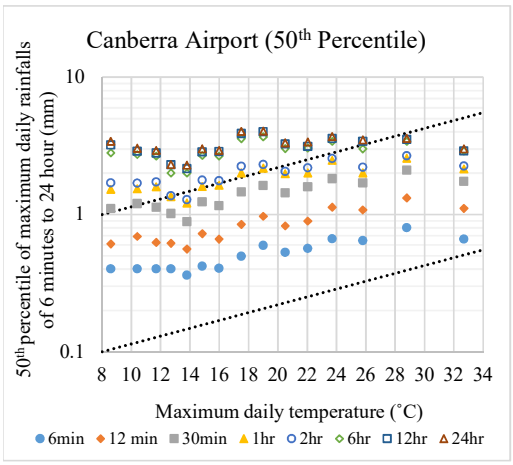
Canberra Airport (50th Percentile)
50th percentile of maximum daily rainfalls of 6 minutes to 24 hour (mm)
10
1
0.1
8 10 12 14 16 18 20 22 24 26 28 30 32 34
Maximum daily temperature (˚C)
6min 12 min 30min 1hr 2hr 6hr 12hr 24hr

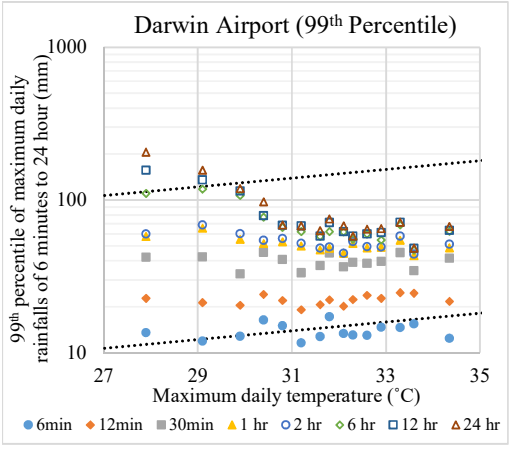
Darwin Airport (99th Percentile)
99th percentile of maximum daily rainfalls of 6 minutes to 24 hour (mm)
1000
100
10
27 29 31 33 35
Maximum daily temperature (˚C)
6min 12min 30min 1 hr 2 hr 6 hr 12 hr 24 hr

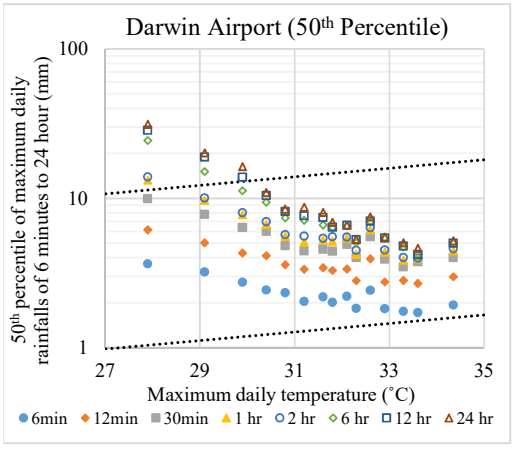
Darwin Airport (50th Percentile)
50th percentile of maximum daily rainfalls of 6 minutes to 24 hour (mm)
100
10
1
27 29 31 33 35
Maximum daily temperature (˚C)
6min 12min 30min 1 hr 2 hr 6 hr 12 hr 24 hr

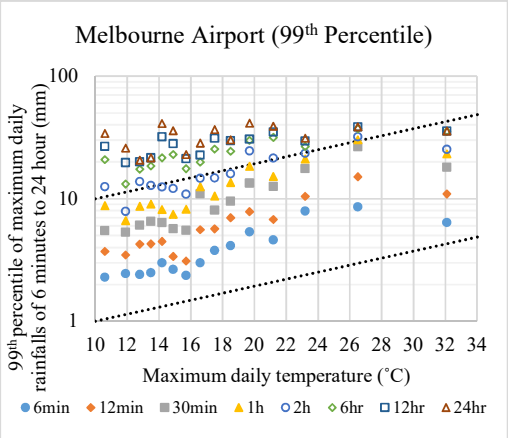

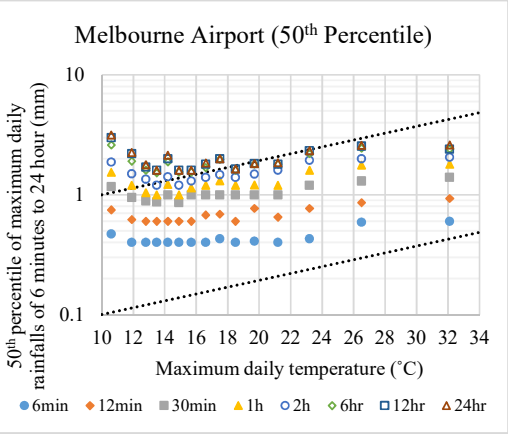

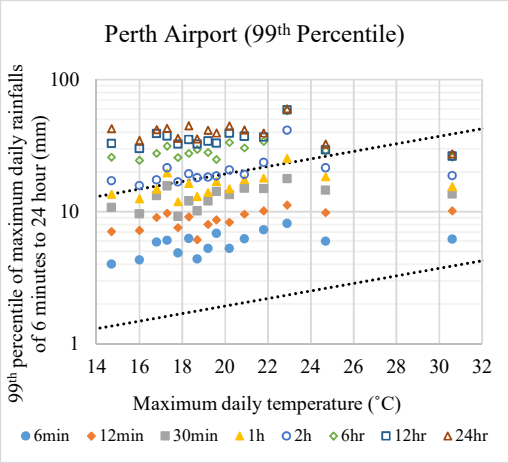

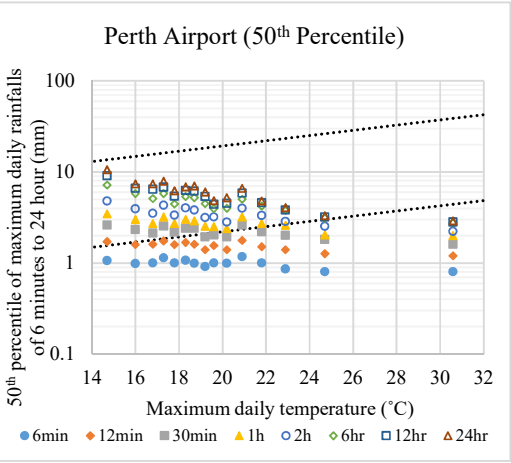

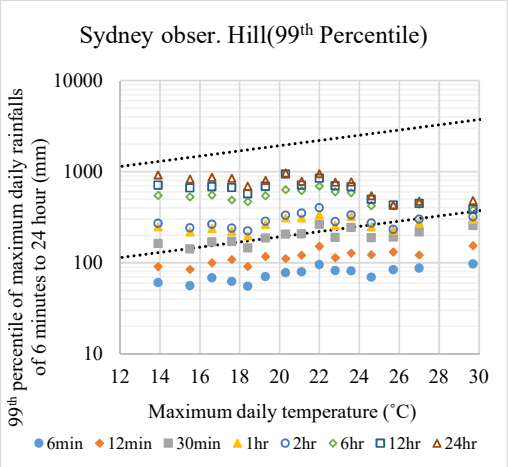

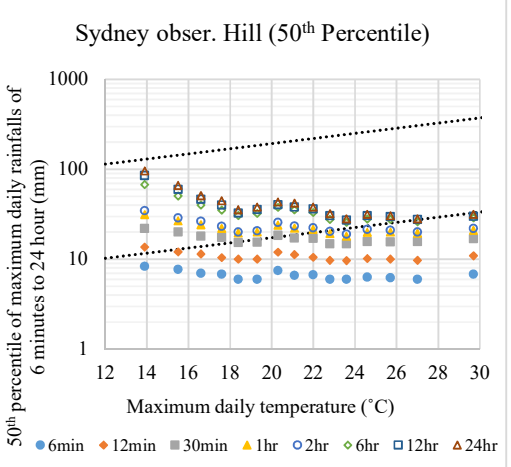

Figure 6.1

Figure 6.2

Figure 6.1: The relationship between daily maximum temperature and the 99th percentile of the maximum daily rainfall

Figure 6.2: The relationship between daily maximum temperature and the 50th percentile of the maximum daily rainfall

Figure 6.3 and Figure 6.4 were developed using equation 6.1 on the percentiles presented in Figure 6.1 and Figure 6.2 respectively, to present the scaling trend. Figure 6.3 describes the variation in scaling of the 99th percentile of the daily maximum rainfall duration (6 minute to 24 hour), while Figure 6.4 describes the variation in scaling of the 50th percentile of the daily maximum rainfall duration (6 minute to 24 hour). Further, these both figures show an approximately similar variation of rainfall–temperature scaling for all stations except Darwin Airport. It is also evident that with the exception of Darwin Airport, the rainfall-temperature scale takes a positive value for 6 minute to 2 hour duration for the 99th percentile. Further, the rate of scale varying for the events with short durations (6 minutes to approximately 2 hours, in some stations it may vary from 6 minutes to 1 hour or 6 hours) is very low, but the rate of scale varying is very high in the long duration events (i.e. 2 hour to 24 hour range). The 6 minute rainfall durations for the Brisbane (7.2%) and Canberra (6.9%) stations show the highest rainfall-temperature scale values. The Melbourne Airport station shows a positive scale for all the durations from 6 minutes to 24 hours, while for all other stations the variation in scale becomes negative for the 2 hour to 24 hour duration range. However, the behaviour of the Darwin Airport station data is different to that from the other stations and, in particular, the data show a negative scale relationship for all the rainfall durations.

The literature confirms that similar trends in scaling have been identified by other researchers for these parts of Australia (Wasko and Sharma, 2015). The data presented in Figure 6.4 show that the 50th percentile rainfall - temperature scale values are lower than the 99th percentile values. The data also show a negative scale trend for all rainfall durations for the Adelaide, Darwin, Perth and Sydney stations, while positive trends are apparent for short duration rainfall events for the Brisbane, Canberra and Melbourne stations.

Furthermore, according to Figure 6.3 and Figure 6.4, the sensitivity of temperature on more extreme rainfall is higher than average extreme rainfall events. It implies that rainfall-temperature scaling relationship is highly visible at more extreme rainfall events which saturate/release total water vapour amount in the atmosphere rather than average extreme rainfall events (Hardwick Jones et al., 2010).

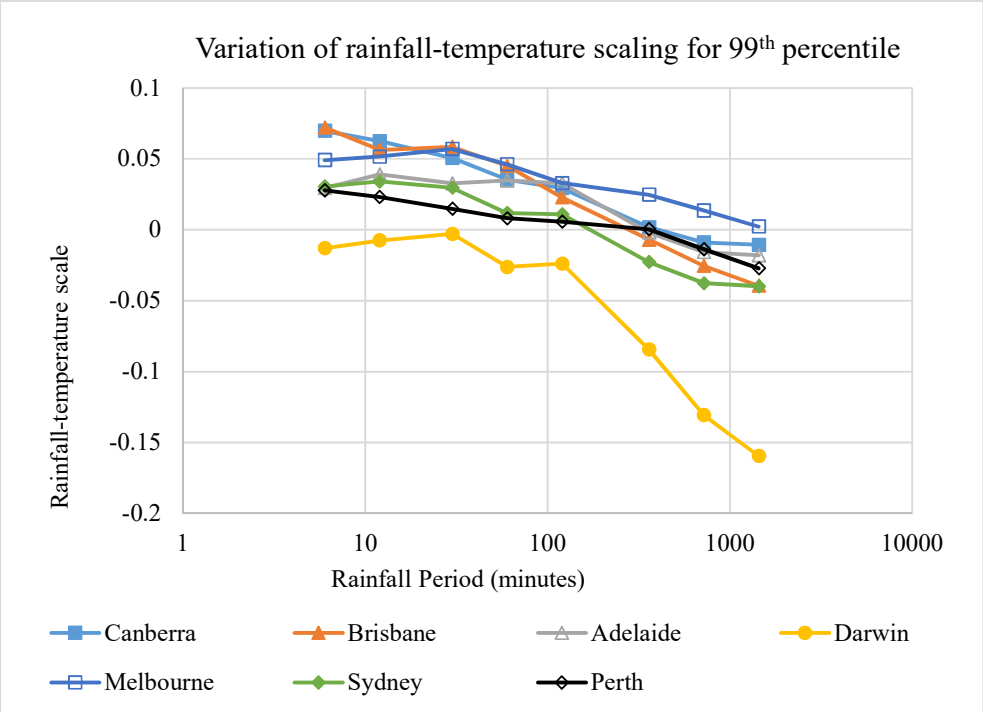

Figure 6.3: Variations in rainfall-temperature scaling with rainfall duration for the 99th percentile of daily maximum rainfall.

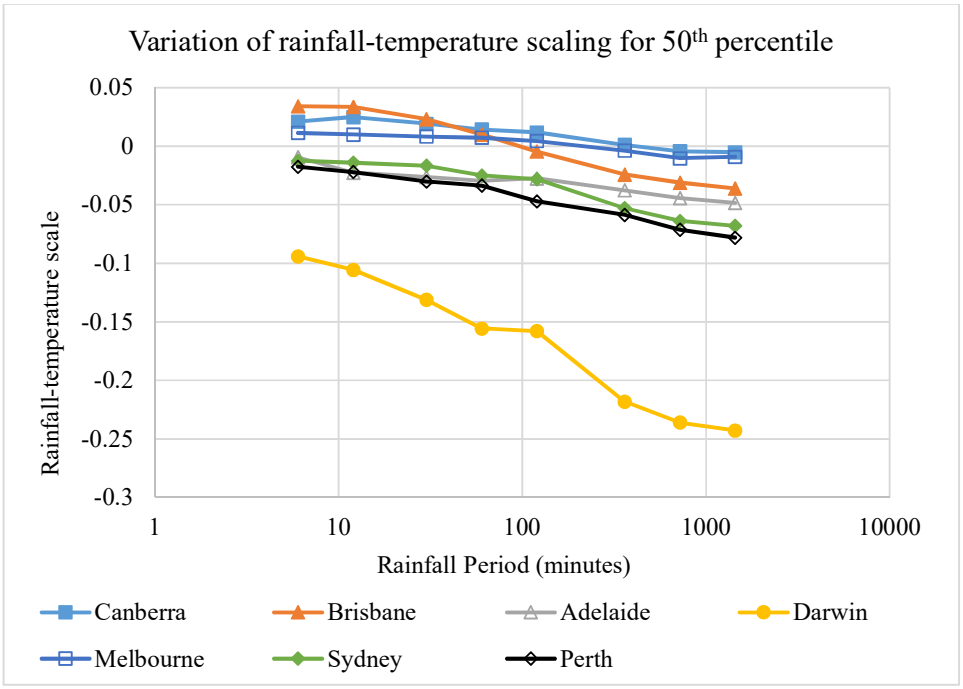

Figure 6.4: Variations in rainfall-temperature scaling with rainfall duration for the 50th percentile of daily maximum rainfall

6.4 Evaluating Changes in Rainfall - Temperature Scale Trends over Time.

The trend in rainfall - temperature scale variation was evaluated for different windows of time. To allocate the adequate number of pairs into a single temperature bin, to minimise the sampling uncertainty, this evaluation was conducted for ten-year time periods. Figure 6.5 to Figure 6.6, Figure 6.7 to Figure 6.8 and Figure 6.9 to Figure 6.10 describe the variation of scale for the 99^{th} and 50^{th} percentiles of 6 minute, 1hour and 24 hour rainfall durations respectively. The least square method is used to determine the scaling variability with the time period.

It can be clearly observed that scales vary from one time slice to the next. In general, all the stations show considerable changes within few decades. It implies that climate factors behind the extreme rain events are changing with the time. As the uncertainty of the regression lines is very low, it clearly verifies that changes are not due to the uncertainty. From Figure 6.5 it can be observed that there is an increasing trend in C-C scale for the 99^{th} percentile for 6 minute extreme rainfall events at all rain stations except Adelaide Airport. Further, Melbourne and Perth Airports show the highest increasing trends. These trends demonstrate that the influence of daily maximum temperature on more extreme rainfall durations (above the 99^{th} percentile) is increasing for all stations except Adelaide. Therefore, there is a high risk of the occurrence of intensified convective rainfall events in the future under the influence of increased daily maximum temperature.

Figure 6.6 presents the scaling trend for the 50^{th} percentile of the 6 minute extreme rainfall event and clearly shows that all rain gauge stations, except Brisbane, display a decreasing trend in scale over time. Among these decreasing trends, the Darwin station shows a comparatively high rate of decrease.

Therefore, the influence of maximum temperature on the 50^{th} percentile of 6 minute duration rainfall events is lesser than the 99^{th} percentile. It implies that the impact of future temperature change for average short period rainfalls is expected to be minimal, whereas the impacts on extreme rainfalls are significantly high.

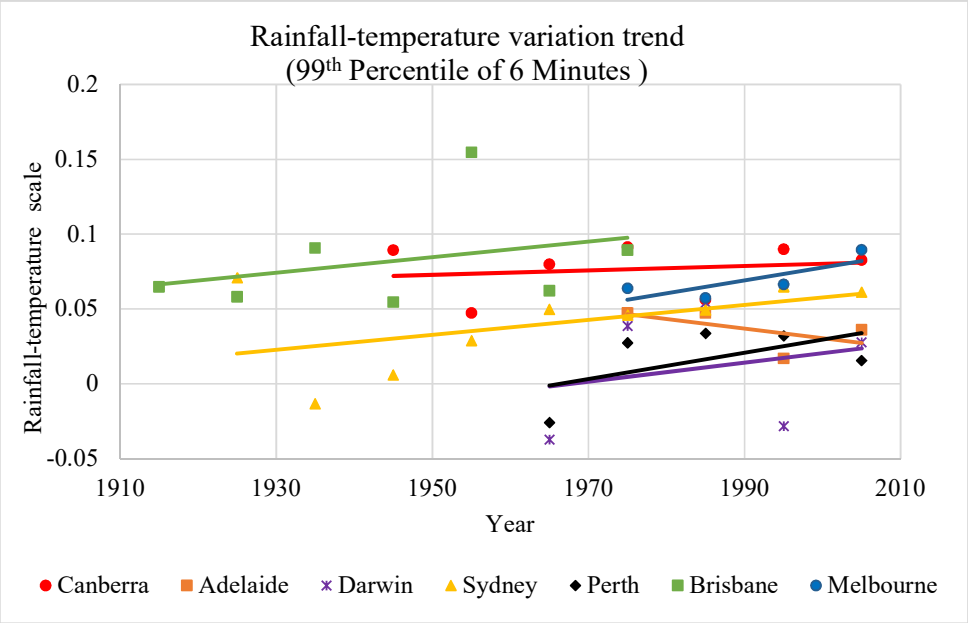

Figure 6.5: Rainfall–temperature scale variation for the 99th percentile of extreme sub-daily rainfall events (6 minute duration)

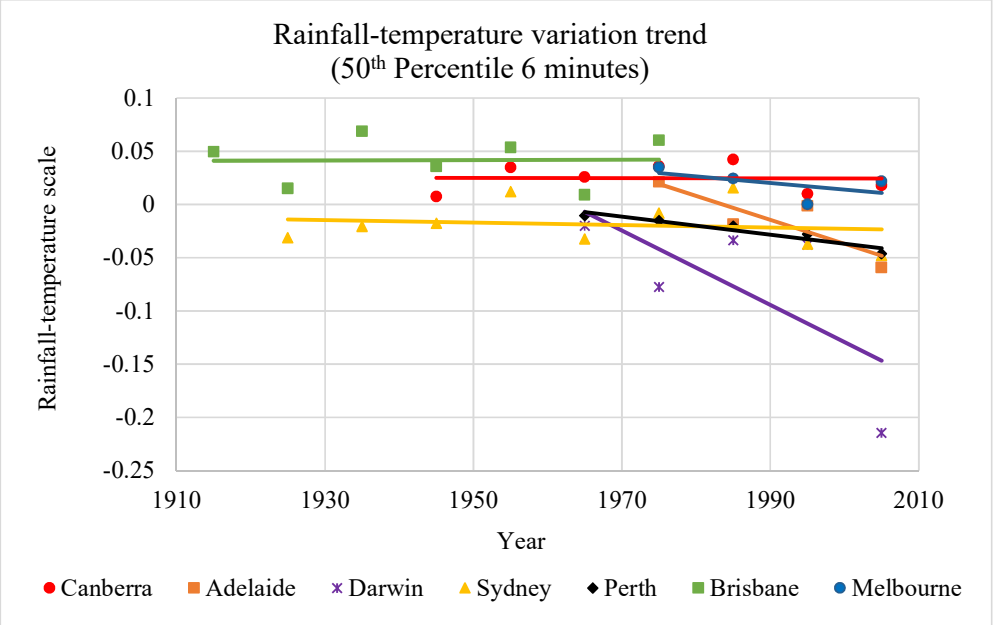

Figure 6.6: Rainfall–temperature scale variation for the 50th percentile of extreme sub-daily rainfall events (6 minute duration)

A similar trend in scale variation of 1 hour daily maximum rainfalls can be observed at all stations except one station in Figure 6.7, the exception being the Darwin station, compared to Figure 6.5. Figure 6.7 shows that the highest increasing trend in scaling occurs at the

Melbourne station, while the Darwin and Adelaide stations display a decreasing trend in scaling. Figure 6.8 describes the trend of scale variation for the 50th percentile of daily maximum 1 hour rainfall duration and daily maximum temperature over time. According to Figure 6.8, all stations show decreasing trends while the Adelaide and Darwin stations show the highest decreasing trend in scaling.

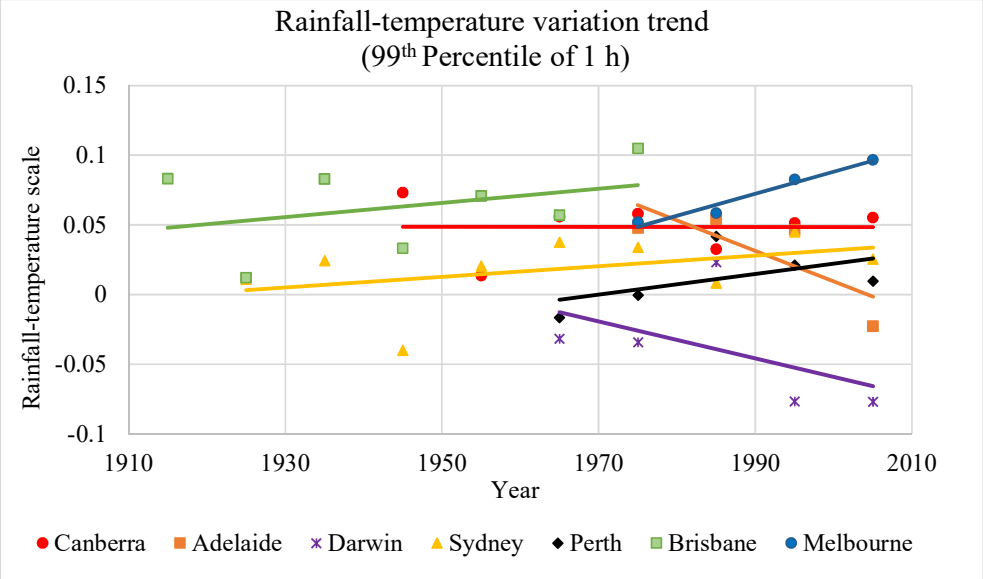

Figure 6.7: Rainfall–temperature scale variation for the 99th percentile of extreme sub-daily rainfall events (1 hour duration)

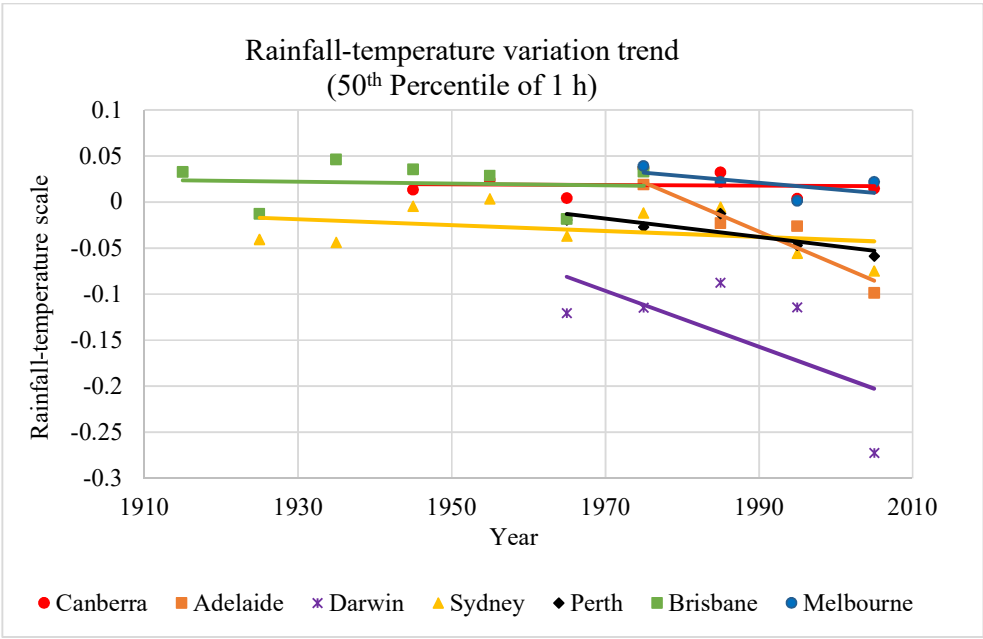

Figure 6.8: Rainfall–temperature scale variation for the 50th percentile of extreme sub-daily rainfall events (1 hour duration)

Figure 6.9 describes the trend in rainfall-temperature scale for daily maximum temperature and the 99th percentile of daily rainfall. It is apparent that the scale changing trend of 99th percentile daily rainfall differs from the scale changing trend of 99th percentile of 6 minute and 1 hour rainfall events. According to Figure 6.9, only the Melbourne, Perth, and Sydney stations show a slight increasing trend in the scale and all other stations show a decreasing trend in the scale. Figure 6.10 describes the scaling trend of the 50th percentile of daily rainfall and it shows a decreasing trend for all stations except Canberra. These trends in extreme daily rainfall events suggest that increasing temperatures will have minimal influence on extreme daily rainfall, in contrast to 6 minute extreme rainfall events. Therefore, it is clear that rainfall–temperature scale variation is highly depended on location, rain duration and the extremeness of the rainfall.

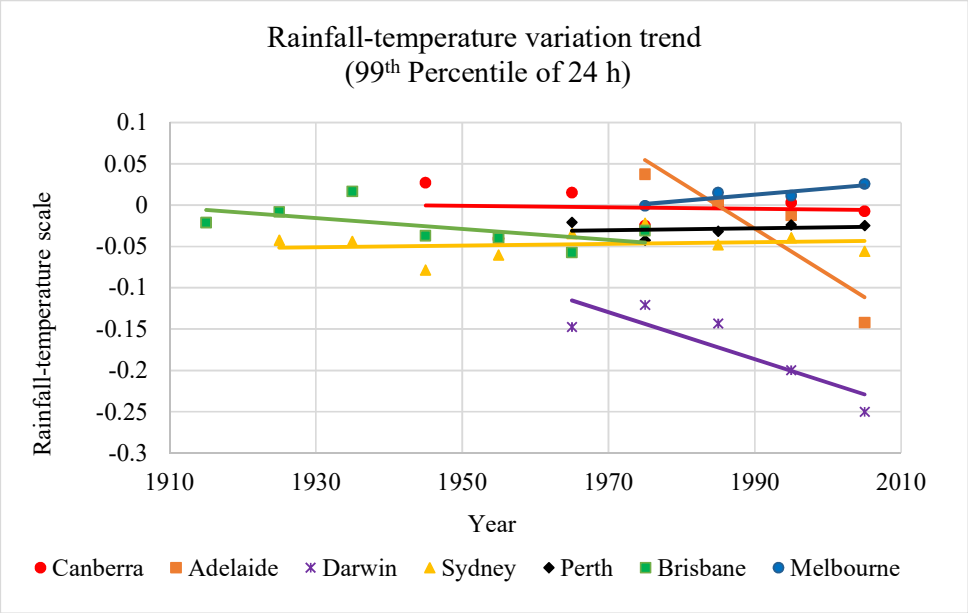

Figure 6.9: Rainfall–temperature scale variation for the 99th percentile of extreme 24 hour rainfall events

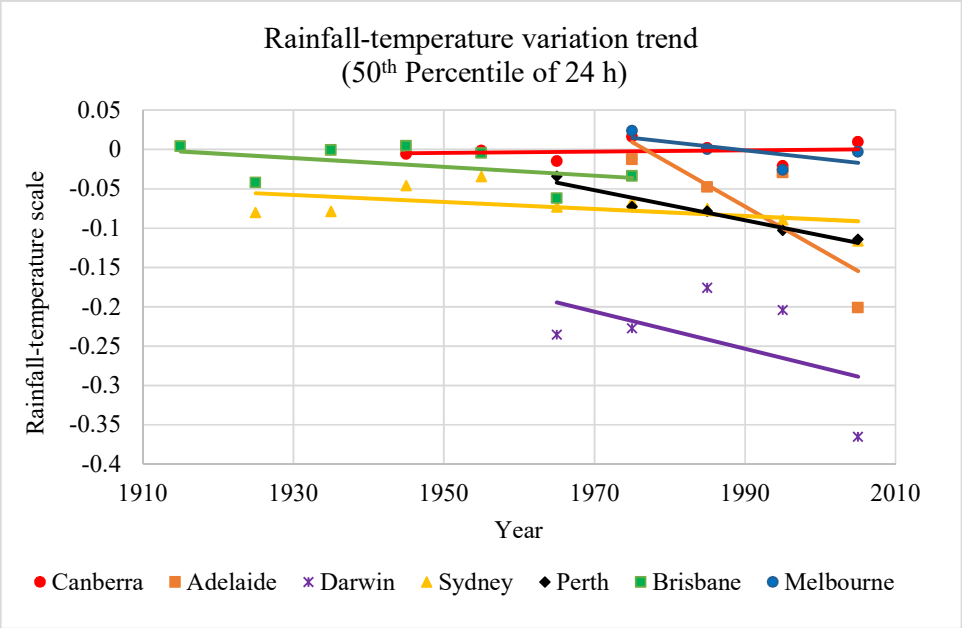

Figure 6.10: Rainfall –temperature scale variation for the 50th percentile of extreme 24 hour rainfall events

To further confirm the accuracy of the described graphical results of rainfall–temperature scale variation trend over time, 95% Confidence Interval (CI) of the slope of proposed trend lines are compared with the estimated variability. To illustrate this, a comparison is presented in Table 6.1 for the 99th percentile of 6 minute, 1 hour and 24 hour rainfall durations. The uncertainty estimates of the trend lines are smaller than the estimated variabilities thus implying that the computed scale slope changes are significant. Further, as estimated 95% CIs do not contain zero value, it justifies the statistical significance of proposed trends (except 24 hour at Sydney and 1 hour at Canberra). Also, the investigation of the uncertainty associated with 50th percentile of rainfall-temperature and seasonal rainfall–temperature scale variation trend lines (see section 6.4.3) confirms that the scale slope changes in times are significant.

Table 6.1: Comparison of uncertainty and variability of trend lines

Duration	Station	95% Confidence Interval	Variability	Station	95% Confidence Interval	Variability
6min		-0.0006 ± 0.00046	0.03026		0.0009±0.0007	0.03223
1 h	Adelaide	-0.0022±0.0010	0.07660	Melbourne	0.0016±0.0004	0.04460
24h		-0.0055±0.0035	0.17938		0.0008±0.0005	0.02668
6min		0.0005±0.0003	0.09643		0.0009±0.0005	0.05942
1 h	Brisbane	0.0005±0.0004	0.09289	Perth	0.0007±0.0001	0.05830
24h		-0.0007±0.0004	0.07407		0.0001±0.00009	0.02134
6min		0.0008±0.0007	0.04392		0.0005±0.0004	0.08430
1 h	Canberra	-0.000004±0.0008	0.05951	Sydney	0.0004±0.0002	0.08481
24h		-0.00009±0.00005	0.06755		0.00001±0.00002	0.05656
6min		0.0006±0.0004	0.09167			
1 h	Darwin	-0.0013±0.0002	0.10004			
24h		-0.0028±0.0019	0.12924			

6.4.3 The Impact of Seasonal Variation on Rainfall- Temperature Scaling Trends

Understanding the average temporal changes of seasonal variation in rainfall-temperature scaling trends is important as it enables the projection of seasonal influence on rainfall extremes in the future. In this analysis, the summer and autumn months (Dec-May) were placed in one group and the winter and spring months (June-November) were placed in the other group. A trend analysis was then conducted to identify the changes in rainfall - temperature scale trend from extreme sub-daily rainfall events to daily maximum temperature. Figure 6.11 describes the trend in the scale variation of the 99th percentile of extreme rainfall and daily maximum temperature seasonally. The data presented in Figure 6.11 show an increasing trend in scale for the Melbourne, Perth and Sydney stations for summer and autumn rainfalls for all durations (six minute; one hour; and 24 hour). In contrast, the winter and spring rainfall events for Melbourne and Perth show increasing trend while Adelaide and Darwin show a decreasing trend. Figure 6.12 presents the seasonal trend variation of the 50th percentile of extreme rainfall events and daily maximum temperature. Based on the data presented in Figure 6.12, the Adelaide, Darwin and Melbourne rain stations show a decreasing trend for both seasonal categories. While the Brisbane and Canberra stations show an increasing trend for the summer and autumn

seasons. Furthermore, the Sydney station shows an increasing trend only for the winter and spring season for the 6 minute duration rainfall events.

By comparing changes in rainfall-temperature scale trend for the seasonal 99th and 50th percentiles, it can be seen that the same trends are evident for the Adelaide and Darwin stations (with the exception of the 6 minute duration events for the summer/autumn rainfall for Darwin). The Melbourne and Perth stations show completely opposite trends in 99th and 50th percentile (with the exception of the 6 minute duration events for the winter/spring rainfall for Perth). However, the magnitude of the scale changing trend is highly variable due to the changes of seasonal storm types, circulation patterns in different stations. Seasonal-scale trends for the Brisbane, Canberra and Sydney stations are varied and it is difficult to identify any patterns.

These observations indicate the important role of different climatic factors play in the occurrence of seasonal rainfalls and rainfall–temperature scale, which is not surprising given that the rainfall driving processes are complex. The intensity of extreme rainfall event depends on the combined impact of many numbers of variables. However, atmospheric temperature is one of the dominant variables driving the occurrence of intense rainfall events. Especially, slow moving thunderstorms, strong low pressure and tropical cyclone have high impacts on local extreme rainfall events which make variations in rainfall - temperature scale. Also, the large-scale motion of the atmosphere (Emori and Brown, 2005) has a considerable impact on extreme rainfall events and changes in moist-adiabatic lapse rates (O'Gorman and Schneider, 2009) is one of the reasons why variations in the scale occur. Furthermore, the local occurrence of rainfall extremes does not scale with water vapour content due to changes in moist-adiabatic lapse rates and temperature anomalies. Changing cloud characteristics during rainfall events (Trenberth et al., 2003, KE, 2011) also have a high impact on rainfall depth. Also, high intense convective rainfall events show high rainfall - temperature scaling relationship rather than stratiform rainfall events (Molnar et al., 2015). Therefore, consequent changing patterns in rainfall-temperature scale could be explained by the combined impact of all these variables.

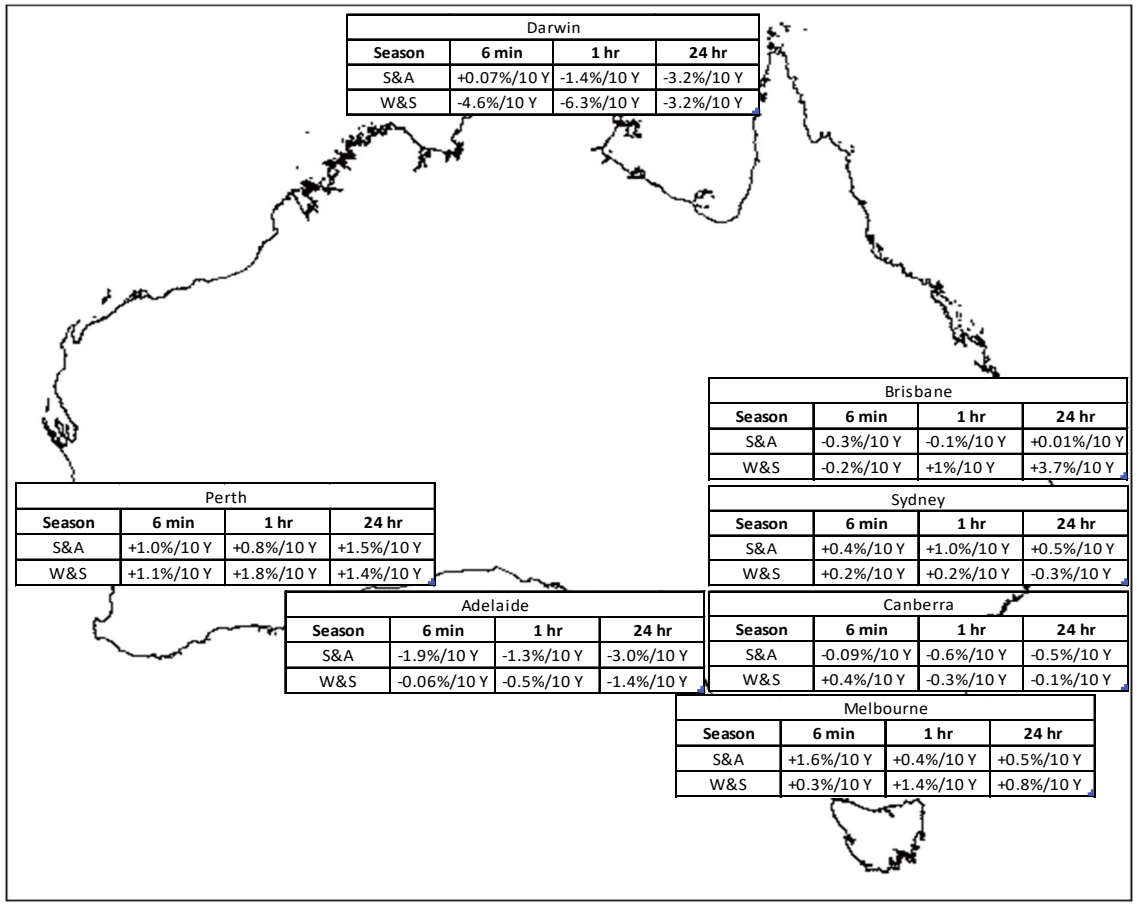

Figure 6.11: Seasonal variations in rainfall–temperature scale trends for the 99th percentile

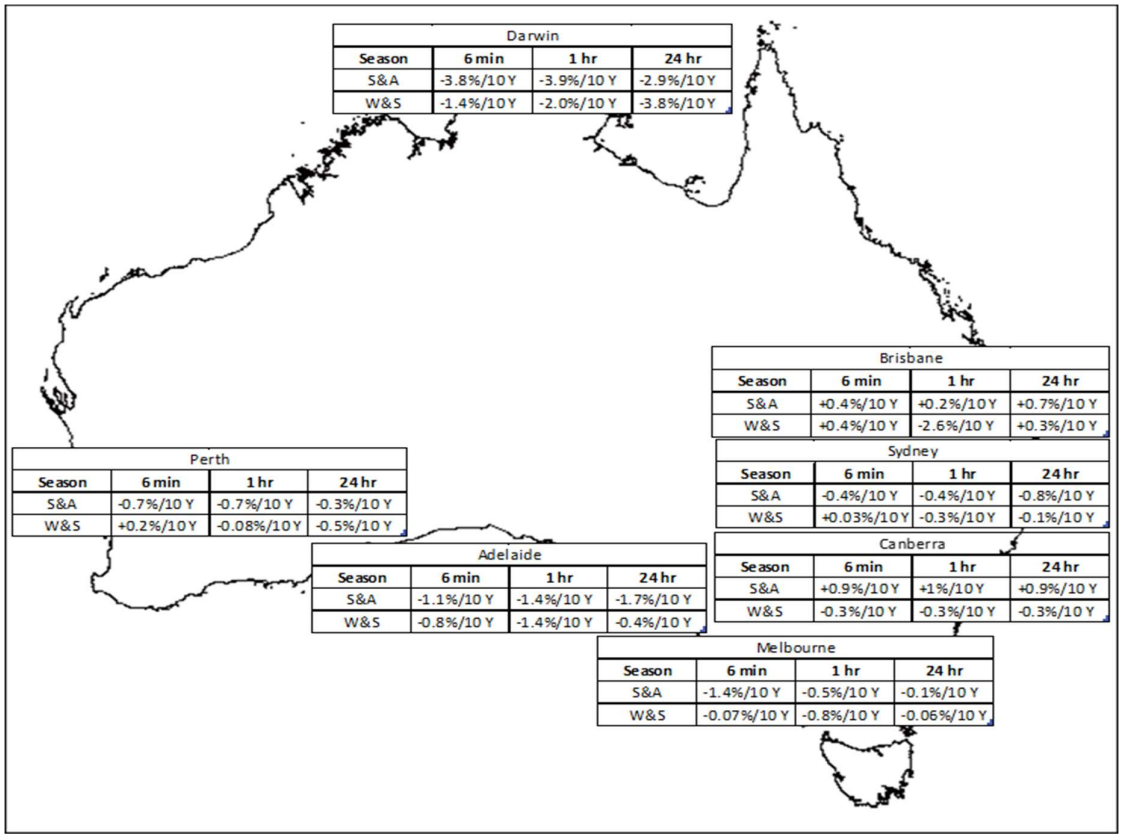

Figure 6.12: Seasonal variations in rainfall–temperature scale trends for the 50th percentile

6.5 Summary

The empirical relationships between extreme intensities on daily maximum temperature were investigated in this study using data from seven weather stations located throughout Australia (Adelaide, Brisbane, Canberra, Darwin, Melbourne, Perth and Sydney). The scaling relationship for daily maximum temperature and the 99^{th} and 50^{th} percentile of 6 minute, 12 minute, 30 minute, 1 hour, 2 hour, 6 hour, 12 hour and 24 hour daily maximum rainfall for wet days (rainfall>0.3mm) was analysed. To minimise the bias associated with C-C scale analysis, a technique placing an equal number of pairs in designated temperature bins was used to analyse the relationship. The initial analysis was conducted by considering the total data period as a single window.

The results of this analysis were consistent with results reported in the literature, with rainfall–temperature scaling relationships found for all stations and evidence that the scale varies with location, rain duration and temperature. Darwin station showed a negative scale relationship for both the 50^{th} and 99^{th} percentiles for all rainfall durations. It is located in the Northern territory, which has tropical climate throughout the year. A similar negative scale at weather stations under tropical climate (in northern territory) are observed by (Hardwick Jones et al., 2010). The other six stations showed similar patterns in scale relationship with the highest scale values resulting for 6 minute rainfall durations and the lowest for 24 hour rainfall durations for both percentiles. These results imply that short duration rainfall events are more dependent on daily maximum temperature than long duration rainfall events. However, scaling values vary with the percentile of the rainfall event, with the 99^{th} percentile always producing a higher value than the 50^{th} percentile. Therefore, we can conclude that the relationship between daily maximum temperature and more extreme rainfall events (not the daily maximum) is stronger than the relationship with average rainfall events. Further, the scale is not constant over a range of temperatures, with deviation especially evident at the lower and upper ends of the temperature range. The results also show that the positive scaling range is a unique for a station. Similar behaviours are identified by other researchers in Australia and other parts of the world (Hardwick Jones et al., 2010, Berg et al., 2009).

To identify the variation of this scale with time, data was then analysed using 10 year data windows. The 99th and 50th percentiles of 6 minute, 1 hour and 24 hour rainfall events were studied. The Adelaide station showed a high decreasing rate of the scale for all rainfall events for both percentiles. The Darwin station also showed a decreasing trend in scale for all events with the exception of the 99th percentile of 6 minute rainfall events. In comparison, the other five stations showed an increasing trend in the scale for the 99th percentile of 6 minute rainfall events. This increasing trend may be caused by frequent intensified convective rainfall events as a result of climate change. Further, the results also show a decreasing trend in the scale, especially for the 50th percentile of long duration rainfall events.

Seasonal variations in the trend of the scale change were analysed by placing the summer and autumn seasons in one group and the winter and spring seasons in another group. The Perth, Melbourne and Sydney (except 24 hour rainfall winter/ spring) stations show an increasing trend of scale for both groups while Adelaide and Darwin show decreasing trend for 99th percentile (except 6 minutes rainfall in summer/autumn). Furthermore, most scaling trends of 50th percentile are decreasing for both groups.

These results clearly show that the rainfall-temperature scaling relationship is limited to certain temperature range, and this relationship depends on the percentile of rainfall, the rainfall duration, analysis period and the season. Both increasing and decreasing scaling trends were observed by periodic analysis. According to these results, it can be expected more extreme short duration rainfalls in some regions of Australia in the future.

CHAPTER 7

7 Modelling of the impacts of climate and land use change on urban catchments

The approach described in this chapter is published at

> H.M.S.M.Herath, B.M.A.P.Basnayaka, P.R. Sarukkalige, V.T.V.Nguyen, Behaviour of urban catchment hydrology to future climate change scenarios, 19th IAHR - APD Congress, 21-24 Sep. 2014, Hanoi, Vietnam.

7.1 Introduction

Hydrological assessment is an essential requirement in all main stages of urban land development projects. Most of the water management authorities in Australia recommends to conduct variety of water management assessments in different scales (i.e. District Water Management Strategy (LWMS), Local Water Management Strategy (LWMS) and Local Water Management Plan (LWMP)). The current stormwater management practice is limited to evaluate the impacts of land use change on the hydrological behaviour of developing catchments. Climate change impact does not address under current stormwater management guidelines and it can be identified as a main drawback of the available approaches. Therefore, assessment of the integrated impacts of climate and land use change on urban catchments is very important for sustainable land development activities.

Rainfall-runoff models are one of the most effective methods for assessing these impacts on catchment hydrological behaviour. Hydrology models help to understand the catchment behaviour and it facilitates in planning, implementing and forecasting of stormwater management strategies. Nowadays, hydrological models are capable to simulate more complex watershed characteristics. As a result, highly developed computational technologies and high accurate data. Also, it has become a compulsory tool in most of the urban stormwater management studies. In urban stormwater

management sector, hydrological models are commonly used to identify the floodplains, drainage structures' capacities and designing flood storage areas etc.

Taking these facts into account, the main purpose of this chapter is to describe an approach to evaluate the combined impacts of land use change and climate change in urban catchments. Also, the other objectives of this case study are;

- Developing a hydrological model by taking catchment parameters into account to simulate the real hydrological process in urban catchments.
- Conducting sensitivity analysis to identify the most sensitive catchment parameters for surface water routing.
- Calibrating and validating the developed model using observed stream data.
- Evaluating the critical events (critical rain duration) which have the highest impacts on surface water routing for 100 year recurrence intervals.
- Identifying vulnerable areas for urban flooding in the future

7.2 Methodology

Urban flooding is a severe problem in most urban watersheds as a result of reduced impervious areas. Influence of changing the climate on rainfall, further increase the severity of this problems and still it is not addressed properly in urban hydrological assessments. With the climate change, rainfall patterns are changed in considerable amount and it is required to assess these variations in the design of the urban stormwater drainage network. Otherwise, stormwater drainage network may fail in high-intensity future rainfall events occurred due to climate change. As discussed in Chapter 5, Intensity Duration Frequency (IDF) relations play a vital role in estimating design storms for drainage capacity designs. Furthermore, Chapter 3-5 describe an

approach of developing IDF relations which represent the climate change impact for future periods. Therefore, it is feasible to use IDF relations for future periods using proposed downscaling approach in hydrological assessments to evaluate the combined impacts of land use change and climate change on urban hydrology. However, there are some limitations in the proposed GCM downscaling approach to develop IDF relations for the future periods. Especially it is required long-term observed rainfall data in sub-daily time steps. Also, availability and reliability of GCM predictors need to be considered in developing IDF relations for future periods.

Development of complex hydrological model is a time consuming and high computational demanded process to assess the stormwater management guideline in developing catchment. Observed and catchment data requirement is very high in hydrological modelling. In some instances, these data are not directly measurable and need to conduct a sensitivity analysis to estimate high accurate values for non-measurable parameters. Also, it requires model calibration and validation prior to applying in scenario analysis in the hydrological study. Therefore, below methodology is adopted in this study to develop an approach to evaluate combined impacts of land use change and climate change on urban catchment.

- Identify suitable urban catchment to apply proposed approach to evaluate the combined impacts of land use change and climate change. When selecting the catchment, the availability of observed sub-daily rainfall data is specially investigated to derive IDF relations for the future period using downscaling of GCM predictors.

- Monitoring, collecting and analysing catchment parameters and hydrological data.

- Identifying high performing rainfall-runoff modelling approach to simulate realistic catchment behaviour under different weather conditions.

- Developing pre-development hydrological model to evaluate the existing hydrological conditions.

- Evaluating sensitivity of catchment parameters, calibrating and validating the model for observed rainfall event under existing condition.

- Developing post-development model and performing series of scenario to evaluate the combined impacts of climate change and land use change on urban catchments.

7.3 Case Study: Stirling City Centre development

7.3.1 Catchment characteristics

To assess the impacts of climate and land use changes on urban catchments, proposed urban development area of Stirling City Centre development project is considered as the study area for this case study. Stirling City Centre development is an ideal case study to assess the future impacts of climate change and also due to the vast land development, it enables to assess the impacts of land use changes on the catchment hydrological characteristics.

Stirling City Centre project is located North Western part of the Perth, approximately 10 km from Perth city. Total proposed development area is 3.5 km^2. However, total catchment area which contributes to the runoff at the end of development area is 17.3 km^2.By considering the accuracy of the rainfall-runoff model, and their boundary conditions model domain has been extended to approximately 37 km^2. Further, Osborn Park Branch Drain (OPBD) is the central hydraulic section in the development area. OPBD enters to development area near to Telford Crescent and exists near to John Sanders Drive. Other secondary local stormwater drainage network mainly consists of underground pipes. Also, this development area consists of landfill area, Freeway section, commercial and residential areas.

To obtain the climate data, Perth airport weather station is selected as it is the nearest ongoing BoM weather station with long period weather records to the study area. Therefore, developed IDF curves for Perth airport region in this research (in Chapter 5), is used in the present hydrological assessment. Figure 7.1 presents an aerial map of the study area, Perth airport and Perth city.

7.3.2 Summary of data for the study

Data requirement in this study is very high and is divided into two categories. i.e data for IDF relation development and data for hydrological model development. For the IDF development sub-daily rainfall at Perth airport stations (009021), NCEP reanalysed data for HadCM3 and CGCM3, Predictor data for HadCM3-A2 and CGCM3-A2 are used. Employed data for IDF developing has been described in previous chapters (section 3.2 and 5.1).

Further, all other required catchment data are collected from GHD Australia, who has conducted some studies in the same catchment as permitted by the City of Stirling.

These data consist of

- Stream flow data
- Weather data
- GIS, topography and survey data

Stream level and flow data are collected at observation station located at downstream of the catchment and it includes 15minute time step observed data for the period of August 2011 to December 2012. Depth sensors are used to record level data and discharge is calculated from these observed level data. In addition, Pan Evaporation data for the Perth Metro BoM weather station (09225) and generated pan evaporation data using the silo patched point data at the centre of model domain is used for the study.

Landgate (Landgate is the business name of Western Australian land information authority) surface geology data, geological mapping data, GIS data including roads, cadastre and imaginary data are used in this study to develop the hydrological model.

Also City of Stirling's stormwater pipe network data, irrigation data are used and the ground survey data is collected from GHD Australia. Further Department of Water (DoW) Lidar data are used in this hydrological modelling study. Groundwater data for October 2011 to January 2013, are obtained from the regional WIN monitoring well data provided by DoW.

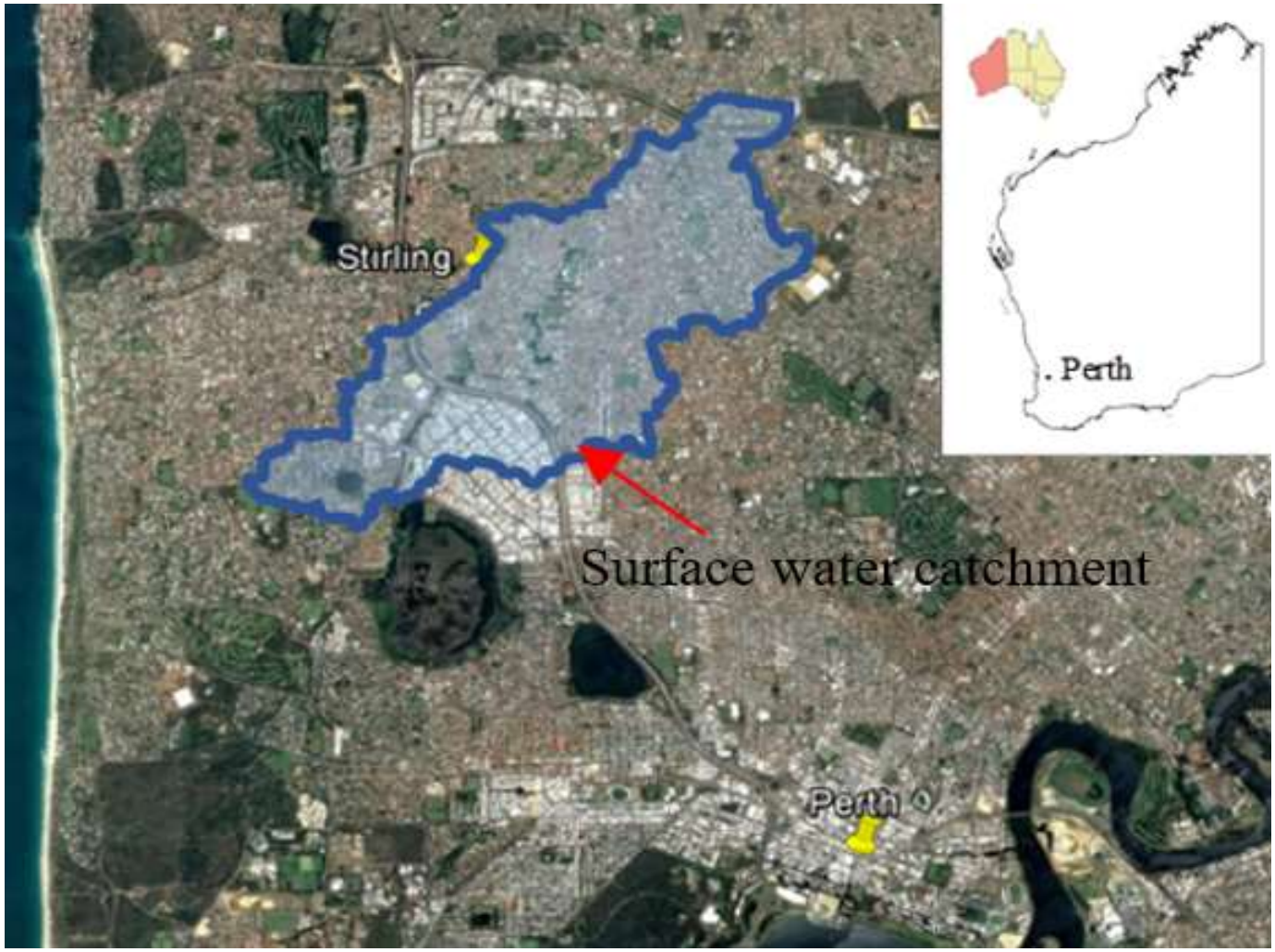

Figure 7.1: Location of the study area

7.3.3 Topography

As a result of surface grading from east and west, the topography of the model domain can be identified as a central valley. It runs from North to South direction. Ground surface elevation variation from North to South is approximately from 25-30 m Australian Hight Datum (AHD) to 5-10 m AHD. Elevation of East and West of the study domain is approximately 75-85 m AHD and 40-50 m AHD respectively. Because of this elevation difference, stormwater drainage discharge is located at the south of the catchment. Figure 7.2 presents the topography of the study area.

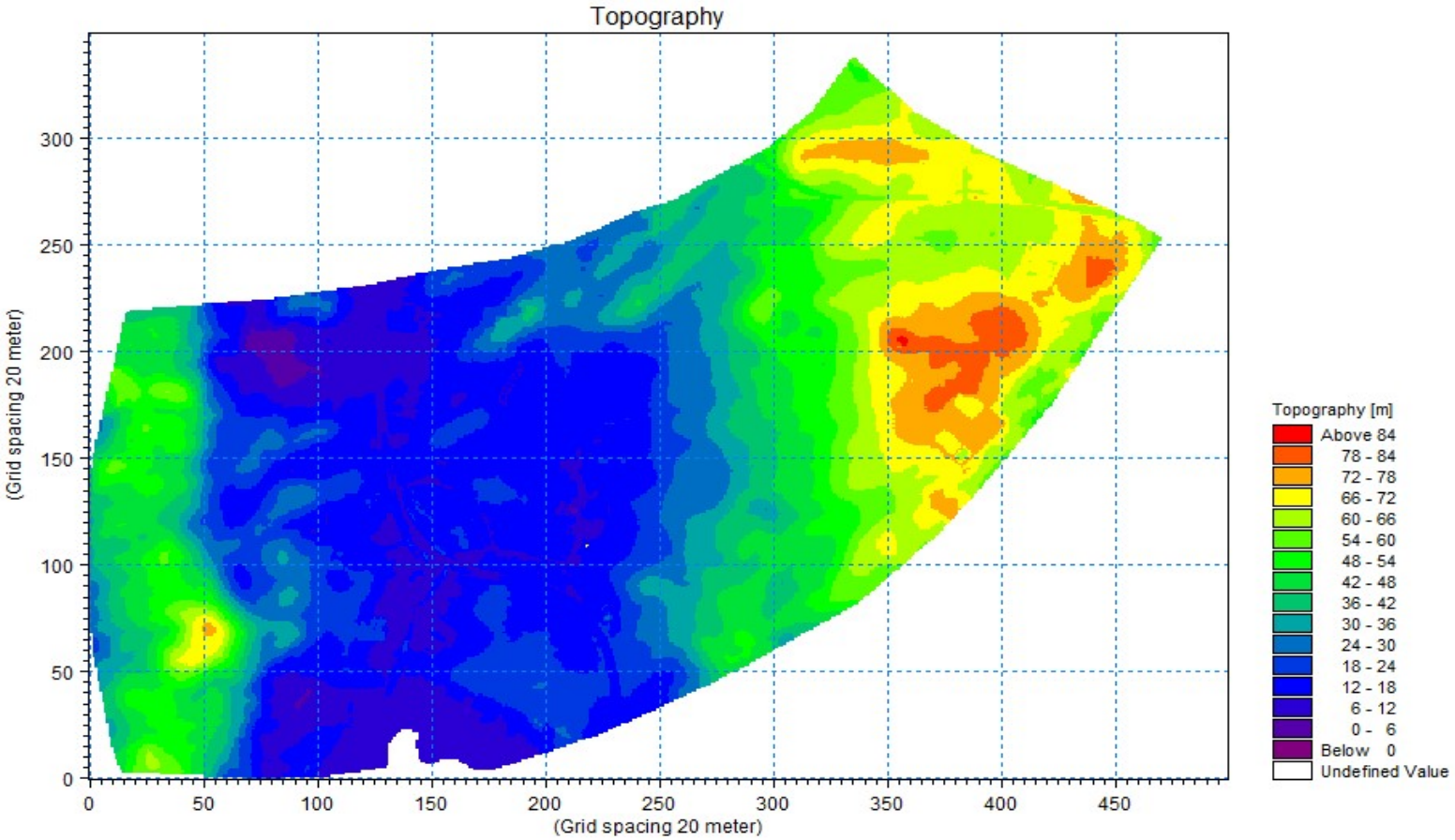

Figure 7.2: Topography map of the model domain

7.3.4 Streamflow and drainage network

As mentioned earlier, OPBD can be identified as the main central streamflow through the study area. Base water flow can be observed throughout the year in OPBD because of the existing shallow groundwater in the area. Also, OPBD is highly sensitive to the rainfall events due to connected stormwater drainage network and groundwater influence. The highest flow rate, approximately 2.5- 2.7 m^3/s could be observed in the winter period and in summer period it drops down to 0.1-0.3 m^3/s.

Two other central drainage systems are located in this area. Beryl Street Branch Drain (BSBD) is an underground pipe network located in the upper catchment. It connects to open drain Albert Street Branch Drain (ASBD) and ASBD connects to OPBD.

There are a number of drainage structures are available in this area. Especially 19 culverts and five weirs are included into the model by considering their influence on surface water routing.

7.3.5 Groundwater

As a broad description, Northeast to Southwest groundwater flow direction can be indicated in the model domain. Groundwater level varies from eastern model boundary to western model boundary from 24 – 27 m AHD to 2 - 4 m AHD respectively. However, these general behaviour is diverted at some specific locations like lakes etc. Further, rainwater infiltration is the dominant groundwater recharging event into the superficial aquifer. In this area 5-14 % of total rainfall recharges to the groundwater (Davidson, 1995).

7.4 Hydrological modelling using MIKE SHE and MIKE 11

MIKE SHE can be identified as one of the greatest physically based modelling software which developed by DHI to address all the main aspects of land phase hydrology(Refsgaard and Storm, 1995). It is an integrated two-dimensional (2-D) model of surface water, groundwater, groundwater recharge and evapotranspiration. Application of MIKE SHE modelling is varied from simple rainfall-runoff modelling to complex hydrology assessments. Common MIKE SHE application area are; integrated catchment hydrology, wetland management, land use and climate change impacts on surface water and groundwater, irrigation and drought management, floodplain management, nutrient fate and management etc. (MIKESHE, 2016). Some of the recent applications of MIKE SHE on land use and climate change impact assessments has discussed in this section by considering their relevancy to the current study.

MIKE SHE is capable of conducting hydrology modelling of small urban catchment as well as large river catchments. Chu et al. (2013) used MIKE SHE to investigate the impacts of urbanization of "Big river" watershed (2381km^2) in USA. Within the period of 1992 to 2006, urban area has been increased by 300% in this watershed. They studied the change of frequency of discharge, velocity and water depth of streamflow as a result of land use change by coupling MIKE SHE and 1-D MIKE 11 hydrodynamic river model. Butts et al. (2014) used MIKE SHE model to study the impact of climate change on groundwater at Skjern river catchment, Denmark. They used the dynamically coupled model of MIKE SHE and HIRHAM regional climate model on open MI (Modelling Interface). Wijesekara et al. (2013) used MIKE SHE/MIKE 11 coupled model to develop a comprehensive land use/hydrological modelling system for scenario simulation. By their study, four scenarios were evaluated for the period of 2010 -2030 in Elbow river watershed, Alberta, Canada.

There is a high impact on the land cover by wildfire. Especially wildfire is the main reason for low infiltration land with high runoff. Moussoulis et al. (2015) investigated the impacts of wildfire on surface runoff in semi-arid catchment located in central Greece. They used MIKE SHE to assess the hydrological response of the catchment after few years follow the wildfire. Further, Keilholz et al. (2015) studied the combined impact of land use change and climate change on groundwater and ecosystem at Tarim

river, China. They used 50 years climate data and land use data to develop MIKE SHE model to assess the impacts on 85km^2 catchment. Also, they projected the probable groundwater and ecosystem changes at 2050 and 2100.

Above recent literature clearly depicts the capability of MIKE SHE to model the different aspects of land use and climate change impact assessments. Also, it shows that MIKE SHE is user-friendly to couple with other modelling software to enhance its performance to apply in various applications.

MIKE 11 is the DHI software for one-dimensional (1-D) river and channel modelling. Therefore, in this study, MIKE SHE model is coupled with MIKE 11 model to evaluate the surface water characteristics. Figure 7.3 presents the MIKE SHE catchment process within the closed water cycle.

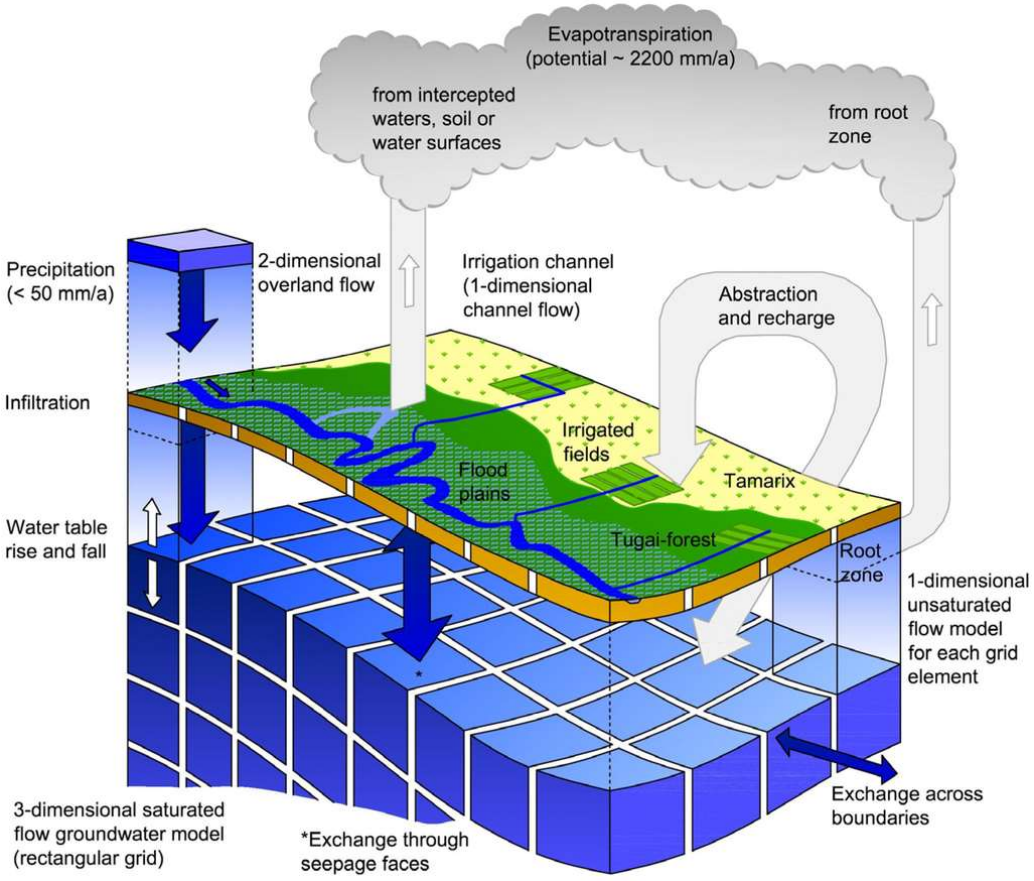

Figure 7.3: Catchment processes simulated by MIKE SHE (Source: DHI 2013)

The concept of MIKE SHE is initially based on the blueprint proposed by Freeze and Harlan (1969) for the hydrologic cycle and it has been developed very rapidly since mid of 1980s by DHI Water and Environment. MIKE SHE provides very flexible simulating options to develop a model based on the user requirement and available data. If the user needs to MIKE SHE model with channel or river, it should be coupled with MIKE 11. Similarly, for sewer modelling MIKE SHE needs to be coupled with Mouse.

The main simulation specifications in MIKE SHE are;

- Overland flow
- Rivers and lakes
- Unsaturated flow
- Evapotranspiration
- Saturated flow
- Water quality

Under these simulation specifications, MIKE SHE provides simple to very complex solving options.

Overland flow modelling

Overland flow option is available in MIKE SHE to simulate the ponded surface water as 2-D. There are two ways to simulate the overland flow.i.e. Finite element method or Sub-catchment method. Finite element method is based on the diffusive wave approximation of Saint Venant equations (de Saint-Venant, 1871). Sub-catchment approach is based on the Manning's equation (Manning, 1891).

Rivers and Lakes

MIKE 11 model is employed in river and lakes modelling. MIKE 11 model is standalone and it can be run separately from MIKE SHE main model. Also, it needs to be constructed separately to MIKE SHE model for 1-D channel flow modelling. There are several options available in MIKE 11 modelling. i.e. Hydrodynamic, Advection-dispersion, Sediment transport, Eco lab, Rainfall–runoff, Flood forecast,

Data assimilation, Ice and encroachment. Also, MIKE 11 model can be run as unsteady or quasi-steady model. Coupling of MIKE 11 to MIKE SHE is possible in three ways.

- River-Aquifer exchange
- Flood codes for inundation
- Overbank spelling to and from MIKE 11

Unsaturated flow

Unsaturated flow simulation is a main function available in MIKE SHE. Rainfall, evapotranspiration and groundwater recharge is associated with this zone and therefore soil moisture amount is fluctuating in the unsaturated zone. In general, water flow in the unsaturated zone is vertical due to the gravity. Based on this assumption MIKE SHE simulates water flow in unsaturated zone as a 1-D vertical flow. Three different equations are available for unsaturated water flow simulation.

- Richards equation
- Gravity flow
- Two-layer water balance method

Richards equation method (Richards, 1931) is more complex and accurate than other methods. However, computationally it is extensive and simulation time increased by several times. Gravity flow method is simple and simulation provides acceptable results with good accuracy. At the presence of shallow groundwater table and high influence of evapotranspiration on groundwater recharge at the root zone, two-layer water balance method is suitable.

Evapotranspiration (ET)

ET modelling is available in MIKE SHE to represent the interception of rainfall by the canopy, draining to soil from canopy, up taking of water by plant root from unsaturated zone, evaporation from canopy and soil surface etc. ET simulation in MIKE SHE is based on the method developed by KRISTENSEN and JENSEN (1975) when Richards equation or Gravity flow methods are used in the unsaturated region. When two-layer

water balance method is employed in unsaturated zone ET simulation model is based on Yan and Smith (1994) approach.

Saturated flow

All the layers below water table are considered as saturated in MIKE SHE and it allows three-dimensional flow in the heterogeneous aquifer. Three-dimensional Darcy equation (Darcy, 1856) is used to describe the spatial and temporal variation of the hydraulic head and iterative finite difference technique is employed for the solving. There are two methods available in MIKE SHE for saturated flow modelling such as finite difference method and linear reservoir method.

Water quality

Water quality modelling section of MIKE SHE is categorized under three subsections. i.e. Advection-dispersion, Reactive transport and Particle tracking

Advection-dispersion concept is mainly used for solute transport in the hydrological cycle. In saturation zone, solute transport modelling can be employed as 1-D, 2-D or 3-D. Under reactive transport; plant uptake, degradation, sorption and desorption options are available to model solute transport. Further, particle tracking option is available in MIKE SHE instead of solute transport modelling,

7.5 Application of the catchment model

Considering the catchment characteristics of the study area, the modelling process should include surface water and groundwater hydrological modelling as well as drainage hydraulic modelling. As integrated MIKE SHE and MIKE 11 modelling approach are capable of handling these complex catchment characteristics. The rainfall-runoff modelling of the catchment, is carried out under two steps.

- MIKE SHE model development,
- MIKE 11 Model development.

As mentioned earlier, MIKE SHE and MIKE 11 are standalong models. MIKE SHE is used to simulate 2-dimensional surface water in the catchment while MIKE 11 is used to simulate 1- dimensional drainage and river network. By coupling of MIKE SHE and MIKE 11 models, it is feasible to develop high accurate distributed hydrological model to assess the real characteristics of the study area.

7.5.1 MIKE SHE model development

MIKE SHE facilitates users by providing "Set up Data Tree" in model development. First major item in the setup tree is "Display" setup. This setup branch does not involve with the simulation and it is available to display background/foreground Figure. Simulation Specification, Model domain and grid, Topography, Climate, Land use, Rivers and lakes (combined with MIKE 11), Overland flow and unsaturated flow and saturated zone are the other key model set up branches in MIKE SHE.

7.5.1.1 Simulation Specification

As shown in

Table 7.1 different simulation methods are employed for different components of the catchment model.

Table 7.1: Simulation components and methods

Simulation component	Method
Overland flow	Finite difference method
Rivers and lakes	MIKE 11
Unsaturated flow	Two-layer Unsaturated Zone (UZ)
Evapotranspiration	Yan and Smith approach
Saturated flow	Finite difference method

Further, simulation time steps are defined in this step. Simulation time and accuracy of the simulation results are the two main concerns in defining the simulation time steps. MIKE SHE recommends to use 0.5 h time as the maximum allowed Over Land

(OL) time step for high realistic simulation. Further, it recommends to use same or larger time step for UZ than the OL. Furthermore, Saturated Zone (SZ) time step should be larger than or equal to the UZ time step. By considering these recommendations, time steps are defined as;

Initial time step – 0.5 h

Maximum allowed OL time step – 0.5 h

Maximum allowed UZ time step – 0.5 h

Maximum allowed SZ time step – 0.5 h

However, at a high intensified rain events MIKE SHE model tends to unstable. To prevent the model unstability, there is an option in MIKE SHE to define precipitation dependant time steps. Under precipitation dependant time step, MIKE SHE defines short time steps by itself to prevent the exceeding of defined values. In this study, following precipitation dependant time steps are defined.

Maximum precipitation depth per time step – 3mm

Maximum infiltration amount per time step – 3 mm

Input precipitation rate requiring its own time step – 1 mm/h

7.5.1.2 Model domain and grid

The Geocentric Datum of Australia (GDA94) is used to create the model domain for the catchment area. Compatibility with Global Positioning System (GPS) and other latest positioning method can be identified as the main advantage of using GDA94 reference system. Further, the current study area is located in ZONE 50 of Map Grid of Australia (MGA) referencing system. When creating the model domain accuracy of simulations and time for the simulations are mainly concerned. By considering these two factors grid size is limited to 20m. Number of grid cells in the domain are 500 and 350 for X and Y direction respectively. Also, the coordinates of the left lower corner

of the model domain is 31°54′48 S, 115°46′45E and right upper corner is 31°51′05S, 115°53′19E.

7.5.1.3 Topography

20 m Digital Elevated Model (DEM) is developed using the surveyed data for the existing condition. Some manual adjustments for the developed DEM are required to well match with the real site situations. Figure 7.2 in section 7.3 presents the developed DEM for existing condition.

DEM is modified to proposed surface elevations to simulate the hydrological parameters of the post-development condition. The proposed DEM of the development area is presented in Figure 7.4.

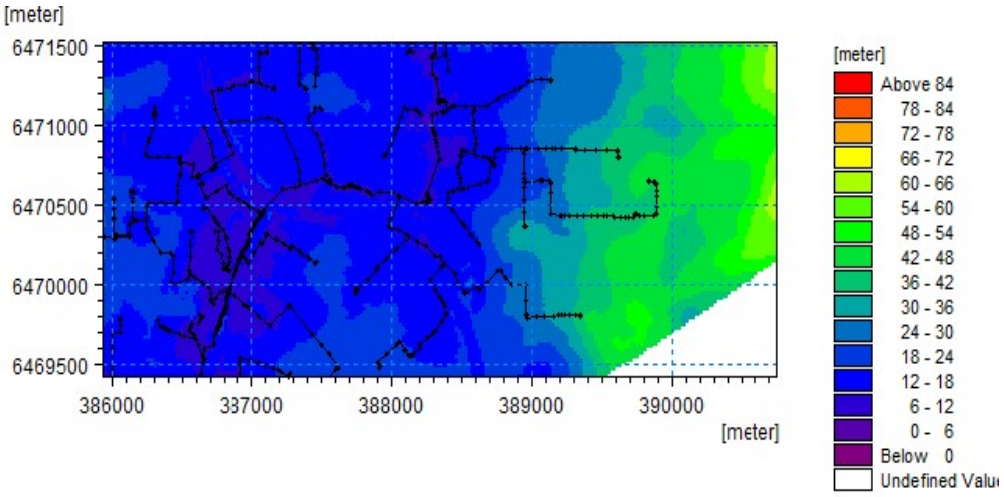

Figure 7.4: Modified DEM map in development area for the post-development stage

7.5.1.4 Climate data

Climate branch comes under two subtitle. i.e. Precipitation and Evapotranspiration. For the model calibration and validation, observed precipitation at Perth Metro BoM weather station (weather station ID 009225) from 03/09/2012 to 06/09/2012 and from

03/11/2012 to 06/11/2012 are used respectively. To evaluate the impact of climate change; developed IDF values in Chapter 5 are used accordingly. Future climate change is evaluated for three periods (2020s, 2050s and 2080s) for HadCM3-A2 and CGCM3-A2 scenarios and existing condition is simulated by the downscaled rainfall for 1960-1990 period using both GCMs. Temporal patterns of future rainfalls are assumed to remain same to the existing temporal pattern in Australian Rainfall and Runoff (ARR) for the Perth region.

Potential evapotranspiration data is obtained from the Perth airport BoM station (weather station ID 009021).

7.5.1.5 Land use

Two land use scenarios are developed to represent the pre-development condition and future post-development condition. Four land use categories are identified in the pre-development stage. Such as Lake, Reserve, Urban and Commercial/Roads etc. These land use types are represented by 1, 2, 3 and 4 grid codes respectively in Figure 7.5. One additional land use category is defined in the post-development stage, known as "proposed" and represented in grid code 5 in Figure 7.6.

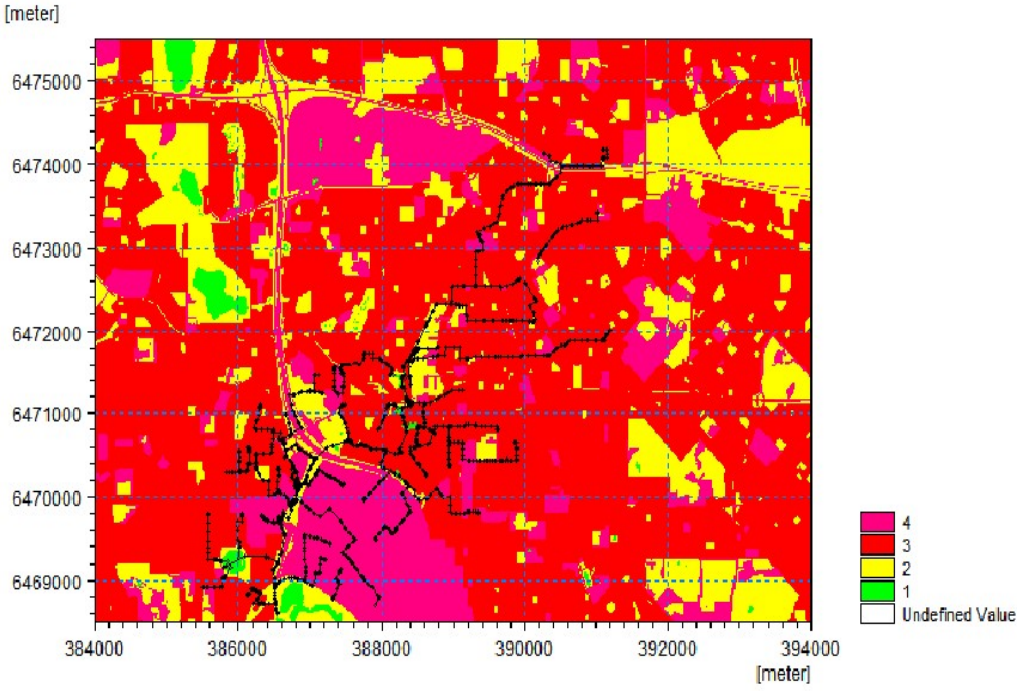

Figure 7.5: Distribution of land use categories in pre-development stage

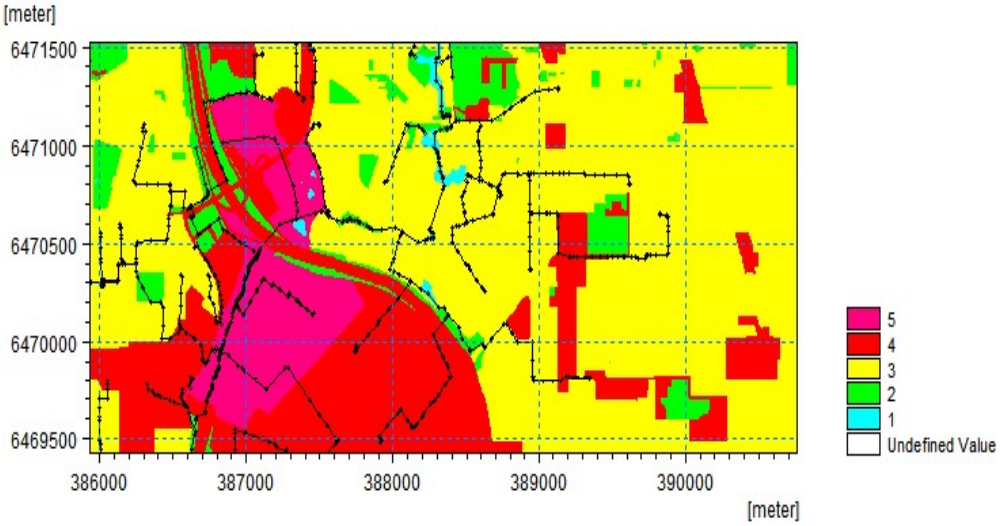

Figure 7.6: Distribution of land use categories in development area (Post-development stage)

7.5.1.6 Overland Flow

There are three main inputs available in overland flow branch. i.e. manning number, detention storage and initial water depth.

Manning number (Manning's coefficient)

Gridded manning numbers are input across the model domain to represent the surface roughness of the land surface. There are four surface types defined in the pre-development stage. Such as lakes, reserves, residential and commercial/road. For the post-development stage, an additional surface type called future development is defined. These identified surface types are presented in Figure 7.7 and Figure 7.8 for pre-development and post-development stages respectively. As surface roughness is a key parameter which having high sensitivity on runoff, sensitivity analysis is conducted to estimate the surface roughness. Therefore, more details about the surface roughness and their sensitivity are included in section 7.7.1.

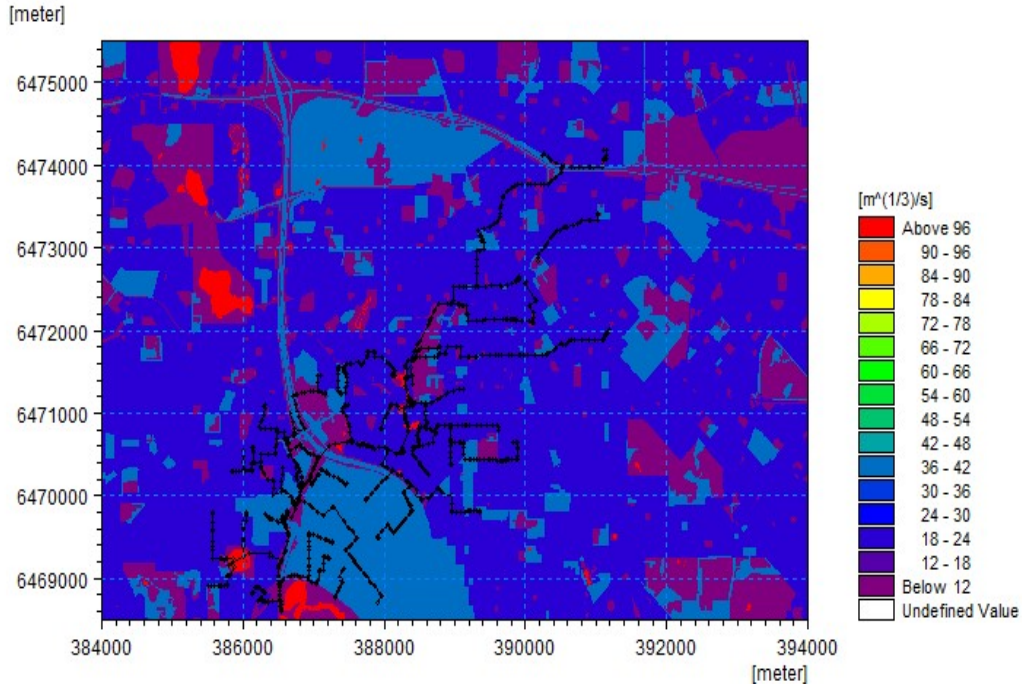

Figure 7.7: Distribution of existing surface roughness (Pre-development)

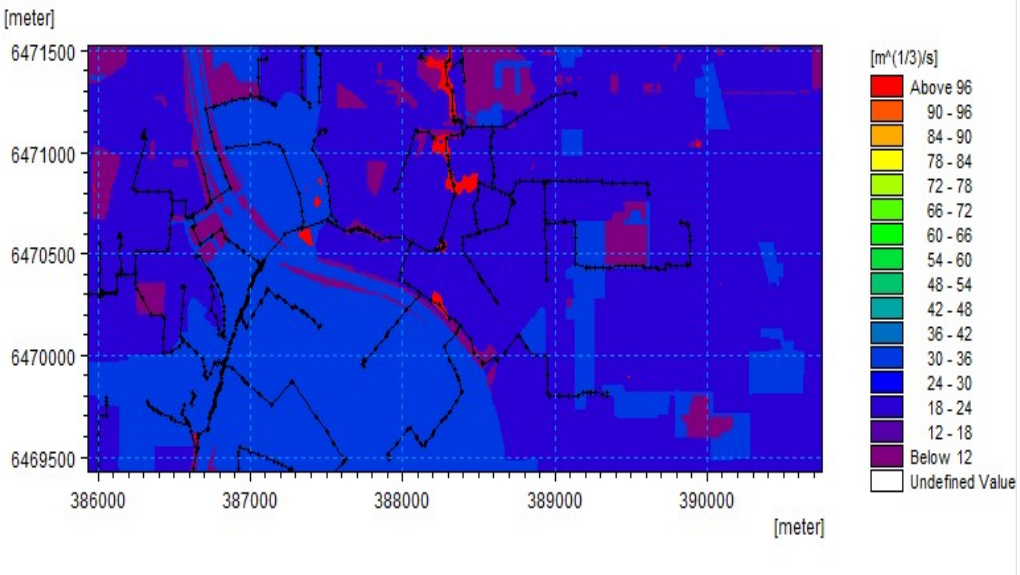

Figure 7.8: Distribution of proposed surface roughness in development area (Post-development)

Detention storage

MIKE SHE uses detention storage to represent the pooled water on the land surface which is not flowing as overland flow. In this study 2 mm depth detention storage over the whole catchment is assumed for the pre-development stage and 5 mm depth detention storage is assumed for the development area in the post-development stage.

Initial water depth

Gridded water depth of lakes and reservoirs are used as the initial water depths. For the other areas 0 mm initial water depth is used.

7.5.1.7 Unsaturated flow

Seven soil types are defined in the pre-development model domain for unsaturated zone. Such as wetland, rivers on sand, urban on sand, commercial on sand, reserves on limestone, urban on limestone and commercial on limestone. Additional soil type known as “proposed” is defined in the post-development stage. Water content at saturation fraction, field capacity fraction and wilting point fraction are assumed as 0.3, 0.1 and 0.05 respectively for all the zones. Evapotranspiration surface depth is assumed as 0.1 m for the area. Distribution of soil types for pre-development stage and the post-development stage are presented in Figure 7.9 and Figure 7.10 respectively (1- Wetland, 2 - Rivers on sand, 3 - Urban on sand, 4 - Commercial on sand, 5 - Reserves on limestone, 6 - Urban on limestone, 7 - Commercial on limestone, 8- Proposed).

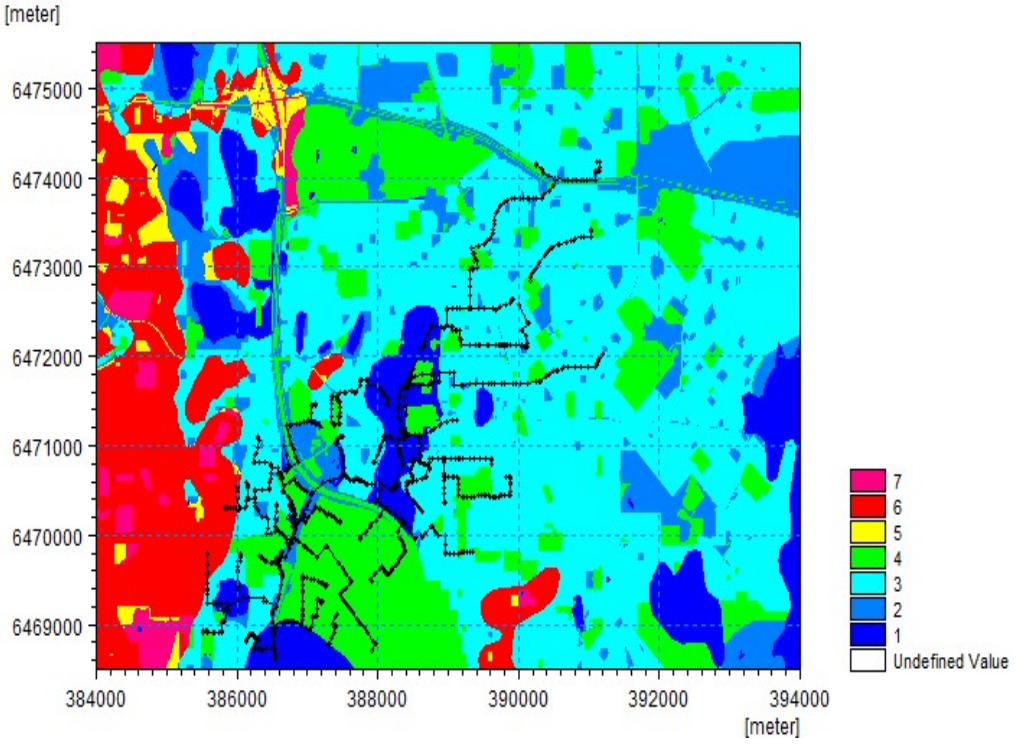

Figure 7.9: Distribution of existing soil types in unsaturated zone (Pre-development)

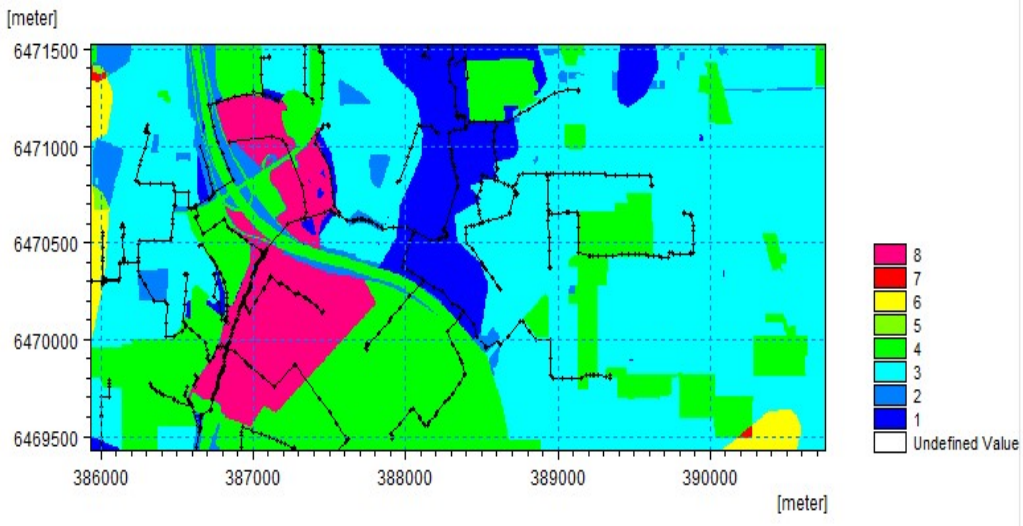

Figure 7.10: Distribution of existing soil types in unsaturated zone (Post-development)

7.5.1.8 Saturated zone

For MIKE SHE saturated zone, data should be provided under three subsections. i.e.) Geological layers, Geological lenses and Computational layers.

According to the borehole data in the development area, the superficial aquifer is modelled using three saturated layers.

Layer 1: Top sand layer

Layer 2: Middle clay layer

Layer 3: Bottom sand layer

Layer 1, 3 and outside of the clay boundaries of layer 2 are considered as homogenous throughout the model domain.

Further, geological lenses are used to control the vertical hydraulic conductivity at the landfill area.

Table 7.2 presents the hydrological properties of saturated zone layers.

Table 7.2: Hydraulic properties of soil layers in saturated zone

Layer Name	Horizontal hydraulic conductivity (m/s)	Vertical hydraulic conductivity (m/s)	Specific yield	Specific Storage (m^{-1})
Sand	$2.89*10^{-4}$	$2.89*10^{-5}$	0.2	$1.0*10^{-6}$
Clay	$1.0*10^{-6}$	$1.0*10^{-6}$	0.2	$1.0*10^{-6}$
Limestone	$1.45*10^{-3}$	$5.79*10^{-5}$	0.2	$1.0*10^{-6}$
Landfill	$1.0*10^{-9}$	$1.0*10^{-9}$	0.1	$1.0*10^{-7}$

In the computation layer setup, regional groundwater level data is used to generate initial potential head. Further, boundary data in Table **7.3** are defined in the saturated zone.

Table 7.3: Boundary types of saturated zone

Boundary	Boundary Type
East (E)	Fixed head
West (W)	Fixed head
North (N)	Zero flux
South (S)	Zero flux
South West (SW)	Zero flux
Herdsman	Fixed head

Furthermore, to represent the water extraction of the area, 100 pumping wells are assumed throughout the model domain.

7.5.2 Development of MIKE 11 model

The drainage network in the study area is modelled using MIKE 11 model. As mention earlier, MIKE 11 one-dimensional river model is a separate and standalone model from the MIKE SHE main model. Therefore, development and simulation can be performed separately to the MIKE SHE. There are four main data inputs (i.e. Network, Cross section, Boundary data and Hydro-Dynamic parameters) are available in MIKE 11 model to couple with MIKE SHE.

7.5.2.1 Drainage Network

The initial step of the MIKE 11 model development is the defining the drainage network. In this case study, OPBD is the main central drainage of the catchment area. Additional 61 drainage branches are defined in the pre-development stage and 64 branches are defined in post-development stage. When defining the drainage network; information on the branch name, topo ID, upstream chainage, downstream chainage, flow direction, the maximum distance between two adjacent water level calculation

points branch type should be provided. Also, upstream and downstream branch connection information should be defined (branch name and chainage etc.). Further, drainage structure information also needs to be provided in MIKE 11 model. Hence, 19 culverts and 5 weirs structure details are fed into the model for pre-development stage. 26 culverts and 4 weirs are defined in post-development stage. Furthermore, runoff and groundwater link development comes under drainage network section. There are 68 runoff/ groundwater links are defined for pre and post-development stages. Under each link, information on location, river-aquifer exchange, weir data for verland river exchange and flood inundation data are provided

Figure 7.11 presents the drainage network in the study area.

7.5.2.2 Cross section data

Providing the cross section data of the branches is the next step in the model development. Under this step, different cross-sections can be defined along the branch. Further, in this step, bed resistance can be defined. In this study bed resistance is defined using Manning's n. According to Chow (1959), following Manning roughness values are used in the pre-development model.

Concrete pipe – 0.013 ($s/m^{1/3}$)

Lakes – 0.018 ($s/m^{1/3}$)

Main central open drain – 0.06 ($s/m^{1/3}$)

Other open drain – 0.027 ($s/m^{1/3}$)

By considering the different channel sections in the proposed development, following Manning's roughness values are used in the post-development stage.

Hard terracing high flow – 0.015 ($s/m^{1/3}$)

Low flow channel – 0.027 ($s/m^{1/3}$)

Open grass high flow – 0.043 ($s/m^{1/3}$)

Stepped short grass high flow – 0.104 ($s/m^{1/3}$)

Dense vegetate high flow – 0.217 ($s/m^{1/3}$)

7.5.2.3 Boundary data

MIKE 11 boundary data section includes boundary description, boundary type, branch name, chainage and boundary ID etc. In the present study, all the upstream boundaries are defined as the closed boundaries. Only one downstream boundary is located at OPBD and it is defined as an opened boundary.

7.5.2.4 Hydro Dynamic parameters (HD parameters)

Under HD parameter section, required supplementary data for MIKE 11 simulation is provided. These data consist with floodplain resistance data, wind data, wave data, mixing coefficients etc. MIKE 11 recommends to use default values in HD parameters in most instances and this study default values of HD parameters are used.

7.5.2.5 Simulation specifications

As MIKE 11 is a standalone model, different simulation specifications can be defined for MIKE 11 from the coupled MIKE SHE model. In this study, one second fixed time step is defined as the simulation time step for the MIKE 11 model.

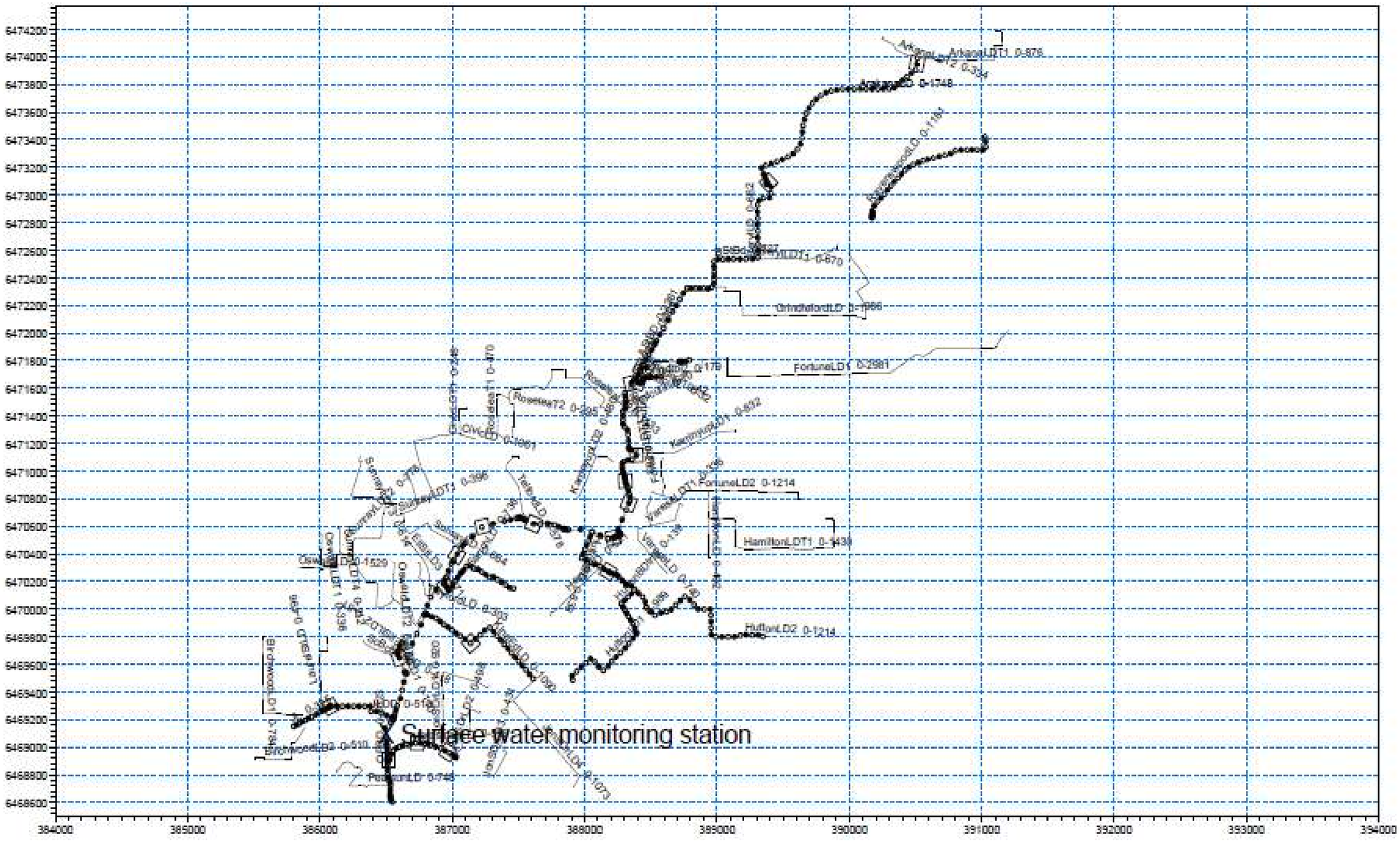

Figure 7.11: Drainage network

7.6 Sensitivity analysis, model calibration and validation

7.6.1 Sensitivity Analysis

Parameter sensitivity analysis is an essential requirement in hydrology and hydraulic modelling as some of the parameters are not directly measurable. However, complex sensitivity analysis is time consuming and computationally high demand process. Therefore, in this case study simple sensitivity analysis is conducted. As the overland flow is the main concern of the study, the sensitivity of detention storage, surface roughness and saturated hydraulic conductivity of the unsaturated zone are evaluated against the overland flow. Further, peak flow at measuring gauge located at chainage 2902.5m, OPBD for the rainfall periods 28/04/2012 – 01/05/2012 is used to sensitivity analysis.

Initially, the sensitivity of detention storage is investigated. In MIKE SHE, detention storage implies the depth of ponded water which does not make overland flow as a result of surface texture. To initiate the overland flow, depth of ponded water should be exceeded the detention storage. Further, in MIKE SHE model, water in detention storage disappears in two ways (through infiltration into unsaturated layers and evapotranspiration). In this study, simulating peak flow at the measuring gauge is investigated for 0 mm to 6 mm detention storage. Figure 7.12 presents the simulated peak flows under different detention storages. As expected, MIKE SHE model simulates highest peak flow of 3.9 m^3/s for 0 mm detention height and lowest of 3.3 m^3/s for 6mm detention height. This peak flow deduction is 16.6 % for 6 mm detention height and it can be identified the sensitivity of the detention storage on peak flow is very high.

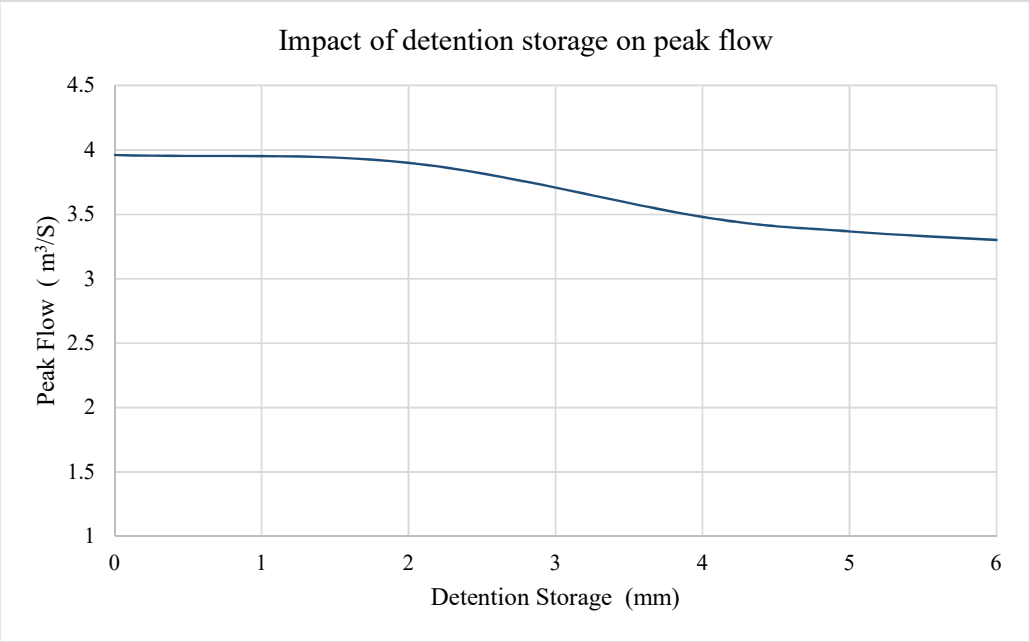

Figure 7.12: Sensitivity of peak flow on detention storage

Saturated hydraulic conductivity of the unsaturated zone is another calibration parameter of the model and subjected to the sensitivity analysis. There are seven surface types with different hydraulic conductivity are defined in the model domain. i.e. wetland, reserves on sand, urban on sand, commercial on sand, reserves on limestone, urban on limestone and commercial on limestone. However, approximately 80% of the total catchment area consists with urban on sand, commercial on sand and urban on limestone surface types. Therefore, hydraulic conductivity of these three types is having the greater impact on the catchment hydrology. Then, these three soil types are subjected to the sensitivity analysis. Figure 7.13, Figure 7.14 and Figure 7.15 present the result of sensitivity analysis conducted on the hydraulic conductivity of urban on sand, commercial on limestone and urban on limestone respectively. As most of these areas are highly developed and presence of high impervious areas, the conductivity of the urban areas (urban on sand and urban on limestone) are investigated for 40 mm/day to 70 mm/day. The conductivity of commercial areas (commercial on sand) is tested for 10 mm/day to 70 mm/day. This analysis is conducted by single variable changing method and therefore other variables are remained constant while investigating variable is changing. According to Figure 7.13, Figure 7.14 and Figure 7.15, it can be observed that there is significance influence of

hydraulic conductivity on the peak flow. Furthermore, Figure 7.14 shows the highest variation of the peak flow. It shows 17% peak flow deduction for the hydraulic conductivity change from 70 mm/day to 10 mm/day of commercial on sand. Urban on sand and urban on limestone show 9 % and 13 % peak flow reduction respectively.

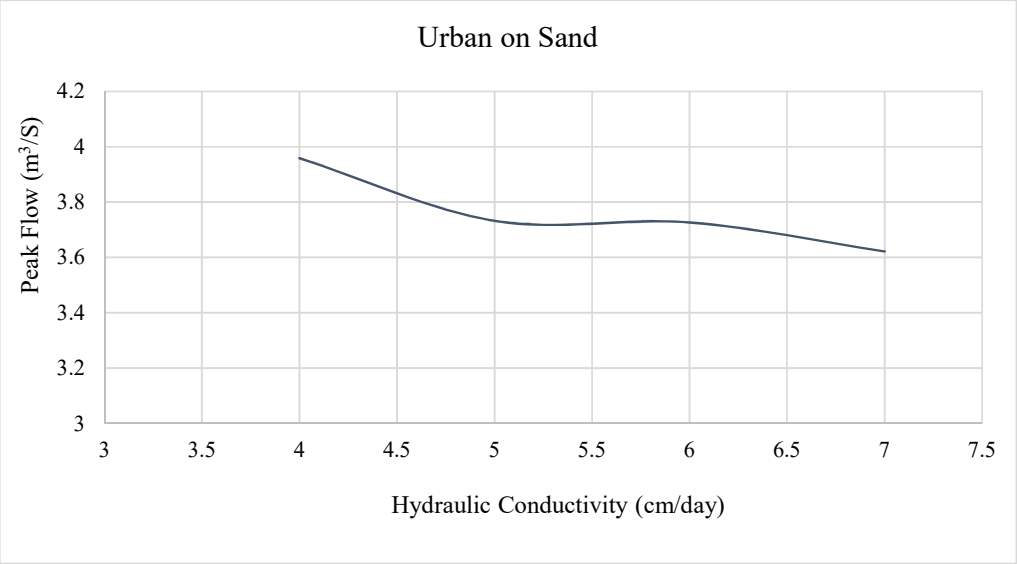

Figure 7.13: Sensitivity of peak flow on saturated hydraulic conductivity (Urban on sand)

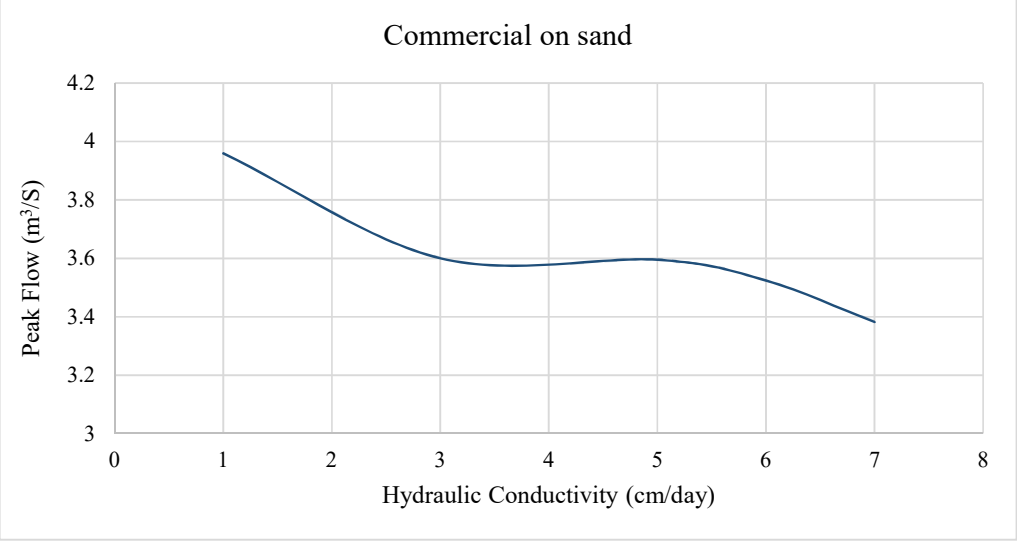

Figure 7.14: Sensitivity of peak flow on saturated hydraulic conductivity (Commercial on sand)

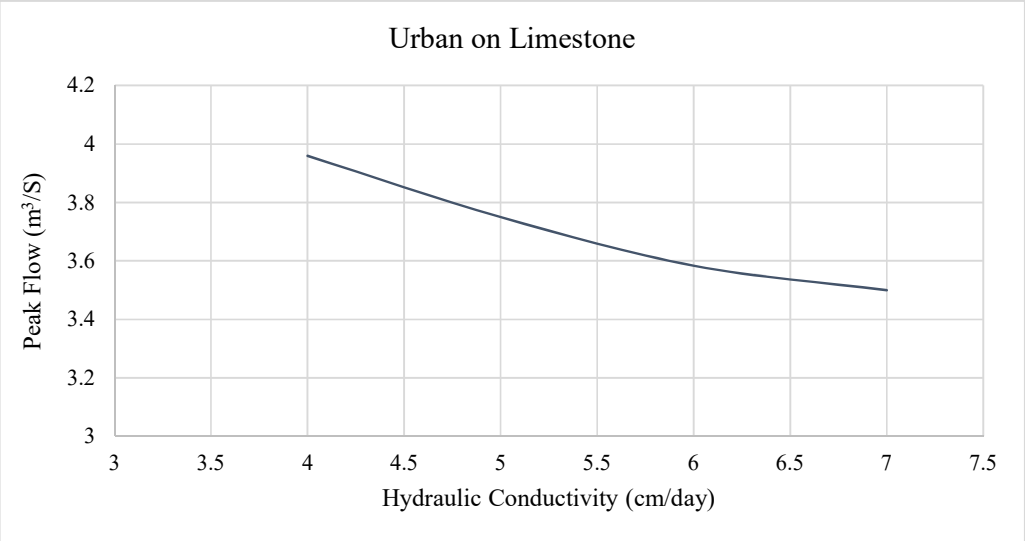

Figure 7.15: Sensitivity of peak flow on saturated hydraulic conductivity (Urban on limestone)

Then the sensitivity of surface roughness on the peak flow is investigated. There are four main surface types are identified in the catchment (i.e. Lake, Reserve, Residential and Commercial). In between these four surface types, surface roughness of reserve, residential and commercial areas are highly uncertain. Furthermore, the area of lake surface is minimum and the area of other three types take a higher proportion of the total catchment area. Therefore, the surface roughness of residential, reserve and commercial areas are subjected to the sensitivity analysis. Figure 7.16, Figure 7.17 and Figure 7.18 are presented the sensitivity of peak flow to the surface roughness of residential area, reserve area and commercial/road area respectively. By considering the high surface roughness of residential areas, it is investigated for 0.05 $s/m^{1/3}$ to 0.075 $s/m^{1/3}$ region. According to Figure 7.16, peak flow is reduced by 10.2% for this surface roughness variation. The sensitivity, of reserve areas (Figure 7.17) are investigated for the region of 0.05 $s/m^{1/3}$ to 0.2 $s/m^{1/3}$ and peak flow variation is 7.5 %. Figure 7.18 presents the sensitivity of surface roughness of commercial/road areas on peak flow. The surface roughness of commercial/road areas is relatively lower than the surface roughness of residential and reserves. Therefore, this sensitivity evaluation is conducted for 0.01 $s/m^{1/3}$ to 0.06 $s/m^{1/3}$ for road and commercial areas and it shows 11.4% deduction percentage of peak flow.

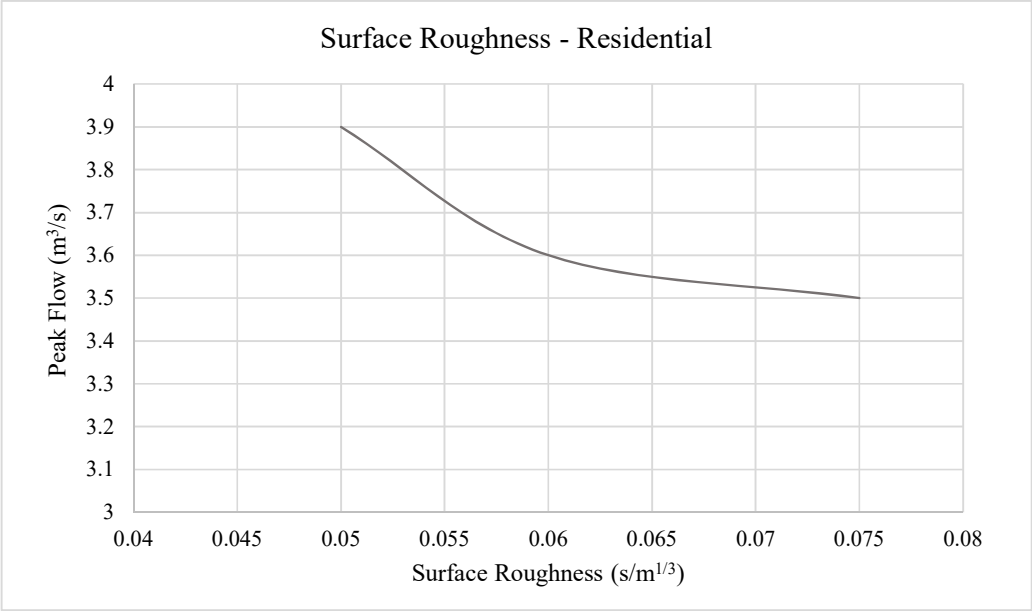

Figure 7.16: Sensitivity of peak flow on surface roughness (Residential)

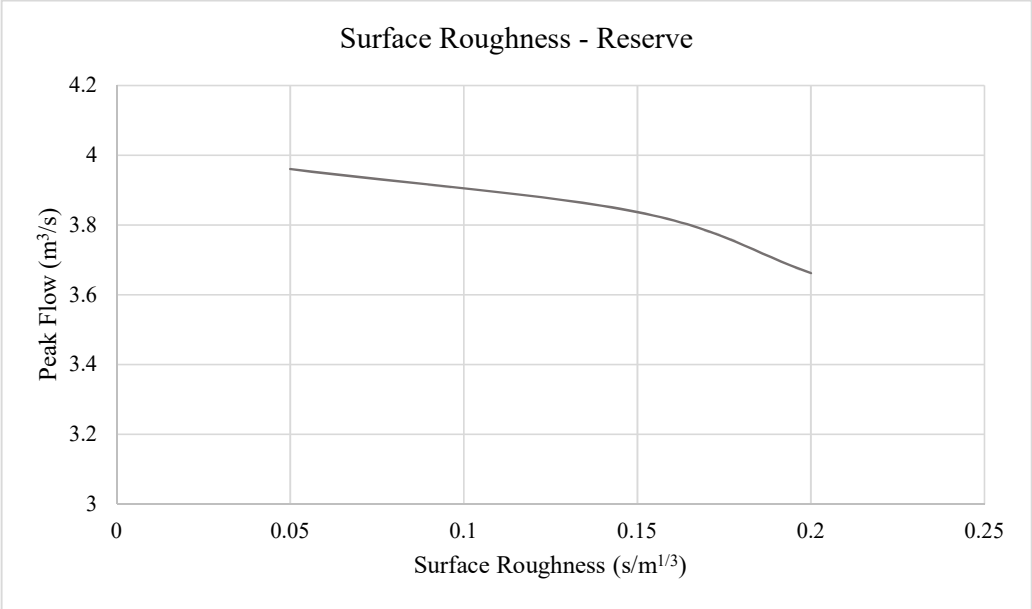

Figure 7.17: Sensitivity of peak flow on surface roughness (Reserve)

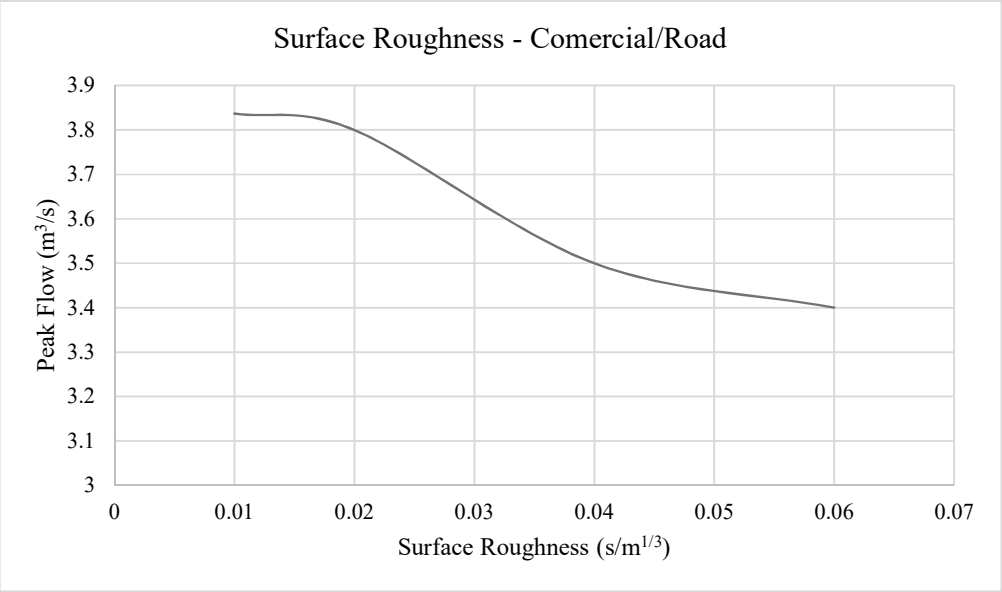

Figure 7.18: Sensitivity of peak flow on surface roughness (Commercial/Road)

7.6.2 Model calibration and validation

Calibration and validation of runoff models verify the accuracy of the developed model prior to use in the hydrological assessments. In this study MIKE SHE/MIKE 11 coupled model is calibrated for 03/09/2012 to 06/09/2012 period and validated for 03/11/2012 to 06/11/2012 period. Best values for the high sensitive hydrological parameters which discussed in previous section 7.6.1 are selected in this process to model the most accurate surface runoff. Thereafter, keeping these values unchanged, the model is run for separate storm event to validate the model.

To facilitate the calibration process, a runoff monitoring data is highly important. At the Stirling Catchment, a surface water monitoring station is located at the downstream of the catchment. Figure 7.19 presents the surface water monitoring station located in the study area. This station is located at chainage 2902.5m, OPBD and close to the southern model boundary. Observed flow data is available for 27/07/2011-29/12/2012 period in 15 minutes interval

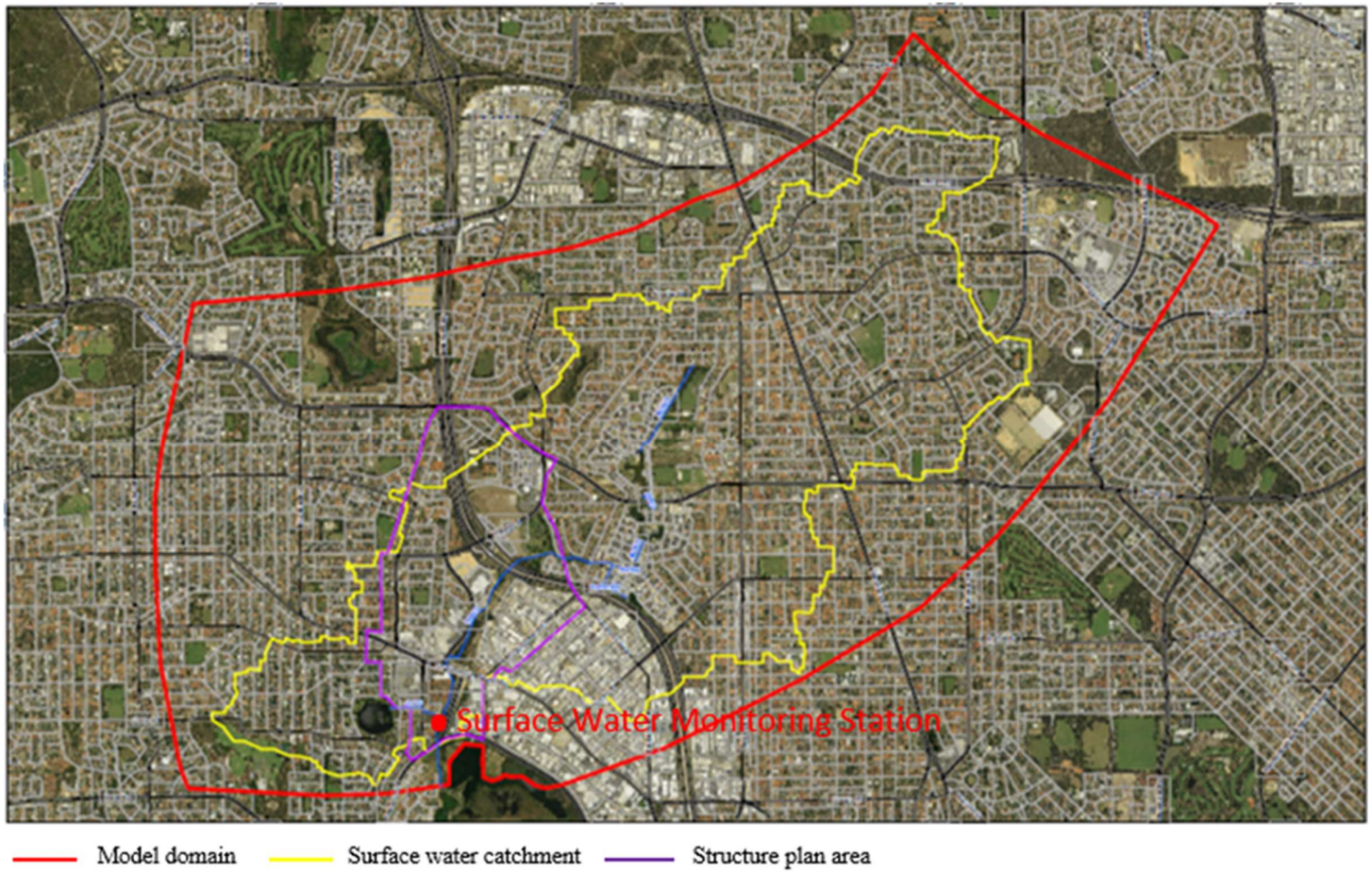

Figure 7.19: Location map of surface water monitoring station and model domain

To evaluate the accuracy of proposed MIKE SHE model, observed peak flow in OPBD channel at 2902.5m chainage is compared with modelled peak flow. In addition to the standard comparisons, RMSE, NSE and PBIAS performance criteria are calculated to identify the model performances in calibration and validation process.

Comparison of modelled peak flow with observed peak flow is presented in Figure 7.20. According to Figure 7.20 runoff model shows slightly high peak flow than observation. Estimated RMSE, NSE and PBIAS values are 0.116, 0.92 and 0.24 respectively. Low RMSE value, NSE value close to 1 and low PBIAS values indicate the high accuracy of developed MIKE SHE/MIKE 11 coupled model for calibration period. Further "negative" sign of PBIAS value indicates the over simulation of the runoff model.

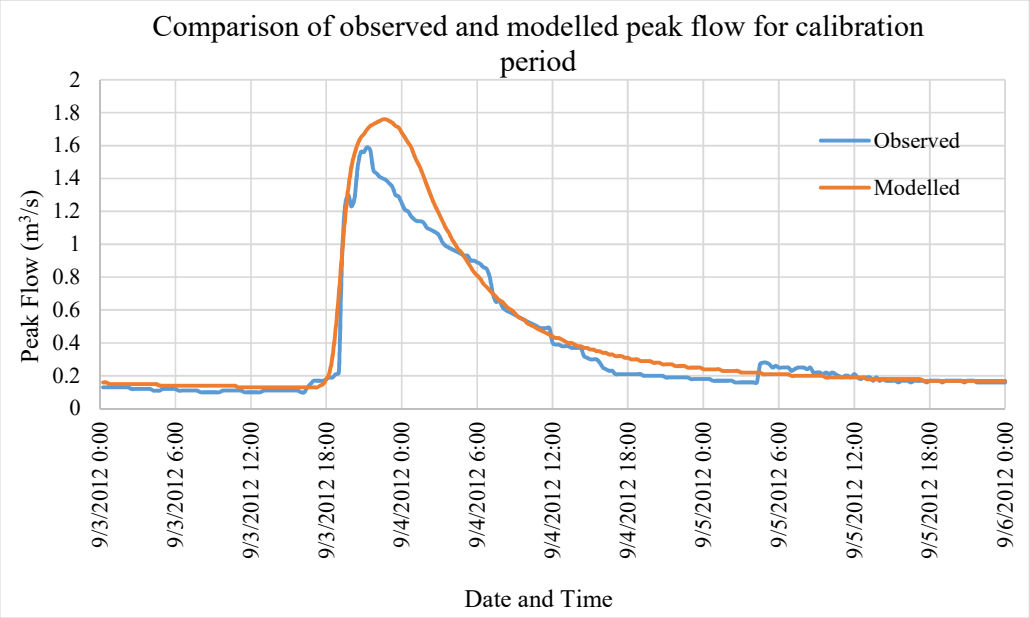

Figure 7.20: Calibration of hydrological model for 03/09/2012 – 06/09/2012 period

Figure 7.21 presents a comparison of observed peak flow and modelled peak flow for validation period. Similar behaviour of modelled peak flow is observed for validation period under same hydrological parameters used in calibration. Corresponding RMSE, NSE and PBIAS values between modelled and observed peak flows are 0.11, 0.91 and 0.14 respectively. Therefore, it is confirmed the accuracy of developed MIKE SHE/ MIKE 11 model to use in other design scenarios in this study.

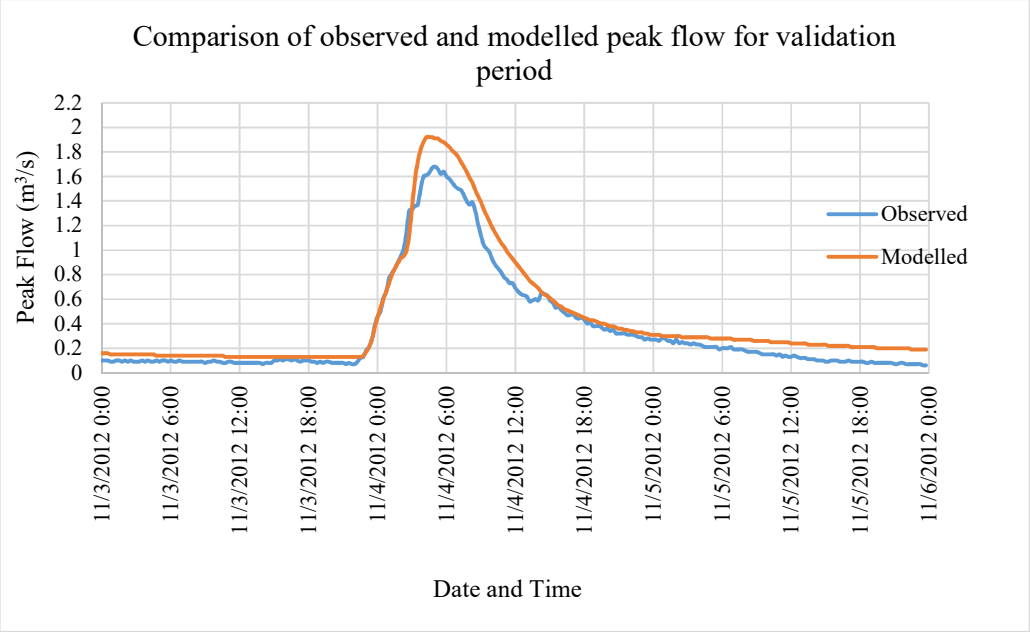

Figure 7.21: Validation of hydrological model for 03/11/2012 – 06/11/2012 period

By considering the accuracy of above presented peak flows for calibration and validation period, model parameters are fixed to the value presented in Table 7.4 to get most realistic surface runoff results.

Table 7.4: Hydrological parameters for the MIKE SHE model

Parameter	Value
Surface roughness ($s/m^{1/3}$)	
Lake	0.01
Reserve	0.2
Residential	0.05
Commercial/ Road	0.025
Future development	0.03
Hydraulic Conductivity (m/s)	
Wetland on all soil	$1*10^{-7}$

Rivers on sand	$1.2*10^{-5}$
Urban on sand	$4.9*10^{-7}$
Commercial on sand	$3.47*10^{-7}$
Reserves on limestone	$1.2*10^{-5}$
Urban on limestone	$4.9*10^{-7}$
Commercial on limestone	$1.2*10^{-7}$
Proposed	$1.2*10^{-7}$
Detention storage (mm)	
Pre-development	2.0
Development area	5.0

7.7 Model result and discussion

7.7.1 Identifying the critical storm

In hydrological modelling process, it is important to identify the critical storm events for the different return periods. After the identification of critical storm for each return period, it is used in the hydrological assessment and designing. The critical storm is decided based on the design criteria to be satisfied according to the stormwater management guideline. In this study, the magnitude of the peak flow is used to identify the critical storm event as the peak flow is a main concern of hydrological assessments in Western Australia. According to Western Australian stormwater management guidelines for land developments; pre-development and post-development peak flows should be same for 100 year return periods (or post-development peak flow should be less than the pre-development peak flow). Therefore, critical storm analysis is conducted for 1 h, 2h, 6 h, 12 h and 24 h rainfalls for 100 year return periods separately. Figure 7.22presents these critical storm analyses for 100 year Average Recurrence Interval (ARI). According to Figure 7.22, 24 hour storm event can be identified as the

critical storm event for both ARI events. Therefore, 24 h storm duration is used to analyse the hydrological behaviour under the future climate scenarios.

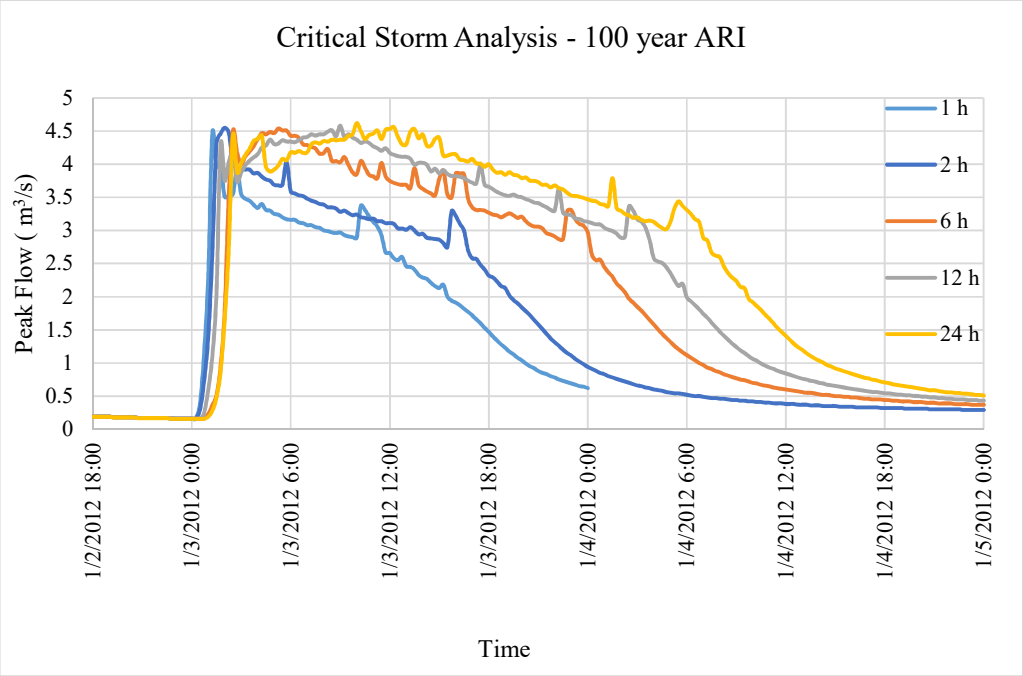

Figure 7.22: Critical storm analysis for 100 year ARI (Note – Given time period presented in the X axis is used for simulation purpose only)

7.7.2 Comparison of pre-development and post-development stages under changing climate scenarios for future periods

7.7.2.1 Comparison of peak flows

The proposed development is mainly consisted with drainage network modifications in the development area. These modifications include dimension and levels changes, introducing new structures and removing existing drainage structures, modifications to the channel bed by introducing vegetation, introducing new embankment slopes and vegetation etc. Also, changes in land usage and surface elevation are come under proposed development. Because of these proposed changes in the post-development stage, significance variations can be expected in the catchment hydrology.

According to the stormwater management guidelines in Western Australia, pre-development and post-development peak flows from the developing catchment should

be same or post-development peak flow should be smaller than pre-development peak flows for 100 year ARI events. To investigate this issue, hydrologists generally use currently available IDF relations and they assume that the IDF relations remain constant for future periods too. However, in this study IDF relations developed in Chapter 5 are used to investigate the behaviour of catchment peak flow. These IDF relations are developed using the downscaled HadCM3-A2 and CGCM3-A2 scenarios for four time periods. Future time period is splitted as 1961-1990, 2011-2040, 2041-2070, 2071-2099/2100 and hereafter these time slices are known as 1960s, 2020s, 2050s and 2080s respectively.

The most downstream point of the OPBD branch is 3304 m chainage and total runoff is drained out through this point. Therefore, peak flow at this point is used to study the peak flow behaviour of the catchment under different scenarios. Figure 7.23 present the peak flow behaviour under HadCM3-A2 downscaled rainfalls for 100 year. According to Figure 7.23, even though peak flow simulated using 1960s rainfall satisfies the guideline, peak flow simulated using IDF relations for 2020s, 2050s and 2080s do not satisfy the stormwater management guidelines in Western Australia. Therefore, it requires more advance approach to stormwater management in the development area.

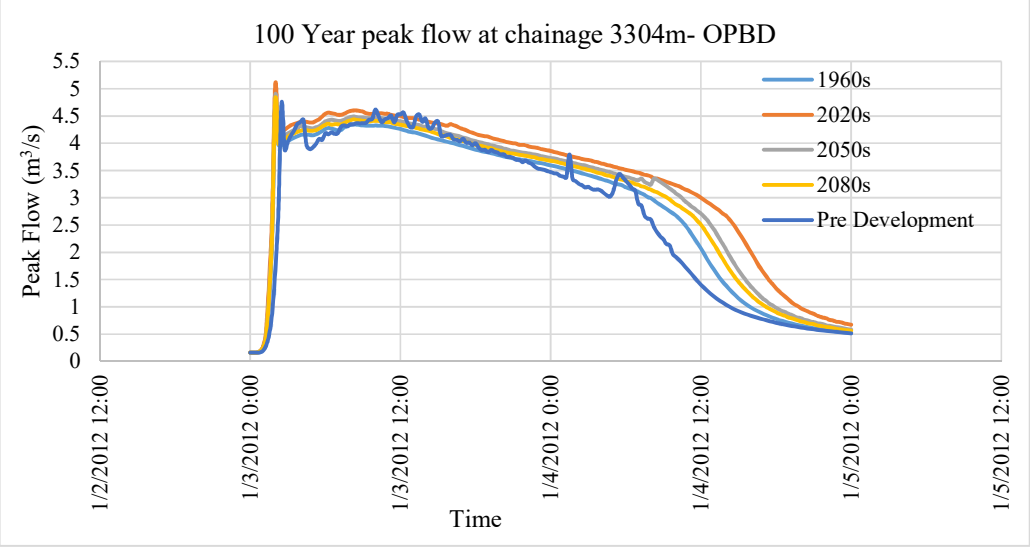

Figure 7.23: Peak flow at chainage 3304m of OPBD for 100 year ARI events under HadCM3-A2 downscaled rainfalls (Note – Given time period presented in the X axis is used for simulation purpose only)

Figure 7.24 shows the simulated peak flow for downscaled rainfall using CGCM3-A2 scenario. Downscaled rainfall depths using CGCM3-A2 scenario show highest rainfalls for 1960s and it shows continuous decreasing trend up to 2080s. Because of rainfall decreasing trend, simulated peak flows satisfy the stormwater management guideline requirement for all the future period for 100 year ARI year respectively.

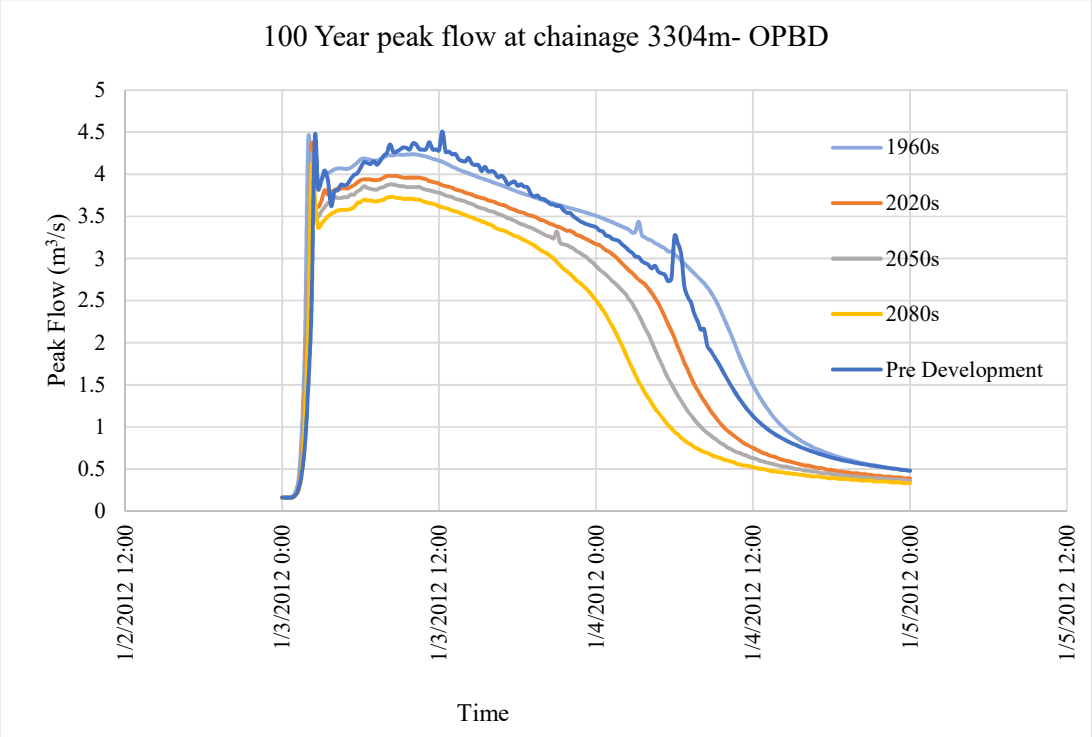

Figure 7.24: Peak flow at chainage 3304m, OPBD for 100 year ARI events under CGCM3-A2 downscaled rainfalls (Note – Given time period presented in the X axis is used for simulation purpose only)

7.7.2.2 Comparison of overland flood for future periods

Distribution of overland flood depth is one of the most important parameter in developing the flood vulnerability and hazard maps. Distribution of overland flood depth at the pre-development stage is compared with the future scenarios. Figure 7.25 describes the overland flow distribution for HadCM3-A2 scenarios for the pre-development stage, 1960s, 2020s, 2050s and 2080s. To improve the resolution of the map, presenting window of the flood depth maps are limited to downstream of the development area. As per these maps, mainly flood inundation can be observed along

the OPBD downstream. Maximum flood depth is varied from 0.8m to 1.2 m along these sections. Also, some sections beside the Jon Sanders Drive and car park near to Selby Street North are inundated. However, the maximum flood depth is lower than OPBD inundation and it takes 0.4m to 0.8m. By comparing the all scenarios, 2020s HadCM3-A2 scenarios show the maximum flood inundation area as a result of increased rainfall intensity. Also, lowest inundation is simulated under 2080s as a result of lowest rainfalls for 2080s. Figure 7.26 presents the flood inundation maps of the model simulations for CGCM3-A2 scenarios. Under CGCM3-A2 scenarios highest rainfall has been simulated for 1960s and lowest for 2080s. Thus, in flood simulation, maximum inundation depths and area are observed for 1960s and lowest for 2080s.

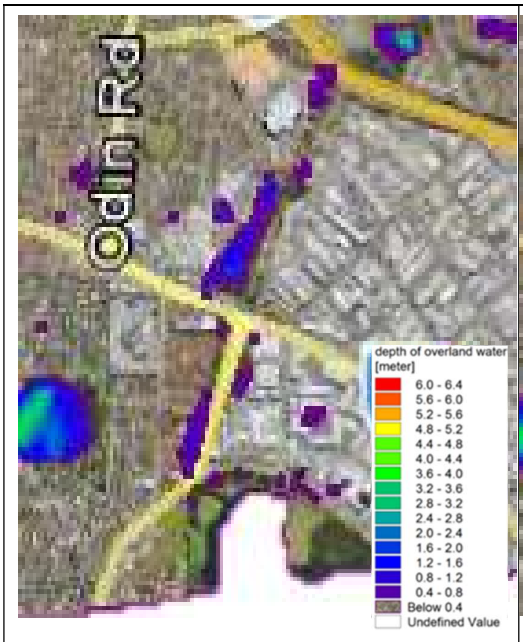	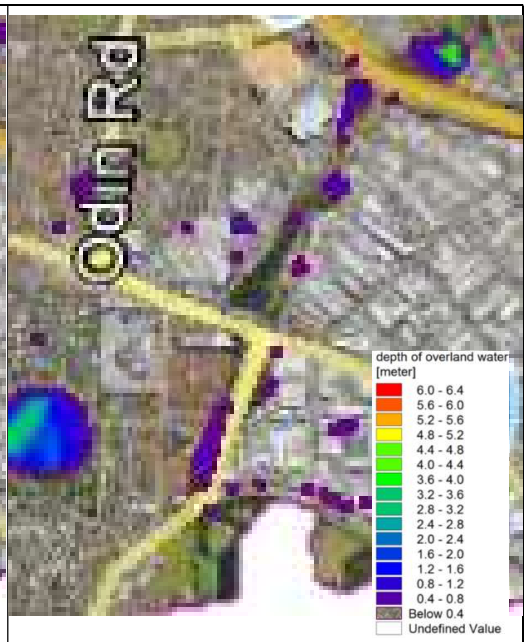
100 Year ARI flood depth for downscaled rainfall 1960s - HadCM3-A2 (Pre-development stage)	100 Year ARI flood depth for downscaled rainfall 1960s - HadCM3-A2 (post-development)

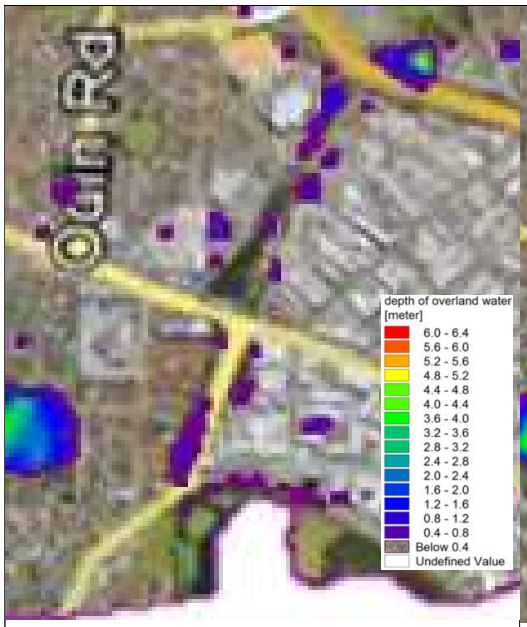

100 Year ARI flood depth for downscaled rainfall 2020s- HadCM3-A2 (post-development)

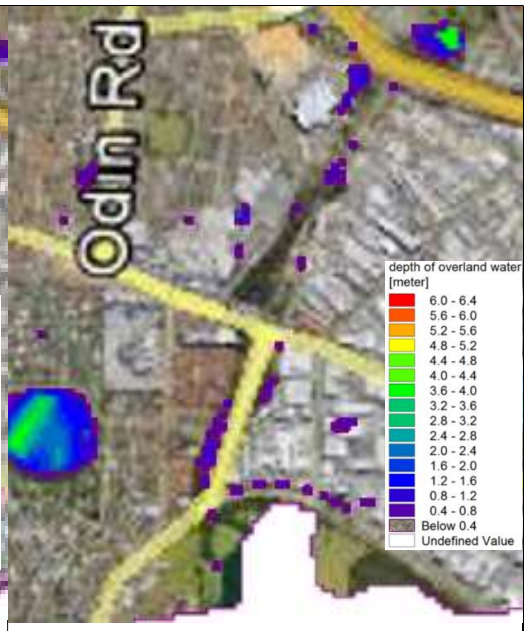

100 Year ARI flood depth for downscaled rainfall 2050s- HadCM3-A2 (post-development)

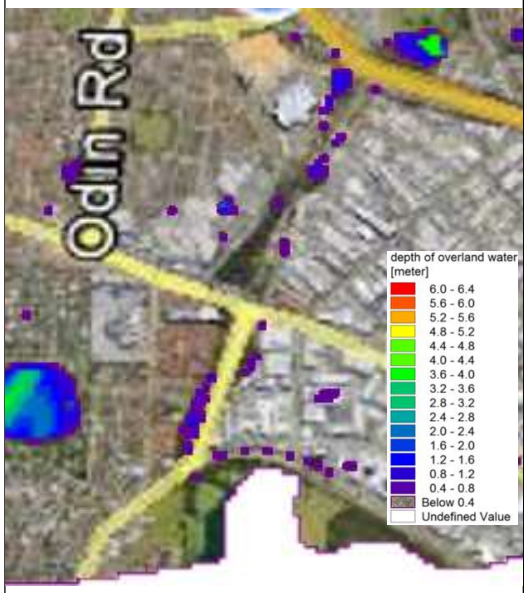

100 Year ARI flood depth for downscaled rainfall 2080s -HadCM3-A2 (post-development)

Figure 7.25: Distribution of overland flow for HadCM3-A2 scenarios

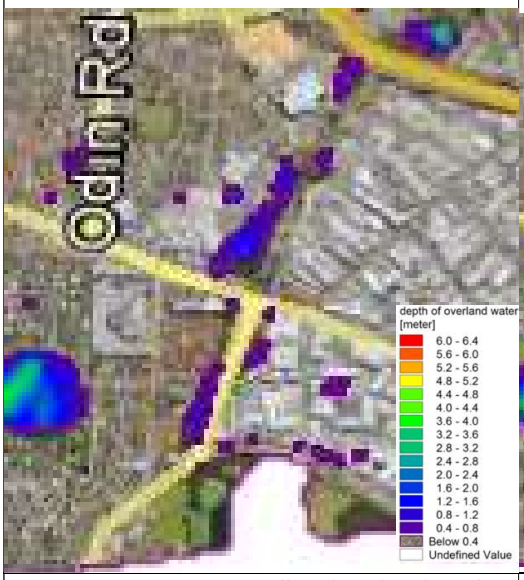

100 Year ARI flood depth for downscaled rainfall 1960s - CGCM3-A2 (pre-development stage)

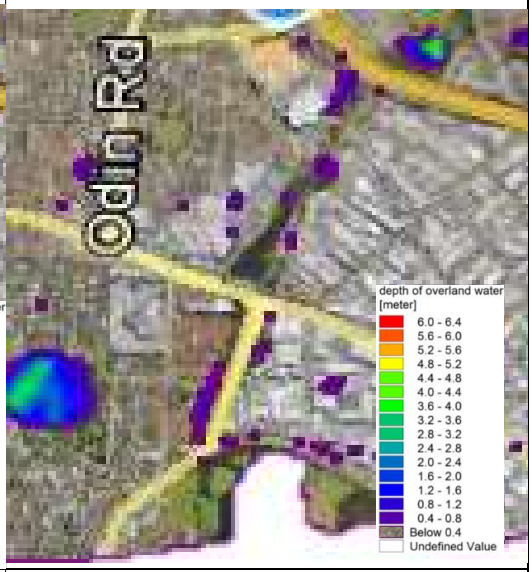

100 Year ARI flood depth for downscaled rainfall 1960s - CGCM3-A2 (post-development)

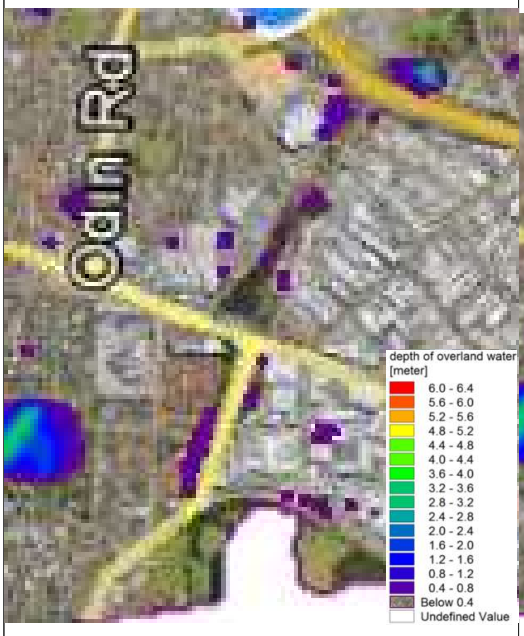

100 Year ARI flood depth for downscaled rainfall 2020s - CGCM3-A2 (post-development)

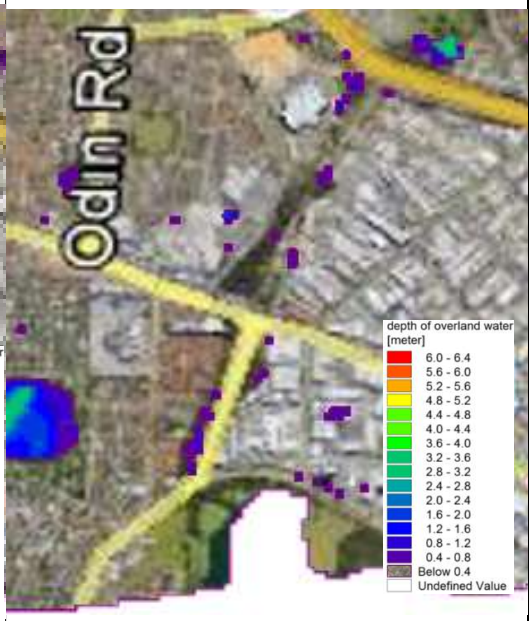

100 Year ARI flood depth for downscaled rainfall 2050s - CGCM3-A2 (post-development)

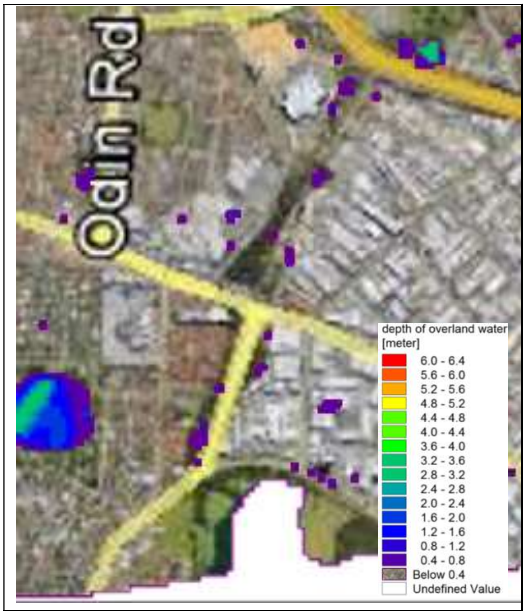

100 Year ARI flood depth for downscaled rainfall 2080s - CGCM3-A2 (post-development)

Figure 7.26: Distribution of overland flow for CGCM3-A2 scenarios

7.7.3 Recommendation for the stormwater management in the catchment for future period

This case study clearly shows the importance of considering the climate change impacts in the urban hydrological studies. Further, it presents that proposed stormwater management plan does not satisfy some guidelines under several future climate projections. Also, expanded flood inundation area around Jon Sanders Drive and car park near to Selby Street North for the future period, emphasise the requirement of further amendments to the proposed stormwater management plan.

In generally, the catchment used in this case study is highly urbanized with less pervious area. Therefore, the opportunities to manage stormwater quantity through infiltration based approaches are limited. However, there are some ways available to increase the on-site infiltration. Especially, the current plan proposed a realignment of OPBD in the development area and it can be facilitated to increase the infiltration through high infiltrating materials to the OPBD beds and slopes. Also, median swale sections with high infiltration capacities can be introduced to the road network in the

development area. These swale sections can be performed as Bio Retention Storages (BRAs) for the catchment. Further, detention storages with side and base infiltration can be recommended to increase the infiltrating water amount from the catchment.

Furthermore, introducing extra Flood Storage Areas (FSAs) to the development area is important in stormwater quantity management. These FSA can be located under the car parks in commercial lots, reservation areas and median swale in the road network. By introducing new FSA to the most downstream of the OPBD, it is feasible to control peak flow and flood inundation around Jon Sanders Drive and car park near to Selby Street North. Also, introducing new stormwater controlling structures is another way of controlling flood in the area. Especially orifices and weirs with detention storages are highly recommended to the OPBD.

7.8 Summary

This chapter presents a case study of stormwater modelling approach of hydrological influences of an urban land development under combined impacts of land use change and climate change. The selected case study site is located in Stirling area, closer to Perth Central Business District (CBD); proposed urban development of Stirling City Centre development.

For the stormwater modelling, one-dimensional MIKE 11 and two-dimensional integrated MIKE SHE models are used. After successful calibration and validation of the hydrological model, it is used to assess the behaviour of catchment hydrology for the proposed land development under different climate changing scenarios using HadCM3-A2 and CGCM3-A2. RMSE, NSE and PBIAS coefficients are estimated to evaluate the model performance in calibration and validation period. Estimated RMSE, NSE and PBIAS values are 0.116, 0.92 and 0.24 respectively for the calibration period and 0.11, 0.91 and 0.14 respectively for the validation period. Then model is run to identify the critical storm event for 100 year recurrence interval. It is identified as 24 h for both recurrence intervals using the peak flow discharge from the development area. Then the model is run for pre-development stage using downscaled rainfall for 1960-1990 period. The peak flow results show that pre-development peak flow from the catchment is 4.67m^3/s and 4.73m^3/s for the downscaled rainfall using

HadCM3-A2 100 year respectively. Peak flow from the catchment is 4.40m^3/s and 4.51m^3/s for the downscaled rainfall using CGCM3-A2 100 year respectively. The results of the post-development model show that 100 year peak flows for downscaled rainfall by HadCM3-A2 for 2020s, 2050s and 2080s exceed the pre-development peak flow. Furthermore, flood inundation maps show the expanded inundation for HadCM3-A2 rainfall for 2020s, 2050s and 2080s.

This assessment implies, even though current stormwater management plan comply with the stormwater management guidelines under present IDF relations, it does not satisfy with some future scenarios. Therefore, the current stormwater management plan should be modified to satisfy under changing climate. This study clearly verifies the importance of the evaluation of combined impacts of climate change and land use change in urban land developments and urban stormwater management.

CHAPTER 8

8 Conclusions and Recommendations

8.1 Conclusions

The study presented in this thesis can be organized under three sub-sections.

- Developing IDF relations using spatial and temporal downscaling of GCM predictors to integrate the impacts of climate change to IDF relations.
- Evaluating the impacts of temperature on daily and sub-daily extreme rainfall.
- Applying the developed IDF relations to evaluate the combined impacts of land use changed and climate change on urban catchment

The available approaches, applications, limitations and drawbacks are discussed in the literature review (Chapter 2) paying special attention to climate change.

In the first section (Chapter 3, 4 and 5) of the thesis, an approach is presented to develop sub-daily IDF relations for future periods under the changing climate. HadCM3 and CGCM3 GCM models with SRES-A2 scenario are selected for the downscaling study as it projects the most severe climate impacts in the future. Perth airport region is selected to verify the accuracy of the proposed approach to develop IDF relations. This approach mainly consists of two stages; spatial downscaling and temporal downscaling. By considering the wide applicability and the high accuracy of SDSM, it is used for the spatial downscaling of future rainfalls. However, the temporal resolution of SDSM outputs is limited to a daily (24 hours) rainfall. Therefore, spatially downscaled daily rainfalls should be subjected to further temporal downscaling to developed sub-daily IDF relations. Scaling invariant based temporal downscaling model is used to temporal disaggregation of spatially downscaled rainfalls. Also, the applicability of proposed temporal downscaling approach is tested for major cities in Australia (Adelaide, Brisbane, Canberra, Darwin, Melbourne and Sydney). Main conclusions of the spatial and temporal downscaling section are;

 SDSM model is feasible in describing fundamental statistical properties of the daily rainfall process.

 However, the downscaled annual daily maximum rainfalls are not accurate as compared to the observed data. Hence, a bias-correction procedure has been proposed to improve the accuracy of the downscaled rainfall.

 The downscaled results of both GCMs show decreasing annual rainfall for future periods (maximum at 2020s, next at 2050s and lowest at 2080s). As expected, the rate of annual rainfall decreasing is not same for HadCM3 and CGCM3. Further, downscaled result by CGCM3-A2 scenario shows a higher deduction rate of daily rainfall than HadCM3-A2 for 2020s, 2050s and 2080s with respect to 1961-1990 period.

 In the seasonal analysis, increasing daily rainfall is observed for autumn season in 2020s and 2050s for HadCM3-A2 downscaled data. Further, increasing spring rainfall for 2020s is observed for CGCM3-A2 downscaled daily time series. However, downscaled rainfall for both GCMs show high reduction in the winter rainfall in the future.

 GEV distribution is a capable probability distribution function to describe annual maximum rainfall events, this is tested in South West region of Western Australia.

 Only NCM method estimates constant shape parameter for annual maximum rainfalls for all the time durations at all selected rainfall stations. Therefore, only NCM method provides a platform to temporal downscaling of daily rainfall using GEV distribution.

 Estimated GEV quantiles for sub-daily rainfall events by NCM methods are useful in constructing IDF curves for ungauged locations and stations with low-resolution rainfall data.

 Scaling behaviour of annual maximum rainfall is studied for major cities in Australia (Adelaide, Brisbane, Canberra, Darwin, Melbourne, Perth, Sydney). It shows that proposed approach is applicable for all these cities to develop IDF relations which successfully presents climate change impacts.

 Also, presented temporal downscaling approach is suitable to use with other spatial downscaling methods (rather than SDSM) which downscale daily rainfall data for future periods.

The second section of the thesis (Chapter 6) evaluates the empirical relationships of daily and sub-daily rainfall with daily maximum temperature in above mentioned major cities. The main objectives of this section are; to identify the relationships between daily and sub-daily extreme rainfall and daily maximum temperature, to evaluate the variation in rainfall-temperature scale for different time slices and analyse the impact of seasonality on rainfall–temperature scale. The scaling relationship between the daily maximum temperature and the 99^{th} and 50^{th} percentile of 6 minute, 12 minute, 30 minute, 1 hour, 2 hour, 6 hour, 12 hour and 24 hour daily maximum rainfall for wet days (rainfall>0.3mm) is analysed. A binning technique is used to identify the rainfall–temperature relationships. To minimize the associated bias in the binning approach, equal number of rainfall–temperature pairs are used in the temperature bins. The main conclusions of the spatial and temporal downscaling section are listed below.

- The rainfall–temperature scaling relationships found for the all stations and evidence that the scale varies with location, rain duration and temperature. Among the selected cities, Darwin station showed a negative scale relationship for both the 99^{th} and 50^{th} percentiles for all rainfall durations. It is located in Northern territory, which has tropical climate throughout the year.

- The other six stations showed similar patterns in scale relationship with the highest scale values resulting for 6 minute rainfall durations and the lowest for 24 hour rainfall durations for both percentiles. These results imply that short duration rainfall events are more dependent on daily maximum temperature than long duration rainfall events.

- Scaling values vary with the percentile of the rainfall event, with the 99^{th} percentile always produce a higher value than the 50^{th} percentile. Therefore, we can conclude that the relationship between daily maximum temperature and more extreme rainfall events (not the daily maximum) is stronger than the relationship with average rainfall events.

- Rainfall–Temperature scale is not constant over a range of temperatures, with deviation especially evident at the lower and upper ends of the temperature range. The results also show that the positive scaling range is independent of station to station.

 To identify the variation of this scale with time, data is analysed using 10-year data windows. The 99th and 50th percentiles of 6 minute, 1 hour and 24 hour rainfall events are studied. The Adelaide station showed a significantly high decreasing rate of the scale for all rainfall events for both percentiles. The Darwin station also showed a decreasing trend in scale for all events with the exception of the 99th percentile of 6 minute rainfall events. In comparison, the other five stations showed an increasing trend in the scale for the 99th percentile of 6 minute rainfall events. This increasing trend may be caused by frequent intensified convective rainfall events as a result of climate change. Further, the results also show a decreasing trend in the scale, especially for the 50th percentile of long duration rainfall events.

 Seasonal variations in the trend of the scale change are analysed by placing the summer and autumn seasons in one group and the winter and spring seasons in another group. The Perth, Melbourne and Sydney (except 24 hour rainfall winter/spring) stations show an increasing trend of scale for both groups while Adelaide and Darwin show decreasing trend for 99th percentile (except 6 minutes rainfall in summer/autumn). Furthermore, the majority of scaling trend of 50th percentile is decreasing for both groups.

 These results clearly show that the rainfall-temperature scaling relationship is limited to certain temperature range, and this relationship depends on the percentile of rainfall, the rainfall duration, analysis period and the season. Both increasing and decreasing scaling trends are observed by periodic analysis. According to these results, it can be expected more extreme short duration rainfalls in some regions in the future.

The third section (Chapter 7) of the thesis presents an application of developed results above to assess an urban catchment using hydrological modelling to evaluate the combined impacts of climate change and land use change on urban catchments. The present practice of hydrological modelling in urban development projects does not address the climate change impacts in the future periods. It only assesses the impacts of land use change on the urban catchments. Therefore, the main objectives of this section are; developing a hydrological model by taking catchment parameter into account to represent the real hydrological process, identifying the critical events (critical rain duration) which have highest impacts on surface water routing, assessing

the impact of future development on hydrological process of the catchment under changing climate.

For the hydrological modelling study, proposed development area of Stirling City Centre development is defined as the case study. The nearest ongoing BoM weather station is Perth airport weather station. Therefore, developed IDF curves which present the climate change impacts for Perth airport region is applied in this hydrological assessment. MIKE SHE and MIKE 11 coupled hydrological model are used to simulate the catchment hydrology. The summarized conclusions of the case study are;.

- Detention storage, saturated hydraulic conductivity and surface roughness are identified as the main sensitive parameters for the surface water modelling. Therefore, these parameters are subjected to the sensitivity analysis.

- Coupled MIKE SHE/MIKE 11 model is calibrated from 03/09/2012 to 06/09/2012 period and validated from 03/11/2012 to 06/11/2012 period. It confirms the capability of proposed modelling approach to simulate the real catchment hydrology in the development area.

- Peak flow from the developing catchment is a main stormwater management parameter according to the stormwater management guidelines, Western Australia. Based on the peak flow from the development area, it is found that 24 hour rainfall event is the critical rainfall event for 100 year recurrence interval.

- The proposed development mainly consists of drainage network modifications in the development area. These modifications include dimensions and levels changes, introducing new structures and removing existing drainage structures, modifications to the channel bed by introducing vegetation, introducing new embankment slopes and vegetation etc.

- Even though above mentioned drainage modifications satisfy the stormwater management requirements under existing climate, it does not satisfy the requirements under changing climate projected by HadCM3-A2 scenario for future periods. Therefore, further modifications are essential for the proposed drainage network.

- Finally, it can be emphasised that combined impacts of climate change and land use change need to be evaluated for more accurate and reliable stormwater management approach in urban areas.

8.2 Recommendations for future research

The outcomes of this study present the importance of evaluating combined impact of climate change and land use change in urban hydrological assessments. The proposed approach is based on the downscaling of GCM predictions for future periods. However, the proposed approach requires further improvements. The following section presents the summary of key factors need to be considered in future research.

- Scaling relationship of NCMs of extreme rainfall event is used in the proposed approach to downscale the future sub-daily rainfall. In the present study, it is limited for seven major cities in Australia and another eight stations in Western Australia. It is highly recommended to investigate the scaling behaviour of NCMs of extreme rainfall across Australian continent using more data from more observation stations.

- Investigate the physical relationships of scaling of extreme rainfall and clustering of weather stations based on the characteristics of NCMs'scaling slope, is encouraged in future research. It will be highly useful in developing IDF relations for future periods.

- The relationship between extreme daily rainfall and the daily maximum temperature is investigated in the current study. It is observed that the rainfall-temperature scaling relation is varied with time. Therefore, it is highly recommended to investigate the physical factors (influence of convective rainfalls etc.) on rainfall – temperature scale.

- The unchanged temporal pattern for future periods is assumed for the hydrological modelling process. However, it should be investigated the changing trends of the temporal pattern of the future rainfalls to capture future temporal changes. Therefore, detailed investigations considering temporal change of future rainfall is highly recommended.

References

ABBOTT, M. B., BATHURST, J. C., CUNGE, J. A., O'CONNELL, P. E. & RASMUSSEN, J. 1986a. An introduction to the European Hydrological System — Systeme Hydrologique Europeen, “SHE”, 1: History and philosophy of a physically-based, distributed modelling system. Journal of Hydrology, 87**,** 45-59.

ABBOTT, M. B., BATHURST, J. C., CUNGE, J. A., O'CONNELL, P. E. & RASMUSSEN, J. 1986b. An introduction to the European Hydrological System — Systeme Hydrologique Europeen, “SHE”, 2: Structure of a physically-based, distributed modelling system. Journal of Hydrology, 87**,** 61-77.

ALEXANDER, L., HOPE, P., COLLINS, D., TREWIN, B., LYNCH, A. & NICHOLLS, N. 2007. Trends in Australia's climate means and extremes: a global context. Australian Meteorological Magazine, 56**,** 1-18.

ALEXANDER, L. V., ZHANG, X., PETERSON, T. C., CAESAR, J., GLEASON, B., KLEIN TANK, A. M. G., HAYLOCK, M., COLLINS, D., TREWIN, B., RAHIMZADEH, F., TAGIPOUR, A., RUPA KUMAR, K., REVADEKAR, J., GRIFFITHS, G., VINCENT, L., STEPHENSON, D. B., BURN, J., AGUILAR, E., BRUNET, M., TAYLOR, M., NEW, M., ZHAI, P., RUSTICUCCI, M. & VAZQUEZ-AGUIRRE, J. L. 2006. Global observed changes in daily climate extremes of temperature and precipitation. Journal of Geophysical Research: Atmospheres, 111**,** D05109.

ALLAN, R. P. & SODEN, B. J. 2008. Atmospheric Warming and the Amplification of Precipitation Extremes. Science, 321**,** 1481-1484.

ANDRAS, B., JIRI, S. & HANS-JOACHIM, C. 2002. Automated objective classification of daily circulation patterns for precipitation and temperature downscaling based on optimized fuzzy rules. Climate Research, 23**,** 11-22.

ARNBJERG-NIELSEN, K., WILLEMS, P., OLSSON, J., BEECHAM, S., PATHIRANA, A., BÜLOW GREGERSEN, I., MADSEN, H. & NGUYEN, V.-T.-V. 2013. Impacts of climate change on rainfall extremes and urban drainage systems: a review. Water Science and Technology, 68**,** 16-28.

ARNOLD, J. G., SRINIVASAN, R., MUTTIAH, R. S. & WILLIAMS, J. R. 1998. LARGE AREA HYDROLOGIC MODELING AND ASSESSMENT PART I: MODEL DEVELOPMENT1. JAWRA Journal of the American Water Resources Association, 34**,** 73-89.

ARYAL, S. K., BATES, B. C., CAMPBELL, E. P., LI, Y., PALMER, M. J. & VINEY, N. R. 2009. Characterizing and Modeling Temporal and Spatial Trends in Rainfall Extremes. Journal of Hydrometeorology, 10**,** 241-253.

BAIGORRIA, G. A. & JONES, J. W. 2010. GiST: A Stochastic Model for Generating Spatially and Temporally Correlated Daily Rainfall Data. Journal of Climate, 23**,** 5990-6008.

BATES, B. C., CHARLES, S. P. & HUGHES, J. P. 1998. Stochastic downscaling of numerical climate model simulations. Environmental Modelling & Software, 13**,** 325-331.

BECK, C., JACOBEIT, J. & JONES, P. D. 2007. Frequency and within-type variations of large-scale circulation types and their effects on low-frequency climate variability in central europe since 1780. International Journal of Climatology, 27**,** 473-491.

BERG, P., HAERTER, J. O., THEJLL, P., PIANI, C., HAGEMANN, S. & CHRISTENSEN, J. H. 2009. Seasonal characteristics of the relationship between daily precipitation intensity and surface temperature. Journal of Geophysical Research: Atmospheres, 114**,** D18102.

BEVEN, K. J., CALVER, A. & MORRIS, E. M. 1987. The Institute of Hydrology distributed model. Wallingford, UK.: Institute of Hydrology.

BEVEN, K. J. & KIRKBY, M. J. 1976. Towards a simple physically based variable contributing model of catchment

hydrology. School of Geography, University of Leeds.

BEVEN, K. J. & KIRKBY, M. J. 1979. A physically based, variable contributing area model of basin hydrology / Un modèle à base physique de zone d'appel variable de l'hydrologie du bassin versant. Hydrological Sciences Bulletin, 24**,** 43-69.

BOM. 2015. Climate outlook overview [Online]. Commonwealth of Australia: Bureau of Meteorology [Accessed 03.04.2015 2015].

BRINKMANN, R. W. A. 1999. Application of Non-hierarchically Clustered Circulation Components to Surface Weather Conditions: Lake Superior Basin Winter Temperatures. Theoretical and Applied Climatology, 63**,** 41-56.

BRINKMANN, W. A. R. 2000. Modification of a correlation-based circulation pattern classification to reduce within-type variability of temperature and precipitation. International Journal of Climatology, 20**,** 839-852.

BUISHAND, T. A. 1978. Some remarks on the use of daily rainfall models. Journal of Hydrology, 36**,** 295-308.

BURLANDO, P. & ROSSO, R. 1996. Scaling and muitiscaling models of depth-duration-frequency curves for storm precipitation. Journal of Hydrology, 187**,** 45-64.

BUSUIOC, A., TOMOZEIU, R. & CACCIAMANI, C. 2008. Statistical downscaling model based on canonical correlation analysis for winter extreme precipitation events in the Emilia-Romagna region. International Journal of Climatology, 28**,** 449-464.

BUTTS, M., DREWS, M., LARSEN, M. A. D., LERER, S., RASMUSSEN, S. H., GROOSS, J., OVERGAARD, J., REFSGAARD, J. C., CHRISTENSEN, O. B. & CHRISTENSEN, J. H. 2014. Embedding complex hydrology in the regional climate system – Dynamic coupling across different modelling domains. Advances in Water Resources, 74**,** 166-184.

CANNON, A. J., WHITFIELD, P. H. & LORD, E. R. 2002. Synoptic map-pattern clasification using recursive partitioning and principal component analysis. Monthly Weather Review, 130**,** 1187.

CARPENTER, T. M. & GEORGAKAKOS, K. P. 2004. Continuous streamflow simulation with the HRCDHM distributed hydrologic model. Journal of Hydrology, 298**,** 61-79.

CHANG, C. W., HIONG, S. Estimating of sub daily IDF curves in Singapore using simple scaling. International conference on climate change effects, May 27-May 30 2013 Potsdam, Germany. 221-230.

CHAU, K., WU, C. & LI, Y. 2005. Comparison of Several Flood Forecasting Models in Yangtze River. Journal of Hydrologic Engineering, 10**,** 485-491.

CHEN, H., XU, C.-Y. & GUO, S. 2012a. Comparison and evaluation of multiple GCMs, statistical downscaling and hydrological models in the study of climate change impacts on runoff. Journal of Hydrology, 434–435**,** 36-45.

CHEN, H., XU, C. Y. & GUO, S. 2012b. Comparison and evaluation of multiple GCMs, statistical downscaling and hydrological models in the study of climate change impacts on runoff. Journal of Hydrology, 434–435**,** 36-45.

CHEN, J., BRISSETTE, F. P. & LECONTE, R. 2010. A daily stochastic weather generator for preserving low-frequency of climate variability. Journal of Hydrology, 388**,** 480-490.

CHEN, Y.-R., YU, B. & JENKINS, G. 2013. Secular Variation in Rainfall Intensity and Temperature in Eastern Australia. Journal of Hydrometeorology, 14**,** 1356-1363.

CHOW, V. T. 1959. Open channel hydraulics, New York, McGraw Hill.

CHU, M. L., KNOUFT, J. H., GHULAM, A., GUZMAN, J. A. & PAN, Z. 2013. Impacts of urbanization on river flow frequency: A controlled experimental modeling-based evaluation approach. Journal of Hydrology, 495**,** 1-12.

CLARKE, L., EDMONDS, J., JACOBY, H., PITCHER, H., REILLY, J. & RICHELS, R. 2007. Scenarios of Greenhouse Gas Emissions and Atmospheric Concentrations. Sub-report 2.1A of Synthesis and Assessment Product 2.1 by the U.S. Climate Change Science Program and the Subcommittee on Global Change Research. Department of Energy. Washington, 7 DC.: Office of Biological & Environmental Research.

COULIBALY, P., DIBIKE, Y. B. & ANCTIL, F. 2005. Downscaling Precipitation and Temperature with Temporal Neural Networks. Journal of Hydrometeorology, 6**,** 483-496.

CRAWFORD, N. H. & LINSLEY, R. K. 1966. Digital simulation in hydrology, Stanford watershed model

IV.: Dep. Civ. Eng., Stanford University.

CROWLEY, T. J. 2000. Causes of Climate Change Over the Past 1000 Years. Science 289**,** 270-277.

CUNNANE, C. 1978. Unbiased plotting positions — A review. Journal of Hydrology, 37**,** 205-222.

DARCY, H. 1856. Les Fontaines Publiques de la Ville de Dijon. Dalmont, Paris.

DARÍO VALENCIA, R. & SCHAKKE, J. C. 1972. A disaggregation model for time series analysis and synthesis. Cambridge, Massachussetts, USA.

DARÍO VALENCIA, R. & SCHAKKE, J. C. 1973. Disaggregation processes in stochastic hydrology. Water Resources Research, 9**,** 580-585.

DAVIDSON, W. A. 1995. Hydrogeology and groundwater resources of the Perth Region. Bulletin 142.

DE SAINT-VENANT, B. 1871. Theorie du mouvement non permanent des eaux, avec application aux crues de rivieras et a l'introduction des marces dans leur lit. Comptes Rendus de l'Academic des Sciences, 73**,** 147-154, 237-240.

DENIS, B. B., LAPRISE, R. R., CAYA, D. D. & CÔTÉ, J. J. 2002. Downscaling ability of one-way nested regional climate models: the Big-Brother Experiment. Climate Dynamics, 18**,** 627-646.

DIAZ-NIETO, J. & WILBY, R. L. 2005. A comparison of statistical downscaling and climate change factor methods: impacts on low flows in the River Thames, United Kingdom. Climatic Change, 69**,** 245-268.

DICKINSON, R. E., . ERRICO, R.M.,GIORGI, F., BATES, G.T., 1989. A REGIONAL CLIMATE MODEL FOR THE WESTERN UNITED STATES Climatic Change, 15**,** 383-422.

EASTERLING, D. R., MEEHL, G. A., PARMESAN, C., CHANGNON, S. A., KARL, T. R. & MEARNS, L. O. 2000. Climate Extremes: Observations, Modeling, and Impacts. Science, 289**,** 2068-2074.

ELIZABETH, N. C., AMANDA, H. L., JOHN, J. C. & MELINDA, R. K. 2006. Classification of synoptic patterns in the western Arctic associated with extreme events at Barrow, Alaska, USA. Climate Research, 30**,** 83-97.

EMBRECHTS, P., KLÜPPELBERG, C. & MIKOSCH, T. 1997. Modelling Extremal Events for Insurance and Finance, New York, Springer.

EMORI, S. & BROWN, S. J. 2005. Dynamic and thermodynamic changes in mean and extreme precipitation under changed climate. Geophysical Research Letters, 32**,** L17706.

ESTEBAN, P., JONES, P. D., MARTÍN-VIDE, J. & MASES, M. 2005. Atmospheric circulation patterns related to heavy snowfall days in Andorra, Pyrenees. International Journal of Climatology, 25**,** 319-329.

FEDER, J. 1988. Fractals, New York, Plenum Press

FISCHER, E. M. & KNUTTI, R. 2015. Anthropogenic contribution to global occurrence of heavy-precipitation and high-temperature extremes. Nature Clim. Change, 5**,** 560-564.

FLETCHER, T. D., ANDRIEU, H. & HAMEL, P. 2013. Understanding, management and modelling of urban hydrology and its consequences for receiving waters: A state of the art. Advances in Water Resources, 51**,** 261-279.

FORSYTHE, N., FOWLER, H. J., BLENKINSOP, S., BURTON, A., KILSBY, C. G., ARCHER, D. R., HARPHAM, C. & HASHMI, M. Z. 2014. Application of a stochastic weather generator to assess climate change impacts in a semi-arid climate: The Upper Indus Basin. Journal of Hydrology, 517**,** 1019-1034.

FOSTER, S. S. D., R., L. A. & L., M. B. 1996. Urban groundwater resource management; priorities for developing cities, London, UK., E & FN Spon.

FOWLER, H. J. & KILSBY, C. G. 2007. Using regional climate model data to simulate historical and future river flows in northwest England. Climatic Change, 80**,** 337-367.

FOWLER, H. J., KILSBY, C. G. & O'CONNELL, P. E. 2000. A stochastic rainfall model for the assessment of regional water resource systems under changed climatic condition. Hydrol. Earth Syst. Sci., 4**,** 263-281.

FREEZE, R. A. & HARLAN, R. L. 1969. Blueprint for a physically-based, digitally-simulated hydrologic response model. Journal of Hydrology, 9**,** 237-258.

FROST, A. J., CHARLES, S. P., TIMBAL, B., CHIEW, F. H. S., MEHROTRA, R., NGUYEN, K. C., CHANDLER, R. E., MCGREGOR, J. L., FU, G., KIRONO, D. G. C., FERNANDEZ, E. & KENT, D. M. 2011. A comparison of multi-site daily rainfall downscaling techniques under Australian conditions. Journal of Hydrology, 408**,** 1-18.

GIORGI, F. 1990. Simulation of Regional Climate Using a Limited Area Model Nested in a General Circulation Model. Journal of Climate, 3**,** 941-963.

GLENIS, V., PINAMONTI, V., HALL, J. W. & KILSBY, C. G. 2015. A transient stochastic weather generator incorporating climate model uncertainty. Advances in Water Resources, 85**,** 14-26.

GOSAIN, A. K., MANI, A. & DWIVEDI, C. 2009. Hydrological modeling review. Climawater, Report No 1.

GRAYSON, R. B., MOORE, I. D. & MCMAHON, T. A. 1992. Physically based hydrologic modeling: 1. A terrain-based model for investigative purposes. Water Resources Research, 28**,** 2639-2658.

GUO, H., HU, Q. & JIANG, T. 2008. Annual and seasonal streamflow responses to climate and land-cover changes in the Poyang Lake basin, China. Journal of Hydrology, 355**,** 106-122.

GUPTA, V. K. & WAYMIRE, E. 1990. Multiscaling properties of spatial rainfall and river flow distributions. Journal of Geophysical Research: Atmospheres, 95**,** 1999-2009.

GUPTA, V. K. & WAYMIRE, E. C. 1993. A Statistical Analysis of Mesoscale Rainfall as a Random Cascade. Journal of Applied Meteorology, 32**,** 251-267.

GUTMANN, E. D., RASMUSSEN, R. M., LIU, C., IKEDA, K., GOCHIS, D. J., CLARK, M. P., DUDHIA, J. & THOMPSON, G. 2012. A Comparison of Statistical and Dynamical Downscaling of Winter Precipitation over Complex Terrain. Journal of Climate, 25**,** 262-281.

HARDWICK JONES, R., WESTRA, S. & SHARMA, A. 2010. Observed relationships between extreme sub-daily precipitation, surface temperature, and relative humidity. Geophysical Research Letters, 37**,** L22805.

HARROLD, T. I., SHARMA, A. & SHEATHER, S. J. 2003. A nonparametric model for stochastic generation of daily rainfall occurrence. Water Resources Research, 39**,** 1300.

HASHMI, M., SHAMSELDIN, A. & MELVILLE, B. 2011. Comparison of SDSM and LARS-WG for simulation and downscaling of extreme precipitation events in a watershed. Stochastic Environmental Research and Risk Assessment, 25**,** 475-484.

HASHMI, M. Z., SHAMSELDIN, A. Y. & MELVILLE, B. W. 2009. Statistical downscaling of precipitation: state-of-the-art and application of bayesian multi-model approach for uncertainty assessment. Hydrol. Earth Syst. Sci. Discuss., 6**,** 6535-6579.

HAUSER, T. & DEMIROV, E. 2013. Development of a stochastic weather generator for the sub-polar North Atlantic. Stochastic Environmental Research and Risk Assessment, 27**,** 1533-1551.

HERATH, S. M., SARUKKALIGE, P. R. & NGUYEN, V. T. V. 2016. A spatial temporal downscaling approach to development of IDF relations for Perth airport region in the context of climate change. Hydrological Sciences Journal, 61**,** 2061-2070.

HESS, P. & BREZOWSKI, H. 1969. Katalog der Gro ̈wetterlagenEuropas. Ber Dt Wetterdienst 113: Offenbach, Wetter-dienst.

HESSAMI, M., GACHON, P., OUARDA, T. B. M. J. & ST-HILAIRE, A. 2008. Automated regression-based statistical downscaling tool. Environmental Modelling & Software, 23**,** 813-834.

HEWITSON, B. & CRANE, R. G. 1996. Climate downscaling: Techniques and application. Climate Research, 7**,** 85-95.

HIJIOKA, Y., MATSUOKA, Y., NISHIMOTO, H., MASUI, M. & KAINUMA, M. 2008. Global GHG emissions scenarios under GHG concentration stabilization targets. Journal of Global Environmental Engineering, 13**,** 97-108.

HOSKING, J. R. M. 1990. L-Moments: Analysis and Estimation of Distributions Using Linear Combinations of Order Statistics. Journal of the Royal Statistical Society. Series B (Methodological), 52**,** 105-124.

HOSKING, J. R. M., WALLIS, J. R. & WOOD, E. F. 1985. Estimation of the Generalized Extreme-Value Distribution by the Method of Probability-Weighted Moments. Technometrics, 27**,** 251-261.

HOSTETLER, S. W., BARTLEIN, P. J., CLARK, P. U., SMALL, E. E. & SOLOMON, A. M. 2000. Simulated influences of Lake Agassiz on the climate of central North America 11,000 years ago. Nature, 405**,** 334-337.

HUTH, R. 2000. A circulation classification scheme applicable in GCM studies. Theoretical and Applied Climatology, 67**,** 1-18.

HUTH, R., BECK, C., PHILIPP, A., DEMUZERE, M., USTRNUL, Z., CAHYNOVÁ, M., KYSELÝ, J. & TVEITO, O. E. 2008. Classifications of Atmospheric Circulation Patterns. Annals of the New York Academy of Sciences, 1146**,** 105-152.

IPCC 2000. IPCC special report on emissions scenarios - Summary for policymakers

Online report available at http://www.ipcc.ch/pdf/special-reports/spm/sres-en.pdf.

JAKOB, D., IMIELSKA, A., CHARLES, S., FU, F., FREDERIKSEN, C., FREDERIKSEN, J., ZIDIKHERI, M., HOPE, P., KEAY, K., GANTER, C. J., LI, Y., PHATAK, A., PALMER, M., WORMWORTH, J., MCBRIDE, J., DARE, R., LAVENDER, S., ABBS, D., ROTSTAYN, L. & RAFTER, T. 2012. Indian Ocean Climate Initiative (2012) Western Australia's Weather and Climate: A Synthesis of Indian Ocean Climate Initiative Stage 3 Research. In: BATES, B., FREDERIKSEN, C. & WORMWORTH, J. (eds.). CSIRO and BoM, Australia.

JOHNSON, F. & SHARMA, A. 2012. A nesting model for bias correction of variability at multiple time scales in general circulation model precipitation simulations. Water Resources Research, 48**,** W01504.

JONES, P. D., HARPHAM, C. & BRIFFA, K. R. 2013. Lamb weather types derived from reanalysis products. International Journal of Climatology, 33**,** 1129-1139.

JONES, R. H., WESTRA, S. & SHARMA, A. 2010. Observed relationships between extreme sub-daily precipitation, surface temperature, and relative humidity. Geophysical Research Letters, 37**,** L22805.

JOSHI, D., ST-HILAIRE, A., OUARDA, T., DAIGLE, A. & THIEMONGE, N. 2014. Comparison of direct statistical and indirect statistical-deterministic frameworks in downscaling river low-flow indices. Hydrological Sciences Journal**,** null-null.

JSCWSC 2009. Evaluating Options for Water Sensitive Urban Design –A National Guide Joint Steering Committee for Water Sensitive Cities

JUNG, M., KIM, H., MALLARI, K. J. B., PAK, G. & YOON, J. 2015. Analysis of effects of climate change on runoff in an urban drainage system: a case study from Seoul, Korea. Water Science and Technology, 71**,** 653-660.

KE, T. 2011. Changes in precipitation with climate change. Climate Research, 47**,** 123-138.

KEILHOLZ, P., DISSE, M. & HALIK, Ü. 2015. Effects of Land Use and Climate Change on Groundwater and Ecosystems at the Middle Reaches of the Tarim River Using the MIKE SHE Integrated Hydrological Model. Water, 7**,** 3040.

KHALILI, M., NGUYEN, V. T. V. & GACHON, P. 2013. A statistical approach to multi-site multivariate downscaling of daily extreme temperature series. International Journal of Climatology, 33**,** 15-32.

KHAN, M. S., COULIBALY, P. & DIBIKE, Y. B. 2006. Uncertainty analysis of statistical downscaling methods. Journal of Hydrology, 319**,** 357-382.

KHARIN, V. V. & ZWIERS, F. W. 2002. Climate predictions with multimodel ensembles. Journal of Climate, 15**,** 793-799.

KNUDSEN, J., THOMSEN, A. & REFSGAARD, J. C. 1986. WATBAL. Hydrology Research, 17**,** 347-362.

KOUTSOYIANNIS, D. & FOUFOULA-GEORGIOU, E. 1993. A scaling model of storm hyetograph. Water Resources Research, 29**,** 2345-2361.

KOUTSOYIANNIS, D. & XANTHOPOULOS, T. 1990. A dynamic model for short-scale rainfall disaggregation. Hydrological Sciences Journal, 35**,** 303-322.

KOZLOWSKI, M. & YUSOF, Y. M. 2016. The role of urban planning and design in responding to climate change: the Brisbane experience. International Journal of Climate Change Strategies and Management, 8**,** 80-95.

KRISTENSEN, K. J. & JENSEN, S. E. 1975. A MODEL FOR ESTIMATING ACTUAL EVAPOTRANSPIRATION FROM POTENTIAL EVAPOTRANSPIRATION. Hydrology Research, 6**,** 170-188.

KUMAR, J., BROOKS, B.-G. J., THORNTON, P. E. & DIETZE, M. C. 2012. Sub-daily Statistical Downscaling of Meteorological Variables Using Neural Networks. Procedia Computer Science, 9**,** 887-896.

LAMB, H. H. 1972. British Isles weather types and a register of daily sequence of circulation patterns. 1861-1971: Geophysical Memoir, 116**,** 85.

LENDERINK, G. & VAN MEIJGAARD, E. 2008. Increase in hourly precipitation extremes beyond expectations from temperature changes. Nature Geoscience, 1**,** 511-514.

LEWIS, A. B. & KEIM, B. D. 2015. A hybrid procedure for classifying synoptic weather types for Louisiana, USA. International Journal of Climatology, 35**,** 4247-4261.

LI, H., SHEFFIELD, J. & WOOD, E. F. 2010. Bias correction of monthly precipitation and temperature fields from Intergovernmental Panel on Climate Change AR4 models using equidistant quantile matching. Journal of Geophysical Research: Atmospheres, 115**,** D10101.

LO PRESTI, R., BARCA, E. & PASSARELLA, G. 2008. A methodology for treating missing data applied to daily rainfall data in the Candelaro River Basin (Italy). Environmental Monitoring and Assessment, 160**,** 1-22.

LUCAS, P. L., VAN VUUREN, D. P., OLIVIER, J. G. J. & DEN ELZEN, M. G. J. 2007. Long-term reduction potential of non-CO2 greenhouse gases. Environmental Science & Policy, 10**,** 85-103.

MANNING, R. 1891. On the flow of water in open channels and pipes. Transactions of theInstitution of Civil Engineers of Ireland, 20**,** 161–207.

MARAUN, D., WETTERHALL, F., IRESON, A. M., CHANDLER, R. E., KENDON, E. J., WIDMANN, M., BRIENEN, S., RUST, H. W., SAUTER, T., THEMEßL, M., VENEMA, V. K. C., CHUN, K. P., GOODESS, C. M., JONES, R. G., ONOF, C., VRAC, M. & THIELE-EICH, I. 2010. Precipitation downscaling under climate change: Recent developments to bridge the gap between dynamical models and the end user. Reviews of Geophysics, 48**,** RG3003.

MAVROMATIS, T. & HANSEN, J. W. 2001. Interannual variability characteristics and simulated crop response of four stochastic weather generators. Agricultural and Forest Meteorology, 109**,** 283-296.

MEARNS, L. O., GIORGI, F., WHETTON, P., PABON, D., HULME, M. & LAL, M. 2003. Guidelines for use of climate scenarios developed from Regional Climate Model experiments. Technical Report. Norwich, UK: The IPCC Data Distribution Centre.

MEHROTRA, R., SHARMA, A. & CORDERY, I. 2004. Comparison of two approaches for downscaling synoptic atmospheric patterns to multisite precipitation occurrence. Journal of Geophysical Research: Atmospheres, 109**,** D14107.

MENABDE, M., SEED, A. & PEGRAM, G. 1999. A simple scaling model for extreme rainfall. Water Resources Research, 35**,** 335-339.

MENEVEAU, C. & SREENIVASAN, K. R. 1987. Simple multifractal cascade model for fully developed turbulence. Physical Review Letters, 59**,** 1424-1427.

MIKESHE. 2016. MIKE SHE - Integrated Catchment Modelling [Online]. Available: https://www.mikepoweredbydhi.com/products/mike-she [Accessed 25.03.2016 2016].

MOLNAR, P., FATICHI, S., GAÁL, L., SZOLGAY, J. & BURLANDO, P. 2015. Storm type effects on super Clausius–Clapeyron scaling of intense rainstorm properties with air temperature. Hydrol. Earth Syst. Sci., 19**,** 1753-1766.

MOUSSOULIS, E., MALLINIS, G., KOUTSIAS, N. & ZACHARIAS, I. 2015. Modelling surface runoff to evaluate the effects of wildfires in multiple semi-arid, shrubland-dominated catchments. Hydrological Processes, 29**,** 4427-4441.

MÜLLER, G. V., COMPAGNUCCI, R., NUÑEZ, M. N. & SALLES, A. 2003. Surface circulation associated with frost in the wet Pampas. International Journal of Climatology, 23**,** 943-961.

MULLER, R. A. 1977. A Synoptic Climatology for Environmental Baseline Analysis: New Orleans. Journal of Applied Meteorology, 16**,** 20-33.

NASH, J. E. The form of the instantaneous unit hydrograph. IUGG Gen. Assem, 1958 Toronto. IAHS.

NGUYEN, T. D., NGUYEN, V. T. V. & DESRAMAUT, N. 2008. Estimation of urban design storms in consideration of GCM-based climate change scenarios. Water and Urban Development Paradigms. CRC Press.

NGUYEN, V. T. V. & NGUYEN, T. D. 2008. Statistical downscaling of daily precipitation process for climate-related impact studies, Colorado, Water Resources Publications.

NGUYEN, V. T. V., NGUYEN, T. D. & ASHKAR, F. 2002. Regional frequency analysis of extreme rainfalls. Water Science and Technology, 45**,** 75-81.

NGUYEN, V. T. V., NGUYEN, T. D. & GACHON, P. 2006. On the linkage of large-scale climate variability with local characteristics of daily precipitation and temperature extremes: an evaluation of statistical downscaling methods. In: N.PARK (ed.) Advances in Geosciences Singapore: World Scientific.

NGUYEN, V. T. V., NGUYEN, T. D. & WANG, H. 1998. Regional estimation of short duration rainfall extremes. Water Science and Technology, 37**,** 15-19.

NKUNA, T. R. & ODIYO, J. O. 2011. Filling of missing rainfall data in Luvuvhu River Catchment using artificial neural networks. Physics and Chemistry of the Earth, Parts A/B/C, 36**,** 830-835.

O'GORMAN, P. A. & SCHNEIDER, T. 2009. The physical basis for increases in precipitation extremes in simulations of 21st-century climate change. Proceedings of the National Academy of Sciences, 106**,** 14773-14777.

O'DRISCOLL, M., CLINTON, S., JEFFERSON, A., MANDA, A. & MCMILLAN, S. 2010. Urbanization Effects on Watershed Hydrology and In-Stream Processes in the Southern United States. Water, 2**,** 605.

OLSSON, J., AMAGUCHI, H., ALSTERHAG, E., DÅVERHÖG, M., ADRIAN, P.-E. & KAWAMURA, A. 2012. Adaptation to climate change impacts on urban storm water: a case study in Arvika, Sweden. Climatic Change, 116**,** 231-247.

PANDEY, G. R. 1995. Regional estimation of floods and rainfalls for ungaged sites. Doctoral Thesis, McGill University.

PANTHOU, G., MAILHOT, A., LAURENCE, E. & TALBOT, G. 2014. Relationship between Surface Temperature and Extreme Rainfalls: A Multi-Time-Scale and Event-Based Analysis*. Journal of Hydrometeorology, 15**,** 1999-2011.

PARK, J.-S., KANG, H.-S., LEE, Y. S. & KIM, M.-K. 2011. Changes in the extreme daily rainfall in South Korea. International Journal of Climatology, 31**,** 2290-2299.

PENG, S., PIAO, S., CIAIS, P., FRIEDLINGSTEIN, P., OTTLE, C., BRÉON, F.-M., NAN, H., ZHOU, L. & MYNENI, R. B. 2012. Surface Urban Heat Island Across 419 Global Big Cities. Environmental Science & Technology, 46**,** 696-703.

PHIEN, H. N. & FANG, T. E. 1989. Maximum likelihood estimation of the parameters and quantiles of the general extreme-value distribution from censored samples. Journal of Hydrology, 105**,** 139-155.

PUI, A., SHARMA, A., MEHROTRA, R., SIVAKUMAR, B. & JEREMIAH, E. 2012. A comparison of alternatives for daily to sub-daily rainfall disaggregation. Journal of Hydrology, 470–471**,** 138-157.

RACSKO, P., SZEIDL, L. & SEMENOV, M. 1991a. A serial approach to local stochastic weather models. Ecological Modelling, 57**,** 27-41.

RACSKO, P., SZEIDL, L. & SEMENOV, M. 1991b. A serial approach to local stochastic weather models. Ecological Modelling, 57**,** 27-41.

REFSGAARD, J. C. & STORM, B. 1995. MIKE SHE, 18, Water Resources Publications, Highlands Ranch, CO.

RIAHI, K., GRÜBLER, A. & NAKICENOVIC, N. 2007. Scenarios of long-term socio-economic and environmental development under climate stabilization. Technological Forecasting and Social Change, 74**,** 887-935.

RICHARDS, L. A. 1931. CAPILLARY CONDUCTION OF LIQUIDS THROUGH POROUS MEDIUMS. Journal of Applied Physics, 1**,** 318-333.

RICHARDSON, C. W. 1981. Stochastic simulation of daily precipitation, temperature, and solar radiation. Water Resources Research, 17**,** 182-190.

RICHARDSON, C. W. & WRIGHT, D. A. 1984. WGEN: A model for generating daily weather variables. US Dept. Agric., Agricultural Research Service

ROCWOOD, D. M. & NELSON, M. L. 1966. Computer application to streamflow synthesis and

reservoir regulation. IV Int. Conf. Irrig. Drain.

RODRIGUEZ-ITURBE, I., COX, D. R. & ISHAM, V. 1987. Some Models for Rainfall Based on Stochastic Point Processes. Proceedings of the Royal Society of London A: Mathematical, Physical and Engineering Sciences, 410**,** 269-288.

ROSE, S. & PETERS, N. E. 2001. Effects of urbanization on streamflow in the Atlanta area (Georgia, USA): a comparative hydrological approach. Hydrological Processes, 15**,** 1441-1457.

RUMMUKAINEN, M. 2010. State-of-the-art with regional climate models. Wiley Interdisciplinary Reviews: Climate Change, 1**,** 82-96.

SACHINDRA, D. A., HUANG, F., BARTON, A. & PERERA, B. J. C. 2013. Least square support vector and multi-linear regression for statistically downscaling general circulation model outputs to catchment streamflows. International Journal of Climatology, 33**,** 1087-1106.

SACHINDRA, D. A., HUANG, F., BARTON, A. & PERERA, B. J. C. 2014a. Statistical downscaling of general circulation model outputs to precipitation—part 1: calibration and validation. International Journal of Climatology, 34**,** 3264-3281.

SACHINDRA, D. A., HUANG, F., BARTON, A. & PERERA, B. J. C. 2014b. Statistical downscaling of general circulation model outputs to precipitation—part 2: bias-correction and future projections. International Journal of Climatology, 34**,** 3282-3303.

SAIDI, H., CIAMPITTIELLO, M., DRESTI, C. & TURCONI, L. 2014. Extreme rainfall events: evaluation with different instruments and measurement reliability. Environmental Earth Sciences, 72**,** 4607-4616.

SCHOOF, J. T. & PRYOR, S. C. 2003. Evaluation of the NCEP–NCAR reanalysis in terms of synoptic-scale phenomena: a case study from the Midwestern USA. International Journal of Climatology, 23**,** 1725-1741.

SEMENOV, M. & BARROW, E. M. 1997a. Use of a stochastic weather generator in the development of climate change scenarios. Climatic Change, 35**,** 397-414.

SEMENOV, M. A. & BARROW, E. M. 1997b. USE OF A STOCHASTIC WEATHER GENERATOR IN THE DEVELOPMENT OF CLIMATE CHANGE SCENARIOS. Climatic Change, 35**,** 397-414.

SHAW, E. M. 1994. Hydrology in Practice, London, UK, Chapman and Hall.

SHAW, S. B., ROYEM, A. A. & RIHA, S. J. 2011. The Relationship between Extreme Hourly Precipitation and Surface Temperature in Different Hydroclimatic Regions of the United States. Journal of Hydrometeorology, 12**,** 319-325.

SHEN, C. & PHANIKUMAR, M. S. 2010. A process-based, distributed hydrologic model based on a large-scale method for surface–subsurface coupling. Advances in Water Resources, 33**,** 1524-1541.

SHERMAN, L. K. 1932. Streamflow from rainfall by the unit graph method. Eng. News Rec., 108**,** 501-505.

SMITHERS, J. C., PEGRAM, G. G. S. & SCHULZE, R. E. 2002. Design rainfall estimation in South Africa using Bartlett–Lewis rectangular pulse rainfall models. Journal of Hydrology, 258**,** 83-99.

SODEN, B. J. & HELD, I. M. 2006. An Assessment of Climate Feedbacks in Coupled Ocean–Atmosphere Models. Journal of Climate, 19**,** 3354-3360.

SUN, W., YUAN, W.-H., LI, J. & YU, R.-C. 2015. CORRELATION BETWEEN PEAK INTENSITY OF EXTREME AFTERNOON SHORT-DURATION RAINFALL AND HUMIDITY AND SURFACE AIR TEMPERATURE IN SOUTHEAST COAST OF CHINA. Journal of Tropical Meteorology, 21**,** 276-284.

TEEGAVARAPU, R. S. V. 2009. Estimation of missing precipitation records integrating surface interpolation techniques and spatio-temporal association rules. Journal of Hydroinformatics, 11**,** 133-146.

TENG, J., VAZE, J., CHIEW, F. H. S., WANG, B. & PERRAUD, J.-M. 2012. Estimating the Relative Uncertainties Sourced from GCMs and Hydrological Models in Modeling Climate Change Impact on Runoff. Journal of Hydrometeorology, 13**,** 122-139.

TODINI, E. 1988. Rainfall-runoff modeling — Past, present and future. Journal of Hydrology, 100**,** 341-352.

TRENBERTH, K. E., DAI, A., RASMUSSEN, R. M. & PARSONS, D. B. 2003. The Changing Character of Precipitation. Bulletin of the American Meteorological Society, 84**,** 1205-1217.

TRIPATHI, S., SRINIVAS, V. V. & NANJUNDIAH, R. S. 2006. Downscaling of precipitation for climate change scenarios: A support vector machine approach. Journal of Hydrology, 330**,** 621-640.

TRIPATI, A. K., ROBERTS, C. D. & EAGLE, R. A. 2009. Coupling of CO2 and Ice Sheet Stability Over Major Climate Transitions of the Last 20 Million Years. Science, 326**,** 1394-1397.

UNITEDNATIONS 2014. World Urbanization Prospects: The 2014 Revision, Highlights (ST/ESA/SER.A/352). New York, USA: United Nations.

UTSUMI, N., SETO, S., KANAE, S., MAEDA, E. E. & OKI, T. 2011. Does higher surface temperature intensify extreme precipitation? Geophysical Research Letters, 38**,** L16708.

VANDENBERGHE, S., VERHOEST, N. E. C., ONOF, C. & DE BAETS, B. 2011. A comparative copula-based bivariate frequency analysis of observed and simulated storm events: A case study on Bartlett-Lewis modeled rainfall. Water Resources Research, 47**,** W07529.

VRAC, M., HAYHOE, K. & STEIN, M. 2007a. Identification and intermodel comparison of seasonal circulation patterns over North America. International Journal of Climatology, 27**,** 603-620.

VRAC, M., STEIN, M. & HAYHOE, K. 2007b. Statistical downscaling of precipitation through nonhomogeneous stochastic weather typing. Climate Research, 34**,** 169-184.

WALSH, C. J., FLETCHER, T. D. & BURNS, M. J. 2012. Urban Stormwater Runoff: A New Class of Environmental Flow Problem. PLoS ONE, 7**,** e45814.

WANG , J., HONG , Y., LI, L., GOURLEY , J. J., KHAN , S. I., YILMAZ , K. K., ADLER , R. F., POLICELLI , F. S., HABIB , S., IRWN , D., LIMAYE , A. S., KORME , T. & OKELLO, L. 2011. The coupled routing and excess storage (CREST) distributed hydrological model. Hydrological Sciences Journal, 56.

WANG, X., YANG, T., SHAO, Q., ACHARYA, K., WANG, W. & YU, Z. 2011. Statistical downscaling of extremes of precipitation and temperature and construction of their future scenarios in an elevated and cold zone. Stochastic Environmental Research and Risk Assessment, 26**,** 405-418.

WAPC 2008. Better Urban Water Management. Perth, Western Australia: Western Australian Planning Commission.

WASKO, C. & SHARMA, A. 2014. Quantile regression for investigating scaling of extreme precipitation with temperature. Water Resources Research, 50**,** 3608-3614.

WASKO, C. & SHARMA, A. 2015. Steeper temporal distribution of rain intensity at higher temperatures within Australian storms. Nature Geosci, 8**,** 527-529.

WESTRA, S., ALEXANDER, L. V. & ZWIERS, F. W. 2013. Global Increasing Trends in Annual Maximum Daily Precipitation. Journal of Climate, 26**,** 3904-3918.

WHEATER, H. S., CHANDLER, R. E., ONOF, C. J., ISHAM, V. S., BELLONE, E., YANG, C., LEKKAS, D., LOURMAS, G. & SEGOND, M. L. 2005. Spatial-temporal rainfall modelling for flood risk estimation. Stochastic Environmental Research and Risk Assessment, 19**,** 403-416.

WHELANS, H. G. M. A. 1994. Planning and Management Guidelines for Water Sensitive Urban (Residential) Design'. Report prepared for the Department of Planning and Urban Development, the Water Authority of Western Australia and the Environmental Protection Authority.

WIJESEKARA, G. N., FARJAD, B., GUPTA, A., QIAO, Y., DELANEY, P. & MARCEAU, D. J. 2013. A Comprehensive Land-Use/Hydrological Modeling System for Scenario Simulations in the Elbow River Watershed, Alberta, Canada. Environmental Management, 53**,** 357-381.

WILBY, R. L., CHARLES, S. P., ZORITA, E., TIMBAL, B., WHETTON, P. & MEARNS, L. O. 2004. Guidelines for use of climate scenarios developed from statistical downscaling methods. Supporting material of the Intergovernmental Panel on Climate Change, available from the DDC of IPCC TGCIA.

WILBY, R. L. & DAWSON, C. W. 2007. SDSM User Manual. UK.

WILBY, R. L. & DAWSON, C. W. 2013. The Statistical DownScaling Model: insights from one decade of application. International Journal of Climatology, 33**,** 1707-1719.

WILBY, R. L., DAWSON, C. W. & BARROW, E. M. 2002. sdsm — a decision support tool for the assessment of regional climate change impacts. Environmental Modelling & Software, 17**,** 145-157.

WILBY, R. L., DAWSON, C. W., MURPHY, C., O'CONNOR, P. & HAWKINS, E. 2014. The Statistical DownScaling Model - Decision Centric (SDSM-DC): conceptual basis and applications. Climate Research, 61**,** 259-276.

WILBY, R. L., HAY, L. E. & LEAVESLEY, G. H. 1999. A comparison of downscaled and raw GCM output: implications for climate change scenarios in the San Juan River basin, Colorado. Journal of Hydrology, 225**,** 67-91.

WILBY, R. L. & WIGLEY, T. M. L. 1997. Downscaling general circulation model output: A review of methods and limitations. Progress in Physical Geography, 21**,** 530-548.

WILKS, D. S. 1999. Multisite downscaling of daily precipitation with a stochastic weather generator. Climate Research, 11**,** 125-136.

WILLEMS, P. & VRAC, M. 2011. Statistical precipitation downscaling for small-scale hydrological impact investigations of climate change. Journal of Hydrology, 402**,** 193-205.

WISE, M., CALVIN, K., THOMSON, A., CLARKE, L., BOND-LAMBERTY, B., SANDS, R., SMITH, S. J., JANETOS, A. & EDMONDS, J. 2009. Implications of Limiting CO2 Concentrations for Land Use and Energy. Science, 324**,** 1183-1186.

WOOD, A. W., LEUNG, L. R., SRIDHAR, V. & LETTENMAIER, D. P. Hydrologic Implications of Dynamical and Statistical Approaches to Downscaling Climate Model Outputs. Climatic Change, 62**,** 189-216.

WOODING, R. A. 1965. A hydraulic model for the catchment-stream problem. Journal of Hydrology, 3**,** 268-282.

WOOLHISER, D. A. & OSBORN, H. B. 1985. A Stochastic Model of Dimensionless Thunderstorm Rainfall. Water Resources Research, 21**,** 511-522.

XU, C. Y. 1999. From GCMs to river flow: a review of downscaling methods and hydrologic modelling approaches. Progress in Physical Geography, 23**,** 229-249.

XU, Z. & YANG, Z.-L. 2012. An Improved Dynamical Downscaling Method with GCM Bias Corrections and Its Validation with 30 Years of Climate Simulations. Journal of Climate, 25**,** 6271-6286.

YAN, J. & SMITH, K. R. 1994. SIMULATION OF INTEGRATED SURFACE WATER AND GROUND WATER SYSTEMS - MODEL FORMULATION1. JAWRA Journal of the American Water Resources Association, 30**,** 879-890.

YARNAL, B., COMRIE, A. C., FRAKES, B. & BROWN, D. P. 2001. Developments and prospects in synoptic climatology. International Journal of Climatology, 21**,** 1923-1950.

YU, R. & LI, J. 2012. Hourly Rainfall Changes in Response to Surface Air Temperature over Eastern Contiguous China. Journal of Climate, 25**,** 6851-6861.

ZHANG, W., YAN, M., CHEN, P. & XU, H. 2008. Advance in application of regional climate models in China. Chinese Geographical Science, 18**,** 93-100.

9 APPENDIX

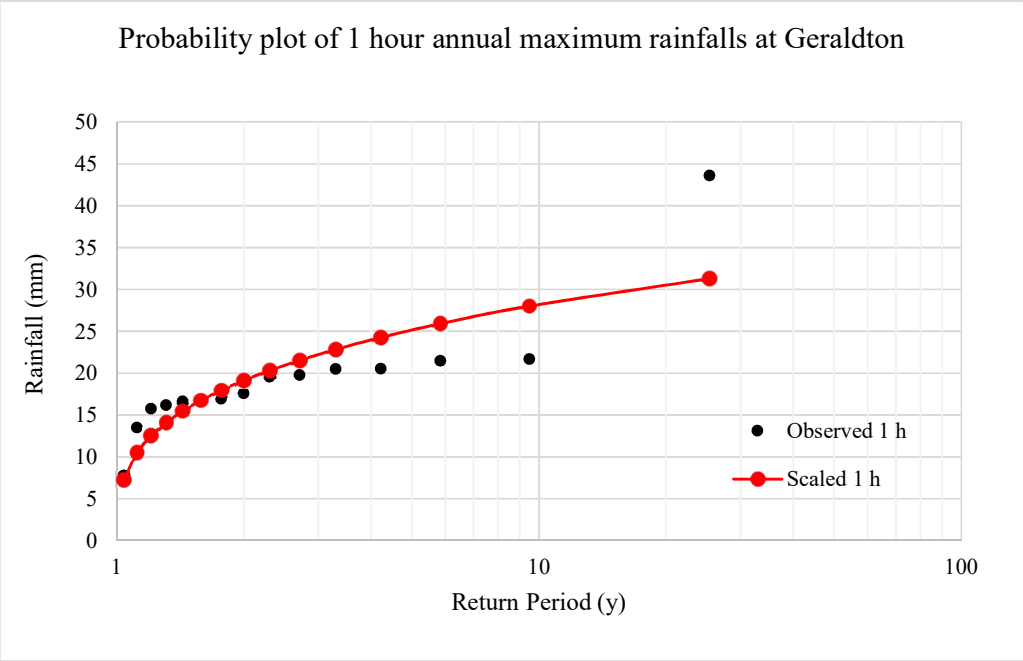

Figure 9.1: Observed and modelled rainfalls at Geraldton

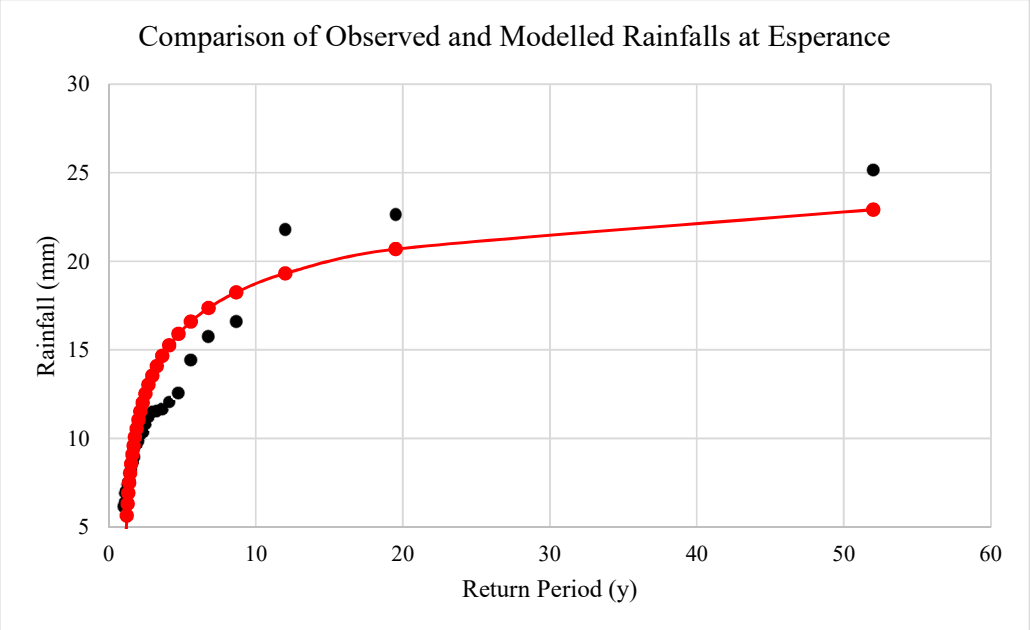

Figure 9.2: Observed and modelled rainfalls at Esperance

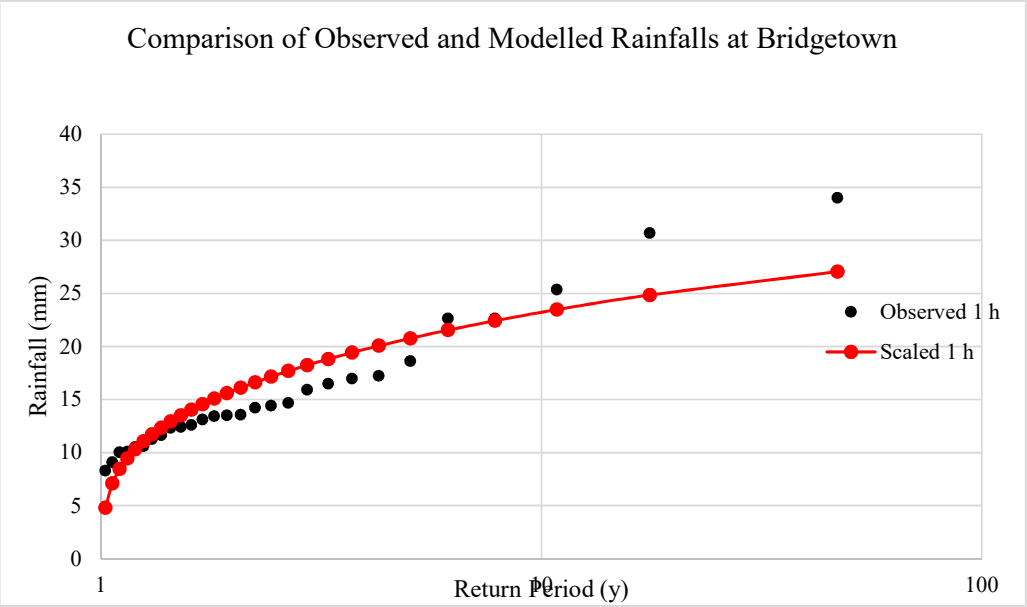

Figure 9.3:Observed and modelled rainfalls at Bridgetown

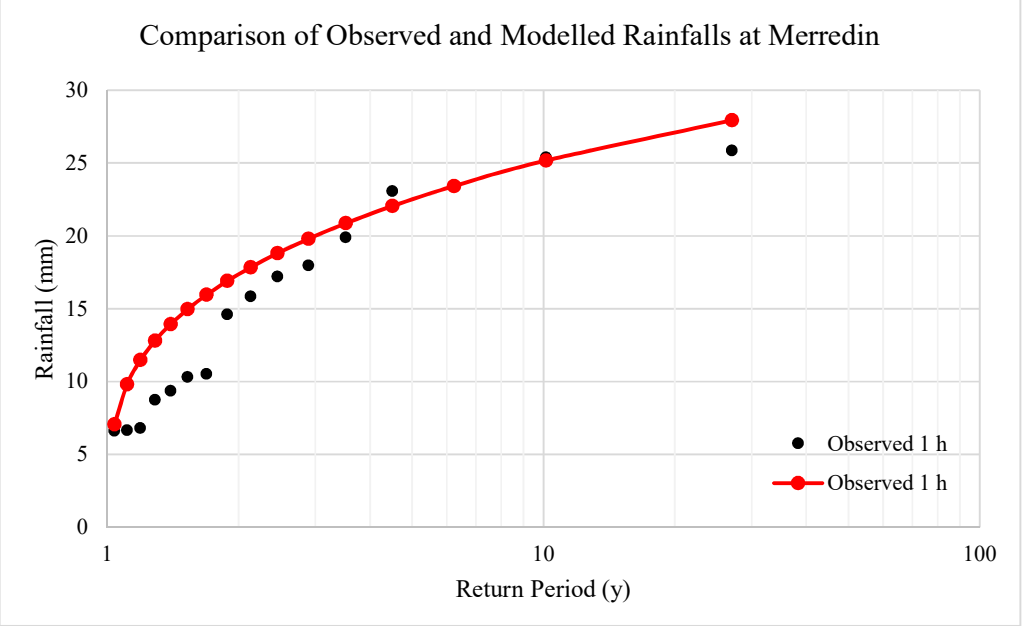

Figure 9.4: Observed and modelled rainfalls at Merredin

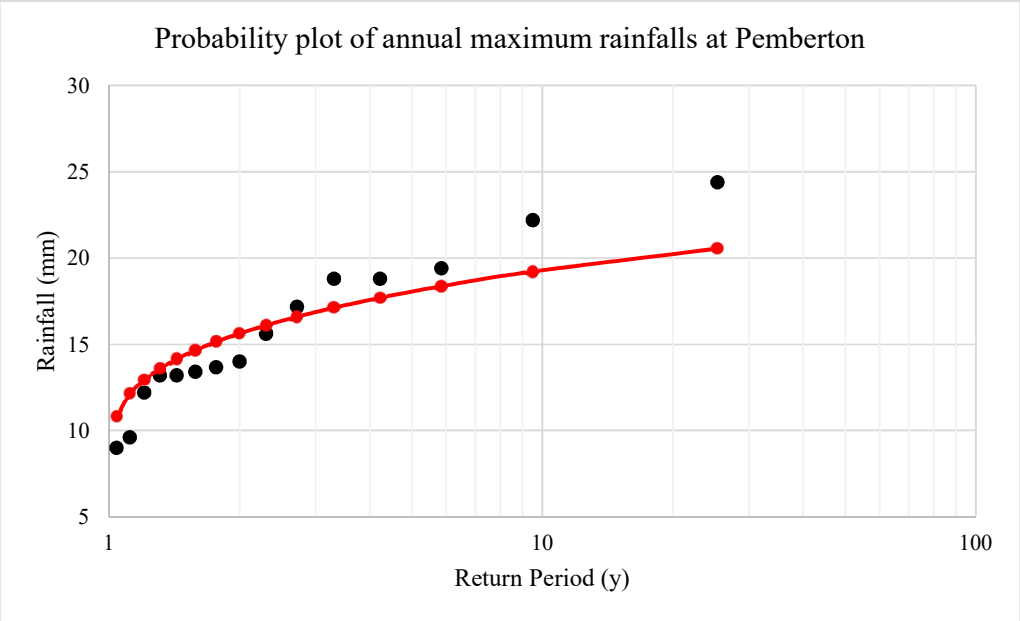

Figure 9.5: Observed and modelled rainfalls at Pemberton

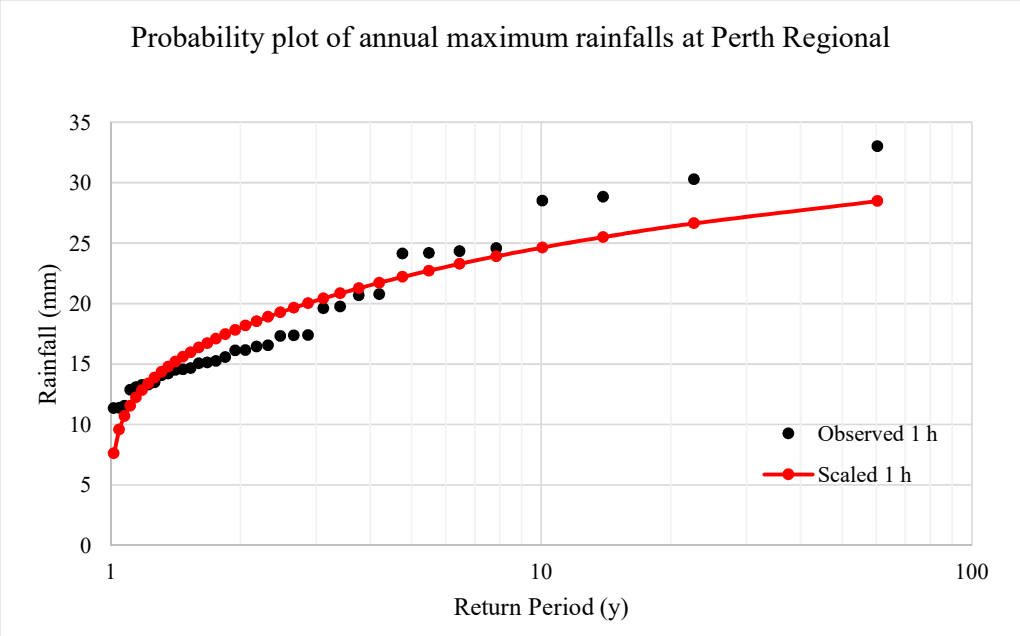

Figure 9.6: Observed and modelled rainfalls at Perth Regional

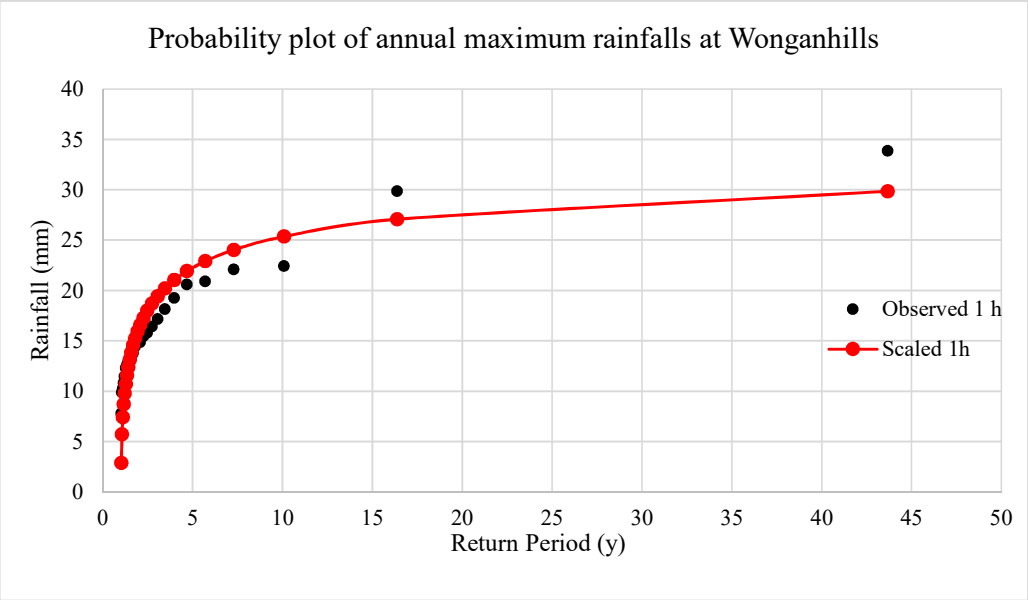

Figure 9.7: Observed and modelled rainfalls at Wongan hills

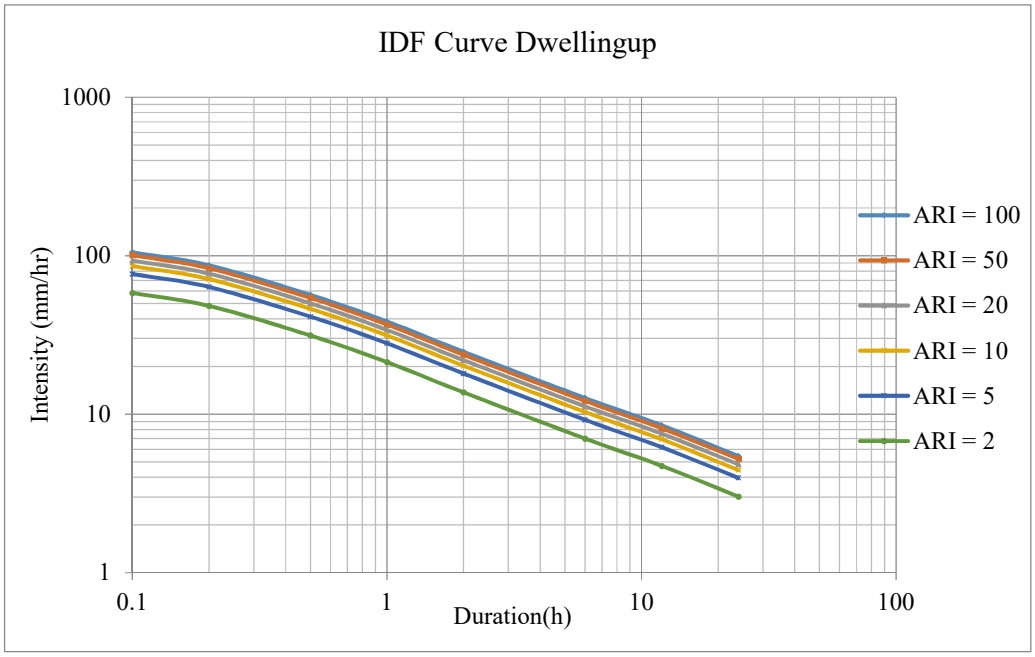

Figure 9.8: Developed IDF curve for Dwellingup

Figure 9.9: Developed IDF curve for Esperance

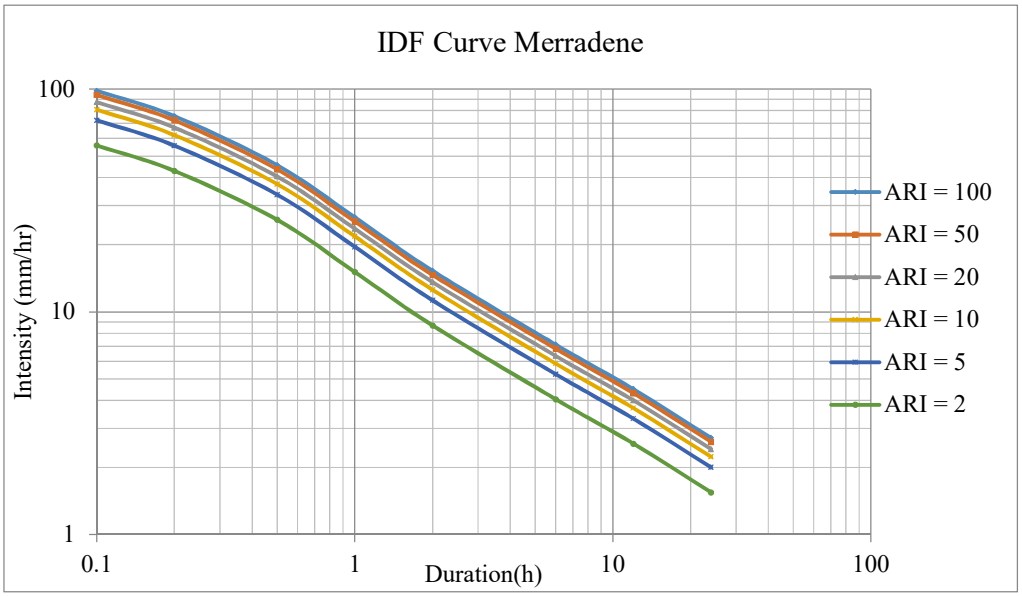

Figure 9.10: Developed IDF curve for Merradene

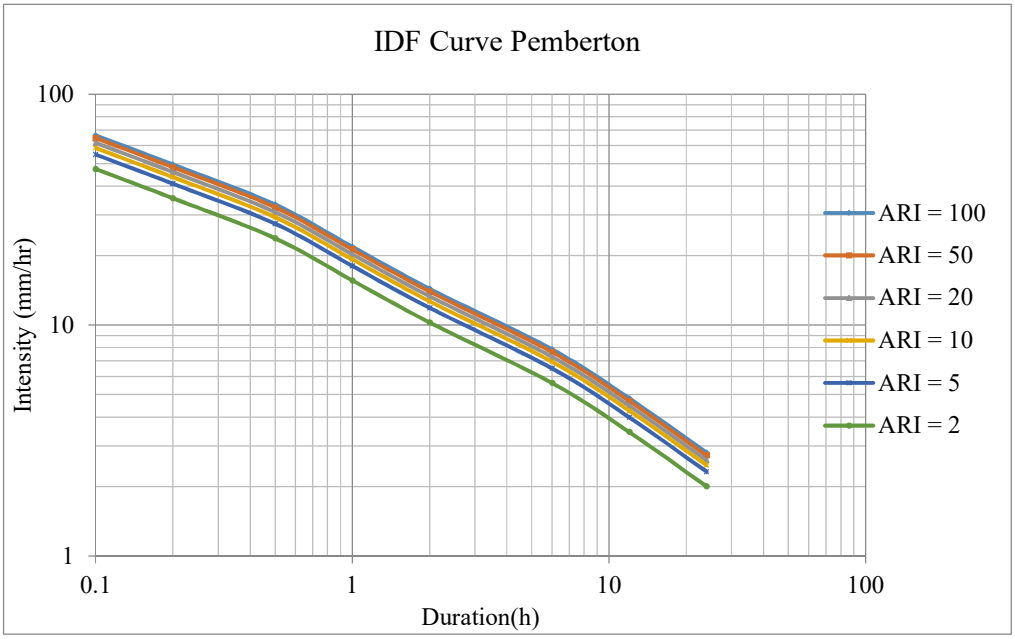

Figure 9.11: Developed IDF curve for Pemberton

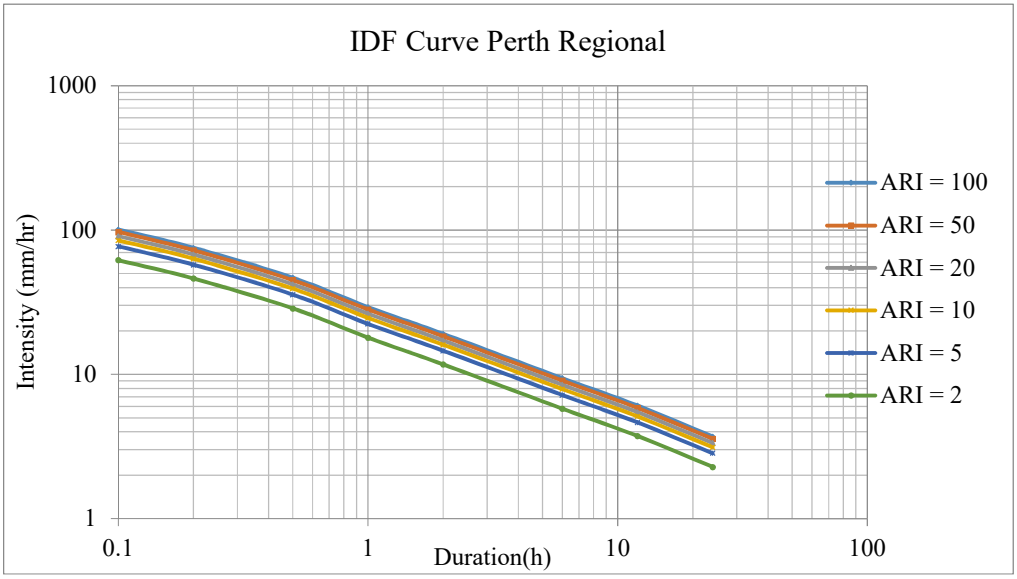

Figure 9.12: Developed IDF curve for Perth Regional

Figure 9.13: Developed IDF curve for Wongan Hills